UNIVERSITY OF CALIFORNIA
SANTA CRUZ

SEA-LEVEL RISE, EL NIÑO, AND THE FUTURE OF THE CALIFORNIA COASTLINE

A dissertation submitted in partial satisfaction
of the requirements for the degree of

DOCTOR OF PHILOSOPHY

in

EARTH SCIENCES

by

Nicole L. Russell

September 2014

The Dissertation of Nicole L. Russell is approved:

____
Professor Gary B. Griggs, Chair

____
Professor Matthew Clapham

____
Dr. Patrick Barnard

____
Tyrus Miller
Vice Provost and Dean of Graduate Studies

TABLE OF CONTENTS

LIST OF FIGURES

CHAPTER ONE

CHAPTER TWO

CHAPTER THREE

LIST OF TABLES

ABSTRACT

Sea-Level Rise, El Niño, and the Future of the California Coastline

Nicole L. Russell

Global mean sea level increased by ~20 cm during the 20th century and the rate is expected to accelerate during this century. Many major cities are already exposed to damaging coastal storms and sea-level rise (SLR) will magnify storm impacts. SLR adaptation can reduce harm, but this new concept is complicated because adaptation plans must be tailored to each community's specifications, due to differences in geologic setting, development, etc. This study designed a process for local SLR adaptation planning, in part through the assessment of the city of Santa Barbara's vulnerability to SLR, including evaluations of shoreline topography and development, historical storm damage, and exposure to SLR. The risk of wave damage to Santa Barbara's shoreline development and infrastructure will be high by 2050 but very high by 2100. The risk of flooding and inundation of low-lying areas will be moderate by 2050 but very high by 2100. The risk of increased cliff erosion rates will be moderate by 2050 but very high by 2100. The threat of beach inundation will be low by 2050 but high by 2100.

Most of the flooding and erosion along the U.S. West Coast are caused by storm surges and wind-driven waves, particularly during strong El Niño events. There

is a need to predict El Niño occurrences for planning purposes, but forecasts from most of the best El Niño Southern Oscillation (ENSO) prediction models have plateaued at a moderate level, leaving room for improvement in ENSO observing systems, models, and data assimilation methods. While the effects of ENSO on wave heights along the U.S. West Coast are well known, no prior studies have examined whether wave heights are also predictive of the phenomenon. This study finds that significant wave heights (H_{sig}) along the U.S. West Coast are slightly suppressed during the summers preceding El Niño winters, but the trend is weak and the data are noisy, so contributions to ENSO forecasts are negligible. The summer H_{sig} trend is strongly associated with the summer North Pacific (NP) Index, which measures the area-weighted sea-level pressure over the Gulf of Alaska (30˚N to 65˚N, 160˚E to 140˚W).

ACKNOWLEDGEMENTS

This work is dedicated to my parents, Ned and Shu San Russell. For your unwavering love, patience, support, wisdom, and good humor, I am eternally grateful. Thank you for always allowing me to be me.

I am very thankful to have received substantial financial support for my research and studies from the Eugene Cota-Robles Fellowship, the California Energy Commission Public Interest Environmental Research Program, and the Hammett Award for Climate Change Research. I would also like to recognize Santa Barbara's City Planning Division, with special thanks to Barbara Shelton, for her tireless assistance with my Santa Barbara City Sea-Level Rise Vulnerability Case Study was indispensable.

To my advisor, Dr. Gary Griggs, thank you for your kindness, enthusiasm, and encouragement throughout my studies. I would also like to acknowledge my other reading committee members, Dr. Matthew Clapham and Dr. Patrick Barnard, for helping me do my best. I am grateful for the many teachers and professors who inspired me over the years, as well. They include my 7th grade teacher, Ms. Diana Barnes, who brought science to life, and Dr. Adina Paytan, who sparked my love of outreach.

Additionally, I would like to recognize my coastal lab mates, whose good cheer, curiosity, and eagerness to help one another have eased this challenging journey. I am also fortunate to have made some outstanding friends since moving to

California. Of these, I extend special thanks to Saffia Hossainzadeh, for her optimism and calm voice of reason have minimized my worries many times. I would also like to express my gratitude for R. Louis Alley, who keeps me in stitches when I take life too seriously and challenges me to think outside the box, whether I like it or not. Also, to Dr. Linda Alley and Stephen Konigsberg, thank you for supporting me as though I were one of your own. Talking with you always leaves me feeling as though anything is possible.

Finally, I would like to acknowledge my wonderful sister, Eileen, who enriches my life and the lives of many others with her kindness, generosity, tremendous wit, and poise. I would also like to thank my extended family, with special recognition of my late grandparents, Ms. Su Yone Lee, Mrs. Wilma Russell, and Dr. Budd Russell. I am forever touched by your empathy, humor, creativity, passion, and inner strength, and I hope to honor you by sharing as much of your good influence and love as I can.

Nicole

CHAPTER ONE

California Sea-Level Rise Vulnerability and Adaptation Guidance Document: A Summary Report

Published in Shore & Beach:
Russell, N.L., and G.B. Griggs (2013a), California sea-level rise vulnerability and adaptation guidance document: A summary report, *Shore & Beach*, *81*(1), 23-29.

1.1 ABSTRACT

Global sea level rose by about 20 cm during the 20th century and observations and projections suggest that it will rise more quickly during the 21st century than it has in the recent past. Many of the world's major coastal cities are already exposed to damaging coastal storms, including hurricanes, with large waves and associated flooding. Sea-level rise is expected to worsen the effects of these events, including increasingly frequent flooding of low-lying areas, increased cliff and bluff erosion rates, increased damage to shoreline infrastructure and development, and narrowing of beaches. One approach to minimizing the harm to coastal communities from such hazards is to begin to adapt to future sea-level rise, using the most recent projections for the coming decades. In California, a 2011 survey of coastal professionals indicated that adaptation to sea-level rise is a high priority for their communities. However, sea-level rise adaptation planning is a relatively new concept, and the survey also revealed a need for technical assistance and translation of scientific information into forms that are readily understood by coastal professionals. Complicating matters is the fact than an adaptation plan must be tailored specifically to a community's unique needs, as coastal communities differ in terms of geologic and topographic setting, infrastructure and development, demographics, politics, and resources. Given these needs, the state of California's Resources Agency funded an effort to develop a guide, *Adapting to Sea-Level Rise: A Guide for California's Coastal Communities*, for assisting local governments in sea-level rise adaptation

planning [see Supplemental File One]. Although the guide is focused on California, much of it is applicable to coastal communities elsewhere.

1.2 INTRODUCTION

1.2.1 Long-Term Sea-Level Rise

Tide gage measurements indicate that global sea level rose by an average of about 1.7 ± 0.5 mm/yr over the 20^{th} century. However, data from satellite altimetry, which has provided records of sea-level rise since 1993, show that the rate of global sea-level rise increased to about 3.1 ± 0.7 mm/yr during the last two decades or so, a near doubling of the 20^{th} century global average, according to a recent study by the National Research Council (2012). The NRC report (2012) provides an up-to-date assessment of both future global sea-level rise and future sea-level rise along the coasts of California, Oregon, and Washington. The governors of those three states and a number of state and federal agencies requested the study in order to assist state agencies and coastal communities in planning for future sea-level rise.

The rate of sea-level rise is not uniform around the world, nor is it the same in every place along the west coast of the United States. Due to regional factors affecting local sea-level rise, including tectonic activity along the coast, ocean and atmospheric circulation patterns, and the gravitational and deformational effects of land ice changes, rates of sea-level rise in specific locations cannot always be assumed to be the same as global rates (NRC 2012). Indeed, the presence of a major plate tectonic boundary at Cape Mendocino causes the U.S. West Coast to behave in different ways on either side of the feature. Between Cape Mendocino and the Mexican border, coastal California is largely subject to strike-slip (lateral) motion along the San Andreas Fault, with relatively little vertical motion. Tide gage data from this portion of the coastline show that rates of sea-level rise over the past 50-100 years have been close to or slightly higher than global values. (Mean values from San Diego to Point Reyes range from about 0.8 to 2.2 mm/yr.) From Cape Mendocino to the Canadian border, the coastline lies above a subduction zone, where accumulating stress tends to raise the coastline. While there are some regional tectonic differences, tide gage data show that rates of sea-level rise are generally lower along this nearly 1000-km stretch of coastline than the global average; in some cases, local sea level is not rising but dropping, instead. This means that coastal communities must tailor sea-level rise adaptation plans to fit the unique needs of their own localities.

The NRC report (2012) thoroughly reviews all of the major contributors to global sea-level rise (oceanic thermal expansion and melting of glaciers and ice sheets; the latter two are the largest components) and combines them to produce a range of projected global sea levels for the years 2030, 2050, and 2100, with uncertainties for each range. In addition, the study accounts for the atmospheric, oceanic, and tectonic variables that affect rates of sea-level rise in individual coastal regions, providing projections for specific stretches of the west coast (also for the years 2030, 2050, and 2100). Thus, the NRC projects different values for future sea-level rise on either side of Cape Mendocino. Relative to the year 2000, sea level is projected to rise along the California coast south of Cape Mendocino by 4 to 30 cm (2 to 12 in) by the year 2030, 12 to 61 cm (5 to 24 in) by 2050, and 42 to 167 (17 to 66 in) by 2100. From Cape Mendocino to Puget Sound in the north, sea level is projected to change by -4 to +23 cm (-2 to +9 in) by 2030, -3 to +48 cm (-1 to +19 in) by 2050, and 10 to 143 cm (4 to 56 in) by 2100 (NRC 2012). However, these figures do not account for the fact that the northern California, Oregon, and Washington coasts will someday experience the next great subduction zone earthquake, which could cause some coastal areas to immediately subside and local sea level to suddenly rise by at least a meter.

The ocean's gradual advance upon low-lying shorelines could allow for the eventual permanent inundation or erosion of beaches that are backed by seawalls, roads, parking lots, etc. This could have a significant impact on California's economy: a 2011 state-commissioned study suggests that a 140-cm (55-in) rise in sea level by the year 2100 (which is close to the upper end of the NRC's projections), could lead to a total loss (i.e. total accumulated loss between now and the year 2100) of at least $440 million in tourism spending and tax revenue at Venice Beach, alone (King *et al*. 2011). This estimate is likely conservative because it assumes that population and income will not grow after the year 2010 (King *et al*. 2011).

1.2.2 Short-Term Phenomena

Although sea level will continue to rise gradually over the long-term, likely by an increasing rate, the most significant threat to California's shoreline over the next few decades will arrive in the form of short-term events, as when sea level is elevated by up to 20-30 cm for several months during ENSO's warm phase and combined with storm waves that approach during high tides (NRC 2010). These events have already been and will continue to be especially damaging when combined with storm surges, high tides, and/or high river flows. The Gulf and East coasts also face similar threats from short-term events, such as hurricanes. Rising sea level is expected to increase the severity of these and other short-term events that coastal communities are already used to experiencing, such as occasional storm flooding (Figure 1.1) and cliff or bluff erosion (Figure 1.2). Additionally, floodwaters and waves can be expected to reach higher elevations and move further inland than they historically have. This will threaten private homes and businesses, public property, including critical low-lying infrastructure such as highways and bridges, power plants, and sewage treatment facilities along the coastline, many of which have already been threatened, damaged, or destroyed by storms in past years (Figure 1.3).

Figure 1.1 East Cliff Drive at Twin Lakes State Beach in Santa Cruz, California, flooded as the result of elevated sea levels coinciding with high tides and storm waves in February 1998 (photo: David Revell).

Figure 1.2 Undercut apartment buildings in the Isla Vista area of Santa Barbara County, California (photo: Kenneth and Gabrielle Adelman, California Coastal Records Project).

Figure 1.3 Apartments in Pacifica, California were threatened by wave attack during the winters of 2009-2010 and 2010-2011 and subsequently evacuated.

1.2.3 Adapting to Sea-Level Rise

Although the precise rate of future sea-level rise is difficult to predict because of the uncertainties in the factors that affect future climate and thus sea level, a 2011 survey of California's coastal professional suggests that most are well aware that sea level is changing and will continue to change well into the future (Finzi Hart *et al*. 2012). Those who participated in the assessment also indicated that adaptation to sea-level rise is a high priority for coastal communities. However, adaptation planning is still in its earliest stages and the survey revealed a need for both technical assistance and for the ongoing translation of scientific information into forms that are readily understood by coastal professionals. Given this insight and the fact that each community is unique in terms of tectonic activity (and thus rate of sea-level change), geography, topography, demographics, politics, etc., the state of California's Resources Agency funded an effort to develop a guide for assisting local governments in their preparations for sea-level rise.

While there are many existing documents regarding climate change vulnerability and adaptation, it appears that none of these have been very specific about *local* sea-level rise. In contrast, the recently published guidance document, *Adapting to Sea-Level Rise: A Guide for California's Coastal Communities*, aims to explain the best available scientific background information about sea-level rise and to walk users through the processes of performing local sea-level rise vulnerability assessments, risk analyses, and formulating and implementing sea-level rise adaptation plans that are tailored to their own communities' specifications [see Supplemental File One]. This guide is now available online, courtesy of the California Ocean Science Trust, at http://calost.org/pdf/announcements/Adapting%20to%20Sea%20Level%20Rise_N%20Russell_G%20Griggs_2012.pdf. It was also printed and distributed to the planning departments, city councils, or boards of supervisors of all of California's coastal communities.

The methods presented in *Adapting to Sea-Level Rise: A Guide for California's Coastal Communities* should largely be applicable to coastal communities outside of California but they were developed through our assessment of the vulnerability of the city of Santa Barbara, California to sea-level rise and related coastal hazards (http://www.climatechange.ca.gov/adaptation/third_assessment/) and influenced by a prior broad study of the vulnerability of the city of Santa Cruz to climate change (http://www.cityofsantacruz.com/Modules/ShowDocument.aspx?documentid=21198). The following is a summary of the key steps in sea-level rise adaptation planning (Figure 1.4), which are described in detail in the guide:

1. *Conduct a sea-level rise and coastal hazards vulnerability assessment*. This could be performed by a consultant or by a team of local government staff, coastal managers, consultants, scientific advisors, etc. Any of these could be appropriate, given a community's size, resources, and prior work with local scientific advisors or consultants. An assessment should identify the areas that are most vulnerable to future flooding, inundation, erosion, and damage from sea-level rise and wave impacts. The consultant or team should complete the following tasks:
    A. *Collect information about the community's historical vulnerability to and past damage from coastal hazards, including reports, maps, surveys, photographs, newspaper archives, etc*. This will help to delineate historically eroded, flooded, and damaged areas and

therefore, the areas that are most likely to be affected or damaged again in the future.

B. *Obtain historic sea level data using the nearest tide gage or gages*. The National Oceanographic and Atmospheric Administration (NOAA) is a good resource for this information (http://tidesandcurrents.noaa.gov/sltrends/sltrends.shtml). This step is necessary because rates of sea-level rise vary from one stretch of coastline to another, especially along the 1760-km length of California's coastline (Figure 1.5), due to differences in tectonic history (uplift or subsidence). Thus, risks and adaptation measures may differ from one region to another as a function of local rates of sea-level rise.

C. *Obtain the most recent sea-level rise projections for different future dates (e.g. 2030, 2050, and 2100).* The estimates provided in the latest NRC report are poised to become the standards used by the state agencies in California that must consider sea-level rise adaptation measures. It makes sense for local communities to use these same values, although adaptation plans should be adjusted as new projections for future sea-level rise become available.

D. *Collect information about short-term increases in sea level, exposure to El Niño events, and changes in wave climate*. Historically, the greatest damage to California's coastal communities, development, and infrastructure has occurred when large waves, high tides, and ENSO's warm phases have occurred simultaneously, as during the winters of 1982-1983 and 1997-1998 (Storlazzi and Griggs 1998; Storlazzi *et al*. 2000). Short-term changes such as these, as well as hurricanes and storm surges on the Gulf and East Coasts, will pose the greatest threats to coastal communities over the next 30-40 years, or until sea level rises by about 30 cm (12 in), the same level that has been reached during some of the largest warm phase ENSO events (Figure 1.6). It is also important to understand that the effects of these individual processes are sometimes cumulative, and any combination will usually be more severe or damaging than a single event. The negative effects of flooding, inundation, and wave attack upon coastal cliffs and bluffs are expected to increase in intensity as the ocean rises to new heights, causing previously unaffected areas of coastline to suffer the combined effects of sea-level rise and coastal storms.

E. *Identify and map the areas that are likely to undergo flooding or inundation in the future, given the most recent sea-level rise projections*. Most communities have not been mapped using high-resolutions (elevations accurate to ≤ 1 ft or 0.3 m). In such cases, it is necessary to use high-resolution land surface elevation data, such as LiDAR data, in order to determine which areas are most likely to be affected by specific future sea levels. The results of the most recent

LiDAR survey can be obtained from NOAA's Digital Coast website (http://csc.noaa.gov/digitalcoast/data/coastallidar), although utilization of the data will require experience in GIS.

F. *Collect all existing information about historic cliff, bluff, dune, and beach erosion rates*. The USGS recently completed two extensive studies of coastal change along the entirety of California's coastline, as part of its National Assessment of Shoreline Change. One of these is focused on coastal land loss along sandy shorelines (Hapke *et al*. 2006) and the other on coastal cliff retreat (Hapke and Reid 2007). Future rates of erosion are expected to be at least as high as historic rates. Griggs *et al*. (2005) provides maps that depict cliff and bluff retreat rates for many locations along the California coast. In addition, many coastal communities have GIS layers or data sets of local shoreline armoring that can supplement national and state data.

2. *Complete a risk assessment*. The consultant or team must evaluate the likelihood that impacts from each sea-level rise-related hazard or process will occur in the future. This assessment should be performed for different endpoints in time, (e.g. 2030, 2050, and 2100), considering the NRC's highest projections for future sea-level rise. The results can be used to determine which areas and assets will require the most attention at different stages in the future. An assessment of risk involves the following steps:

A. *Assess adaptive capacity*. Vulnerability to sea-level rise depends on both the physical stressors to the shoreline and the ability of the affected community to respond and adapt to those changes (NOAA 2010). In part, a community's vulnerability reflects the types of public and private development, resources, and infrastructure that will be at risk from exposure to sea-level rise at different future time periods. The second consideration is a community's adaptive capacity: the ability to prepare for, respond to, and recover from hazards related to sea-level rise. For example, some shoreline parks, parking lots, and roads might be tolerant of occasional flooding. Others could potentially be relocated without great expense. In such cases, there is a high capacity for adaptation. On the other hand, adaptive capacity might be low for large facilities and developments, such as low-lying sewage treatment plants, coastal power plants, large hotels, and other visitor facilities, as they must be planned for decades in advance and replacement or relocation costs are apt to be very high.

B. *Develop a risk assessment*. A risk assessment should evaluate both the probabilities of the future occurrences of individual events and the magnitudes of the consequences of those events. Because it is a key step in prioritizing adaptive actions, the consultant or team should summarize the assessment of the community's expected exposure to sea-level rise and related hazards for different future times (Tables 1.1A and B). A summary should consider the following:

i. Actual future threats or hazards of concern (e.g. flooding, cliff or bluff erosion, inundation, beach loss, etc.)
ii. Economic importance and value of public facilities and infrastructure
iii. Value and importance of private development sectors, both commercial and residential
iv. Importance of municipal emergency services
v. Magnitude of impacts of future hazardous events
vi. Timing and frequency of hazardous events
vii. Certainty of projected impacts to the degree that they can be expected (e.g. given that sea level reaches a particular elevation, certain structures will be flooded during storms of a given magnitude)

3. *Develop an adaptation plan*. Once the vulnerability and risk assessments are complete, they should be used together as the basis for defining a specific plan of action. Communities will likely not have the resources to address all sea-level rise impacts at once. Thus, it is best to start by focusing on the most

important and threatened planning areas, such as facilities and developments that are sited at the lowest elevations, infrastructure that is critical for meeting the needs of the community (e.g. sewage lines, pumping stations, or treatment plants), and structures or infrastructure that are closest to the edges of eroding bluffs or cliffs. The consultant or team should take the following steps:

A. *Identify all adaptation options for each projected hazard*. These should account for the differences between undeveloped and developed land and the differences between public and private property. (Adaptation strategies for these varied types of planning zones are detailed in the guide.) Furthermore, the consultant or team should conduct a careful review of the existing local policies and regulations that might only need to be modified or strengthened. In particular, it is important to review the community's general plan or Local Coastal Program (LCP). Visit http://www.coastal.ca.gov/lcps.html for more information about LCPs.
B. *Specify the criteria for assessing each option*. These could include actual effectiveness, cost-effectiveness, ease of design and implementation, and public and political acceptability.
C. *Evaluate all options and develop recommendations*. Using the criteria from the previous step, the consultant or team should evaluate each potential adaptation measure individually and recommend to decision-

makers only the strategies that are most likely to be successfully implemented.

D. *Draft a plan and complete an internal review*.

4. *Review and adopt the adaptation plan*.

   A. *Review by individual public agencies, the public, and the community's planning commission*.

   B. *Prepare a revised draft adaptation plan*.

   C. *Final review, editing, and adoption by governing body (either city council or board of supervisors)*: Adaptation plan approval is unlikely to be immediate or automatic, although this will depend upon the community's vulnerability, resources, and political climate. It is important to include elected officials from the initiation of adaptation plan development in order to keep them aware of and involved in the plan.

5. *Implement the adaptation plan*. Following approval, it becomes the responsibility of the city or county planning department (or another local government department or agency, such as city management or public works) to implement the sea-level rise adaptation plan. The plan will likely include policies that could require changes to existing land use plans (e.g. general plan, ordinances, zoning, etc.). When a measure requires regulatory decisions, or

when it must be implemented through agencies that share jurisdictions and responsibilities, it cannot be assumed that there will be effective coordination and communication between all parties. However, these challenges and administrative, institutional, and political barriers can be overcome through discussions, leadership from the top, and a shared sense of purpose. (Additional information about this and information about obtaining and raising funds for the implementation of adaptation plans can be found in the guide.)

6. *Monitor, review, and update the adaptation plan*. Once the adaptation plans are enacted, all measures should be monitored regularly in order to determine their effectiveness because stakeholders need to know whether policies are fulfilling their intended purposes. Local consultants or university research groups could perform this task. Adaptation plans should be reviewed and revised when deemed necessary, based upon the most recent occurrences of hazardous events, changes in the rate of sea-level rise, and changes in community growth and development.

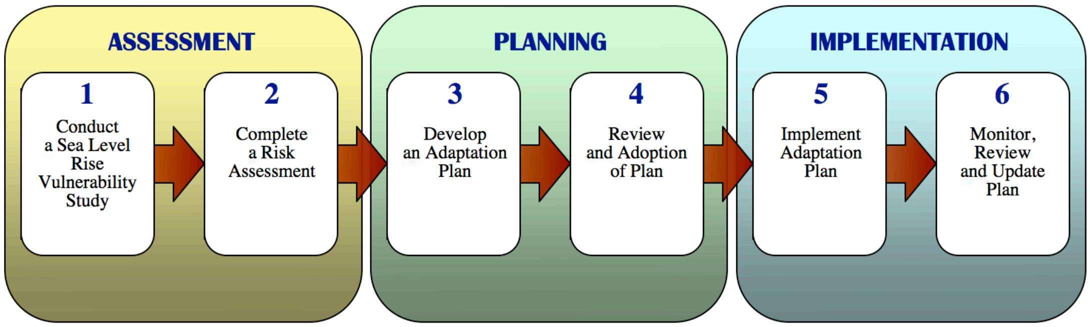

Figure 1.4 Steps for developing and implementing a sea-level rise adaptation plan.

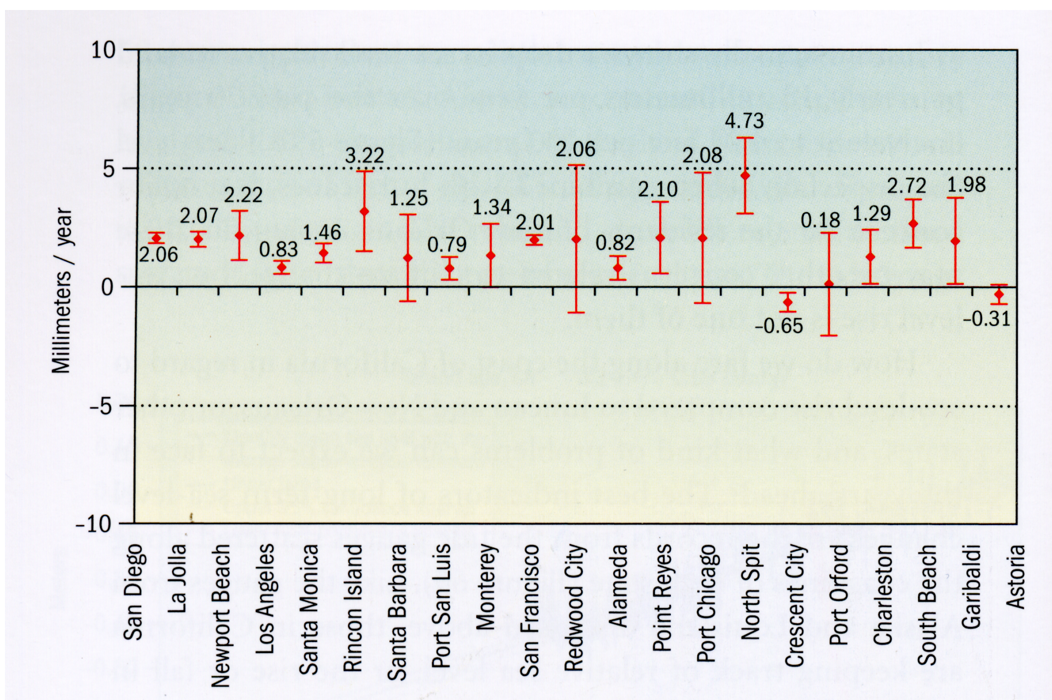

Figure 1.5 Local rates of sea-level rise from NOAA tide gages vary along the coasts of California and Oregon (from Griggs 2010).

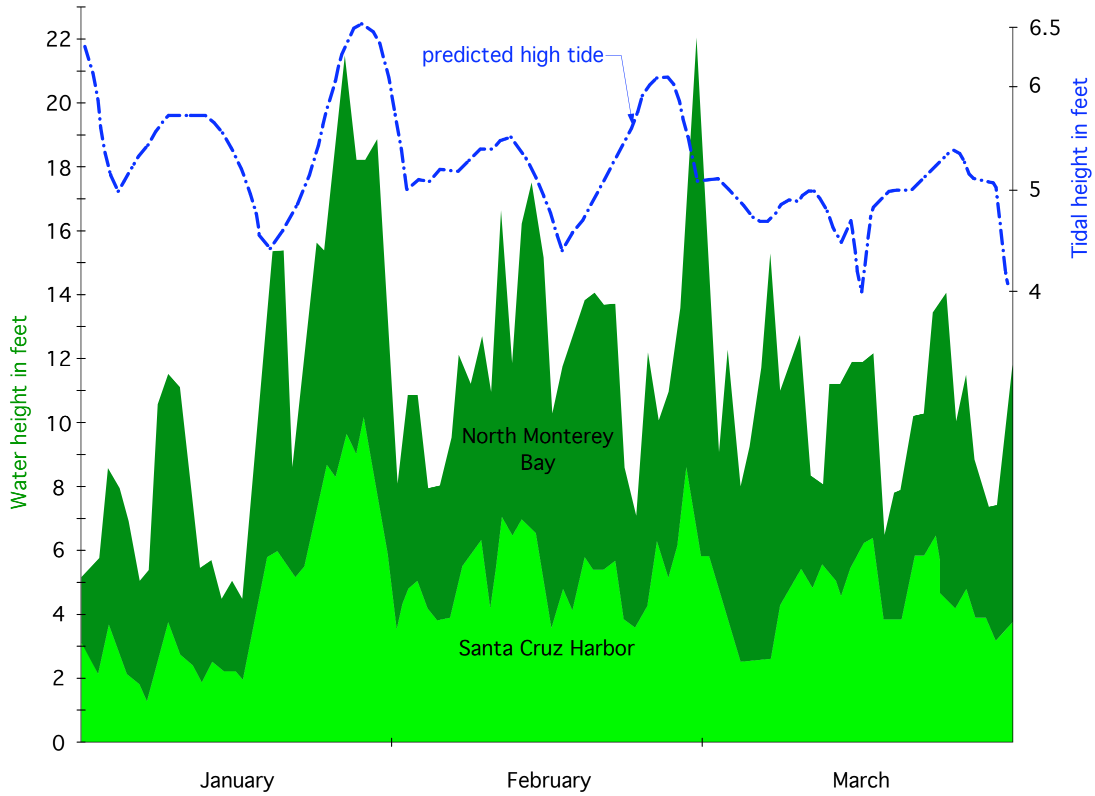

Figure 1.6 During the 1983 El Niño, the arrival of large storm waves during high tides caused millions of dollars in damage along the entirety of California's coastline. Wave height records from Santa Cruz Harbor (shallow-water nearshore buoy) and North Monterey Bay (deep-water offshore buoy) are shown. Predicted high tide is the higher high water for each day.

Table 1.1: *Example of (A) short to intermediate-term (2013-2050) and (B) intermediate to long-term (2050-2100) risk from sea-level rise and related processes. Risk = (Probability) • (Consequence). Colors from green to red indicate increasing risk levels. Risks in red boxes are of the highest priority for adaptation action because they will cause the greatest impacts and occur most frequently.*

A		Probability / Likelihood of Occurrence (2013-2050)			
		Low	Moderate	High	Very High
Magnitude of Consequence	Low			Passive beach erosion	
	Moderate			Increase in coastal cliff/bluff erosion rates	Wave attack on coastal infrastructure and development
	High			Flooding of low-lying coastal areas	

B		Probability / Likelihood of Occurrence (2050-2100)			
		Low	Moderate	High	Very High
Magnitude of Consequence	Low				
	Moderate				Passive erosion of beaches
	High				Inundation of low-lying areas; Wave attack on infrastructure and development; Increase in cliff/bluff erosion rates

1.3 CONCLUSIONS

Sea-level rise will likely become an increasingly important concern to many U.S. coastal communities and state agencies in the coming decades, as it is expected to increase the frequency and magnitude of coastal flooding, as well as cliff, bluff, and beach erosion, with associated damage to shoreline infrastructure and development. Adapting to sea-level rise is one important local approach to minimizing the impacts of future sea-level rise on coastal communities. Because sea-level rise adaptation planning is still in its early stages, it will be very useful for coastal communities to publicize the results of their adaptation planning and to share them not only with local government staff, elected officials, and the public, but also with other coastal communities, which face common issues related to sea-level rise and could benefit from the insight. *Adapting to Sea-Level Rise: A Guide for California's Coastal Communities* is a resource that should aid coastal communities in and outside of California during the organization and management stages of their efforts to plan for sea-level rise.

1.4 REFERENCES

Committee on Sea-Level Rise in California, Oregon, and Washington; Board on Earth Sciences and Resources; Ocean Studies Board; Division on Earth and Life Studies; National Research Council (2012), *Sea-level rise for the coasts of California, Oregon, and Washington: Past, present, and future*. Washington, DC: National Academies Press, 275 pp. http://www.nap.edu/catalog.php?record_id=13389

Finzi Hart, J.A., P.M. Grifman, S.C. Moser, A. Abeles, M.R. Myers, S.C. Schlosser, and J.A. Ekstrom (2012), Rising to the Challenge: Results of the 2011 coastal California adaptation needs assessment. USCSG-TR-01-2012.

Griggs, G.B. (2010). *Introduction to California's beaches and coast*. University of California Press: 311 pp.

Griggs, G.B., K.B. Patsch, and L.E. Savoy (2005). *Living with the changing California coast*. University of California Press: 540 pp.

Hapke, C.J., and D. Reid (2007), National assessment of shoreline change part 4: Historical coastal cliff retreat along the California coast, USGS Open File Report, 2007-1133, 51 pp. http://pubs.usgs.gov/of/2007/1133/

Hapke, C.J., D. Reid, B.M. Richmond, P. Ruggiero, and J. List (2006), National assessment of shoreline change part 3: Historical shoreline change and associated coastal land loss along sandy shorelines of the California coast, USGS Open File Report, 2006-1219, 72 pp. http://pubs.usgs.gov/of/2006/1219/

King, P.G., A.R. McGregor, and J.D. Whittet (2011), *The economic costs of sea-level rise to California beach communities*. California Department of Boating and Waterways and San Francisco State University, 97 pp. http://www.dbw.ca.gov/PDF/Reports/CalifSeaLevelRise.pdf

National Oceanic and Atmospheric Administration (2010), *Adapting to climate change: A planning guide for state coastal managers*. NOAA Office of Ocean and Coastal Resource Management, 138 pp. http://coastalmanagement.noaa.gov/climate/docs/adaptationguide.pdf

Russell, N.L, and G.B. Griggs (2012), *Adapting to sea-level rise: A guide for California's coastal communities.* Sacramento, California: California Energy Commission, Public Interest Environmental Research Program, 52 pp.

Storlazzi, C.D., and G.B. Griggs (1998), The 1997-1998 El Niño and erosion processes along the central coast of California, *Shore & Beach*, *66*(3), 12-17.

Storlazzi, C.D., C.M. Willis, and G.B. Griggs (2000), Comparative impacts of the 1982-83 and 1997-98 El Niño winters on the central California coast, *Journal of Coastal Research*, *16*(4), 1022-1036.

CHAPTER TWO

City of Santa Barbara Sea-Level Rise Vulnerability Assessment: A Summary Report

Published in Shore & Beach:
Russell, N.L., and G.B. Griggs (2013b), City of Santa Barbara sea-level rise vulnerability assessment: A summary report, *Shore & Beach*, *81*(4), 38-51.

2.1 ABSTRACT

In 2010, the California Resources Agency funded a project to develop a guide for assisting local governments in sea-level rise adaptation planning: "*Adapting to Sea-Level Rise: A Guide for California's Coastal Communities*" (Russell and Griggs 2012; see Supplemental File One). An assessment of the vulnerability of the city of Santa Barbara to future sea-level rise (by the years 2050 and 2100) and related coastal hazards served as a case study [see Supplemental File Two] for the development of the adaptation guide. Historically damaging events, shoreline topography and development, and exposure to sea-level rise and wave attack were evaluated for Santa Barbara, as were the likely impacts of potential future coastal hazards to specific areas of the city, risk levels, the city's ability to respond, and potential adaptation measures. The case study finds that the risk of wave damage to shoreline development and infrastructure in Santa Barbara will be high by 2050 and very high by 2100. Choices are limited and adaptive capacity will be moderate, with retreat as the most viable long-term option. By 2050, flooding and inundation of low-lying coastal areas will present a moderate risk to the city, which will have a moderate capacity for adaptation. The risks are expected to be very high and adaptive capacity will be low by 2100. Cliff erosion has taken place for decades, threatening public and private property in the Mesa area. The risk of increased cliff erosion rates will be moderate by 2050 and very high by 2100. Because armoring is ineffective along the Mesa and retreat would necessitate the relocation of structures, adaptive capacity will be low. Inundation of beaches presents a low threat to the city by 2050 but a high

threat by 2100. The city faces a dilemma: protect oceanfront development and infrastructure or remove barriers and let beaches migrate inland. By 2100, structures will have to be moved if beaches are to be maintained.

2.2 INTRODUCTION

Global sea level is rising. As a result, many coastal communities will face tough choices for adapting to the future conditions and/or dealing with the consequences. Although the precise rate of future sea-level rise is impossible to predict because of the uncertainties in the factors that affect future climate and thus sea level, a 2011 survey of California's coastal professionals suggests that most are aware that sea level is changing and will continue to change well into the future (Finzi Hart *et al.* 2012). Participants in the assessment also indicated that adaptation to sea-level rise is a high priority for coastal communities. Fortunately, the state of California is supporting their cause. The California Coastal Commission recently announced that it will award a total of $1 million in grants in early 2014 to local governments that successfully apply for assistance to update their Local Coastal Programs, with special consideration for updates that address the effects of climate change. (See http://www.coastal.ca.gov/lcp/lcpgrantprogram.html for additional information.)

Tide gage records indicate that the average rate of global sea-level rise was 1.7 ± 0.5 mm/yr during the 20th century. However, data from satellite altimetry, which has provided precise records of sea-level rise since 1993, show that the rate increased to about 3.1 ± 0.7 mm/yr during the last two decades, a near doubling of the 20th century global average (NRC 2012). Because rates of local sea-level rise are affected by regional factors, including uplift and subsidence, ocean and atmospheric circulation patterns, and the gravitational and deformational effects of land ice changes, local sea-level rise rates cannot be assumed to be the same everywhere (NRC 2012). Indeed, a major plate tectonic boundary at Cape Mendocino (northern California) produces different effects on either side of this feature. Between Cape Mendocino and the Mexican border, coastal California is largely subject to strike-slip (lateral) motion along the San Andreas Fault, with relatively little vertical motion. Tide gage data from this portion of the coastline show that rates of sea-level rise over the past 50 to 100 years have been close to or slightly higher than global rates, with mean values from San Diego (southern California) to Point Reyes (just northwest of San Francisco Bay) ranging from about 0.8 to 2.2 mm/yr (Figure 2.1). From Cape Mendocino to the Canadian border, the coastline lies above a subduction zone, where accumulating stress tends to raise the land. While there are some regional tectonic differences along this nearly 1000-km (600-mi) stretch of coastline, tide gage data show that local rates of sea-level rise are generally lower than the global average and in some cases, local sea level is dropping because the rate of uplift outpaces the rate of sea-level rise. These phenomena suggest that coastal communities must tailor sea-level rise adaptation plans to fit the unique needs of their own localities.

Relative to the year 2000, sea level is projected to rise along the California coast south of Cape Mendocino by 5 to 30 cm (2 to 12 in) by the year 2030, 13 to 61 cm (5 to 24 in) by 2050, and 43 to 168 cm (17 to 66 in) by 2100. From Cape Mendocino to Puget Sound (Washington) in the north, sea level is projected to change by -5 to +23 cm (-2 to +9 in) by 2030, -3 to +48 cm (-1 to +19 in) by 2050, and 10 to 142 cm (4 to 56 in) by 2100 (NRC 2012). (These projections have ranges due to the consideration of multiple climate models.) However, these figures do not account for the next great Cascadia Subduction Zone earthquake, which would likely cause much of the region north of Cape Mendocino to immediately subside and local sea level to suddenly rise by at least one meter (3.3 feet) (NRC 2012).

The ocean's gradual advance upon low-lying shorelines will lead to the eventual permanent inundation or erosion of beaches that are backed by development or barriers, such as seawalls, roads, parking lots, and other structures. While permanent inundation is expected to occur gradually over the long-term, the most significant threats to California's shoreline over the next few decades will continue to be short-term episodic events, such as storms. Storm waves and associated storm surges that arrive during high tides are especially damaging when sea level is elevated during strong El Niño winters (NRC 2012). However, a rising sea level is expected to increase the frequency and severity of these and other short-term events that coastal communities are used to experiencing, such as occasional storm flooding (Figure 2.2) and cliff or bluff erosion (Figure 2.3). Additionally, floodwaters and waves can be expected to reach higher elevations and move further inland than they have in the recent past. This will threaten private homes, businesses, and public property, including critical low-lying infrastructure, such as highways, bridges, power plants, and sewage treatment facilities along the coastline, many of which have already been threatened, damaged, or destroyed by storms in past years.

It is likely that sea-level rise will have a significant impact on California's economy. A 2011 state-commissioned study (King *et al.*) uses sea-level rise projections to estimate the potential economic losses due to flooding and beach erosion for five California beach communities. A 1.4-m (55-in) rise in sea level by the year 2100 could lead to a total loss (i.e. total accumulated loss between now and the year 2100) of at least $440 million in tourism spending and tax revenue at Venice Beach alone (King *et al*. 2011). This estimate is likely conservative because it assumes that population and income will not grow after the year 2010.

Adaptation planning is still in its early stages and there is a need for technical assistance and the ongoing translation of scientific information into forms that are readily understood by coastal planners and managers (Finzi Hart *et al.* 2012). Given this insight and the fact that each community is unique in terms of land motion (and thus rate of local sea-level change), topography, demographics, politics, etc., California's Resources Agency funded an effort to develop a guide for assisting local governments in their preparations for future sea-level rise.

While there are many existing documents about climate change vulnerability and adaptation, it appears that few have been focused specifically on local sea-level rise. "*Adapting to Sea-Level Rise: A Guide for California's Coastal Communities*" [Supplemental File One] provides scientific background information about sea-level rise and walks users through the processes of performing local sea-level rise vulnerability assessments, risk analyses, and formulating and implementing sea-level rise adaptation plans (Russell and Griggs 2012). This guide is now available online, courtesy of the California Ocean Science Trust, at http://calost.org/pdf/announcements/Adapting to Sea Level Rise_N Russell_G Griggs_2012.pdf. The methods presented in this guide were developed in part through our assessment of the vulnerability of the city of Santa Barbara, California to sea-level rise and related coastal hazards, which can serve as an example for other coastal communities (Griggs and Russell 2012). "*City of Santa Barbara Sea-Level Rise Vulnerability Study"* [Supplemental File Two] is available online at http://www.climatechange.ca.gov/adaptation/third_assessment/.

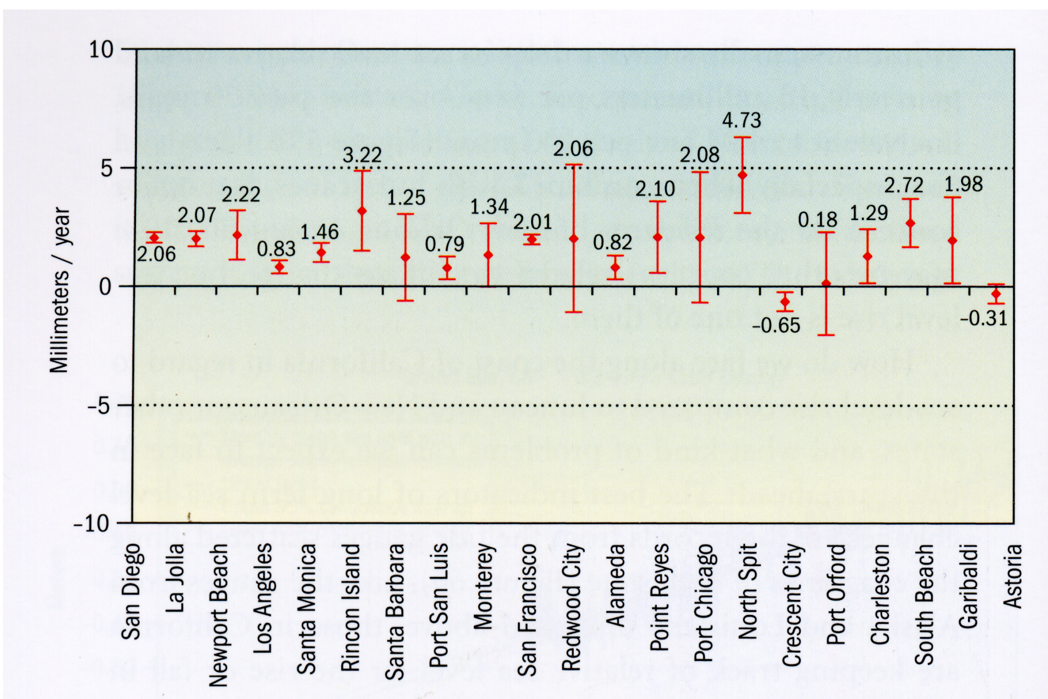

Figure 2.1 Local rates of sea-level rise from NOAA tide gages vary along the coasts of California and Oregon (from Griggs 2010).

Figure 2.2 The Santa Barbara Airport parking lot flooded in 1969 (source: Santa Barbara Airport).

Figure 2.3 Cliffs are actively eroding along the Clarke Estate and the adjacent cemetery (photo: Kenneth and Gabrielle Adelman, California Coastal Records Project).

2.2.1 Sea-Level Rise and the City of Santa Barbara

The city of Santa Barbara is located along the central California coast, about 145 km (90 mi) northwest of Los Angeles. Its approximately 8-km (5-mi) east-west trending coastline faces south and includes cliffs, bluffs, and beaches (Figures 2.4 and 2.5). The low-lying Santa Barbara Airport is also part of the city, although it is located about 5 km (3 mi) west of the city proper. "*City of Santa Barbara Sea-Level Rise Vulnerability Study"* (Griggs and Russell 2012) evaluates the vulnerability and adaptive capacity of the city of Santa Barbara to sea-level rise by the years 2050 and 2100. Sea-level rise is expected to increase the magnitude of coastal hazards and loss of resources from storm damage, flooding, sea cliff and bluff erosion, and shoreline erosion. A variety of physical, ecological, economic, and social consequences can be expected to result from these changes. The vulnerability study qualitatively assesses risks to the city, emphasizing the potential consequences for public property and infrastructure, as well as private property and development along the coastline.

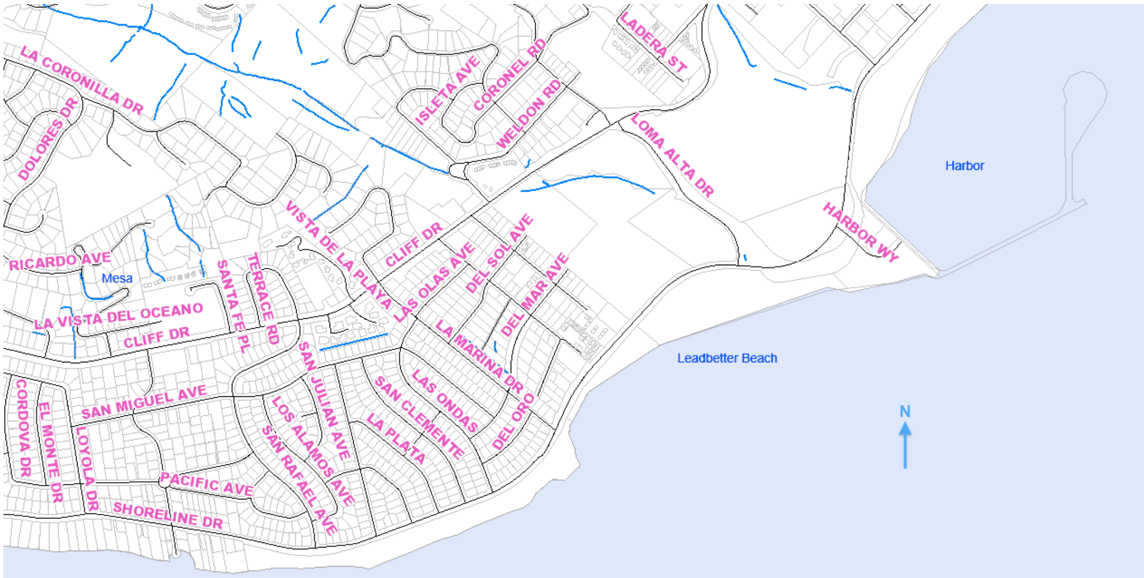

Figure 2.4 Map depicts relative locations of Santa Barbara's Mesa, which extends to the west side of the city, as well as Shoreline Drive, Leadbetter Beach, and the harbor (source: City of Santa Barbara).

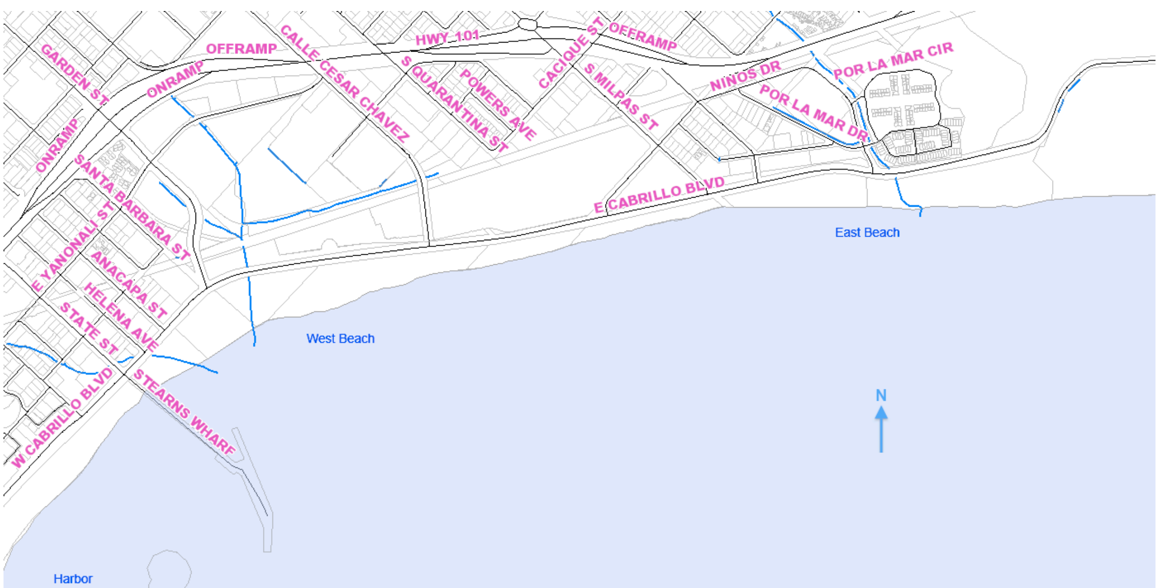

Figure 2.5 Map depicts relative locations of Stearns Wharf, West Beach, and East Beach, on the city of Santa Barbara's east side (source: City of Santa Barbara).

2.3 MATERIALS AND METHODS

This project was initiated while the city of Santa Barbara was completing a general plan revision and an environmental impact report (EIR) that included a climate change component. At the beginning, we met with relevant city departments to explain the project's objectives, ask for information and suggestions, and find out what kinds of information were desirable to city staff. Follow-ups provided useful information and photographs of historical coastal storm damage, flooding, and cliff erosion.

Historical aerial photographs from the California Coastal Records Project (http://www.californiacoastline.org) proved to be very useful for evaluating conditions and development along the city's coastline. In addition, the city's revised general plan and EIR highlighted areas that were historically and/or are currently vulnerable to coastal storms, flooding, and erosion, as well as the areas that will likely be vulnerable to coastal impacts associated with future sea-level rise. We used the state of California's sea-level rise projections to assess hazards: 25-43 cm (10-17 in) by 2050 and 1-1.4 m (3.3-4.6 ft) by 2100 (projections relative to the year 2000). (These values were recommended in 2010, prior to the release of the 2012 NRC report.) City department staff reviewed draft versions of the vulnerability assessment and adaptation recommendations.

For adaptation to future changes, a coastal community must have an understanding of both its *vulnerability* to the expected changes and the *risk* of its exposure to them, as adaptation to sea-level rise is a risk management strategy for an uncertain future. For the purposes of this study, *vulnerability* is defined as the degree of exposure to a relatively high sea level or to the combined effects of an elevated sea level plus a major coastal storm and/or high tide. On the other hand, *risk* includes both the *probability* that a future event (i.e. coastal flooding, inundation, or increased cliff erosion) is likely to occur, as well as the *magnitude* (or level of severity) of the event. Thus, a *vulnerability assessment* should include an evaluation of the level of a community's exposure to coastal hazards, as well as the potential magnitudes of the damages or losses from events that are known to elevate sea level significantly, such as large El Niño storms or storm surges.

Finally, *adaptive capacity* must be evaluated. *Adaptation* is defined as the adjustment of natural or human systems in response to actual or expected events and their effects, such that losses are minimized. Thus, a coastal community's *adaptive capacity* is defined by its ability to respond to sea-level rise and its associated impacts, including the avoidance, reduction, or moderation of potential damages, as well as its ability to cope with the expected or predicted consequences of such impacts.

2.3.1 Conducting the Assessment

Several types of coastal processes have the potential to affect communities like Santa Barbara. Each of the following needs to be evaluated and considered in planning efforts:

A. Sea-level rise
B. Coastal storm damage

C. Runoff and flooding

D. Cliff or bluff retreat

E. Shoreline or beach retreat

It is also important to understand that the effects of these individual processes can be cumulative and any combination can be more severe or damaging than a single event. The city of Santa Barbara has been damaged during such events in the past and will experience them again in the future, most likely with an increased frequency under rising sea levels. The impacts of those events are also expected to increase in magnitude as a result of sea-level rise.

The first step in conducting a sea-level rise and coastal hazards vulnerability assessment is to collect information about a community's historical vulnerability to coastal hazards using reports, maps, surveys, photographs, newspaper archives, interviews, etc. that detail past damages. This will help to delineate historically eroded, flooded, or damaged areas and, therefore, the areas that are most likely to be affected again in the future. Because future rates of erosion are expected to be at least as high as historic rates, a community will need to obtain data for historic cliff, bluff, dune, and beach erosion rates. It is also important to look for information about previous short-term increases in sea level and exposure to El Niño events. Potential adaptation responses can then be recommended for reducing exposure to future hazards. In this study, specific areas of the city of Santa Barbara were analyzed in order to determine the likely impacts of sea-level rise, the risks that are posed by these hazards, and the city's ability to respond to them.

The second step is to obtain historic sea-level rise rates using the nearest tide gage or gages, as these can serve as a community's baseline data. The National Oceanographic and Atmospheric Administration (NOAA) is a good resource for this information (http://tidesandcurrents.noaa.gov/sltrends/sltrends.shtml). This step is necessary because rates of sea-level change vary by tectonic setting along the 1770-km (1100-mi) length of California's coastline.

The third step is to obtain the most recent sea-level rise projections for different future dates (e.g. 2050 and 2100). The estimates provided in the latest NRC report are the standards that were recently adopted by the California state agencies that must consider sea-level rise adaptation measures. It makes sense for local communities to use the same values, although adaptation plans should be adjusted as new sea-level rise projections become available. As previously stated, the Santa Barbara study uses the state of California's 2010 sea-level rise projections of 25-43 cm (10-17 in) by the year 2050 and 1-1.4 m (40-55 in) by 2100 (relative to sea level of the year 2000), as the NRC's 2012 values (13-61 cm or 5-24 inches by 2050 and 43-168 cm or 17-66 inches by 2100), were not yet available prior to this study's completion.

The final step in assessing vulnerability is to identify and map the areas that are likely to undergo flooding in the future, given the most recent sea-level rise projections (for 2050 and 2100). It is best to use the latest high-resolution land surface elevation data, such as LiDAR data, which can be obtained from NOAA's Digital Coast website (http://csc.noaa.gov/dataviewer/index.html?action=advsearch&qType=in&qFld=projectid&qVal=1005), although utilization of this data requires experience in GIS.

For the latest analysis of Santa Barbara's potential future flood elevations, 2010 LiDAR data were obtained as digital elevation models from NOAA's *2009-2011 CA Coastal Conservancy Coastal LiDAR Project* (2011). The horizontal positional accuracy of these data is 51 cm (20 in) or better and the vertical accuracy is 18 cm (7 in) or better (NOAA 2011). Contour lines representing (a) the 1.35-m (4.43-ft) mean high water level (from Hapke *et al.* 2006), (b) the 100-year flood (0.9-m or 3-ft flood) level on top of mean high water plus 60 cm (2 ft) of sea-level rise (the highest projected sea-level rise by 2050, from NRC 2012), and (c) the 100-year flood level (0.9-m flood) on top of mean high water plus 1.7 m (5.5 ft) of sea-level rise (the highest projected sea-level rise by 2100, from NRC 2012) were added using ArcGIS software. Contour layers were exported as shapefiles and then converted to KML format for use in Google Earth.

The next course of action is to complete a *risk assessment* for different endpoints in time (e.g. 2050 and 2100) by evaluating the likelihood that impacts from each sea-level rise-related hazard or process from the vulnerability assessment will occur in the future, as well as the magnitudes of the consequences of those events. An assessment of risk also includes an evaluation of *adaptive capacity*, or the ability of a community to respond to, adapt to, or recover from the changes associated with sea-level rise at different future time periods (NOAA 2010). For this study, we considered the future threats of concern along the city's coastline (e.g. flooding, cliff and bluff erosion, inundation, and beach loss), the economic importance and value of public facilities and infrastructure, and the value and importance of residential development. Additionally, we assessed the magnitudes of the impacts of future hazardous events, the timing and frequency of such events, and the certainty of occurrences to the degrees that they can be projected (e.g. given that sea level reaches a particular elevation, certain structures will be flooded during storms of a given magnitude). The future risks from hazards that are associated with sea-level rise were evaluated for both a *short to intermediate timeframe* (2012-2050) and an *intermediate to long-term timeframe* (2050-2100). We used three different levels for the magnitude of impact: *low, moderate*, and *high*; and four different levels for the probability or likelihood of occurrence**:** *low, moderate, high,* and *very high*. Although the terms "low, moderate, high, and very high" are based upon the sea-level rise scenarios that were originally suggested for use by California's state agencies, they are used qualitatively in the Santa Barbara report.

Finally, we used the vulnerability and risk assessments to identify adaptation options for each projected hazard. Communities should consider overall effectiveness, general cost-effectiveness, and ease of design and implementation of various strategies. Adaptation to sea-level rise is a relatively new concept and most coastal communities have limited resources for dealing with the consequences of climate change. Ideally, a city or county would determine the economic/historic/cultural, etc. values of all of its coastal infrastructure, development, recreational areas, etc., for the purpose of ranking their relative levels of vulnerability and importance to the community. Planning staff could then focus upon the critical areas, such as facilities and development that are sited at the lowest elevations, infrastructure that is critical for meeting the needs of the community (e.g. sewage transmission lines, pumping stations, or treatment plants), and structures or infrastructure that are closest to the edges of eroding cliffs or bluffs. In this way, a community could stagger its adaptive efforts in phases, rather than attempting to tackle all areas simultaneously.

We utilized a ranking system for the various risks to the city of Santa Barbara's coastline by the years 2050 and 2100 using California's 2010 projections for sea-level rise and emphasized the effects of anticipated future sea-level rise on public property and infrastructure, as well as private property (Tables 2.1A and B). Suggested adaptation measures include a broad range of approaches: future planning for hazard avoidance, engineering (including retrofitting, rebuilding, construction, and protection), and retreat or relocation.

Table 2.1: *Short to intermediate-term (2012-2050) and (B) intermediate to long-term (2050-2100) risk from sea-level rise and related processes. Risk = (Probability) • (Consequence). Colors from green to red indicate increasing risk levels. Risks in red boxes are of the highest priority for adaptation action because they will cause the greatest impacts and occur most frequently.*

A		Probability / Likelihood of Occurrence (2012-2050)			
		Low	Moderate	High	Very High
Magnitude of Consequence	Low	Passive beach erosion			
	Moderate		Inundation of low-lying areas; Increased cliff erosion rates		
	High			Wave damage to shoreline development	

B		Probability / Likelihood of Occurrence (2050-2100)			
		Low	Moderate	High	Very High
Magnitude of Consequence	Low				
	Moderate			Passive beach erosion	
	High			Inundation of low-lying areas	Wave damage to shoreline development; Increased cliff erosion rates

2.4 RESULTS AND DISCUSSION

2.4.1 Flooding

Santa Barbara has a NOAA tide gage (established in 1973) but due to displacement during various construction projects, the record is discontinuous and of limited value (Figure 2.6). However, if the tide gage remains stationary in the future, the record should become reliable and over time, it will provide a long-term indication of the rate of local sea-level rise. The study recommends that all precautions be taken in order to protect the existing NOAA tide gage at the breakwater from future construction or disturbance, such that a long-term record of local sea level change can be established.

As sea level rises, there will be an increased number of extreme high water events, which tend to occur when high tides coincide with winter storms and their associated high winds, storm surges, and wave run-up. Santa Barbara has suffered the effects of such events in the past. While sea level is temporarily elevated for several months during El Niño years, a particularly devastating storm during the 1983 El Niño was also accompanied by high tides, large waves, and storm surge, which eroded portions of the beachfront park facilities, damaged the yacht club and harbormaster's office, and reached almost to Shoreline Drive (Figures 2.7-9; Figure 2.4 shows location of Shoreline Drive). Waves also carried debris onto Cabrillo Boulevard at Palm Park along East Beach (Figure 2.10; Figure 2.5 shows location of Cabrillo Boulevard).

Where streams meet the coast, backwater conditions can occur as elevated sea levels (from high tides, storm surges, or, over the long-term, from rising sea levels) prevent floodwaters from draining rapidly, causing streams to back up or slow down, which can lead to upstream flooding. Currently, flooding occurs during high tides and major storm events but these problems will be exacerbated in the future with increasing sea levels.

The city's 2009 coastal flood hazard map was updated using NOAA's (2011) LiDAR data, which has improved surface elevations. The new images show contour lines for the present mean high water level and for the potential future extent of 100-year flooding, based on the NRC's 2012 sea-level rise projections for the years 2050 and 2100. The images were created using ArcGIS and Google Earth in order to produce maps with easily identifiable geographic features (Figures 2.11A and B). Both the 2009 city map and the new maps are limited in that the areas highlighted as being subject to flooding include *all* areas that are lower than the critical elevations, even though some of those areas are inland and not directly connected to the shoreline.

An increase in the number of extreme high water events will likely accelerate rates of cliff retreat and increase damage to public and private oceanfront properties and development, including city infrastructure. These types of events pose the greatest threats to the Santa Barbara coastline for the near-term future (until about 2050). Historically, damage to shoreline structures and infrastructure has been *moderate* but this is expected to increase to *high* in the near-term (by 2050) with 36 cm (14 in) of sea-level rise (pre-NRC 2012 value) because damage is already happening at present-day sea level (Table 2.1A). The magnitude of damage will increase to *very high* by the year 2100 if sea level rises by 1.2 or more meters (at least 3.9 feet; pre-NRC 2012 value) above the year 2000 sea level (Table 2.1B). Park facilities, parking lots, development at the harbor, the municipal wharf, Shoreline Drive, Cabrillo Boulevard, and associated infrastructure and development that serve visitors along Cabrillo Boulevard will all eventually be at risk from wave attack.

There are limited adaptive measures for the city's low-lying shoreline areas: beach sand nourishment, armor to protect in place, or relocation of facilities (retreat). Although Leadbetter Beach (Figure 2.4) was widened by hundreds of feet following breakwater construction in the late 1920s, significant damage still occurred landward of the beach during the 1983 El Niño winter. West and East Beaches (Figure 2.5) are now nourished by the discharge of sand dredged from the harbor entrance. Without increasing the height and length of the breakwater, additional sand will probably not solve the challenges that are posed by a significant increase in sea level by 2050. Furthermore, it is unclear whether there is a source of sand that would be large enough for such a project. While a seawall can help to buffer or protect oceanfront development from wave attack over the short to intermediate-term (until 2050), this may require significant investment in the Leadbetter, harbor, West, and East Beach areas. Over the long-term (from 2050-2100), if 0.9-1.2 m (3-4 ft) of sea-level rise were to occur and the city beaches were greatly reduced in width or eliminated as buffers for the winter months, a seawall would need to be of substantial height. The lifetime of the structure, the protection that would be offered by it, and its potential costs and benefits would need to be carefully weighed against a gradual retreat, which might be the only long-term option, as sea level continues to rise.

In addition, rising sea levels and a high water table could begin to interfere with wastewater discharge and/or potentially increase flood hazards at treatment plants in low-lying areas (CCC 2009). The city's El Estero Wastewater Treatment Plant is located within 400 m (0.25 mi) of the shoreline, at a ground elevation of about 3.6-4.2 m (12-14 ft) above historic mean sea level. While it does not appear likely that the plant could be subject to flooding with a modest sea-level increase, projections show that the facility would be increasingly vulnerable over time to a 100-year flood event with 1.4 meters (4.6 feet) of sea-level rise. Thus, sea-level rise may necessitate the modification of plant facilities or operations in the coming decades.

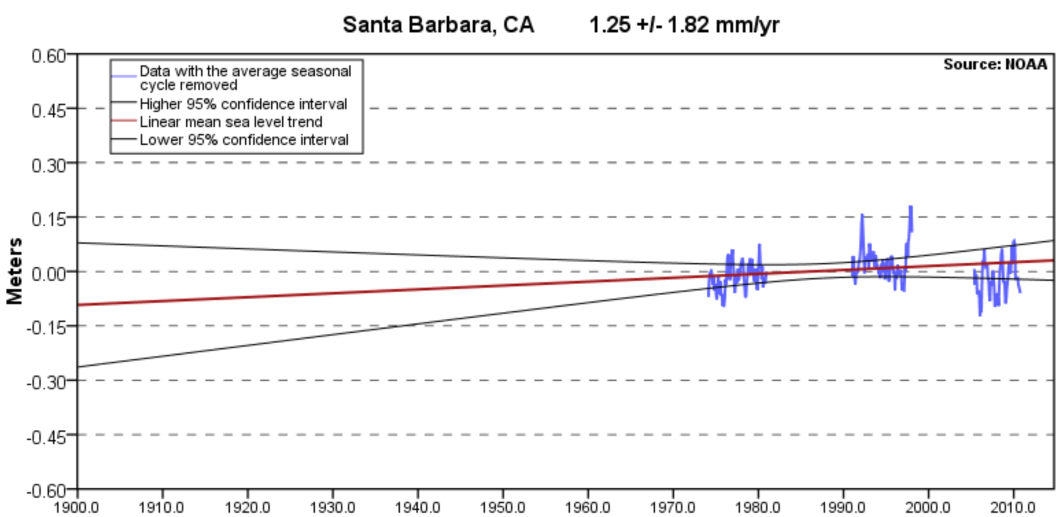

Figure 2.6 The sea-level record from Santa Barbara's tide gauge is discontinuous due to several harbor construction projects, which required relocation of the gauge (source: NOAA).

Figure 2.7 Beach erosion extended beneath the Santa Barbara Yacht Club in March 1983 (source: Santa Barbara News-Press).

Figure 2.8 Erosion removed part of the Leadbetter Beach parking lot during the 1983 El Niño.

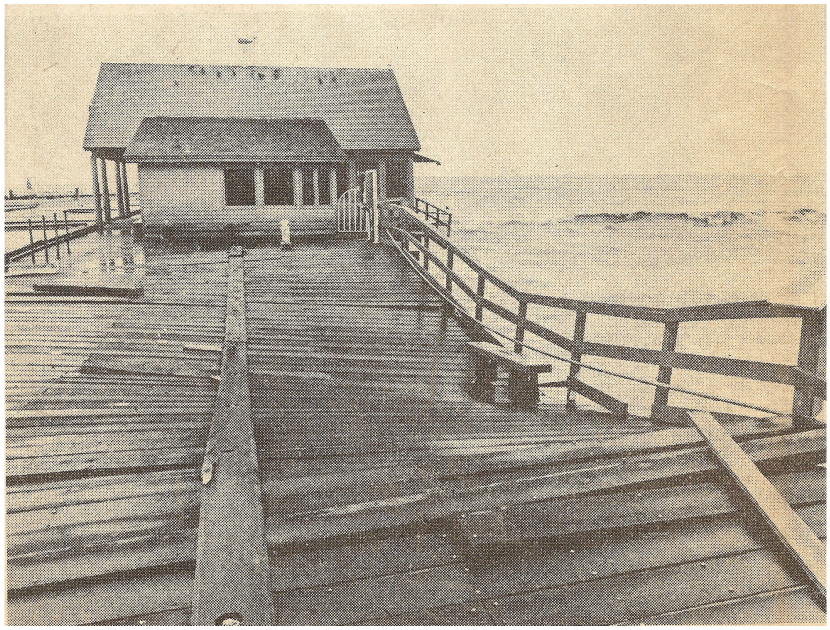

Figure 2.9 Large waves that arrived during high tide and an elevated sea level in March 1983 left Stearns Wharf sagging from a loss of pilings (source: Santa Barbara News-Press).

Figure 2.10 Palm Park, on Cabrillo Boulevard, was strewn with debris, including a picnic table that was carried in by waves that had overtopped East Beach in March 1983 (source: Santa Barbara News-Press).

Figure 2.11 Projected future coastal flood inundation maps using NOAA's 2010 LiDAR data and Google Earth. Blue lines show the present mean high water level at 4.4 feet (1.35 meters). Green lines show extent of 100-year flood (3-ft flood) on top of 2 feet of sea-level rise (NRC's most recent high sea-level rise projection relative to sea level of the year 2000) at high water, for a total elevation of 9.4 feet for the year 2050. Red lines show extent of 100-year flood (3-ft flood) on top of 5.5 feet of sea-level rise at high water for a total elevation of 12.9 feet for the year 2100. Maps show (A) Santa Barbara Harbor and surrounding area and (B) Santa Barbara's east side.

A.

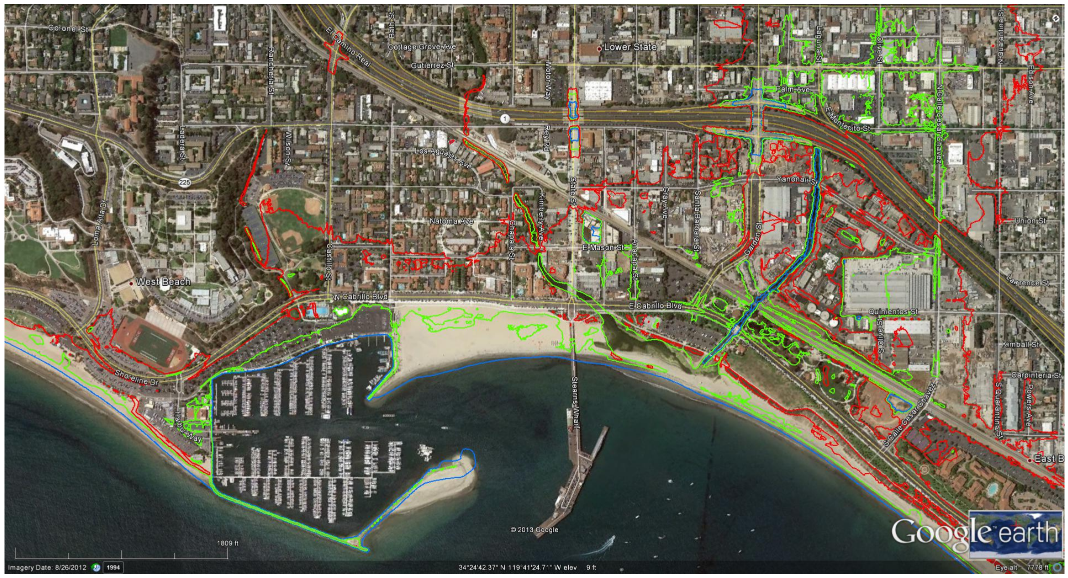

Lower State
West Beach
Google earth

B.

Waterfront
Google earth

2.4.2 Airport Flooding and Inundation

The Santa Barbara Municipal Airport, located about 13 km (8 mi) west of downtown Santa Barbara, is the largest commercial service airport on the California coast between San Jose and Los Angeles, providing a major economic benefit to the South Coast. The airport was originally built on artificial fill within and upon the margins of the Goleta Slough. As such, it is located only a few feet above sea level, much like the San Francisco and Oakland International Airports, as well as many other airports in coastal cities around the world. Because it lies in an area where five streams converge, the airport has historically been subject to flooding. In 1969, water completely surrounded the main terminal (Figures 2.2 and 2.12). In 1995 and 1998, all three runways were flooded, closing the airport for several days (Figure 2.13). Public buildings and structures are threatened by inundation during heavy rains and runway flooding poses a safety hazard, preventing planes from taking off and landing.

Even without sea-level rise, flooding will occur during intense and prolonged rainfall, which will increase runoff from the streams that drain into the Goleta Slough and combine with high tides. With a rising sea level, the frequency and magnitude of flooding in the area can be expected to increase. NOAA (2011) LiDAR data were used to update the city's 2009 flood map for the airport area. With 61 cm (24 in) of sea-level rise by 2050, a 100-year flood could reach the runways and get close to the terminals (Figure 2.14). By 2100, 1.7 m (5.6 ft) of sea-level rise would allow 100-year floodwaters to extend across the entire airport (Figure 2.14).

Thus, the probability of airport flooding is *high* in the short to intermediate-term (to 2050). If sea-level rise approaches or exceeds 1.2 m (3.9 ft) by 2100, the probability of flooding, with some permanent inundation of the site, will be *very high*. There are two areas of concern regarding short-term flooding and permanent inundation: 1] the airport terminal and parking areas and 2] the runways and associated areas for airplanes. While temporary flooding of the runways and airport parking areas will be short-term inconveniences, as they have in the past, permanent inundation presents an unacceptable risk. The adaptive capacity of the Santa Barbara Airport to future flooding and inundation in the short to intermediate-term is believed to be *moderate*. It seems possible, although very expensive, to raise the runways in order to accommodate the 100-year flood conditions for the projected high sea level of 2050. However, it appears that neither the terminal nor the runways can easily be adapted to the 100-year flood conditions of 2100 with high projected sea-level rise.

Figure 2.12 The airfield flooded in 1969 (source: Santa Barbara Airport).

Figure 2.13 The Santa Barbara Airport flooded in 1995 (source: Santa Barbara Airport).

Figure 2.14 Projected future coastal flood inundation map for the Santa Barbara Airport using NOAA's 2010 LiDAR data and Google Earth. Blue lines show the present mean high water level at 4.4 feet (1.35 meters). Green lines show extent of 100-year flood (3-ft flood) on top of 2 feet of sea-level rise (NRC's most recent high sea-level rise projection relative to sea level of the year 2000) at high water, for a total elevation of 9.4 feet for the year 2050. Red lines show extent of 100-year flood (3-ft flood) on top of 5.5 feet of sea-level rise at high water for a total elevation of 12.9 feet for the year 2100.

2.4.3 Cliff and Bluff Retreat

There are 6.4 km (4 mi) of coastal cliffs within Santa Barbara's city limits. Monterey Shale, capped by unconsolidated marine terrace deposits, comprises the majority of these cliffs, which are 15-30 m (49-98 ft) high. They are susceptible to erosion from both wave attack and terrestrial runoff and they are also prone to landslides and slumps. The bedrock is deformed and tilted throughout this area and in some places, bedding dips (tilts) towards the beach. This is highly conducive to bluff failure, in which sliding occurs along exposed bedding planes. The cliffs at both ends of the city are experiencing active erosion and retreat. Historic aerial photographs were used to determine average long-term erosion rates, which range from about 15 to 30 cm/yr (6 to 12 in/yr) (Griggs *et. al* 2005). Hapke and Reid (2007) completed a statewide assessment that compares cliff edge position on aerial photographs from the 1930s with LiDAR data from 1998 (approximately a 70-year period) and obtained similar values: an average of 10 to 46 cm/yr (4 to 18 in/yr) for the Mesa area in the west (Figure 2.4) and about 15 cm/yr (6 in/yr) for the Clarke Estate/Cemetery cliffs in the east. The range in erosion rates is a product of local variations in bedrock strength, bedding plane orientation, and the effects of development and human interference, including the placement of protective riprap on the fronting beaches. However, the overall linear trend of the bluff edge along the Mesa indicates that long-term rates of cliff retreat are fairly uniform alongshore.

Cliffs may appear to go unchanged for years until the right combination of groundwater saturation, tidal height, wave attack, and/or seismic shaking, causes episodic failure. The loss of two homes on the Mesa in 1978 illustrates how landsliding along the bluff edge can result in the nearly instantaneous loss of oceanfront property and structures. The winter of 1978 saw the first large El Niño event in years, and rainfall was heavy in Santa Barbara for several weeks prior to the slide. The Mesa failure was a typical rotational slump on a curved failure (rupture) surface, with a nearly vertical head scarp.

Google Earth was used to measure distances from the cliff edge to homes along the Mesa. There are about 98 cliff-front dwellings along the Mesa and nearly half of these are within 30 m (98 ft) of the cliff edge, while eight of them are within 15 m (49 ft). These homes were constructed at different times and setback distances from the cliff edges vary. Some homes or their additions (such as decks, patios, and other accessory structures) are located immediately adjacent to or within 5-10 m (16-33 ft) of the cliff edge (Figures 2.15 and 2.16). The proximity of a large number of homes and their additions to the cliff edge, combined with the cliff's general instability and long-term retreat rates, results in a *moderately high* vulnerability to future cliff retreat and accelerated erosion due to a rising sea level.

On January 25, 2008, Shoreline Park (on the Mesa) suffered a landslide that extended 20 m along the cliff and moved the cliff edge inland by as much as 12 m (39 ft) (Figure 2.17). Since the park's construction in the late 1960s, different sections of the cliff have retreated intermittently. As erosion has occurred, walkways, picnic tables, and fencing have been relocated inland. Progressive retreat of the cliff fronting Shoreline Park is expected to continue, possibly by an increased rate, in the future.

The cliffs that front the Clarke Estate and the adjacent cemetery on the city's east side are also subject to landsliding (Figure 2.3). Riprap was placed at the base of the bluff below the estate in the 1980s. This has reduced wave impact but it has not halted the failure of overlying materials, which appears to proceed primarily due to terrestrial processes. Below the cemetery, on the east end of the bluffs, an old concrete seawall gradually deteriorated, so riprap and some cliff-top retaining walls were constructed in its place, in an attempt to slow erosion. Many years ago, several groins were built in this area in order to trap littoral drift and widen the beach but these have also deteriorated over time and are no longer effective. Some of the gravesites that were once closest to the cliff edge have been moved back over time.

A continued rise in sea level will allow waves to attack the bases of cliffs and bluffs with an increased frequency, which will increase erosion. With average historic retreat rates between 15-30 cm/yr (6 to 12 in/yr), a loss of at least 3-6 m (10-20 ft) can be expected over the 20-year lifespan (by 2030) of *Plan Santa Barbara*. Total retreat could be higher than that in places where uncontrolled drainage, historic landslides, or adverse bedding planes exist (AMEC 2010). Over the short to intermediate-term (2012-2050), the probability of significantly increased cliff erosion rates is considered to be *moderate* (Table 2.1A). However, the probability is likely to increase substantially to *high* or *very high* over the intermediate to long-term (2050-2100; Table 2.1B). If cliff erosion rates on the Mesa remain close to their historical values or double (to 30-60 cm/yr or 12-24 in/yr), the cliff edge could retreat by 12-24 m (39-79 ft) by 2050. Such retreat would directly threaten 30 or more homes, as well as a number of secondary structures. With increased erosion rates, Santa Barbara can expect to see 24-50 m (79-164 ft) of erosion from the present cliff edge by 2100. This will affect oceanfront walkways, trails, a playground, picnic areas, and two restrooms at Shoreline Park that are located within 15 m (49 ft) of the present cliff edge.

This magnitude of retreat would threaten or necessitate the relocation or removal of about 67 cliff-top homes on the city's west side. If erosion rates increase in the future, the number of affected homes will also increase. With nearly all of the oceanfront Mesa-area homes likely to be affected by 2100, this is deemed to have a *high* impact over the intermediate to long-term timeframe (Table 2.1B). A conservative prediction here and in other similar areas is that the rate of cliff erosion will increase in the future and the rate of increase will be related to the extent of sea-level rise, as well as any changes in wave climate. The study recommends the establishment of a cliff edge monitoring program with a set of surveyed transects that can be regularly re-measured in order to document and track rates of retreat along all sea cliffs within city limits.

There are two basic approaches for adapting to cliff or bluff erosion within the city of Santa Barbara or elsewhere: armor or retreat. Because of the height of the cliffs and the typical failure mechanisms (large slumps or landslides), armoring is not likely to be an effective long-term solution. The situation along the cliffs below the Clarke Estate and the cemetery is similar to that of the Mesa. Although scattered riprap has been placed there over the years, it has been ineffective in halting cliff erosion because failure is occurring high on the cliff, as a result of terrestrial processes. While beach-level armoring is unlikely to be an effective mechanism for halting cliff erosion in this location, the land at the Clarke Estate and the cemetery is not highly developed, so retreat is a relatively easy option.

Retreat, or gradual relocation of the cliff-top homes or infrastructure, is the most effective long-term approach. The overall capacity of the city to adapt to the hazards of increased cliff retreat is *low* because there is no buffer zone or physical space to allow for retreat without relocation of structures.

Figure 2.15 Some structures along the Mesa are virtually at the cliff's edge (photo: Kenneth and Gabrielle Adelman, California Coastal Records Project).

Figure 2.16 A number of homes along the Mesa are within 15 meters (49 feet) of the cliff edge (photo: Kenneth and Gabrielle Adelman, California Coastal Records Project).

Figure 2.17 In January 2008, a landslide at Shoreline Park moved the cliff edge inland by as much as 12 meters (39 feet) and eliminated a portion of the sidewalk.

2.4.4 Inundation of Beaches

The likelihood of the inundation of city beaches (i.e. passive erosion or permanent coverage by seawater) will depend upon beach widths and elevations, as well as the future rate(s) of sea-level rise. Inundation, as opposed to short-term flooding, is defined as an essentially permanent condition. Leadbetter (Figure 2.4), West, and East beaches (Figure 2.5) have all eroded or flooded temporarily in the past, with waves reaching Cabrillo Boulevard under severe storm conditions (Figures 2.9 and 18). Over short to intermediate timeframes (i.e. 2012 to 2050), there is a *low* probability of the permanent loss of city beaches under the 36-cm (14-in) sea-level rise scenario (Table 2.1A). There may be some beach narrowing by 2050 but this is not likely to be very noticeable. An El Niño event will likely cause more beach flooding than will gradual sea-level rise but the former is a short-term phenomenon, lasting only a few days or weeks. Over the long-term (2050-2100), sea-level rise will gradually begin to cover low-lying areas that are fixed by back-beach barriers (such as seawalls, parking lots, buildings, etc.), which will eventually include all of the shoreline and beach areas closest to sea level. Seawater will reach progressively further inland as sea-level rise continues, permanently covering previously dry land. For instance, areas that would have flooded only temporarily during very high tides or El Niño conditions, such as freeway underpasses, will gradually begin to be submerged permanently. All city beaches could potentially narrow, gradually disappear, and be replaced by shallow water or wet sand at low tide by 2100. This would negatively affect tourism, beach use, and recreation. Any narrowing or loss of these beaches would progressively expose public facilities, such as the coastal bike trail, public parking lots, restrooms, and development at the Santa Barbara Harbor, Stearns Wharf, and along shoreline streets, to periodic flooding and/or increased damage from wave action. The study recommends the establishment and annual survey of a set of beach profiles along the city shoreline and a set of winter and summer profiles from Cabrillo Boulevard to the shoreline, with profile spacing of about 500 feet (150 m). This would track both seasonal and long-term changes.

The ability to adapt to the potential inundation or loss of Santa Barbara's beaches is *low* to *moderate*, depending on the particular beach in question. Allowing beaches to migrate inland and the shoreline to retreat as sea level gradually rises presents challenges for the city because there is valuable development and infrastructure along the entire back edge of the beaches, from Leadbetter to East Beach. Ultimately, park facilities and parking lots could be abandoned and the structures could be removed in order to allow the beach to migrate inland across the former shoreline. By the time that the ocean reaches Shoreline Drive, a major thoroughfare, projections for sea-level rise in the decades between 2050 and 2100 will likely have improved, such that the risks and options for adaptation can be assessed more accurately than they can be today. If Santa Barbara's beaches are to be maintained, adaptation may ultimately require removal or relocation of the facilities between the shoreline and Cabrillo Boulevard. Adaptive capacity is deemed *moderate* because most of these facilities are potentially movable.

Figure 2.18 A boat was beached against a seawall just west of Stearns Wharf during the storms of 1914.

2.5 CONCLUSIONS

Sea-level rise is becoming an increasingly significant concern to many U.S. coastal communities and state and federal agencies, especially in light of the recent devastation caused by Hurricane Sandy. A rising sea level is expected to exacerbate the effects of all coastal storms, increasing the magnitude of coastal flooding, as well as the extent and rate of cliff, bluff, and beach erosion, with associated damage to shoreline infrastructure and development. Adaptation to sea-level rise is one important local approach to minimizing future risks and damages to coastal communities.

Sea-level rise adaptation is still an emergent concept, so there are few case studies and scarce information for city planners and coastal managers who want to begin the processes of assessing local vulnerability, performing risk analyses, and formulating and implementing their own adaptation plans. *Adapting to Sea-Level Rise: A Guide for California's Coastal Communities* (Russell and Griggs 2012) is a resource that should aid coastal communities both in and outside of California during the organization and management stages of their efforts to plan for sea-level rise.

The city of Santa Barbara has taken a critical first step towards sea-level rise adaptation by addressing these issues in its 2011 General Plan update and Environmental Impact Report, as well as in its 2012 Climate Action Plan, which incorporates data collection and adaptation planning recommendations from the *City of Santa Barbara Sea-Level Rise Vulnerability Study*. Furthermore, the city has applied for the California Coastal Commission's Local Coastal Program Assistance

Grant Program to update its Local Coastal Program to reflect the expected impacts of climate change, including sea-level rise.

It will be very useful for Santa Barbara and other coastal communities to publicize the results of their adaptation planning and to share them not only with local government staff, elected officials, and the public but also with other coastal communities, which face common issues related to sea-level rise and could benefit from the experience and insight.

2.6 REFERENCES

AMEC Earth & Environmental Inc. (2010), *Proposed Final Program Environmental Impact Report for the Plan Santa Barbara General Plan Update.* Santa Barbara, California, 762 pp.

Committee on Sea-Level Rise in California, Oregon, and Washington; Board on Earth Sciences and Resources; Ocean Studies Board; Division on Earth and Life Studies; National Research Council (2012), *Sea-level rise for the coasts of California, Oregon, and Washington: Past, present, and future*. Washington, DC: National Academies Press, 275 pp. http://www.nap.edu/catalog.php?record_id=13389

Department of Commerce, National Oceanic and Atmospheric Administration, National Ocean Service, Coastal Services Center (2011), *2009-2011 CA Coastal Conservancy Coastal Lidar Project*. NOAA's Ocean Service, Coastal Services Center (CSC).

Finzi Hart, J.A., P.M. Grifman, S.C. Moser, A. Abeles, M.R. Myers, S.C. Schlosser, and J.A. Ekstrom (2012), Rising to the Challenge: Results of the 2011 coastal California adaptation needs assessment. USCSG-TR-01-2012.

Griggs, G.B. (2010). *Introduction to California's beaches and coast*. University of California Press: 311 pp.

Griggs, G.B., K.B. Patsch, and L.E. Savoy (2005). *Living with the changing California coast*. University of California Press: 540 pp.

Griggs, G.B., and N.L. Russell (2012), *City of Santa Barbara Sea-Level Rise Vulnerability Study*. Sacramento, California: California Energy Commission, Public Interest Environmental Research Program, 87 pp.

Hapke, C.J., and D. Reid (2007), National assessment of shoreline change part 4: Historical coastal cliff retreat along the California coast, USGS Open File Report, 2007-1133, 51 pp. http://pubs.usgs.gov/of/2007/1133/

Hapke, C.J., D. Reid, B.M. Richmond, P. Ruggiero, and J. List (2006), National assessment of shoreline change part 3: Historical shoreline change and associated coastal land loss along sandy shorelines of the California coast, USGS Open File Report, 2006-1219, 72 pp. http://pubs.usgs.gov/of/2006/1219/

Heberger, M., H. Cooley, P. Herrera, P.H. Gleick, and E. Moore (2009), *The impacts of sea-level rise on the California coast*. The Pacific Institute, 99 pp. www.pacinst.org/reports/sea_level?rise/report.pdf

King, P.G., A.R. McGregor, and J.D. Whittet (2011), The economic costs of sea-level rise to California beach communities, California Department of Boating and Waterways and San Francisco State University, 97 pp. http://www.dbw.ca.gov/PDF/Reports/CalifSeaLevelRise.pdf

National Oceanic and Atmospheric Administration (2010), *Adapting to climate change: A planning guide for state coastal managers*. NOAA Office of Ocean and Coastal Resource Management, 138 pp. http://coastalmanagement.noaa.gov/climate/docs/adaptationguide.pdf

Russell, N.L, and G.B. Griggs (2012), *Adapting to sea-level rise: A guide for California's coastal communities.* Sacramento, California: California Energy Commission, Public Interest Environmental Research Program, 52 pp.

CHAPTER THREE

Can El Niño-Southern Oscillation Forecasts be Improved Using U.S. West Coast Significant Wave Heights?

3.1 ABSTRACT

Most of the flooding and erosion along the U.S. West Coast are caused by storm surges and wind-driven waves, particularly during strong El Niño events. There is a need to predict El Niño occurrences for coastal planning purposes, but forecasts from most of the best El Niño Southern Oscillation (ENSO) prediction models have plateaued at a moderate level. Ample room remains for improvement in ENSO observing systems, models, and data assimilation methods. In particular, current coupled forecasts suffer from both a lack of observational data for sufficient model initialization and an inability to make effective use of available data. Additionally, gaps in observing systems and the recent failure to properly maintain the Tropical Atmosphere Ocean array (TAO) have also been detrimental to current ENSO forecasting systems. Thus, it makes sense to explore existing oceanographic data that have not traditionally been used for ENSO prediction to determine their potential for enhancing predictions. While the effects of ENSO on wave heights along the U.S. West Coast are relatively well known, no prior studies have examined whether wave heights are also predictive of the phenomenon. This study finds that significant wave heights (H_{sig}) along the U.S. West Coast are slightly suppressed during the summers preceding El Niño winters, but the trend is weak and the data are noisy, so contributions to ENSO forecasts are negligible. The summer H_{sig} trend is strongly associated with the summer North Pacific (NP) Index, which measures the area-weighted sea-level pressure over the region 30˚N to 65˚N, 160˚E to 140˚W, in the Gulf of Alaska.

3.2 INTRODUCTION

3.2.1 Long-Term Sea-Level Rise vs. Short-Term Regional Sea Level Variation along the U.S. West Coast

A recent report by the National Research Council (2012) estimates that sea level could rise along the U.S. West Coast by 12 to 61 cm south of Cape Mendocino and -3 to 48 cm north of Cape Mendocino (Figure 3.1) by the year 2050 (using year 2000 sea level as baseline). This will present challenges to coastal communities, including the inundation of low-lying land areas and the amplification of storm surges and high waves (Heberger et al. 2009 and 2011). However, these changes are expected to occur gradually, whereas short-term climate fluctuations, such as the El Niño Southern Oscillation (El Niño), can temporarily raise regional sea levels significantly—by 10 to 30 cm [through a combination of increased ocean temperatures (steric), shifts in the Ekman transport of surface waters, and the transmission of coastally-trapped Kelvin waves] for several months (Figure 3.2); these effects are likely to be exacerbated by long-term sea-level rise (Enfield and Allen 1980; Chelton and Davis, 1982; Huyer and Smith 1985; Flick 1998; Ryan and Noble 2002; Bromirski et al. 2003; Allan and Komar 2006; Komar et al. 2011).

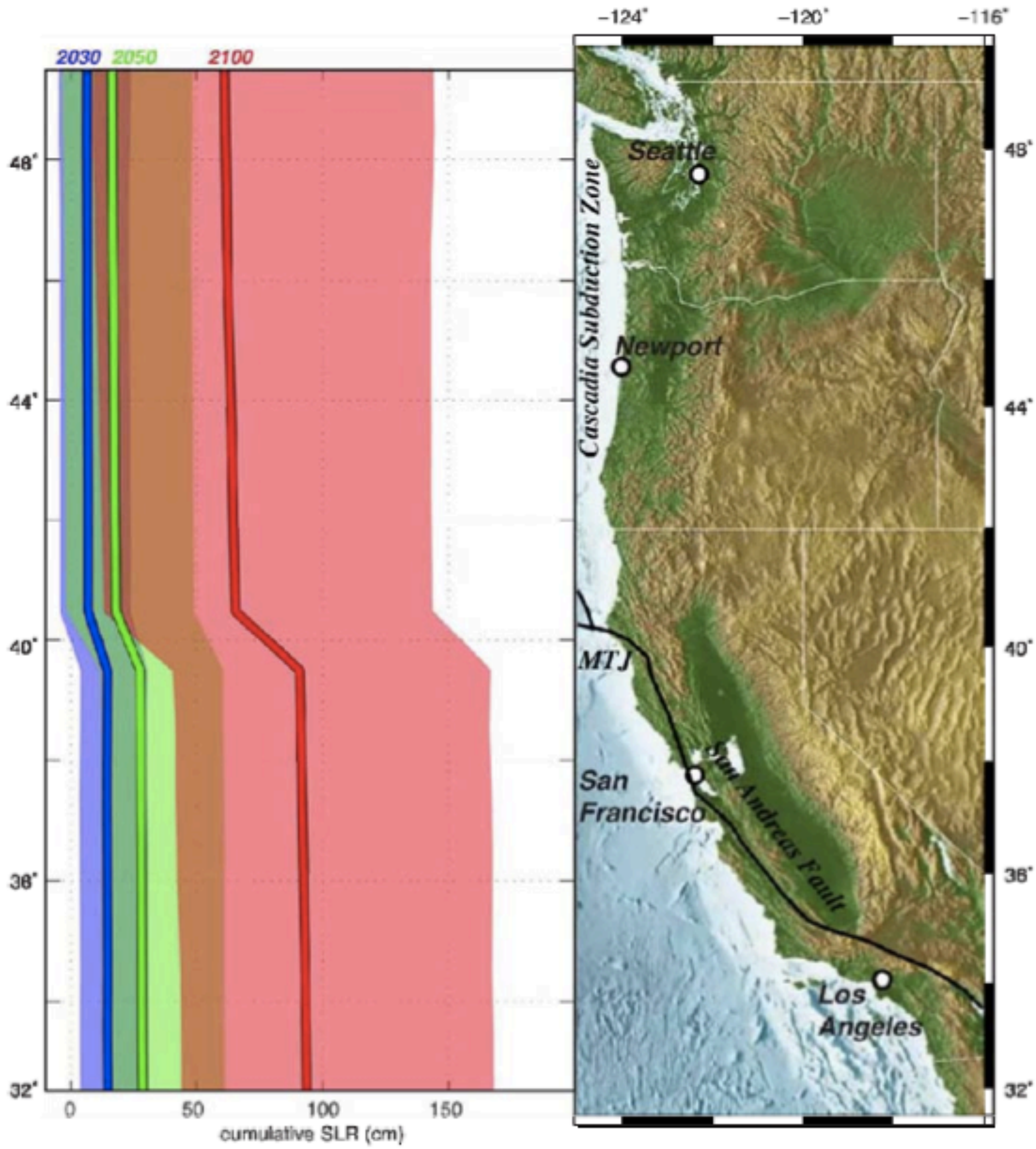

Figure 3.1 The National Research Council's most recent sea-level rise projections for California, Oregon, and Washington, as a function of latitude. Solid lines represent projections and shaded areas represent ranges, which overlap (brown and blue-green). Blue represents projections for 2030, green represents projections for 2050, and pink represents projections for 2100, all relative to the year 2000. "MTJ" stands for the Mendocino Triple Junction, where the San Andreas Fault meets the Cascadia Subduction Zone (from NRC 2012).

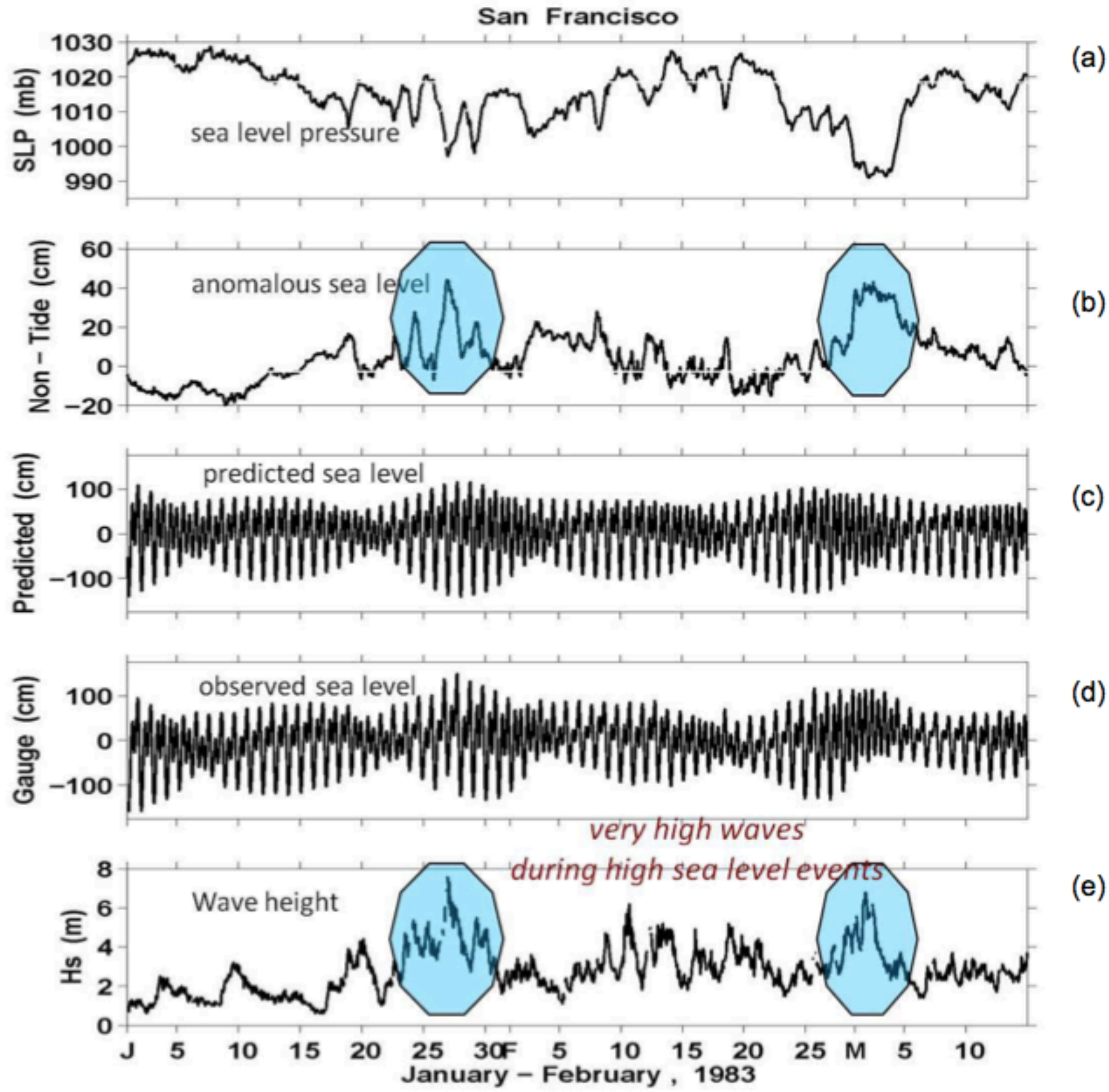

Figure 3.2 (a) Hourly sea-level pressure, (b) sea-level anomaly above tide predictions, (c) predicted and (d) observed sea level relative to a mean sea-level datum, and (e) significant wave height (the average height of the highest one-third of waves) from a buoy near San Francisco during the El Niño winter of 1983 (from NRC 2012).

3.2.2 El Niño Southern Oscillation (ENSO) and Detrimental Impacts of Major Events on the California Coastline and Worldwide

The El Niño Southern Oscillation (ENSO) is a pattern of climate variability that occurs across the tropical Pacific Ocean and atmosphere quasi-periodically, about every two to seven years. It is characterized by two extremes: El Niño and its opposite phase, La Niña. During a typical El Niño, a maximum warm sea surface temperature (SST) anomaly occurs in the eastern Pacific, accompanied by relatively high air surface pressures in the western Pacific. ("Southern Oscillation" refers to the reversal in air surface pressure between the eastern and western tropical Pacific.) In addition to raising regional sea levels along the U.S. West Coast, El Niños also affect predominant storm tracks in the North Pacific, thereby altering regional wave climates temporarily (Storlazzi and Griggs 2000; Graham and Diaz 2001; Allan and Komar 2002). Major El Niños, such as the 1982-83 and 1997-98 events, displace the predominant winter extratropical storm tracks from their usual positions over the Pacific Northwest coast of Oregon and Washington to the south (Seager et al. 2010). This both increases wave energy off the coast of California and causes waves to approach the California coastline from a more southerly direction than usual, which can reverse net littoral sediment transport and enhance the erosion of sea cliffs at the southern ends of headland-bounded littoral cells (Kaminsky et al. 1998; Sallenger et al. 2002; Allan and Komar 2006). It can also enhance the erosion of beaches that are normally protected from dominant waves from the northwest (Griggs and Brown 1998).

The impacts of the most recent extreme El Niños on the California coast are well documented. For instance, during the winter of 1983, the California coast suffered over $213 million in damage (2013 dollars), including the complete destruction of 33 oceanfront homes and damage to more than 3,000 homes and businesses, due to the combination of elevated water levels (Figure 3.2) and a series of large storms that arrived during high astronomical tides (Griggs et al. 2005). At one point during the 1982-83 event, sea levels were the highest ever recorded in San Diego, Los Angeles, and San Francisco (29.0, 32.3, and 53.8 cm above predicted high tides, respectively), and low-lying areas were flooded due to a combination of heavy rainfall and high sea levels, which also increased the level of wave action on beaches and bluffs (Storlazzi and Griggs, 2000). Given that most of the flooding and erosion along the U.S. West Coast are caused by storm surges and wind-driven waves, particularly during strong El Niño events, the ability to predict the occurrence of El Niño is highly valuable for coastal planning purposes (Allan and Komar 2006).

ENSO also affects other regions of the world considerably, triggering disastrous floods in places like Peru and Ecuador and causing sizable droughts in Indonesia, Africa, Australia, and India. Additionally, the phenomenon has been tied to severe winter weather in Europe, abnormal monsoon dynamics in eastern Asia, incidences of epidemic diseases in various locations, and the intensity of tropical cyclones, including hurricanes in the Caribbean (Wen 2002; Kovats et al. 2003; Brönnimann et al. 2004; Donnelly and Woodruff 2007; Corral et al. 2010). Strong El Niño events have even been implicated in the fates of entire societies. Mike Davis'

2001 book, "Late Victorian Holocausts: El Niño Famines and the Making of the Third World," examines the relevant late 19th-century droughts in India, China, and Brazil that resulted in the deaths of 30 to 50 million people.

3.2.3 El Niño Southern Oscillation (ENSO) Prediction Models: A Brief History

After the disastrous 1982-83 El Niño event took scientists by surprise, the National Oceanographic and Atmospheric Administration (NOAA) collaborated with the international community to test and deploy a moored array to monitor the temperature of the upper layer of the tropical Pacific Ocean (to a depth of 500 meters) and the atmospheric conditions above it, providing real-time measurements. By 1994, the Tropical Atmosphere Ocean array (TAO) included nearly 70 moorings (Figure 3.3), which, along with satellite data and computer models, have contributed to major progress in the observation and theory of ENSO, playing a crucial role in the prediction of subsequent events (Latif et al. 1998; McPhaden et al. 1998; Neelin et al. 1998).

Many ENSO models depend on the low-dimensional nature (i.e. just a few distinctive modes) of the coupled instability of the tropical Pacific's ocean-atmosphere system, taking into account its two basic elements: (1) the positive feedback between the zonal winds resulting from the seesawing (Southern Oscillation) of atmospheric mass between the eastern and western Pacific (which sets up sea-level pressure gradients) and the equatorial sea surface temperature (SST) gradient (which is powered by wind-driven upwelling and thermocline fluctuation), and (2) the dynamics of the equatorial Pacific, with non-dispersive and out-of-phase Kelvin and Rossby waves allowing for oscillation between warm (El Niño) and cold (La Niña) phases (Bjerknes 1969; Zebiak and Cane 1987; Battisti and Hirst 1989; Cane et al. 1990; Jin 1997; Chen and Cane 2008). One such representation, the Zebiak-Cane (or LDEO) model, a dynamical ocean-atmosphere coupled system of intermediate complexity, is the first to have successfully forecasted El Niño (the 1986-87 event) in real time (Cane and Zebiak 1985; Cane et al. 1986; Zebiak and Cane 1987). The mid-1980s saw a few other attempts to forecast El Niño, including statistical models (Graham et al. 1987; Xu and Storch 1990) and a standalone ocean model (Inoue and O'Brien 1984), although the standalone system only predicts the onset of El Niño because it ignores feedbacks between the ocean and the atmosphere (Chen and Cane 2008). A case study (Barnett et al. 1988) reviewing the performances of three different classes of numerical models shows that the 1986-87 El Niño was effectively predicted at lead times of three to nine months.

Since those early successes of the mid-1980s, numerous ENSO prediction models with varying levels of complexity were developed. They mainly fall into three categories (Chen and Cane 2008):

- *Fully physical ocean-atmosphere coupled models*: Generally considered to be at the top of the hierarchy, these models treat the atmosphere and the ocean as different types of fluids, and their behaviors are described by complex systems of differential equations. Models range from intermediate coupled versions of the "shallow water" type, with simplified physics (Cane et al. 1986; Kleeman

1991), to coupled general circulation models (Ji et al. 1994; Kirtman et al. 1997).

- *Purely statistical models*: These models derive statistical relationships from past El Niño occurrences. Most of the frameworks use linear regression, in which matrix operations maximize the association between or covariance of the chosen predictor (atmospheric—sea-level pressure or surface wind, oceanic—sea surface temperature or a measure of upper ocean heat content, or a combination of oceanic and atmospheric quantities) and predictand fields (Graham et al. 1987; Xu and Storch 1990; Barnston and Ropelewski 1992), but there are also nonlinear models based on artificial neural networks that can adapt and recognize patterns (Tang et al. 1997) and self-evolving Markov models (Xue et al. 2000). While these systems are computationally efficient, especially with respect to fully physical ocean-atmosphere coupled models, the timespan of oceanic and atmospheric observations is short, and purely statistical models do not describe the physics of the phenomena, so their predictions are limited in accuracy.
- *Physical ocean-statistical atmosphere hybrid models*: Hybrid models take advantage of both the accuracy of physical ocean models and the computational efficiency of statistical frameworks (which are used to represent the atmosphere). Specifically, such a system links the SST field of a given physical ocean model to the surface wind field driving the model with a statistical relationship (Neelin 1990; Barnett et al. 1993). These models

assume that the coupled system's memory is contained solely within the ocean's thermocline state (with the ocean also containing the limiting nonlinearity of the structure), with the atmosphere responding instantaneously to SST changes, as the fast component of a stiff system. For most purposes, the latter assumption works for timescales that are longer than one season, and it is largely applicable to ENSO if the importance of high frequency, internal atmospheric variability is discounted (Neelin et al. 1994). This is due to the fact that the atmospheric response to SST is rapidly redistributed vertically (especially in convective regions) and is nonlocal horizontally on timescales longer than dynamical adjustment times (a few days to a month), whereas the ocean responds on a wide range of timescales, from days (as with some features of the mixed layer) to millennia (as with deep-ocean thermal adjustment).

A review by Latif et al. (1998) concludes that models from each of the above categories are useful for predicting typical ENSO indices at 6-12 month lead times. For lead times of six months or fewer, the skills of statistical models are comparable to those of fully physical coupled models, but the latter appear to have the edge for long lead times (Barnston et al. 1994).

Kirtman et al. (2002) also examined one statistical and six dynamical prediction systems (all state-of-the-art for the time) using relatively consistent evaluation metrics and long periods of retrospective forecasts of sea surface temperature anomalies in the NINO3 area (150˚-90˚W, 5˚S-5˚N) of the tropical

Pacific. The study again showed that both statistical and dynamical models are skilled in forecasting the peak phase of ENSO up to two seasons in advance, but it also discovered that, due to errors in both the initial conditions and the models themselves, a forecast developed as a consensus of at least three separate prediction systems is far more reliable than any one individual model. Although both the statistical and dynamical models are useful for forecasting the peak phases of the extreme warm and cold ENSO phases, their predictive skills are time-dependent. That is to say that none of the frameworks sufficiently capture the detailed life cycle of the different ENSO phases and none are especially skilled in predicting the timing of the initialization of El Niño events (Kirtman et al. 2002). For instance, researchers who examined forecasts from a large number of models concluded that none were able to predict the entirety of the large 1997-98 El Niño (Barnston et al. 1999; Landsea and Knaff 2000).

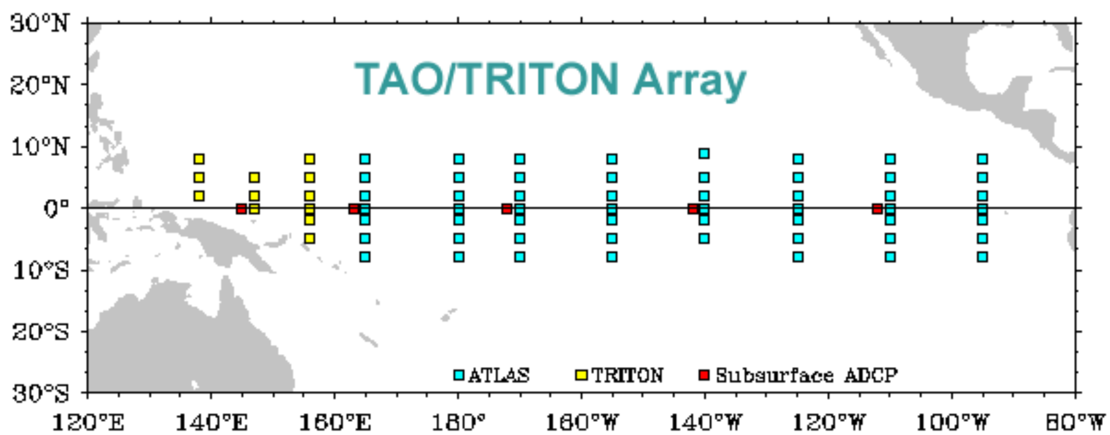

Figure 3.3 Locations of buoys in the Tropical Atmosphere Ocean array; yellow boxes represent buoys maintained by the Japan Agency for Marine-Earth Science and Technology (JAMSTEC), and blue boxes represent US instruments (from NOAA).

3.2.4 El Niño Southern Oscillation (ENSO) Prediction: The Current State and Challenges

Today, the periods of retrospective forecasting are mostly too short (about 1-3 decades, covering a relatively small number of ENSO events, so there are few degrees of freedom) to adequately distinguish between the skills of various ENSO prediction models and confidently estimate how well we are able to forecast ENSO overall (Kirtman et al. 2002). The lack of observational data for sufficient model initialization is mostly to blame, as even small errors in the initial conditions can compound and change forecast results significantly, but the inability of current models to make effective use of available data is also problematic (Chen and Cane 2008).

A recent (2004) unprecedented, retrospective (covering 148 years) forecast experiment by Chen et al. was able to predict most of the warm and cold ENSO events at a six-month lead time, using only reconstructed SST data for model initialization. The model was especially good at forecasting large El Niño and La Niña events, but it had trouble predicting small events and no-shows. These outcomes are representative of the current status of ENSO forecasting, despite vast differences in the complexity of present-day models (for operational predictions by many research groups worldwide, see the quarterly Experimental Long lead Forecast Bulletin at http://www.iges.org/ellfb/ and the International Research Institute for Climate and Society's forecast website at http://iri.columbia.edu/our-expertise/climate/forecasts/enso/), which exhibit comparative predictive skills and seem to have plateaued at a moderate level, making real-time forecasts that do not appear to be more skillful than those made years ago (Barnston et al. 1999; Chen and Cane 2008).

According to a review of the present status of ENSO prediction and predictability studies by Chen and Cane (2008), the current skill of ENSO forecasting is limited by four factors: inherent limits to predictability, gaps in observing systems, model flaws, and suboptimal use of observational data. While the inherent limits to predictability have been debated, increasing evidence suggests that those limits have yet to be reached, leaving room for improvement in our observing systems, models, and data assimilation methods (Chen and Cane 2008). Already, researchers have made great strides in all of those areas since the early days of ENSO forecasting: data from observation networks, including the TAO array and satellite altimetry and scatterometry, have been invaluable for ENSO monitoring and have significantly improved ENSO prediction skill at multi-season lead times (Ji and Leetma 1997; McPhaden 1999; Clarke and Van Gorder 2003; McPhaden 2003); regional and global models of differing levels of complexity have continuously improved in their physics and computational capabilities; and various data assimilation and forecasting strategies have been developed and employed in operational ENSO prediction (Chen and Cane 2008).

Unfortunately, recent (2012) budget cuts at NOAA have kept the TAO array from being properly maintained, causing nearly half of the buoys to fail in the last two years and partially blinding us to early El Niño development in the tropical

Pacific (Figure 3.4). Scientists are now collecting data from only 40% of the array (Tollefson 2014). Nearly all of the initial ENSO forecasts for this year (2014) suggest that a moderate to severe El Niño or neutral conditions will appear in the coming months, so researchers are trying to see whether warm water will continue to flow eastward across the tropical Pacific toward South America (Figure 3.5). Although NOAA has promised to restore most of the TAO array by the end of 2014, the timing will be well after critical El Niño forecasts are (or ought to have been) released (Tollefson 2014). For now, researchers will have to supplement the TAO data with satellite observations of water temperature and sea level, which can serve as stand-ins for the depth of the wave of warm water moving across the tropical Pacific.

Despite the recent setbacks in ENSO forecasting, it appears as though researchers are still making headway. For instance, Ludescher et al. (2014) developed an alternative forecasting approach (Ludescher et al. 2013) based on complex network analysis (Tsonis et al 2006; Yamasaki et al. 2008; Donges et al. 2009; Gozolchiani et al. 2011) for predicting the occurrences of El Niño events by about one year in advance, thus overcoming the "spring barrier" (Webster 1995; Goddard et al. 2001) that has prevented other models from detecting El Niño events by more than six months in advance (during the boreal spring, anomalies that develop randomly in the western Pacific reduce the signal-to-noise ratio for the dynamics relevant to ENSO, making it difficult to predict across the barrier). Ludescher et al.'s 2014 univariate model links current daily surface atmospheric temperatures at grid points of a Pacific network (Figure 3.6) to future sea surface temperatures at grid points both inside and outside of the “El Niño basin” (comprised of the NINO1, NINO2, NINO3, and NINO3.4 regions plus one grid point south of the NINO3.4 region, as in Yamasaki et al. 2008 and Gozolchiani et al. 2011), based on Ludescher et al.’s 2013 findings, which indicate that El Niño is a cooperative phenomenon, wherein teleconnections between the El Niño basin and the rest of the Pacific tend to build up during the year prior to an El Niño event (the study examines the time evolution of the teleconnections between pairs of grid points, as opposed to the time dependence of climate records at single grid points). By the ends of the years 2011 and 2012, the model correctly predicted the absences of El Niño events in 2012 and 2013, respectively. Such results are not trivial, given that as late as August of 2012, the Climate Prediction Center/International Research Institute (CPC/IRI) for Climate and Society Consensus Probabilistic ENSO forecast, which focuses on the SSTs in the NINO3.4 area (Figure 3.6), predicted a 4-in-5 likelihood for an El Niño event in 2012, which turned out to be incorrect just a few months after the prediction was made (to view archived forecasts, visit http://iri.columbia.edu/our-expertise/climate/forecasts/enso/ and http://www.cpc.ncep.noaa.gov/products/analysis_monitoring/enso_advisory/). By September of 2013, Ludescher et al.’s 2014 model already forecasted the return of El Niño in late 2014 with a 3-in-4 likelihood, while the CPC/IRI Consensus Probabilistic ENSO forecast predicted only a 1-in-5 likelihood at the same time, which increased to a 1-in-3 likelihood by November of 2013. Because Ludescher et al.’s method is based entirely on high-quality instrumental readings that are easily accessible, the results of their studies (2013; 2014) can be reproduced in a straightforward manner, standing in contrast to the outputs of algorithms that make use of model data. If the method turns out to be sound, it would be a major improvement to ENSO forecasting and the understanding of ENSO dynamics.

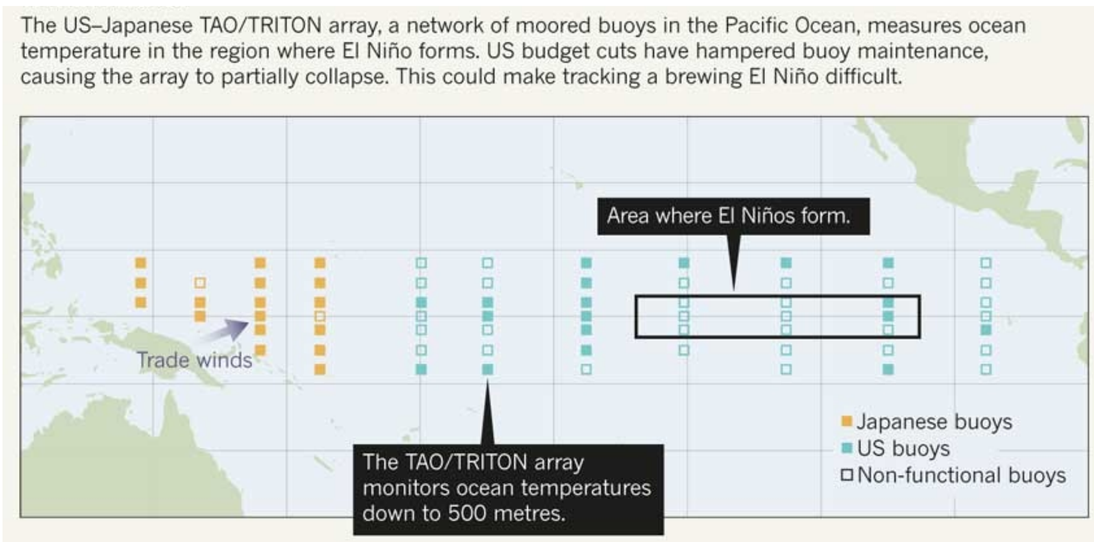

Figure 3.4 Locations of buoys in the Tropical Atmosphere Ocean array that are non-functional due to budget cuts at NOAA; open blue boxes represent non-functional U.S. buoys (modified from Tollefson 2014; originally from NOAA).

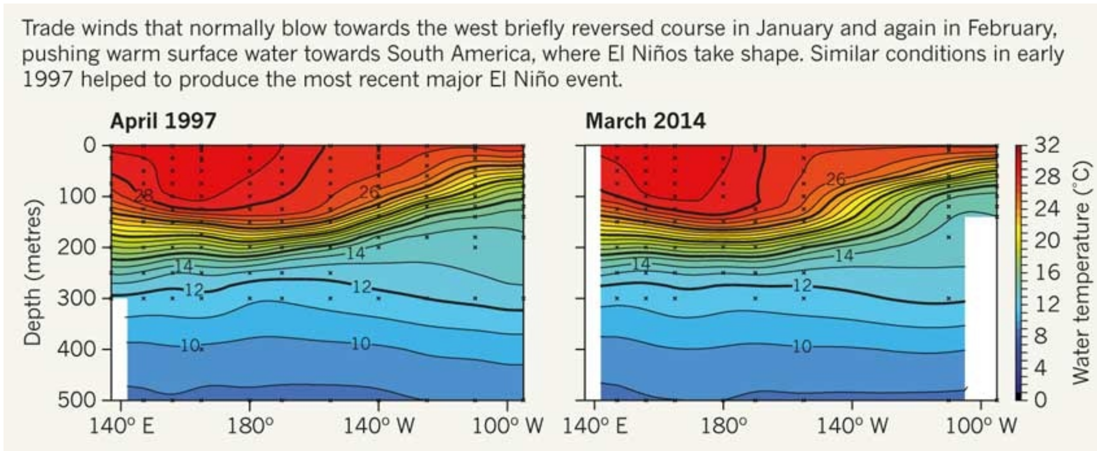

Figure 3.5 Warm surface waters have been moving eastward across the tropical Pacific early since 2014, which resemble the conditions in early 1997 that preceded one of the largest El Niños; if these conditions persist, another moderate to severe El Niño could develop (modified from Tollefson 2014; originally from NOAA).

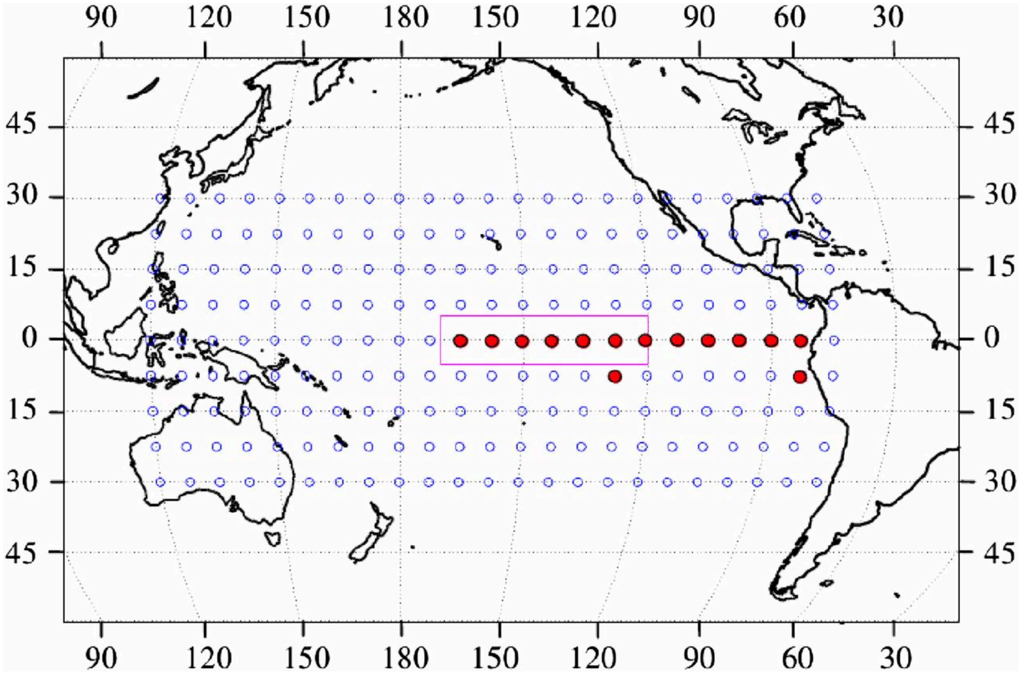

Figure 3.6 Locations of grid points (nodes) in the climate network used by Ludescher et al. (2013; 2014) to predict El Niño events by about one year in advance, based on dynamic fluctuations of the teleconnections (links in the network) between grid points in the El Niño basin and the rest of the Pacific. The network includes 14 nodes in the El Niño basin (denoted by solid red dots) and 193 nodes outside of the basin (denoted by blue circles). Each node inside of the basin is linked to each node outside of the basin. The strengths of the links are determined by cross-correlations between the observed sea-surface-level air temperatures in the grid points. The magenta box indicates the area where the NINO3.4 index is measured. The NINO3.4 index tracks and quantifies the ENSO phenomenon and is defined as the average of the sea surface temperature anomalies at the grid points located within the box. An El Niño episode is said to occur when the index is above 0.5˚C for at least five consecutive months (from Ludescher et al. 2013).

3.2.5 El Niño Southern Oscillation (ENSO) Prediction: U.S. West Coast Significant Wave Heights (H_{sig})

While it is well established that wave heights along the U.S. West Coast are affected by ENSO (as described in section 3.2.2), no one has yet attempted to determine whether wave heights are also predictive of the phenomenon. Although the predictions of most purely statistical models have been limited in accuracy because of their inability to describe the physics of the ocean-atmosphere system, the short timespan of oceanic and atmospheric observations, and the lack of freedom to tweak parameters (as opposed to the freedom of coupled models), the recent promise of Ludescher et al.'s 2014 statistical model suggests that it may be possible to obtain reliable ENSO predictions from purely statistical frameworks.

This paper seeks to determine whether significant wave heights (H_{sig}) along the U.S. West Coast can provide a predictive lead on El Niño, using data from NOAA's National Data Buoy Center (NDBC, at http://www.ndbc.noaa.gov/) and Scripps Institution of Oceanography's Coastal Data Information Program (CDIP, at http://cdip.ucsd.edu/). The potential for H_{sig} to predict El Niño by itself is examined, but because current coupled forecasts suffer from both a lack of observational data for sufficient model initialization and an inability to make effective use of available data (Chen and Cane 2008) and because generally, consensus forecasts are far more skillful than individual models (Kirtman et al. 2002), this study also examines H_{sig} in combination with an established ENSO index to see whether the addition of H_{sig} data can improve its predictions. Gaps in observing systems and the recent failure to maintain the TAO array have been detrimental to current ENSO forecasting systems, as well (Chen and Cane 2008; Tollefson 2014), so it makes sense to explore existing oceanographic data that have not traditionally been used for ENSO prediction in this novel way.

3.3 METHODS

Two sources of buoy data collected from off the U.S. West Coast are employed in this study (Table 3.1): NOAA's National Data Buoy Center (NDBC, at http://www.ndbc.noaa.gov/) and Scripps Institution of Oceanography's Coastal Data Information Program (CDIP, at http://cdip.ucsd.edu/). The NDBC's offshore deep-water buoys record hourly oceanographic and atmospheric data, including significant wave height (H_{sig}). The CDIP buoys also record hourly oceanographic and atmospheric data now, including H_{sig}, but the number of records increased from 4 to 8 times per day during the 1980's and again in 1996 to 24 times per day.

Due to buoy failures and maintenance operations, both the NDBC and CDIP datasets have dropouts that range from weeks to years (Appendix A and Supplemental File 3), although the latter case is most common amongst the CDIP buoys. For this reason, each dataset was normalized using the cumulative distribution function for one of the analyses (as noted in section 3.3.3). Also, only datasets containing relevant information from at least 15 of the seasons of interest were included in the analyses (seasons are from consecutive years wherever possible but in all cases, the 15-season threshold is high enough to sample El Niño conditions). In other words, NOAA buoy 46027 was included in both the summer (defined in this study as June through August) and autumn (September through November) H_{sig} analyses because its record contains H_{sig} data from at least 15 summers and at least 15 autumns. Data from 2013 and 2014 were not included in any of the analyses because the NDBC did not release its 2013-2014 data by the time this study was conducted and the 2013 CDIP data were incomplete prior to the analyses (the 2013 calendar year had not yet drawn to a close by this study's completion).

Where possible, open-ocean buoys were selected preferentially (Figure 3.7A) to avoid picking up the effects of interference with the waves. However, the open-ocean requirement significantly reduces the number of available buoys off the coast of Southern California, due to the relatively small number of stations located offshore of the Southern California Bight. Thus, some of the buoys that might be affected by the islands and banks in the bight were included in the analyses (Figure 3.7B).

For the purpose of El Niño prediction, El Niño summers and autumns are those preceding El Niño winters. Thus, for the 1997-1998 El Niño, only data from the summer and autumn of 1997 were considered to be subject to El Niño conditions, whereas data from the summer and autumn of 1998 were not. El Niño years and relative El Niño strengths were identified using the Multivariate ENSO Index (MEI, at http://www.esrl.noaa.gov/psd/enso/mei/; Figure 3.8), which combines the six main observed variables over the tropical Pacific: sea-level pressure, zonal and meridional components of the surface wind, sea surface temperature (SST), near-surface air temperature, and total cloudiness fraction of the sky (Wolter and Timlin 1993, 1998, and 2011). Since the MEI incorporates more information than other indices (such as SST indices or the Southern Oscillation Index, which is based on observed sea-level pressure differences between Tahiti and Darwin, Australia), it is a better reflection of the nature of the coupled ocean-atmosphere system than single-component indices.

The multiple components of the MEI also decrease its vulnerability to intermittent data dropouts in its monthly update cycles.

Table 3.1: *Buoy locations and historical significant wave height record lengths (not including breaks, which are presented in detail for summers and autumns through 2012 in Appendix A). Red numbers indicate that a station was disestablished.*

Region	Source	Buoy	Station	Latitude N.	Longitude W.	Water Depth (m)	Wave Height Record (yrs)
Washington	NDBC	Cape Elizabeth	46041	47°20'58"	124°42'30"	114.3	1987-2013
		Columbia River Bar	46029	46°9'32"	124°30'52"	144.8	1984-2013
	CDIP	Grays Harbor	36	46°85'81"	124°24'39"	38.5	1981-2014
	NDBC	West Washington	46005	46°5'59"	131°0'5"	2,981	1976-2012
Oregon	NDBC	Stonewall Bank	46050	44°38'20"	124°32'2"	128	1991-2013
		West Oregon	46002	42°35'21"	130°28'28"	3,444	1975-2013
Northern California	NDBC	St Georges	46027	41°51'1"	124°22'52"	48	1985-2013
		Southeast Papa	46006	40°45'16"	137°27'51"	4,151	1977-2013
		Eel River	46022	40°43'25"	124°34'41"	674	1982-2013
		Pt Arena	46014	39°14'6"	123°58'26"	256	1981-2013
Central California	NDBC	West California	46059	38°2'49"	129°58'8"	4,627	1994-2012
		Bodega Bay	46013	38°14'31"	123°18'2"	116	1981-2013
		San Francisco	46026	37°45'18"	122°50'21"	53	1982-2013
		Half Moon Bay	46012	37°21'45"	122°52'52"	208	1980-2013
		Monterey	46042	36°47'7"	122°28'9"	2,098	1987-2013
		Cape San Martin	46028	35°44'29"	121°53'3"	1,158	1983-2013
Southern California	CDIP	Diablo Canyon	76	35°12'23"	120°51'56"	23	1983-2014
	NDBC	Santa Maria	46011	35°0'0"	120°59'30"	412	1980-2013
		Point Arguello	46023	34°42'50"	120°58'0"	384	1982-2010
	CDIP	Harvest	71	34°27'48"	120°46'9"	549	1995-2014
	NDBC	West Santa Barbara	46054	34°16'28"	120°27'42"	460	1994-2013
		East Santa Barbara	46053	34°14'52"	119°50'28"	450	1994-2013
		Santa Monica Basin	46025	33°44'58"	119°3'10"	905	1982-2013
	CDIP	San Pedro	92	33°37'07"	118°19'00"	457	1981-2014
		Oceanside Offshore	45	33°10'76"	117°28'28"	220	1997-2014
		Mission Bay Offshore	93	32°44'86"	117°22'17"	192	1981-2014
	NDBC	Tanner Bank	46047	32°24'11"	119°32'8"	1,399	1991-2013

Figure 3.7 Maps showing (a) locations of all buoys used in this study and (b) close-up of buoy locations in the Southern California Bight. Light blue anchors represent NDBC stations and dark blue anchors represent CDIP stations.


A
West Washington
Cape Elizabeth
Grays Harbor
Columbia River Bar
Stonewall Bank
West Oregon
Southeast Papa
St Georges
Eel River
West California
Point Arena
Bodega Bay
San Francisco
Half Moon Bay
Monterey
Cape San Martin
Diablo Canyon
Santa Maria
Pt Arguello
East Santa Barbara
West Santa Barbara
Santa Monica Basin
San Pedro
Tanner Bank
Oceanside Offshore
Mission Bay Offshore
830 mi
US Dept of State Geographer
© 2013 Google
Image Landsat
Data SIO, NOAA, U.S. Navy, NGA, GEBCO
Google earth
Imagery Date: 4/10/2013
43°23'50.77" N 109°46'23.76" W elev 7809 ft eye alt 2471.98 mi

B
Santa Maria
Pt Arguello
Harvest
West Santa Barbara
East Santa Barbara
San Miguel Island
Santa Cruz Island
Santa Rosa Island
Anacapa Island
Santa Monica Basin
San Pedro
San Nicolas Island
Santa Catalina Island
Oceanside Offshore
San Clemente Island
Tanner Bank
Mission Bay Offshore
Data LDEO-Columbia, NSF, NOAA
© 2013 Google
Image Landsat
Data SIO, NOAA, U.S. Navy, NGA, GEBCO
107 mi
Imagery Date: 4/10/2013 33°45'32.67" N 118°30'21.64" W elev -471 ft eye alt 440.14 mi
Google earth

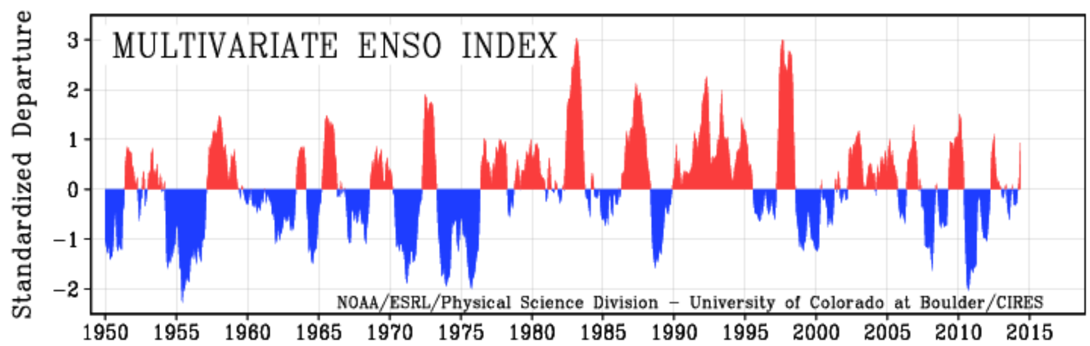

Figure 3.8 Time series of the Multivariate ENSO Index (MEI) since 1950 (from http://www.esrl.noaa.gov/psd/enso/mei/). Negative values (blue) represent cold ENSO phases (La Niña conditions) and positive values (red) represent warm ENSO phases (El Niño conditions).

3.3.1 Significant Wave Height (H_{sig}): All El Niño vs. Non-El Niño

In order to quickly reveal any obvious differences between the significant wave height (H_{sig}) data from El Niño years (1976, 1979, 1982, 1986, 1991, 1994, 1997, 2002, 2004, 2006, 2009) and non-El Niño years, observed H_{sig} values were averaged over all El Niño summers, all non-El Niño summers, each month for El Niño summers (one average for June, one for July, and one for August), and each month for non-El Niño summers for each of the 21 NOAA buoys and 6 CDIP buoys. Here, both ENSO-neutral/normal years and La Niña years were categorized as "non-El Niño" years. This allowed for some simplification, in that only two discrete categories (either "yes, El Niño" or "no, not El Niño") were used. The same process was repeated for all El Niño autumns, all non-El Niño autumns, each month for El Niño autumns (one average for September, one for October, and one for November), and each month for all non-El Niño autumns for each buoy. Summer and autumn H_{sig}

values were also averaged for each region (Washington, Oregon, Northern California, Central California, and Southern California).

3.3.2 Significant Wave Height (H_{sig}): Moderate to Strong El Niño vs. Non-El Niño to Weak El Niño

In order to compare some of the effects of using a strict definition of El Niño to those of an inclusive (as in section 3.3.1) version, observed significant wave height (H_{sig}) data from moderate to strong El Niño (MEI ranking of at least 0.750; Figure 3.8) years (1982, 1986, 1991, 1994, 1997, 2002, 2009) and non-El Niño to weak El Niño years were averaged for the same seasonal and monthly scenarios as described in section 3.3.1 for each of the same 27 buoys.

3.3.3 Summer Significant Wave Height (H_{sig}): Individual Summers vs. Average

In this analysis, a series of Kolmogorov-Smirnov tests (K-S test; Massey 1951) were performed to compare each individual summer's observed H_{sig} cumulative distribution function (CDF) to its respective buoy's overall observed summer H_{sig} CDF (including data from the entire summer record length, through 2012) for each of the 27 buoys. The resulting D-statistics were then evaluated against the distribution of D-values produced by a 10,000-trial Monte Carlo computer simulation (Metropolis and Ulam 1949), in which 6,422 values (representative of the number of H_{sig} data points in a typical summer) were randomly subsampled [using Python's "random.sample(*population*, *k*)" function for random sampling without replacement] from one buoy's overall observed summer H_{sig} record (through 2012) and compared (as a CDF) using the K-S test to the same buoy's overall observed summer H_{sig} record (CDF; record through 2012) for each trial.

3.3.4 Summer Significant Wave Height (H_{sig}) vs. the Winter Multivariate El Niño Southern Oscillation (ENSO) Index (MEI)

In this analysis, the average winter MEI (average of December-January, January-February, and February-March indices) was plotted as a function of the percentage difference between the average summer (June-August) H_{sig} for each year and the overall average summer H_{sig} for every buoy over the 1976-2012 period (linear regression; each pair of values included a given year's average winter MEI and the previous year's summer H_{sig} percentage difference) to determine the extent to which the observed summer H_{sig} data are associated with winter values from a commonly used ENSO index. To state it another way, average winter MEI was plotted as a function of [100*((average H_{sig} for a given year) – (average summer H_{sig})) / (average summer H_{sig})]. MEI values were obtained from http://www.esrl.noaa.gov/psd/enso/mei/table.html. An exact, two-tailed binomial test (an exact test of the statistical significance of deviations from the theoretically expected distribution of observations in two categories—in this case, negative slope vs. positive slope) was used to measure the significance of the deviance of the slope types of the 27 plots from what is expected when drawing randomly from the same populations (with normal distributions). The following code was used in R to obtain the p-value of the hypothesis test: binom.test(x, n, (p =0.5)). "x" represents the number of successes (one slope type), "n" represents the number of trials (27, as there are 27 buoys and thus, 27 plots), and "p = 0.5" is the hypothesized probability of success.

Then, in order to assess the likelihood of observing the outcome of the above analysis by chance, the slopes were compared to the distribution of those produced by a 10,000-trial Monte Carlo computer simulation, in which the average winter MEI (from the 1976-2012 period) was plotted as a function of values representing the previous summers' H_{sig} percentage differences (linear regression), drawn randomly (using a random number generator) from a Gaussian distribution centered on zero, with a standard deviation that is representative of the distributions of observed summer H_{sig} percentage differences (the data from the buoy records through 2012).

3.3.5 Yearly Significant Wave Height (H_{sig}) vs. the Winter Multivariate El Niño Southern Oscillation (ENSO) Index (MEI)

In order to determine the extent to which the observed yearly H_{sig} data are associated with winter MEI values, the same process as in section 3.3.4 was used to plot average winter MEI as a function of the yearly H_{sig} percentage difference (yearly H_{sig} percentage difference = [100*((average H_{sig} for each year) – (overall average H_{sig})) / (overall average H_{sig})]) for every buoy over the 1976-2012 period (i.e. each pair of values included a given year's average winter MEI and the previous year's H_{sig} percentage difference). Then, in order to evaluate the likelihood of observing a chance outcome that resembles the results of the above analysis, the slopes were compared to the distribution of those produced by the 10,000-trial Monte Carlo computer simulation described in section 3.3.4.

3.3.6 Summertime ENSO Forecasting: The Multivariate El Niño Southern Oscillation (ENSO) Index (MEI)

In this analysis, the average winter MEI (average of December-January, January-February, and February-March indices) was plotted as a function of the average MEI of the previous summer (average of May-June, June-July, and July-August indices) for every year since 1975 (linear regression) to determine the extent to which the average summer MEI relates to the (following year's) average winter MEI.

Then, Python packages "numpy," "pandas," "pylab," and "statsmodels" were used to calculate and plot the probability of winter El Niño occurrence (with winter El Niño defined as MEI $\geq$ 1.0 for the average of the November-December, December-January, and January-February bimonthly seasons) as a function of the average summer MEI for 1975-2012, using the method for binary logistic regression that is described here: http://blog.yhathq.com/posts/logistic-regression-and-python.html. First, two arrays were generated for input to the "statsmodels Logit.fit()" function, where the independent variable was the average summer MEI and the dependent dummy variable represented the presence of winter El Niño conditions (dummy variable = 1 for El Niño or 0 for no El Niño). Next, the highest and lowest summer

MEI values and eight evenly spaced points between them were selected. The probability of winter El Niño occurrence was then calculated for each point using the regression coefficients and the "statsmodels predict()" function. Finally, the resulting values were plotted to show the probability of winter El Niño occurrence as a function of the range of average summer MEI values.

3.3.7 Summertime ENSO Forecasting: Combining the Multivariate El Niño Southern Oscillation (ENSO) Index (MEI) with Significant Wave Height (H_{sig})

In order to determine whether a combination of the average summer MEI and average summer H_{sig} better relates to the (following year's) average winter MEI than does the average summer MEI alone, a multiple linear regression analysis was performed for each buoy (for the duration of each buoy's record through 2012) and the outcome was compared to the results from section 3.3.6. The ordinary least-squares (OLS) regression was performed with x_1 = average summer MEI (average of May-June, June-July, and July-August indices), x_2 = summer average H_{sig}, and y = average winter MEI (average of December-January, January-February, and February-March indices), using the method described here: http://www.datarobot.com/blog/ordinary-least-squares-in-python/.

3.3.8 Summer Significant Wave Height (H_{sig}) vs. The Summer North Pacific (NP) Index

In this analysis, the same process as in section 3.3.4 was used to plot the observed monthly summer H_{sig} percentage difference between the average summer monthly (June, July, or August) H_{sig} for each year and the overall monthly average summer H_{sig} (for June, July, or August) as a function of the corresponding monthly summer Northern Pacific (NP) Index (Trenberth and Hurrell 1994) in order to determine the extent to which the observed summer H_{sig} data relate to summer values from the NP Index. Standard format NP values were obtained from this website: http://140.172.38.100/psd/gcos_wgsp/Timeseries/NP/.

Plots were generated for each buoy over the 1975 to 2010 time period because the NP Index has not been updated since 2011. Despite the lack of recent updates, the NP Index is still considered to be a good indicator of the intensity of the Aleutian Low pressure cell in the Gulf of Alaska, which is important to North Pacific and North American Climate. Specifically, it results from a simple but robust measure of the circulation in the North Pacific: the area-weighted mean sea-level pressure over the region 30˚N to 65˚N, 160˚E to 140˚W (Trenberth and Hurrell 1994).

3.4 RESULTS AND DISCUSSION

3.4.1 Significant Wave Height (H_{sig}): Preliminary Exploration of the Observed Data

As described in sections 3.3.1 and 3.3.2, observed H_{sig} values were averaged (including seasonal, monthly, and regional means) and compared across the following scenarios for every buoy:

i. all El Niño summers vs. non-El Niño summers,

ii. all El Niño autumns vs. non-El Niño autumns,

iii. moderate to strong El Niño summers vs. non-El Niño to weak El Niño summers, and

iv. moderate to strong El Niño autumns vs. non-El Niño to weak El Niño autumns.

Results for the "ii," "iii," and "iv" scenarios are presented in appendices B, C, and D, respectively. Table 3.2 contains the seasonal and monthly average H_{sig} values for El Niño and non-El Niño summers (scenario "i"). It appears from the H_{sig} percentage differences that El Niño summer average H_{sig} values are lower than non-El Niño summer average H_{sig} values at most stations (Table 3.2). In general, the standard deviations for this "i" scenario are high relative to the averages, though, so no strong claims can be made regarding the apparent trend in the H_{sig} percentage differences. Switching to a strict definition of El Niño (scenario "iii") results in practically the same outcome (Appendix C and Supplemental File 5) for the summer as does using an inclusive definition (as in scenario "i").

The autumn averages yield some potentially interesting results that might warrant further study. For instance, scenario "ii's" seasonal H_{sig} percentage differences suggest that El Niño autumn H_{sig} values are higher than non-El Niño autumn H_{sig} values, on average (Appendix B and Supplemental File 4). However, the standard deviations are relatively high (and generally higher than the summer standard deviations), indicating some variability over the season. Indeed, scenario ii's monthly H_{sig} percentage differences reveal that October is the "odd man out," in that it suggests the opposite of autumn's (overall) seasonal trend, but standard deviations from the individual autumn months are also relatively high, so no strong claims regarding any apparent trends can be made at this point. For the most part, switching to a strict definition of El Niño (scenario "iv") has no major effect on the autumn results (Appendix D and Supplemental File 6), but it looks as though H_{sig} percentage differences for the southern region are more positive with a strict definition than they are with an inclusive definition (as in scenario "ii") for the month of October. However, again, the high standard deviations prevent the formation of any final conclusions without further research. While additional analyses of the autumn H_{sig} data might unearth some trends that could contribute to the understanding of the behavior of El Niño, the remainder of this paper focuses on the summer "i" scenario, as the identification of a strong relationship between El Niño summer H_{sig} and winter El Niño conditions would provide a two-season predictive lead on El Niño, as opposed to an autumn one-season lead, which is of low utility.

It should also be noted that some of the southernmost buoys (numbers 46025, 92, 45, and 93) seem to have consistently low standard deviations (relative to the other stations') on their H_{sig} averages, across the board. The Southern California Bight is located just offshore of these buoys (Figure 3.7B). The bight's interference with the waves (due to island blocking, refraction, diffraction, and shoaling of incident deep water waves) lowers the level of wave energy and thus the level of variation in wave heights when the waves reach the bight before they reach the buoys, as is the case with storms that are generated off the Aleutian Islands (O'Reilly and Guza 1993 and 1998).

Another study of wave climate variation (using wave spectral density data; Bromirski et al. 2005) shows that variations in wave energy at different buoys off the U.S. West Coast for the same storm event result from differences in the buoys' proximities to the strong wind sector of the storm, fetch parameters, and wavefront spreading, while bottom interactions that cause refraction and shoaling in relatively shallow coastal waters can be prominent, as well. Bromirski et al. (2005) specifically mention that station 46025 in the Southern California Bight is shielded (by Point Conception and the Channel Islands) from waves propagating from storm centers to the northwest. They find that long-term monthly means of band-limited wave energy are substantially lower (about 65% lower) at station 46025 than at station 46023, which is located nearby. Even so, the dominant portion of the long-period (wave period $T > 12$ s, which results primarily from swell) and intermediate-period ($6 \text{ s} \leq T \leq 12$ s, which probably results from a mixture of local and regional wind forcing) wave energy observed at station 46025 is generated primarily in the open ocean and reflects mostly open ocean wave variability (Bromirski et a. 2005), as opposed to effects from local seas (which would be indicated by dominant short-period waves; T < 6 s).

Table 3.2: *Average summer significant wave heights (H_{sig}) over (a) the entire season and over the months of (b) June, (c) July, and (d) August for all El Niño years and non-El Niño years. Blue cells indicate that average H_{sig} during El Niño summer months were lower than during non-El Niño summer months.*

A.

Region	Station	Summer Average Hsig (m)					
		All El Niño	StDev	Non-El Niño	StDev	El Niño – Non-El Niño	% Difference
Washington	46041	1.41	0.61	1.40	0.55	0.00	0.3
	46029	1.51	0.60	1.48	0.54	0.03	2.2
	36	1.35	0.53	1.32	0.48	0.03	2.0
	46005	1.67	0.69	1.71	0.65	-0.03	-1.9
	regional	1.49	0.62	1.47	0.57	0.02	1.2
Oregon	46050	1.60	0.61	1.61	0.57	-0.01	-0.5
	46002	1.71	0.61	1.79	0.63	-0.08	-4.7
	regional	1.67	0.61	1.71	0.61	-0.04	-2.4
Northern California	46027	1.74	0.76	1.71	0.69	0.03	1.8
	46006	1.59	0.60	1.64	0.64	-0.05	-3.2
	46022	1.81	0.82	1.80	0.78	0.01	0.5
	46014	1.85	0.74	1.95	0.72	-0.10	-5.2
	regional	1.75	0.74	1.79	0.72	-0.03	-1.9
Central California	46059	1.97	0.66	1.91	0.65	0.06	3.3
	46013	1.75	0.69	1.88	0.71	-0.14	-7.6
	46026	1.45	0.57	1.51	0.57	-0.06	-3.9
	46012	1.62	0.62	1.69	0.62	-0.07	-4.4
	46042	1.72	0.59	1.78	0.59	-0.06	-3.6
	46028	1.95	0.63	1.96	0.63	-0.01	-0.7
	regional	1.72	0.65	1.78	0.65	-0.06	-3.6
Southern California	76	1.20	0.36	1.24	0.36	-0.03	-2.7
	46011	1.63	0.54	1.68	0.57	-0.06	-3.3
	46023	1.76	0.56	1.82	0.57	-0.06	-3.3
	71	1.75	0.55	1.84	0.55	-0.09	-5.0
	46054	1.61	0.52	1.68	0.52	-0.06	-3.9
	46053	1.01	0.35	1.03	0.35	-0.01	-1.2
	46025	0.96	0.26	1.00	0.26	-0.04	-4.2
	92	0.82	0.19	0.85	0.21	-0.02	-3.0
	45	0.88	0.20	0.89	0.19	-0.01	-1.7
	93	0.96	0.22	0.99	0.23	-0.03	-3.5
	46047	1.72	0.50	1.85	0.57	-0.14	-7.7
	regional	1.29	0.56	1.33	0.58	-0.04	-3.2

B.

Region	Station	June Average Hsig (m)					
		All El Niño	StDev	Non-El Niño	StDev	El Niño – Non-El Niño	% Difference
Washington	46041	1.53	0.75	1.56	0.65	-0.03	-2.1
	46029	1.72	0.72	1.62	0.64	0.09	5.6
	36	1.43	0.61	1.44	0.56	0.00	-0.1
	46005	1.82	0.86	1.90	0.77	-0.08	-4.4
	regional	1.62	0.76	1.61	0.68	0.01	0.5
Oregon	46050	1.71	0.72	1.74	0.66	-0.03	-1.8
	46002	1.76	0.67	1.90	0.71	-0.14	-7.5
	regional	1.74	0.69	1.83	0.69	-0.09	-5.0
Northern California	46027	1.75	0.81	1.83	0.72	-0.08	-4.7
	46006	1.75	0.71	1.87	0.79	-0.11	-6.3
	46022	1.89	0.89	2.01	0.81	-0.12	-6.1
	46014	1.99	0.89	2.14	0.79	-0.15	-7.1
	regional	1.85	0.84	1.98	0.79	-0.12	-6.4
Central California	46059	2.08	0.66	2.05	0.70	0.03	1.4
	46013	1.93	0.87	2.14	0.78	-0.21	-10
	46026	1.72	0.72	1.73	0.64	-0.01	-0.7
	46012	1.81	0.78	1.98	0.74	-0.18	-9.4
	46042	1.98	0.75	2.02	0.69	-0.03	-1.7
	46028	2.21	0.77	2.19	0.73	0.01	0.7
	regional	1.94	0.79	2.02	0.73	-0.07	-3.6
Southern California	76	1.39	0.44	1.41	0.42	-0.02	-1.2
	46011	1.85	0.70	1.92	0.67	-0.08	-4.1
	46023	1.97	0.71	2.05	0.68	-0.08	-4.0
	71	2.01	0.69	2.05	0.65	-0.04	-1.9
	46054	1.90	0.65	1.87	0.62	0.03	1.8
	46053	1.18	0.41	1.13	0.41	0.05	4.3
	46025	1.05	0.30	1.08	0.31	-0.02	-2.1
	92	0.87	0.23	0.89	0.25	-0.03	-3.1
	45	0.93	0.19	0.94	0.20	0.00	-0.4
	93	1.02	0.23	1.08	0.28	-0.06	-5.6
	46047	1.93	0.64	2.04	0.68	-0.11	-5.7
	regional	1.43	0.67	1.47	0.68	-0.04	-2.8

C.

Region	Station	July Average Hsig (m)					
		All El Niño	StDev	Non-El Niño	StDev	El Niño – Non-El Niño	% Difference
Washington	46041	1.36	0.48	1.35	0.47	0.00	0.2
	46029	1.44	0.48	1.47	0.46	-0.03	-2.1
	36	1.28	0.43	1.30	0.41	-0.02	-1.3
	46005	1.59	0.53	1.56	0.51	0.04	2.2
	regional	1.41	0.49	1.41	0.47	0.00	0.3
Oregon	46050	1.59	0.51	1.61	0.51	-0.01	-0.9
	46002	1.69	0.56	1.73	0.55	-0.04	-2.1
	regional	1.66	0.54	1.68	0.54	-0.02	-1.1
Northern California	46027	1.81	0.77	1.70	0.70	0.12	6.6
	46006	1.51	0.49	1.52	0.50	0.00	-0.1
	46022	1.88	0.83	1.76	0.80	0.12	6.6
	46014	1.93	0.68	1.94	0.70	0.00	-0.1
	regional	1.79	0.73	1.74	0.71	0.05	2.9
Central California	46059	1.89	0.68	1.89	0.65	0.01	0.4
	46013	1.72	0.55	1.80	0.67	-0.08	-4.7
	46026	1.41	0.44	1.44	0.50	-0.03	-1.9
	46012	1.59	0.45	1.63	0.56	-0.04	-2.4
	46042	1.63	0.42	1.73	0.53	-0.10	-6.0
	46028	1.84	0.50	1.90	0.58	-0.06	-3.2
	regional	1.66	0.52	1.72	0.60	-0.06	-3.6
Southern California	76	1.12	0.25	1.18	0.30	-0.05	-4.6
	46011	1.55	0.42	1.62	0.50	-0.06	-4.0
	46023	1.67	0.44	1.77	0.50	-0.10	-5.9
	71	1.67	0.42	1.79	0.48	-0.12	-6.7
	46054	1.51	0.41	1.60	0.46	-0.09	-6.1
	46053	0.93	0.29	0.99	0.33	-0.06	-5.9
	46025	0.93	0.20	0.99	0.24	-0.06	-6.5
	92	0.82	0.16	0.84	0.18	-0.02	-2.1
	45	0.84	0.18	0.87	0.17	-0.03	-3.6
	93	0.93	0.19	0.98	0.20	-0.05	-5.4
	46047	1.61	0.39	1.80	0.49	-0.18	-11
	regional	1.23	0.48	1.29	0.53	-0.06	-4.7

D.

Region	Station	August Average Hsig (m)					
		All El Niño	StDev	Non-El Niño	StDev	El Niño – Non-El Niño	% Difference
Washington	46041	1.36	0.59	1.31	0.48	0.04	3.3
	46029	1.42	0.55	1.37	0.49	0.05	3.4
	36	1.34	0.52	1.24	0.43	0.10	7.5
	46005	1.62	0.63	1.70	0.62	-0.08	-4.7
	regional	1.44	0.59	1.40	0.54	0.04	2.6
Oregon	46050	1.50	0.55	1.49	0.50	0.01	0.7
	46002	1.68	0.60	1.74	0.61	-0.07	-4.0
	regional	1.61	0.59	1.63	0.57	-0.01	-0.9
Northern California	46027	1.65	0.67	1.61	0.63	0.05	2.8
	46006	1.51	0.54	1.56	0.55	-0.05	-3.4
	46022	1.67	0.70	1.66	0.69	0.00	0.2
	46014	1.62	0.57	1.78	0.62	-0.16	-9.5
	regional	1.61	0.63	1.66	0.63	-0.05	-3.0
Central California	46059	1.94	0.62	1.77	0.56	0.16	8.8
	46013	1.59	0.55	1.70	0.58	-0.11	-6.8
	46026	1.26	0.41	1.34	0.45	-0.08	-6.5
	46012	1.43	0.48	1.51	0.45	-0.08	-5.2
	46042	1.56	0.45	1.63	0.47	-0.07	-4.6
	46028	1.77	0.47	1.81	0.52	-0.04	-2.5
	regional	1.55	0.53	1.62	0.53	-0.07	-4.4
Southern California	76	1.09	0.29	1.12	0.29	-0.03	-2.8
	46011	1.50	0.41	1.51	0.43	-0.02	-1.1
	46023	1.68	0.46	1.65	0.43	0.02	1.4
	71	1.58	0.39	1.69	0.43	-0.11	-6.8
	46054	1.48	0.41	1.57	0.39	-0.09	-5.8
	46053	0.93	0.28	0.96	0.27	-0.03	-3.1
	46025	0.90	0.22	0.96	0.22	-0.05	-5.8
	92	0.79	0.17	0.82	0.18	-0.03	-3.6
	45	0.85	0.22	0.87	0.18	-0.01	-1.3
	93	0.92	0.22	0.93	0.19	0.00	-0.3
	46047	1.61	0.37	1.73	0.49	-0.12	-7.0
	regional	1.21	0.47	1.23	0.48	-0.03	-2.1

3.4.2 Summer Significant Wave Height (H_{sig}): Individual Summers vs. Average

In this analysis, the K-S test was used (as described in section 3.3.3) to determine whether the normalized distributions of summer H_{sig} observed data from individual years differ significantly from the overall (normalized) distributions of summer H_{sig} observed data for each buoy (Table 3.3, Appendix E, and Supplemental File 7). However, with very large datasets, the likelihood that the K-S test will declare that any observed differences are statistically significant is high, so an additional analysis is needed to evaluate the likelihood of occurrence of the D-statistics resulting from the tests of observed data. Thus, the D-statistics resulting from the first set of K-S tests (Table 3.3), which represent the maximum differences between the observed (normalized) individual summer and the overall (normalized) summer H_{sig} distributions, were compared to the large distribution of D-statistics (Figure 3.9) resulting from the 10,000-trial Monte Carlo computer simulation described in section 3.3.3 [in which the K-S test was used to compare randomly subsampled distributions of H_{sig} values representing single typical summers ("typical," in that there are no distinct representations of any "types" of summer, such as El Niño, La Niña, or neutral) to station 46005's overall observed summer H_{sig} record through 2012 (33 summers)] to determine how likely it is to observe the outcome of the first set of K-S tests (Table 3.3 and Appendix E) by chance.

Table 3.3 and Appendix E show that virtually all of the D-statistics from the K-S tests of the distributions of summer H_{sig} observed data from individual years vs. the overall distributions of summer H_{sig} observed data are significant, according to the confidence intervals generated by the Monte Carlo simulation (Figure 3.9). This suggests that year-to-year summer H_{sig} variations are large enough that H_{sig} distributions from most years deviate significantly from the average summer H_{sig}. Thus, H_{sig} data from individual summers are not likely to be useful for ENSO prediction and if there is indeed a trend in the summer El Niño H_{sig} data, it is probably most apparent when the El Niño summer data are viewed collectively.

Table 3.3: *K-S test results for normalized distributions of individual summer H_{sig} observed data vs. normalized distributions of overall summer H_{sig} observed data for each Washington buoy (Appendix E contains results from all stations). Data from El Niño summers are indicated in bold typeface. A sign on a D-statistic indicates whether the greatest difference between an individual summer's H_{sig} distribution and that of the overall summer for its station is positive or negative. Red color indicates that the results of the K-S test are not significant. Confidence levels of the observed D-statistics relative to the outcome of the Monte Carlo simulation (Figure 3.9) are also presented in the last column on the right.*

Region	Station	Year	D-statistic	p < 0.05?	Monte Carlo Confidence
Washington	46041	1987	-0.070	yes	99%
		1988	0.035	yes	99%
		1989	-0.167	yes	99%
		1990	0.039	yes	99%
		1991	**-0.067**	**yes**	**99%**
		1992	-0.069	yes	99%
		1993	-0.083	yes	99%
		1994	**-0.051**	**yes**	**99%**
		1995	-0.057	yes	99%
		1996	-0.069	yes	99%
		1997	**0.087**	**yes**	**99%**
		1998	-0.143	yes	99%
		1999	-0.097	yes	99%
		2000	0.038	yes	99%
		2001	0.022	yes	99%
		2002	**0.060**	**yes**	**99%**
		2003	0.049	yes	99%
		2004	**0.069**	**yes**	**99%**
		2005	0.076	yes	99%
		2006	**-0.154**	**yes**	**99%**
		2007	0.323	yes	99%
		2008	0.065	yes	99%
		2009	**0.032**	**yes**	**99%**
		2010	0.111	yes	99%
		2011	0.062	yes	99%
		2012	0.071	yes	99%

Region	Station	Year	D-statistic	p < 0.05?	Monte Carlo Confidence
Washington	46029	1984	-0.127	yes	99%
		1985	0.216	yes	99%
		1986	**0.132**	**yes**	**99%**
		1987	0.347	yes	99%
		1991	**0.219**	**yes**	**99%**
		1992	-0.082	yes	99%
		1993	-0.148	yes	99%
		1994	**0.031**	**yes**	**99%**
		1995	-0.094	yes	99%
		1996	-0.362	yes	99%
		1997	**-0.035**	**yes**	**99%**
		1998	-0.061	yes	99%
		1999	0.091	yes	99%
		2000	-0.099	yes	99%
		2001	0.068	yes	99%
		2002	**-0.038**	**yes**	**99%**
		2003	0.030	yes	99%
		2004	**-0.051**	**yes**	**99%**
		2005	-0.097	yes	99%
		2006	**0.071**	**yes**	**99%**
		2007	-0.027	yes	99%
		2008	-0.083	yes	99%
		2009	**0.081**	**yes**	**99%**
		2010	0.104	yes	99%
		2011	0.040	yes	99%
		2012	0.155	yes	99%

Region	Station	Year	D-statistic	p < 0.05?	Monte Carlo Confidence
Washington	36	**1982**	**-0.371**	**yes**	**99%**
		1987	0.133	yes	99%
		1988	-0.193	yes	99%
		1989	0.104	yes	99%
		1990	-0.047	no	n/a
		1991	**-0.105**	**yes**	**99%**
		1992	-0.114	yes	99%
		1993	-0.142	yes	99%
		1994	**-0.153**	**yes**	**99%**
		1995	0.052	yes	99%
		1996	0.065	yes	99%
		1997	**-0.070**	**yes**	**99%**
		1998	-0.034	yes	99%
		1999	-0.056	yes	99%
		2000	-0.039	yes	99%
		2001	-0.037	yes	99%
		2002	**0.039**	**yes**	**99%**
		2003	0.017	no	n/a
		2004	**0.091**	**yes**	**99%**
		2005	0.098	yes	99%
		2006	**0.081**	**yes**	**99%**
		2007	-0.070	yes	99%
		2008	0.068	yes	99%
		2009	**-0.042**	**yes**	**99%**
		2010	0.082	yes	99%
		2011	-0.069	yes	99%
		2012	-0.091	yes	99%

Region	Station	Year	D-statistic	p < 0.05?	Monte Carlo Confidence
Washington	46005	**1976**	**-0.135**	**yes**	**99%**
		1977	0.278	yes	99%
		1978	-0.145	yes	99%
		1979	**-0.152**	**yes**	**99%**
		1980	-0.063	yes	99%
		1981	0.032	yes	99%
		1982	**-0.105**	**yes**	**99%**
		1983	-0.051	yes	99%
		1984	0.068	yes	99%
		1985	-0.255	yes	99%
		1986	**-0.074**	**yes**	**99%**
		1987	0.130	yes	99%
		1988	0.025	yes	99%
		1989	-0.098	yes	99%
		1990	0.087	yes	99%
		1991	**-0.046**	**yes**	**99%**
		1992	-0.051	yes	99%
		1993	0.081	yes	99%
		1994	**0.059**	**yes**	**99%**
		1995	0.069	yes	99%
		1996	-0.083	yes	99%
		1997	**-0.025**	**yes**	**99%**
		1998	0.085	yes	99%
		1999	0.092	yes	99%
		2000	-0.034	yes	99%
		2001	0.084	yes	99%
		2002	**0.030**	**yes**	**99%**
		2003	0.057	yes	99%
		2004	**0.067**	**yes**	**99%**
		2006	**-0.109**	**yes**	**99%**
		2007	0.038	yes	99%
		2008	0.054	yes	99%
		2010	-0.148	yes	99%
		2011	-0.064	yes	99%
		2012	0.139	yes	99%

Frequency of D-statistics Resulting from 10,000-Trial Monte Carlo Simulation of K-S Tests of Distributions of Random Individual Summers' H_{sig} Values vs. 33 Years of Summer H_{sig} Values

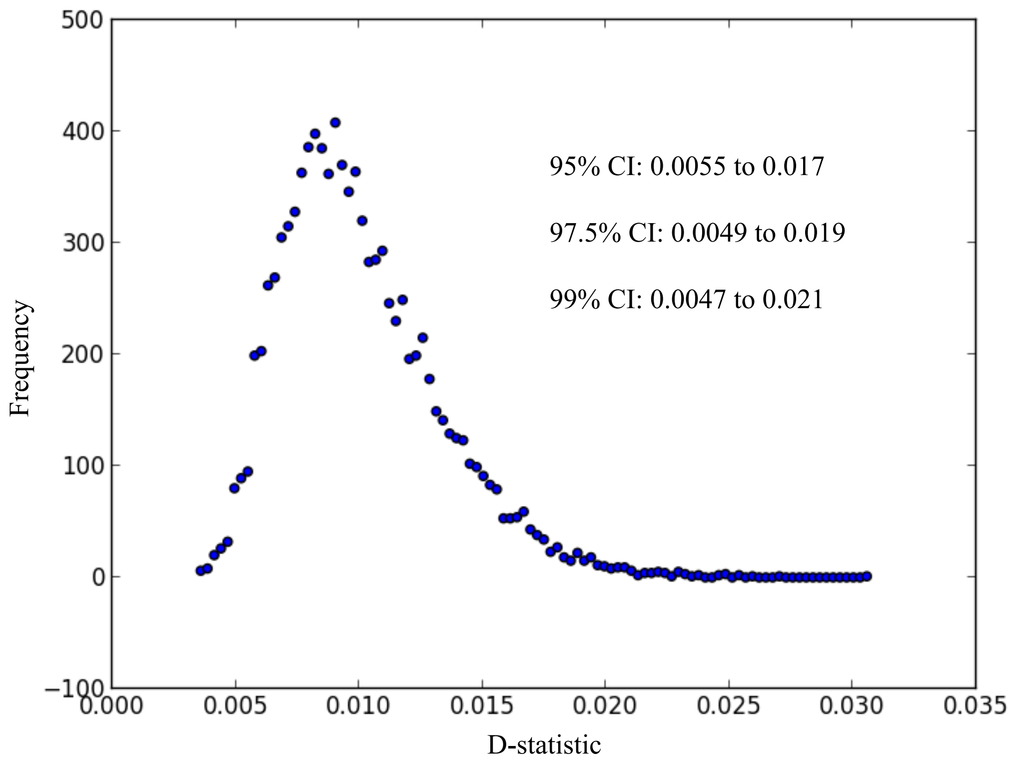

Figure 3.9 Distribution of D-statistics resulting from a 10,000-trial Monte Carlo simulation of K-S tests of distributions of individual summers' H_{sig} values vs. all summer H_{sig} values from station 46005's record through 2012 (33 summers included). Confidence intervals (CI) are shown.

3.4.3 Summer Significant Wave Height (H_{sig}) vs. the Winter Multivariate El Niño Southern Oscillation (ENSO) Index (MEI)

In order to examine the predictive potential of the summer H_{sig} observed data, the average winter MEI was plotted as a function of the percentage difference between the average summer H_{sig} for each year and the overall average summer H_{sig} for each buoy over its timespan of available summer H_{sig} data, as described in section

3.3.4. 7/27 stations have summer H_{sig} percentage differences that are significantly associated with the average winter MEI, including 1/2 Oregon stations (station 46050 has a weak significance at the $p < 0.05$ level), 1/4 Northern California stations (46014), 2/6 Central California stations (46013 and 46026), and 3/11 Southern California stations (46011, 71, and 93), with the average winter MEI increasing as summer H_{sig} percentage difference decreases in all of the aforementioned cases (Table 3.4). While the data are not very tightly clustered (Appendix F), 19/27 of the plots have negative slopes. This is unusual given the expected outcome; if the data were drawn randomly from the same populations, one would expect half of the slopes to be negative and half positive (in a normal distribution). An exact, two-tailed binomial test puts the likelihood of the actual outcome (19/27 plots with negative slopes) at $p = 0.052$, which falls just short of significance, but as with all tests of significance, just because the null hypothesis (that the observed outcome does not deviate significantly from the expected 50-50 outcome) cannot be rejected at this stage does not necessarily mean that it is true. Excluding the two plots with zero slopes makes $p = 0.014$ ($p < 0.05$) for 19/25 plots with negative slopes, but there is no rationale for eliminating any of the results.

The above analysis is limited and even at $p = 0.052$, an outcome of 19/27 plots with negative slopes still appears to be unusual compared to that which is expected. Since there is not yet sufficient evidence to reject the null hypothesis, it is worthwhile to compare the above results to the large simulated distribution of slopes (Figure 3.10) that could result by chance (as described in section 3.3.4; values representing summer H_{sig} percentage differences were drawn randomly from a Gaussian distribution centered on zero, with a standard deviation of seven), in order to determine the likelihood that the observed H_{sig} data vs. MEI plots would have slopes that differ from zero. According to the confidence intervals (CI) generated through the Monte Carlo simulation (Figure 3.10), seven of the negative slopes (and one positive slope) from the observed summer H_{sig} percentage difference vs. average winter MEI plots (Table 3.4) are significant at the 97.5% level and five of those negative slopes (as well as the positive slope) are also significant at the 99% level. This suggests that the weak trend in the observed summer H_{sig} data (average H_{sig} during El Niño summers is slightly lower than during neutral and La Niña summers) may be robust.

Table 3.4: *Linear regression coefficients for the plots (Appendix F contains the graphs) of the average winter Multivariate ENSO Index (MEI) vs. the previous summer's significant wave height (H_{sig}) percentage difference for each buoy. Negative slopes are highlighted in blue.*

Region	Station	Summer H_{sig} Percentage Difference vs. Average Winter MEI Correlation Results			
		a	b	R2	p < 0.05?
Washington	46041	0.033	0.134	0.069	no
	46029	0.000	-0.052	0.000	no
	36	-0.037	0.183	0.044	no
	46005	-0.019	0.160	0.020	no
Oregon	46050	-0.075	-0.023	0.203	yes
	46002	-0.005	0.373	0.002	no
Northern California	46027	0.021	0.030	0.025	no
	46006	-0.003	0.174	0.001	no
	46022	0.015	0.191	0.007	no
	46014	-0.066	0.148	0.181	yes
Central California	46059	0.071	-0.229	0.052	no
	46013	-0.059	0.032	0.246	yes
	46026	-0.038	0.170	0.138	yes
	46012	-0.032	0.158	0.118	no
	46042	0.000	0.047	0.000	no
	46028	0.017	0.088	0.013	no
Southern California	76	-0.027	0.067	0.032	no
	46011	-0.079	0.158	0.154	yes
	46023	-0.034	0.200	0.036	no
	71	-0.095	-0.307	0.306	yes
	46054	-0.038	-0.088	0.061	no
	46053	-0.044	-0.250	0.084	no
	46025	0.017	0.156	0.012	no
	92	-0.088	-0.294	0.192	no
	45	-0.040	-0.109	0.036	no
	93	-0.075	0.330	0.246	yes
	46047	-0.045	-0.135	0.182	no

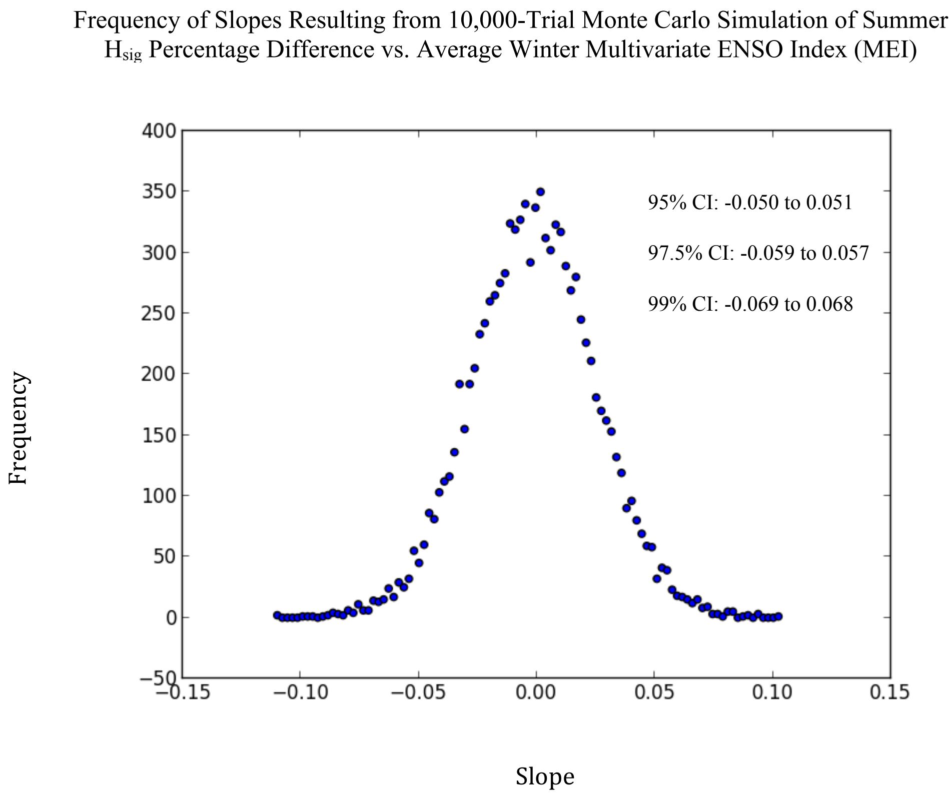

Figure 3.10 Distribution of slopes resulting from a 10,000-trial Monte Carlo simulation of summer H_{sig} percentage difference vs. average (following) winter Multivariate ENSO Index (MEI). Confidence intervals (CI) are shown.

3.4.4 Yearly Significant Wave Height (H_{sig}) vs. the Winter Multivariate El Niño Southern Oscillation (ENSO) Index (MEI)

In order to determine whether opening up the analysis to include the entire spectrum of wave heights might increase or decrease the relationship between H_{sig} and the average winter MEI compared to using just the summer H_{sig} data, the above evaluation (section 3.4.3) was repeated using yearly H_{sig} percentage difference in place of summer H_{sig} percentage difference, as mentioned in section 3.3.5. At first glance, the outcome for the yearly H_{sig} data (Table 3.5) does not appear to be very different from the outcome for the summer H_{sig} data (Table 3.4). Both analyses result in slopes that are close to zero, with many more negative slopes than positive slopes (20/27 for the yearly data and 19/27 for the summer data). A few of the yearly H_{sig} vs. average winter MEI plots with negative slopes even have significant relationships (Table 3.5), although they are less numerous than are the significant summer H_{sig} vs. average winter MEI plots (7/27 with significant results).

It is impossible to say whether the yearly H_{sig} data are any better or worse for ENSO prediction (using the MEI) than are the summer H_{sig} data when using only the information contained in Tables 3.4 and 3.5. Thus, the above results were compared to the large simulated distribution of slopes (Figure 3.10) that could result by chance (as mentioned in section 3.3.5) in order to determine the likelihood that the observed yearly H_{sig} data vs. MEI plots would have slopes that differ from zero. As it turns out, the standard deviation that is representative of the distributions of observed yearly H_{sig} percentage differences (seven) is the same as the standard deviation that is representative of the distributions of observed summer H_{sig} percentage differences, so the slopes from the observed yearly H_{sig} percentage difference data vs. the average winter MEI plots were evaluated by comparison with the Monte Carlo simulation outcome from section 3.4.3 (Figure 3.10). According to the confidence intervals (CI) generated through the Monte Carlo simulation (Figure 3.10), six of the negative slopes from the observed yearly H_{sig} percentage difference vs. average winter MEI plots (Table 3.5) are significant at the 95% level and four of those slopes are also significant at the 99% level. This suggests that the yearly H_{sig} data are a bit more random than the summer H_{sig} data and thus have lower predictive potential than the summer H_{sig} data.

Table 3.5: *Linear regression coefficients for the plots of the average winter Multivariate ENSO Index (MEI) vs. the previous year's significant wave height (H_{sig}) percentage difference for each buoy. Negative slopes are highlighted in blue.*

Region	Station	Yearly H_{sig} Percentage Difference vs. Average Winter MEI Correlation Results			
		a	b	R2	p < 0.05?
Washington	46041	0.033	0.134	0.069	no
	46029	0.016	0.110	0.046	no
	36	0.004	0.156	0.003	no
	46005	-0.011	0.184	0.013	no
Oregon	46050	0.029	0.067	0.120	no
	46002	-0.030	0.242	0.101	no
Northern California	46027	0.004	0.115	0.001	no
	46006	-0.025	0.201	0.062	no
	46022	-0.044	0.170	0.100	no
	46014	-0.050	0.160	0.086	no
Central California	46059	0.005	-0.088	0.002	no
	46013	-0.037	0.160	0.053	no
	46026	-0.039	0.170	0.132	yes
	46012	-0.036	0.156	0.083	no
	46042	-0.016	0.075	0.016	no
	46028	-0.033	0.076	0.043	no
Southern California	76	-0.008	0.076	0.006	no
	46011	-0.047	0.153	0.110	no
	46023	-0.089	0.200	0.202	yes
	71	-0.030	-0.328	0.090	no
	46054	-0.052	-0.088	0.063	no
	46053	-0.109	-0.250	0.226	no
	46025	-0.025	0.170	0.030	no
	92	-0.191	-0.096	0.441	yes
	45	-0.091	-0.109	0.213	no
	93	-0.024	0.204	0.097	no
	46047	0.028	-0.010	0.030	no

3.4.5 Summertime El Niño Southern Oscillation (ENSO) Forecasting: The Multivariate ENSO Index (MEI)

In order to establish how well ENSO can be forecasted using the MEI alone (over the period of available observed significant wave height data, 1975-2012), the average winter MEI was plotted as a function of the average summer MEI (Figure 3.11), as described in section 3.3.6. Since the MEI is widely regarded as one of the best indices for overall monitoring of the ENSO phenomenon (and use in worldwide correlation with surface temperature and rainfall, for example; Wolter and Timlin 2011), it is unsurprising that the average summer MEI is by itself an excellent predictor of the average winter MEI [R2 = 0.59 is good, given the current status of ENSO forecasting (Barnston et al. 1999; Chen and Cane 2008)], with the average winter MEI increasing as a function of an increasing average summer MEI (Figure 3.11). This stands in stark contrast to the weak relationship between summer significant wave height (H_{sig}) percentage difference and the average winter MEI (Table 3.4; Appendix F). Of course, this is not an entirely equal comparison of independent variables, as H_{sig} is a static parameter, whereas all seasonal MEI values [calculated separately for each of 12 sliding bimonthly seasons (December-January, January-February,…, November-December)] are standardized with respect to each season and to the 1950-1993 reference period (Wolter and Timlin 1993, 1998, and 2011). (Because of the MEI's autocorrelation, its seasonal values can change with each monthly update, but the changes are usually smaller than ± 0.1.)

In order to demonstrate how the average summer MEI affects the probability of El Niño occurrence (average winter MEI ≥ 1) during the following winter, the probability of winter El Niño occurrence as a function of the average summer MEI for 1975-2012 was calculated and plotted (Figure 3.12) using the method for binary logistic regression, as described in section 3.3.6. A logistic regression model is a non-linear transformation of a linear regression. It results in an S-shaped distribution function and while it is similar to a standard normal distribution, it makes for easily calculated probabilities (it constrains estimated probabilities to between zero and one, while mapping the probabilities to log odds ranging from zero to positive infinity).

Table 3.6 contains the results of the logistic regression analysis, including the overall model fit quality, the fit of the coefficient (for average summer MEI), the odds ratio, and the confidence interval. Rather than indicating the rate of change in the dependent variable (likelihood of El Niño occurrence during the winter) as the average (previous) summer MEI changes, as in a linear regression analysis, the estimated coefficient here is the log odds ratio. This is not very intuitive, so the odds ratio, which results from taking the exponential of the coefficient, is computed for a different interpretation. Table 3.6c gives an odds ratio of 1.79 (an odds ratio of 1.79 is equivalent to a probability of 0.64), which indicates that the odds of winter El Niño occurrence increase by 179% for every 1-unit increase in the average (previous) summer MEI. The confidence interval shows how uncertainty in the average summer MEI can affect the probability of El Niño occurrence during the following winter. The confidence interval is wide, which suggests that the coefficient for average summer MEI is not exact. The results of the z-test (Table 3.6b) also seem to indicate that the null hypothesis (that there is no relationship between average summer MEI and winter El Niño occurrence) cannot be rejected.

However, while the plot of the average winter MEI as a function of the average summer MEI (Figure 3.11) does show that the summer and winter indices are not perfectly related, the currently moderate skill levels of ENSO forecasting models (and the MEI's reputation as one of the best indices for overall monitoring of the ENSO phenomenon) should also be considered when evaluating this model. In other words, while this model is not perfect, it is probably good enough for making rough predictions. Figure 3.12 provides a visual representation of the chances that El Niño (average winter MEI ≥ 1) will occur during the winter following a given summer average MEI. The points are spaced at intervals of 0.41 along the x-axis (because the average summer MEI ranges from -1.45 to 2.68 and including the highest and lowest average summer MEI values, 10 evenly spaced average summer MEI values were chosen for the plot).

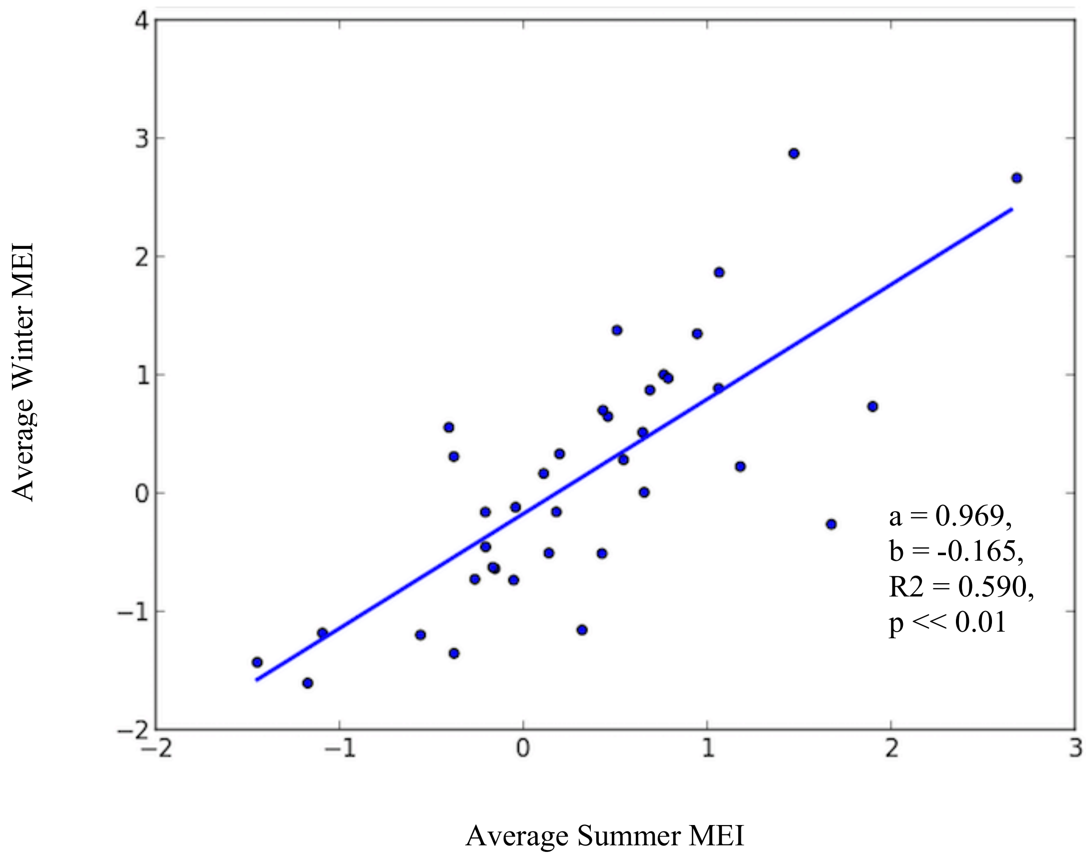

Figure 3.11 The average winter Multivariate ENSO Index (MEI) as a function of the average (previous) summer MEI from 1975 to 2012.

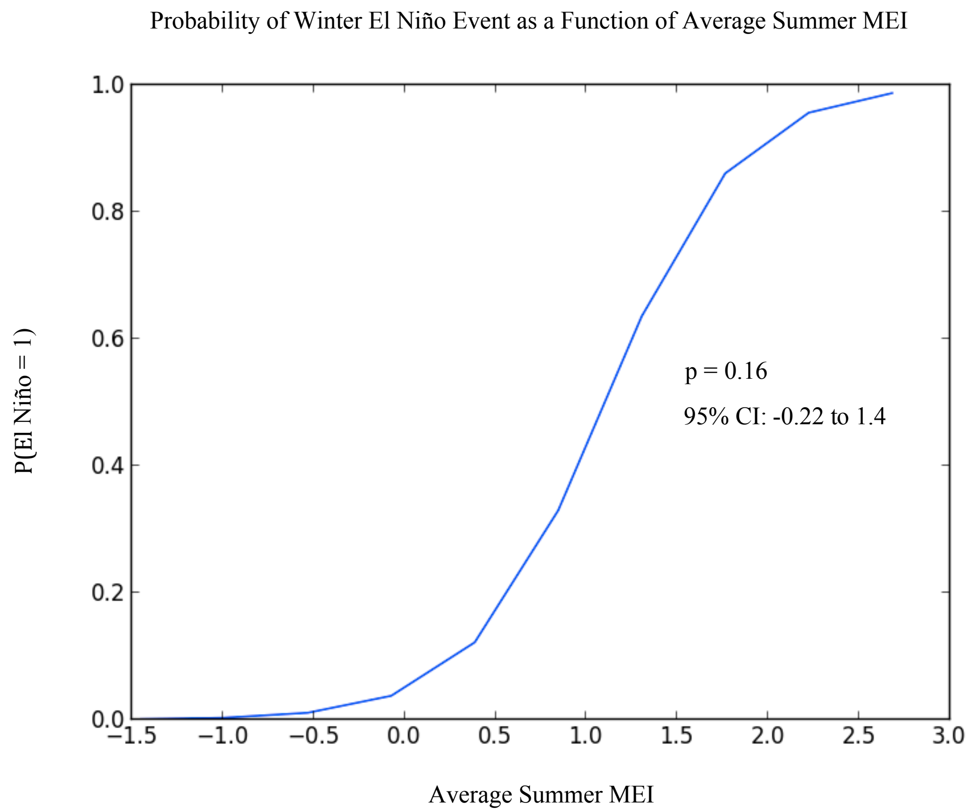

Figure 3.12 The probability of winter El Niño occurrence as a function of the previous summer's average MEI. Table 3.6 contains information about the logistic regression fit quality and odds ratio.

Table 3.6: *Results of logistic regression analysis of the probability of winter El Niño occurrence as a function of the previous summer's average MEI. Reports are shown for (a) overall model fit quality, (b) coefficient and fit, and (c) odds ratio (OR) and confidence interval.*

A.

Logit Regression Results			
Dep. Variable:	El Niño	Df Residuals:	36
Model:	Logit	Df Model:	0
Method:	MLE	Pseudo R-squ.:	-0.2696
converged:	True	Log-Likelihood:	-24.524
		LL-Null:	-19.317
		LLR p-value:	1.000

B.

name of term	coef	std err	z	P>|z|	[95.0% Conf. Int.]	
average_summer_mei	0.5824	0.411	1.418	0.156	-0.223	1.388

C.

Odds Ratio and Confidence Interval			
name of term	2.5%	97.5%	OR
average_summer_mei	0.8003	4.005	1.790

3.4.6 Summertime ENSO Forecasting: Combining the Multivariate El Niño Southern Oscillation (ENSO) Index (MEI) with Significant Wave Height (H_{sig})

From the above analysis, it is clear that the average summer MEI is by itself a good predictor of the average winter MEI. In contrast, while there appears to be a robust (albeit very small) trend in the (normalized) El Niño summer H_{sig} observed data (section 3.4.2), there is only a weak relationship between summer H_{sig} percentage difference and the average winter MEI (section 3.4.3), so it does not make sense to try to predict winter ENSO conditions (based on the average winter MEI, at least) using the summer H_{sig} data alone. However, it is possible to use a combination of the average summer MEI and average summer H_{sig} to see whether the inclusion of H_{sig} data can improve the average summer MEI vs. average winter MEI model (section 3.4.5). To that end, multiple linear regression analyses were performed for each buoy, using x_1 = average summer MEI, x_2 = summer average H_{sig}, and y = average winter MEI, as described in section 3.3.7.

Table 3.7 shows the results of the ordinary least-squares (OLS) multiple regression analysis for station 46014. Results for the other stations, which are similar to station 46014's, are contained in Appendix G (and Supplemental File 8). In Table 3.7a, "coef" is the estimated value of the coefficient. Each coefficient provides an indication of the impact of a change in its associated variable (x_1 or x_2) after accounting for the other variable (x_2 or x_1, respectively). A coefficient of zero (or nearly zero) indicates that the associated explanatory variable is not helpful for the model. As expected, the signs on the coefficients are consistent with the relationships between the respective variables and the average winter MEI (Table 3.4; Appendix F; Figure 3.11). The report (Table 3.7a) shows that the coefficient for the average summer MEI (x_1) is significant with greater than 95% confidence (in relation to x_2) and in all likelihood, describes a real relationship with the average winter MEI. The same cannot be said of the coefficient for summer average H_{sig} (x_2), which has only a 93.4% chance of describing a real relationship (in relation to x_1) with the average winter MEI (and thus does not contribute significantly to the model). In Table 3.7b, "Adj. R-squared" is an adjustment of R2 that accounts for the fact that R2 generally increases as the number of independent variables increases, even when irrelevant variables are included, because increasing the number of parameters improves the fit of the regression line. According to Table 3.7b, an adjusted R2 of 0.61 indicates that

61% of the variance in the observed values of the dependent variable (average winter MEI) is explained by the model, while 39% of the differences remain unexplained (in the error term). While this model is a huge improvement over using just the summer average H_{sig} to predict the average winter MEI (Table 3.4), the improvement over using just the average summer MEI to predict the average winter MEI (Figure 3.11) is tiny, at just 2%.

A biased model might perform well in some areas or given a particular range of values for the dependent variable (average winter MEI, y) but otherwise perform poorly in general. However, the R2 value cannot reveal such biases. Thus, additional tests are conducted to assess the distribution of the residuals (over/under predictions). For instance, OLS assumes that the relationships in the model are linear. In a properly specified OLS model, the residuals are normally distributed about a mean of zero, whereas a biased model might be skewed positively or negatively (and/or it could be affected by outliers). In Table 3.7c, "Jarque-Bera(JB)" and "Prob(JB)" indicate whether skewness and kurtosis are statistically significant. A histogram of the summer H_{sig} data for station 46014 shows that the data are positively skewed (Figure 3.13). If this were a significant issue, performing a log transformation on the H_{sig} data (to increase its linearity) could potentially reduce the bias, but the Jarque-Bera test indicates that skewness does not affect the whole model significantly, which does not come as a surprise, given how little the H_{sig} data contribute to the fit. Ultimately, there is no compelling reason to recommend combining the average summer MEI with summer average H_{sig} data to predict the average winter MEI.

Table 3.7: *Results of the ordinary least-squares (OLS) multiple (linear) regression analysis for station 46014, with x_1 = average summer MEI, x_2 = summer average H_{sig}, and y = average winter MEI. Reports are shown for (a) each coefficient, (b) model fit and goodness of fit, and (c) statistical tests for assessment of the distribution of the residuals. (Appendix G contains results from the other stations.)*

A.

Station 46014						
name of term	coef	std err	t	P > |t|	[95.0% Conf. Int.]	
x1	0.9248	0.159	5.819	0.000	0.599	1.251
x2	-0.0356	0.019	-1.913	0.066	-0.074	0.003
const	-0.1916	0.142	-1.347	0.189	-0.483	0.100

B.

Dep. Variable:	y	R-squared:	0.637
Model:	OLS	Adj. R-squared:	0.610
Method:	Least Squares	F-statistic:	23.67
No. Observations:	30	Prob (F-statistic):	1.16E-06
Df Residuals:	27	Log-Likelihood:	-30.725
Df Model:	2	AIC:	67.45
		BIC:	71.65

C.

Omnibus:	1.389	Durbin-Watson:	2.130
Prob(Omnibus):	0.499	Jarque-Bera(JB):	0.561
Skew:	-0.299	Prob(JB):	0.755
Kurtosis:	3.300	Cond. No.	10.1

Station 46014

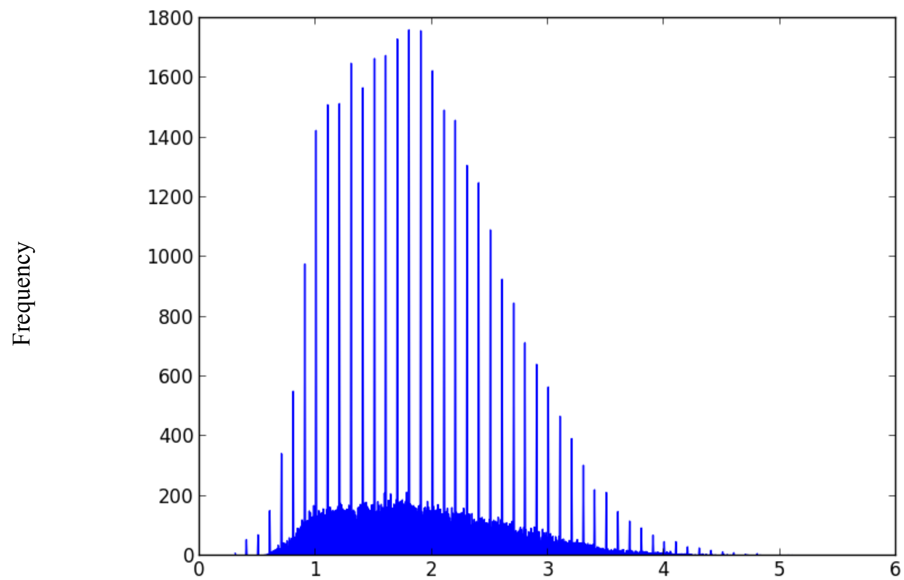

H_{sig} (m)

Figure 3.13 Histogram of all summer H_{sig} data from station 46014 for the1981-2012 period. Combed effect is due to the relatively small binwidth.

3.4.7 Summer Significant Wave Height (H_{sig}): Explaining the Trend

Part of a recent study (Seymour 2011) examined monthly mean H_{sig} values from U.S. West Coast buoys (NDBC and CDIP) in relation to monthly means of three climate indices [Pacific Decadal Oscillation (PDO, which measures sea surface temperature), Multivariate ENSO Index (MEI, which indicates ENSO condition), and Northern Pacific (NP Index or "NPI," which measures the mean sea-level pressure over the region 30˚N to 65˚N, 160˚E to 140˚W) Index] over two time periods (1984 to 1995 and 1996 to 2007) for two consolidated regions ("North," including records from Washington in the north to Point Conception in the south; and "Southern

California," including records from south of Point Conception) to determine the degree to which wave energy along the coast can be predicted by the three indices. (The data were split into two time periods for the main purpose of determining whether mean wave energy changed from the first period to the second.) Seymour (2011) found that monthly mean H_{sig} records are strongly associated with the NP Index over both regions and time periods, whereas neither the MEI nor the PDO are very significantly associated with the data (Table 3.8).

In order to determine the extent to which summer H_{sig} observed data relate to the NP Index, monthly summer H_{sig} percentage difference was plotted as a function of the monthly summer NP Index for each buoy through 2010 (Appendix H), as described in section 3.3.8. Table 3.9, which contains the linear regression coefficients for the plots, shows that there is a strong relationship between monthly summer H_{sig} percentage difference and the monthly summer NP Index, with R2 values ranging from 0.296 to 0.585. Monthly summer H_{sig} percentage difference decreases as the NP Index rises, indicating that monthly H_{sig} percentage difference is lower than average during the summer when the intensity of the Aleutian Low pressure cell in the Gulf of Alaska rises. Most of the plots (Appendix H) appear to have high concentrations or clusters of points on the extreme end of the summer NP Index (around 1015 to 1020 mbar), which suggests that a sizable portion of the monthly H_{sig} percentage differences is low during the summer.

While the R2 values from the monthly summer H_{sig} percentage difference vs. monthly summer NP Index plots (Table 3.9) are high, the regression fits do not fully describe the summer H_{sig} trend. Monthly means of the NP Index, MEI, and PDO all exhibit significant year-to-year and seasonal variability (Figure 3.14), so part of the relationship between the monthly NP Index and the monthly mean H_{sig} could be coincidental, since both time series have well-defined annual cycles (Seymour 2011). The monthly MEI and monthly PDO vary on timescales that are far longer than that of the NP Index. Seymour 2011 investigated the possibility of associations among combinations of the three indices because the influence of the MEI and the PDO could be important for producing extreme wave heights, as a result of coincidence with each other or with the atmospheric pressure in the Gulf of Alaska (as would be indicated by the NP Index). Table 3.10 shows the significant relationships among the indices. The NP Index is weakly and negatively associated with the PDO during the 1996-2007 period, which suggests that atmospheric pressure near the Aleutian Islands trends toward low values when sea surface temperatures are warm in the Pacific (and conditions for El Niño are favorable), but the NP Index is not significantly associated with the MEI (Seymour 2011).

Some of the spread in the monthly summer H_{sig} percentage difference vs. monthly summer NP Index plots (Table 3.9 and Appendix H) is likely due to local random noise, but changes in wave energy at particular stations can also result from a persistent shift in the proximity or orientation of storm activity or from changes in storm intensity (Bromirski et al. 2005). The wave climate in the U.S. northeast Pacific is characterized by three dominant modes: the northern hemisphere swell, the southern hemisphere swell, and local wind-driven seas (Moffatt and Nichol Engineers

1989). Northern hemisphere swell is usually generated by cyclones off the Aleutian Islands in the north Pacific, but it can also be produced by subtropical storms north of Hawaii, tropical hurricanes, and strong winds in the eastern Pacific (Flick 1994). During the summer, southern hemisphere swell is generated by storms and cyclones off New Zealand, Indonesia, Central and South America, generally producing smaller waves (with very long periods of $T \geq 20$ s because of the intensity and persistence of storms in the Antarctic vicinity) than does northern hemisphere swell (Benumof et al. 2000). Local wind-driven swell develops rapidly when low-pressure systems track near the coastline during the winter and when strong sea breezes are generated during the spring and summer (Benumof et al. 2000). Unfortunately, wave direction records are limited, so there is some ambiguity as to cause(s) of changes in the observed H_{sig} data. That is to say, without looking at wave spectral density data, which would allow for some differentiation between distant and local wave generation, it is difficult to tell whether changes in H_{sig} result primarily from changes in storm intensity, storm location (shifting storm tracks), or from a combination of the two (Bromirski et al. 2005).

Table 3.8: *Linear regression fits for regional monthly mean significant wave heights (H_{sig}) vs. monthly means of the Northern Pacific Index (NPI), the Pacific Decadal Oscillation (PDO), and the Multivariate ENSO Index (MEI) for U.S. West Coast buoys over two time periods (from Seymour 2011).*

Era	Region	Index	R	Limit
1984–1995	North	NPI	−0.599	>99%
1984–1995	So. Calif.	NPI	−0.538	>99%
1996–2007	North	NPI	−0.714	>99%
1996–2007	So. Calif.	NPI	−0.671	>99%
1996–2007	So. Calif	PDO	0.163	95%
1984–1995	So. Calif.	MEI	0.125	>85%
1996–2007	North	MEI	−0.134	>85%

Table 3.9: *Linear regression coefficients for the plots (plots are contained in Appendix H) of the monthly summer significant wave height (H_{sig}) percentage difference vs. the monthly summer Northern Pacific (NP) Index for each buoy.*

Region	Station	Monthly Summer Northern Pacific Index vs. Monthly Summer H_{sig} Percentage Difference			
		a	b	R2	p < 0.05?
Washington	46041	-4.54	4600	0.358	yes
	46029	-4.50	4557	0.376	yes
	36	-4.72	4779	0.410	yes
	46005	-5.23	5296	0.521	yes
Oregon	46050	-4.72	4779	0.448	yes
	46002	-4.52	4574	0.455	yes
Northern California	46027	-3.56	3601	0.428	yes
	46006	-6.00	6079	0.585	yes
	46022	-3.83	3877	0.437	yes
	46014	-3.17	3214	0.427	yes
Central California	46059	-4.27	4325	0.436	yes
	46013	-3.08	3123	0.409	yes
	46026	-3.46	3502	0.434	yes
	46012	-3.11	3149	0.381	yes
	46042	-3.19	3227	0.406	yes
	46028	-2.37	2399	0.296	yes
Southern California	76	-3.90	3953	0.544	yes
	46011	-3.27	3310	0.391	yes
	46023	-2.73	2763	0.362	yes
	71	-2.74	2777	0.415	yes
	46054	-3.19	3228	0.468	yes
	46053	-3.49	3535	0.514	yes
	46025	-2.91	2947	0.383	yes
	92	-3.06	3100	0.477	yes
	45	-1.06	1073	0.117	yes
	93	-2.58	2612	0.298	yes
	46047	-2.54	2567	0.384	yes

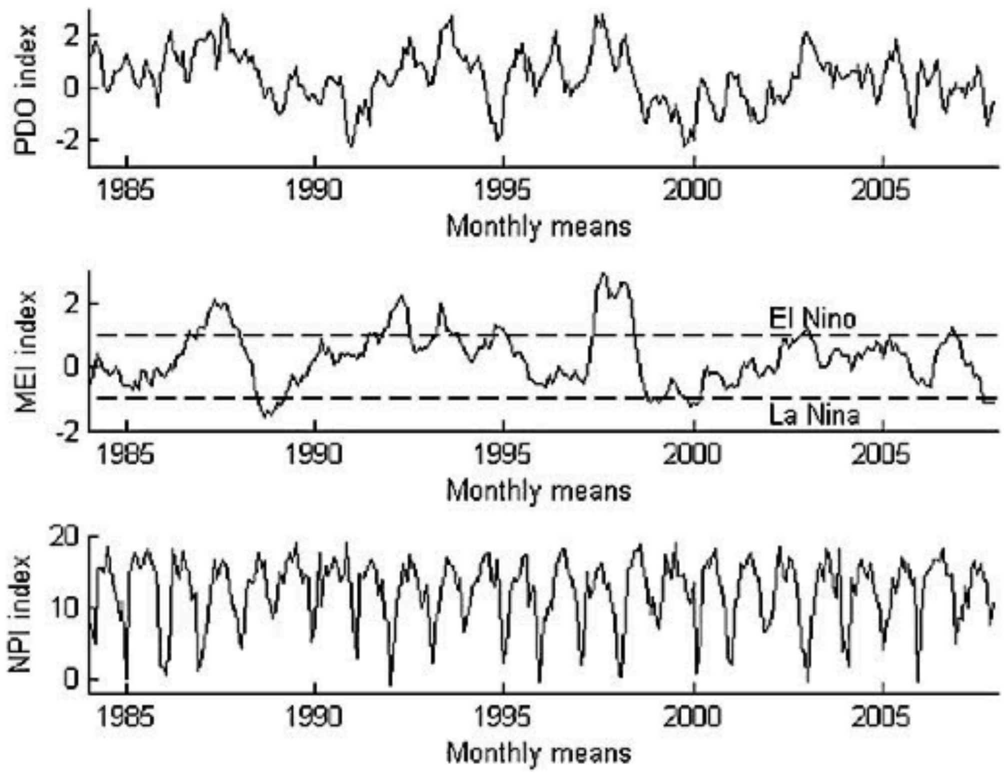

Figure 3.14 Time series of the monthly means of the Pacific Decadal Oscillation (PDO), Multivariate ENSO Index (MEI), and Northern Pacific Index (NPI) show significant variation over different time scales (from Seymour 2011).

Table 3.10: *Significant relationships among climate indices, including the Northern Pacific Index (NPI), the Pacific Decadal Oscillation (PDO), and the Multivariate ENSO Index (MEI) over two time periods (from Seymour 2011).*

Era	Index pair	R	Limit
1984–1995	MEI/PDO	0.316	>99%
1996–2007	MEI/PDO	0.637	>99%
1996–2007	NPI/PDO	−0.164	>95%

3.5 CONCLUSIONS

The El Niño Southern Oscillation (ENSO) is a pattern of climate variability that occurs across the tropical Pacific Ocean and atmosphere semi-periodically, about every two to seven years. One of ENSO's two main phases, El Niño, has been known to cause costly floods and coastal erosion across the U.S. West Coast during strong events, due to a combination of elevated water levels, storm surges, and wind-driven waves, so predicting ENSO events is critical for coastal planning purposes (Allan and Komar 2006). While scientists have made great strides in ENSO forecasting since the mid-1980's, the best frameworks have mostly stalled at a moderate level, leaving room for improvement in ENSO observing systems, models, and data assimilation methods (Chen and Cane 2008).

In the hierarchy of ENSO prediction models, purely statistical systems are usually at a disadvantage (compared to fully coupled models and hybrid models) because of their inability to describe the physics of the ocean-atmosphere system, the short timespan of oceanic and atmospheric observations, and the lack of freedom to adjust parameters as information evolves. However, Ludescher et al.'s (2014) model, which uses an alternative forecasting approach (Ludescher et al. 2013) based on complex network analysis (Tsonis et al 2006; Yamasaki et al. 2008; Donges et al. 2009; Gozolchiani et al. 2011), appears to be able to predict the occurrences of El Niño events by about one year in advance, thus overcoming the "spring barrier" (Webster 1995; Goddard et al. 2001) that has prevented other models from detecting

El Niño events by more than six months in advance and suggesting that there may be hope for purely statistical ENSO frameworks.

Currently, one of the biggest obstacles to ENSO prediction is NOAA's recent failure (due to 2012 budget cuts) to maintain the Tropical Atmosphere Ocean array (TAO), which normally provides real-time measurements of the temperature of the upper layer of the tropical Pacific Ocean (to a depth of 500 meters) and the atmospheric conditions above it, playing a crucial role in ENSO prediction (Latif et al. 1998; McPhaden et al. 1998; Neelin et al. 1998). Scientists are now partially blind to early El Niño development in the tropical Pacific, since nearly half of the buoys in the array have failed during the last two years (Tollefson 2014). NOAA is dedicated to restoring most of the array by the end of 2014.

Gaps or dropouts in ENSO observing systems and a lack of observational data for sufficient coupled model initialization (Chen and Cane 2008) call for the use of proxy data and the exploration of existing oceanographic data that have not traditionally been employed in ENSO prediction. For instance, no previous studies have attempted to determine whether significant wave height (H_{sig}) data from buoys off the U.S. West Coast are predictive of ENSO, although it is clear that wave heights in that region are affected by the phenomenon (Storlazzi and Griggs 2000; Graham and Diaz 2001; Allan and Komar 2002).

In this study, significant wave height (H_{sig}) data from 27 deep-water buoys located off the U.S. West Coast (operated by NOAA's National Data Buoy Center and Scripps Institution of Oceanography's Coastal Data Information Program) were examined to determine whether they could provide a predictive lead on El Niño. This study finds the following:

- While it appears that on the whole, El Niño summer average H_{sig} values are slightly lower than non-El Niño summer average H_{sig} values at most stations, the standard deviations are high, indicating a fair amount of variability over the season (Table 3.2).
- Plotting the average winter Multivariate ENSO Index (MEI) as a function of the percentage difference between the average (previous) summer H_{sig} for each year and the overall average summer H_{sig} for each buoy over its timespan of available summer H_{sig} data (through 2012) yields 7/27 stations with summer H_{sig} percentage differences that relate significantly to the average winter MEI (Table 3.4). In each of those cases, the average winter MEI increases as summer H_{sig} percentage difference decreases. The data are not tightly clustered, but 19/27 of the plots have negative slopes (Appendix F). An exact, two-tailed binomial test puts the likelihood of the actual outcome (19/27 plots with negative slopes) at $p = 0.052$, which falls just short of significance but still seems unusual, given the expected outcome (50:50 positive and negative slopes for a normal distribution).
- According to confidence intervals (CI) generated through a Monte Carlo simulation of linear regression analyses of summer H_{sig} percentage difference vs. the average (following) winter MEI (Figure 3.10), seven of the negative slopes (and one positive slope) from the observed summer H_{sig} percentage

difference vs. average winter MEI plots (Table 3.4) are significant at the 97.5% level. This suggests that the weak trend in the observed summer H_{sig} data (average H_{sig} during El Niño summers is slightly lower than during neutral and La Niña summers) may be robust and not due to natural variation.

- An analysis of yearly H_{sig} percentage difference vs. the average (following) winter MEI (section 3.4.4) shows that the yearly data are a bit more random than the summer H_{sig} data and thus have lower predictive potential than the summer data. However, in either case, the relationship between H_{sig} percentage difference and the winter MEI is weak and there is too much noise to consider using H_{sig} as an ENSO predictor on its own.
- A plot of winter MEI as a function of the average (previous) summer MEI over the 1975 to 2012 time period shows that the average summer MEI is by itself an excellent predictor of the average winter MEI [R2 = 0.59 is good, given the current status of ENSO forecasting (Barnston et al. 1999; Chen and Cane 2008)], with the average winter MEI increasing as a function of an increasing average summer MEI (Figure 3.11). This comes as no surprise, as the MEI is regarded as one of the best indices for overall ENSO monitoring (Wolter and Timlin 2011).
- Since consensus forecasts are usually far more skillful than individual models (Kirtman et al. 2002), multiple linear regression analyses were performed for each buoy, using x_1 = average summer MEI, x_2 = summer average H_{sig}, and y = average winter MEI (section 3.3.7) to see whether the addition of H_{sig} data

could improve the ability of the average summer MEI to forecast ENSO conditions. Although the combination model is much better than using only the summer average H_{sig} to predict the average winter MEI, it is unreasonable to recommend combining the average summer MEI with summer average H_{sig} data to predict the average winter MEI because the improvement over using just the average summer MEI to predict the average winter MEI (Figure 3.11) is negligible, at just 2%.

- Plots of monthly summer H_{sig} percentage difference as a function of the monthly summer Northern Pacific (NP) Index (which measures the mean sea-level pressure over the region 30˚N to 65˚N, 160˚E to 140˚W, indicating the intensity of the Aleutian Low pressure cell in the Gulf of Alaska), for each buoy through 2010 (Appendix H) suggest that the summer H_{sig} observed data may be largely explained by the NP Index (Table 3.9), with monthly summer H_{sig} percentage difference decreasing as the NP Index rises.
- Some of the spread in the monthly summer H_{sig} percentage difference vs. monthly summer NP Index plots (Table 3.9 and Appendix H) is likely due to local random noise, but without adequate wave direction information, it is difficult to say whether differences in wave energy result from persistent shifts in the proximity or orientation of storm activity, changes in storm intensity, or some combination of the two (Bromirski et al. 2005). Some of the summer H_{sig} differences could be explained by southern hemisphere swell generated by storms and cyclones off New Zealand, Indonesia, Central and

South America, which generally produce smaller waves than does the predominating northern hemisphere swell (Benumof et al. 2000). Another source is local wind-driven swell, which develops rapidly when strong sea breezes are generated during summer (Benumof et al. 2000). Perhaps these effects are heightened (to a small degree) during the summers leading up to El Niño winters.

While there is no good reason to use summer H_{sig} observed data from off the U.S. West Coast in ENSO prediction, it is interesting to note that there appears to be a weak relationship between summer H_{sig} and the winter MEI, as this contributes to the growing body of knowledge about ENSO. Further study could benefit from the use of wave hindcasts, such as the ERA-40 wave reanalysis, which extends back in time to 1957 (http://www.ecmwf.int/products/data/archive/descriptions/e4/), or NCEP (http://www.ncep.noaa.gov/), which extends back to 1948. This would both lengthen the observed H_{sig} dataset (from the buoys) substantially beyond its currently limited (~30-year) timespan and smooth over any dropouts in the raw data.

3.6 REFERENCES

Akaike, H. (1974), A new look at the statistical model identification, *IEEE Transactions on Automatic Control*, *19*, 716-723.

Allan, J.C., and P.D. Komar (2002), Extreme storms on the Pacific Northwest Coast during the 1997–98 El Niño and 1998–99 La Niña, *Journal of Coastal Research*, *18*(1), 175–193.

Allan, J.C., and P.D. Komar (2006), Climate controls on US West Coast erosion processes, *Journal of Coastal Research*, *22*(3), 511–529, doi:10.2112/030108.1.

Barnett, T.P., N.E. Graham, N.A. Cane, S.E. Zebiak, S.C. Dolan, J.J. O'Brien, and D.M. Legeler (1988), On the prediction of the El Niño of 1986-1987, *Science*, *241*, 192-196.

Barnett, T.P., N. Graham, S. Pazan, W. White, M. Latif, and M. Flügel (1993), ENSO and ENSO-related predictability, Part I: Prediction of equatorial Pacific sea surface temperature with a hybrid coupled ocean–atmosphere model, *Journal of Climate*, *6*, 1545-1566.

Barnston, A.G., M.H. Glantz, and Y.X. He (1999), Predictive skill of statistical and dynamical climate models in SST forecasts during the 1997/98 El Niño episode and the 1998 La Niña onset, *Bulletin of the American Meteorological Society*, *80*, 217-243.

Barnston, A.G., and C.F. Ropelewski (1992), Prediction of ENSO episodes using canonical correlation analysis, *Journal of Climate*, *5*, 1316-1345.

Barnston, A.G., H.M. van den Dool, S.E. Zebiak, T.P. Barnett, M. Ji, D.R. Rodenhuis, M.A. Cane, A. Leetma, N.E. Graham, C.R. Ropelewski, V.E. Kousky, E.A. O'Lenic, and R.E. Livezey (1994), Long-lead seasonal forecasts—where do we stand?, *Bulletin of the American Meteorological Society*, *75*, 2097-2114.

Battisti, D.S., and A.C. Hirst (1989), Interannual variability in a tropical atmosphere-ocean model: Influence of the basic state, ocean geometry, and nonlinearity, *Journal of Atmospheric Science*, *46*, 1687-1712.

Benumof, B.T., C.D. Storlazzi, R.J. Seymour, and G.B. Griggs (2000), The relationship between incident wave energy and seacliff erosion rates: San Diego County, California, *Journal of Coastal Research*, *16*, 1162-1178.

Bjerknes, J. (1969), Atmospheric teleconnections from the equatorial Pacific, *Monthly Weather Review*, *97*, 163-172.

Bromirski, P.D., D.R. Cayan, and R.E. Flick (2005), Wave spectral energy variability in the northeast Pacific, *Journal of Geophysical Research*, *110*, 15 pp.

Bromirski, P.D., R.E. Flick, and D.R. Cayan (2003), Storminess variability along the California coast: 1858–2000, *Journal of Climate*, *16*(6), 982–993, doi:10.1175/1520-0442(2003)016<0982:SVATCC>2.0.CO;2.

Brönnimann, S., J. Luterbacher, J. Staehelin, T.M. Svendby, G. Hansen, and T. Svenøe (2004), Extreme climate of the global troposphere and stratosphere in1940-42 related to El Niño, *Nature*, *431*, 971-974.

Burnham, K.P., and D.R. Anderson (2002), *Model selection and multimodel inference: a practical information-theoretic approach*, Springer.

Cane, M.A., M. Munnich, and S.E. Zebiak (1990), A study of self-excited oscillations of the tropical ocean-atmosphere system. Part 1: Linear analysis, *Journal of Atmospheric Science*, *47*, 1562-1577.

Cane, M.A., and S.E. Zebiak (1985), A theory for El Niño and the Southern oscillation, *Science*, *228*, 1085-1087.

Cane, M.A., S.E. Zebiak, and S.C. Dolan (1986), Experimental forecasts of El Niño, *Nature*, *321*, 827-832.

Chelton, D.B., and R.E. Davis (1982), Monthly mean sea-level variability along the west coast of North America, *Journal of Physical Oceanography*, *12*, 757-784.

Chen, D., and M.A. Cane (2008), El Niño prediction and predictability, *Journal of Computational Physics*, 227, 3625-3640.

Chen, D., M.A. Cane, A. Kaplan, S.E. Zebiak, and D. Huang (2004), Predictability of El Niño over the past 148 years, *Nature*, *428*, 733-736.

Clarke, A.J., and S. Van Gorder (2003), Improving El Niño prediction using a space-time integration of Indo-Pacific winds and equatorial Pacific upper ocean heat content, *Geophysics Research Letters*, *30*, 1399, doi:10.1029/2002GL016673.

Committee on Sea-Level Rise in California, Oregon, and Washington; Board on Earth Sciences and Resources; Ocean Studies Board; Division on Earth and Life Studies; National Research Council (2012), *Sea-level rise for the coasts of California, Oregon, and Washington: Past, present, and future*. Washington, DC: National Academies Press, 275 pp. Available at: http://www.nap.edu/catalog.php?record_id=13389

Corral, A., A. Ossó, and J.E. Llebot (2010), Scaling of tropical-cyclone dissipation, *Nature Physics*, *6*, 693-696.

Davis, M. (2001), *Late Victorian Holocausts: El Niño Famines and the Making of the Third World*, Verso, London.

Donges, J.F., Y. Zou, N. Marwan, and J. Kurths (2009), The backbone of the climate network, *EPL (Europhysics Letters)*, *87*, 48007.

Donnelly, J.P., and J.D. Woodruff (2007), Intense hurricane activity over the past 5,000 years controlled by El Niño and the West African monsoon, *Nature*, *447*, 465-468.

Enfield, D.B., and J.S. Allen (1980), On the structure and dynamics of monthly mean sea level anomalies along the Pacific coast of North and South America, *Journal of Physical Oceanography*, *10*, 557–578, doi:10.1175/1520-0485(1980)010<0557:OTSADO>2.0.CO;2.

Flick, R.E. (1994), *Shoreline Erosion Assessment and Atlas of the San Diego Region,* Volume 1, Sacramento, California: Department of Boating and Waterways and the San Diego Association of Governments, 135 pp.

Flick, R.E. (1998), Comparison of tides, storm surges, and mean sea level during the El Niño winters of 1982-83 and 1997-98, *Shore & Beach*, *66*, 7-17.

Goddard, L., S.J. Mason, S.E. Zebiak, C.F. Ropelewski, R. Basher, and M.A. Cane (2001), Current approaches to seasonal to interannual climate predictions, *International Journal of Climatology*, *21*, 1111-1152.

Gozolchiani, A., S. Havlin, and K. Yamasaki (2011), Emergence of El Niño as an autonomous component in the climate network, *Physical Review Letters*, *107*, 148501.

Graham, N.E., and H.F. Diaz (2001), Evidence for intensification of North Pacific winter cyclones since 1948, *Bulletin of the American Meteorological Society*, *82*, 1869–1893, doi:10.1175/1520-0477(2001)082<1869:EFIONP>2.3. CO;2.

Graham, N.E., J. Michaelsen, and T.P. Barnett (1987), An investigation of the El Niño-Southern oscillation cycle with statistical models. 2. Model results, *Journal of Geophysical Research*, *92*, 14271-14289.

Griggs, G.B., and K. Brown (1998), Erosion and shoreline damage along the Central California coast: A comparison between the 1997-98 and 1982-83 winters, *Shore & Beach*, *66*(3), 18-23.

Griggs, G.B., K.B. Patsch, and L.E. Savoy (2005). *Living with the changing California coast*. University of California Press: 540 pp.

Heberger, M., H. Cooley, P. Herrera, P.H. Gleick, and E. Moore (2009), *The impacts of sea-level rise on the California coast*. The Pacific Institute, 99 pp. www.pacinst.org/reports/sea_level?rise/report.pdf

Heberger, M., H. Cooley, P. Herrera, P.H. Gleick, and E. Moore (2011), Potential impacts of increased coastal flooding in California due to sea-level rise, *Climatic Change*, *109*, 229-249.

Huyer, A., and R.L. Smith (1985), The signature of El Niño off Oregon, 1982–1983, *Journal of Geophysical Research*, *90*(C4), 7133–7142, doi:10.1029/JC090iC04p07133.

Inoue, M., and J.J. O'Brien (1984), A forecasting model for the onset of El Niño, *Monthly Weather Review*, *112*, 2326-2337.

International Research Institute for Climate and Society Earth Institute, IRI/CPC ENSO Quick Look, available at http://iri.columbia.edu/our-expertise/climate/forecasts/enso/.

Ji, M., A. Kumar, and A. Leetma (1994), An experimental coupled forecast system at the National Meteorological Center: some early results, *Tellus*, *46A*, 398-418.

Ji, M., and A. Leetma (1997), Impact of data assimilation on ocean initialization and El Niño prediction, *Monthly Weather Review*, *125*, 742-753.

Jin, F.F. (1997), An equatorial recharge paradigm for ENSO. Part I: Conceptual model, *Journal of Atmospheric Science, 54*, 811–829, doi:10.1175/1520-0469(1997)054<0811:AEORPF>2.0.CO;2.

Kaminsky, G.M., P. Ruggiero, and G.R. Gelfenbaum (1998), Monitoring coastal change in southwest Washington and northwest Oregon during the 1997/98 El Niño, *Shore & Beach*, *66*(3), 42–51.

Kirtman, B.P., J. Shukla, M. Balmaseda, N. Graham, C. Penland, Y. Xue, and S. Zebiak (2002), Current status of ENSO forecast skill. A report to the Climate Variability and Predictability (CLIVAR) Numerical Experimentation Group (NEG), CLIVAR Working Group on Seasonal to Interannual Prediction.

Kirtman, B.P., J. Shukla, B. Huang, Z. Zhu, and E.K. Schneider (1997), Multiseasonal predictions with a coupled tropical ocean global atmosphere system, *Monthly Weather Review*, *125*, 789-808.

Kleeman, R. (1991), A simple model of the atmospheric response to ENSO sea surface temperature anomalies, *Journal of Atmospheric Science*, *48*, 3-18.

Komar, P.D., J.C. Allan, and P. Ruggiero (2011), Sea level variations along the U.S. Pacific Northwest coast: Tectonic and climate controls, *Journal of Coastal Research, 27*(5), 808–823. West Palm Beach (Florida), ISSN 0749-0208.

Kovats, R.S., M.J. Bouma, S. Hajat, E. Worrall, and A. Haines (2003), El Niño and health, *Lancet*, *362*, 1481-1489.

Landsea, C.W., and J.A. Knaff (2000), How much skill was there in forecasting the very strong 1997/98 El Niño?, *Bulletin of the American Meteorological Society*, *81*, 2107-2119.

Latif, M., D. Anderson, T. Barnett, M. Cane, R. Kleeman, A. Leetmaa, J.J. O'Brien, A. Rosati, and E. Schneider (1998), A review of the predictability and prediction of ENSO, *Journal of Geophysical Research*, *103*, 14,375-14,393, doi:10.1029/97JC03413.

Ludescher, J., A. Gozolchiani, M.I. Bogachev, A. Bunde, S. Havlin, and H.J. Schellnhuber (2013), Improved El Niño forecasting by cooperativity detection, *Proceedings of the National Academy of Sciences*, *110*, 11742-11745.

Ludescher, J., A. Gozolchiani, M.I. Bogachev, A. Bunde, S Havlin, and H.J. Schellnhuber (2014), Very early warning of next El Niño, *Proceedings of the National Academy of Sciences*, *111*, 2064-2066, doi: 10.1073/pnas.1323058111.

Massey, F.J., Jr. (1951), The Kolmogorov-Smirnov Test for goodness of fit, *Journal of the American Statistical Association*, *46*(253), 68-78.

Matsumoto, M, and T. Nishimura (1998), Mersenne Twister: A 623-dimensionally equidistributed uniform pseudo-random number generator, *Association for Computing Machinery Transactions on Modeling and Computer Simulation*, *8*, 3-30.

McPhaden, M.J. (1999), Genesis and evolution of the 1997-98 El Niño, *Science*, *283*, 950-954.

McPhaden, M.J. (2003), Tropical Pacific Ocean heat content variations and ENSO persistence barriers, *Geophysics Research Letters*, *30*, 1480, doi:10.1029/2003GL016872.

McPhaden, M.J., A.J. Busalacchi, R. Cheney, J.-R. Donguy, K.S. Gage, D. Halpern, M. Ji, P. Julian, G. Meyers, G.T. Mitchum, P.P. Niiler, J. Picaut, R.W. Reynolds, N. Smith, and K. Takeuchi (1998), The Tropical Ocean-Global Atmosphere observing system: A decade of progress, *Journal of Geophysical Research*, *103*, 14169-14240.

Metropolis, N., and S. Ulam (1949), The Monte Carlo method, *Journal of the American Statistical Association*, *44*, 335-341.

Moffatt and Nichol Engineers (1989), *Historic Wave and Sea Level Data Report, San Diego Region*, Coast of California Storm and Tidal Waves Study 88-6, Los Angeles, California: U.S. Army Corps of Engineers.

Neelin, J.D. (1990), A hybrid coupled general circulation model for El Niño studies, *Journal of Atmospheric Sciences*, *47*, 674-693.

Neelin, J.D., D.S. Battisti, A.C. Hirst, F.-F. Jin, Y. Wakata, T. Yamagata, and S.E. Zebiak (1998), ENSO theory, *Journal of Geophysical Research*, *103*, 14261-14290.

Neelin, J.D., M. Latif, and F. Jin (1994), Dynamics of coupled ocean-atmosphere models: The tropical problem, *Annual Review of Fluid Mechanics*, *26*, 617-659.

O'Reilly, W.C., and R.T. Guza (1993), A comparison of two spectral wave models in the Southern California Bight, *Coastal Engineering*, *19*, 263-282.

O'Reilly, W.C., and R.T. Guza (1998), Assimilating coastal wave observations in regional swell predictions. Part I: Inverse methods, *American Meteorological Society*, *28*, 679-691.

Ryan, H.F., and M. Noble (2002), Sea level response to ENSO along the central California coast: How the 1997–1998 event compares with the historic record, *Progress in Oceanography*, *54*, 149–169, doi:10.1016/S0079-6611(02)00047-2.

Sallenger, A.H., W. Krabill, J. Brock, R. Swift, S. Manizade, and H. Stockton (2002), Sea-cliff erosion as a function of beach changes and extreme wave runup during the 1997–1998 El Niño, *Marine Geology*, *187*, 279–297, doi:10.1016/S0025-3227(02)00316-X.

Seager R., N. Naik, M. Ting, M.A. Cane, N. Harnik, and Y. Kushnir (2010), Adjustment of the atmospheric circulation to tropical Pacific SST anomalies: Variability of transient eddy propagation in the Pacific–North America sector, *Quarterly Journal of the Royal Meteorological Society*, *136*, 277–296, doi:10.1002/qj.588.

Seymour, R.J. (2011), Evidence for changes to the Northwest Pacific wave climate, *Journal of Coastal Research*, *27*, 194-201.
Stahl, S. (2006), The evolution of the normal distribution, *Mathematics Magazine*, *79*, 96-113.

Storlazzi, C.D., and G.B. Griggs (2000), Influence of El Niño-Southern Oscillation (ENSO) events on the evolution of central California's shoreline, *Geological Society of America Bulletin*, *112*(2), 236-249.

Takeuchi, K. (1976), Distribution of informational statistics and a criterion of model fitting, *Suri-Kagaku (Mathematical Sciences)*, *153*, 12-18.

Tang, F.T., W.W. Hsieh, and B. Tang (1997), Forecasting the equatorial Pacific sea surface temperature by neural network models, *Climate Dynamics*, *13*, 135-147.

Tollefson, J. (2014), El Niño tests forecasters, *Nature*, *508*, 20-21.

Trenberth, K.E., and J.W. Hurrell (1994), Decadal atmosphere-ocean variations in the Pacific, *Climate Dynamics*, *9*, 303-319.

Tsonis, A.A., K.L. Swanson, and P.J. Roebber (2006), What do networks have to do with climate?, *Bulletin of the American Meteorological Society*, *87*, 585-595.

Webster, P.J. (1995), The annual cycle and the predictability of the tropical coupled ocean-atmosphere system, *Meteorology and Atmospheric Physics*, *56*, 33-55.

Wen, C. (2002), Impacts of El Niño and La Niña on the cycle of the East Asian winter and summer monsoon, *China Journal of Atmospheric Sciences*, *5*, 595-610.

Wolter, K., and M.S. Timlin (1993), Monitoring ENSO in COADS with a seasonally adjusted principal component index, *Proceedings of the 17th Climate Diagnostics Workshop*, Norman, OK, NOAA/NMC/CAC, NSSL, Oklahoma Climate Survey, CIMMS and the School of Meteorology, University of Oklahoma, 52-57.

Wolter, K. and M.S. Timlin (1998), Measuring the strength of ENSO events: How does 1997/98 rank?, *Weather, Royal Meteorological Society*, *53*(9), 315–324.

Wolter, K., and M.S. Timlin (2011), El Niño/Southern Oscillation behaviour since 1871 as diagnosed in an extended multivariate ENSO index (MEI. ext), *International Journal of Climatology*, *31.7*, 1074-1087.

Xu, J.S., and H. Storch (1990), Principal oscillation patterns – prediction of the state of ENSO, *Journal of Climate*, *3*, 1316-1329.

Xue, Y., A. Leetmaa, and M. Ji (2000), ENSO prediction with Markov models: The impact of sea level, *Journal of Climate*, *13*, 849-871.
Yamasaki, K., A. Gozolchiani, and S. Havlin (2008), Climate networks around the globe are significantly affected by El Niño, *Physical Review Letters*, *100*, 228501.

Zebiak, S.E., and M.A. Cane (1987), A model El Niño-Southern oscillation, *Monthly Weather Review*, *115*, 2262-2278.

APPENDIX A

Number of Significant Wave Height Records by Month and Year

Number of significant wave height (Hsig) records by month and year for each station. El Niño records are highlighted in yellow. Additionally, moderate to strong El Niño records are noted in bold, while missing data are displayed in red text.

Region	Station	Year	# of Hsig Records by Month					
			June	July	August	September	October	November
Washington	46041	1987	506	741	740	674	742	709
		1988	719	739	735	716	740	718
		1989	0	299	733	714	734	711
		1990	709	737	741	698	738	714
		1991	**716**	**733**	**710**	**707**	**732**	**672**
		1992	701	724	716	657	693	648
		1993	653	705	691	662	691	668
		1994	**709**	**700**	**735**	**72**	**0**	**215**
		1995	716	726	647	0	0	242
		1996	717	827	787	715	732	689
		1997	**294**	**0**	**0**	**0**	**0**	**0**
		1998	373	718	759	680	731	692
		1999	169	698	658	642	584	575
		2000	661	704	592	455	699	712
		2001	708	741	721	709	724	689
		2002	**101**	**739**	**738**	**717**	**739**	**719**
		2003	719	707	742	712	738	719
		2004	716	736	740	719	741	715
		2005	716	743	742	708	742	712
		2006	220	742	742	717	737	357
		2007	0	0	0	0	476	710
		2008	720	743	742	720	744	719
		2009	**714**	**741**	**715**	**700**	**700**	**675**
		2010	713	744	744	720	709	623
		2011	720	744	744	718	487	714
		2012	718	742	733	702	713	580
	46029	1984	715	735	726	713	740	710
		1985	0	0	0	0	0	0
		1986	**0**	**0**	**0**	**0**	**0**	**0**
		1987	0	0	0	0	0	0
		1988	0	0	0	0	0	0
		1989	0	0	0	0	0	0

		1990	0	0	0	0	0	0
		1991	0	0	0	0	512	712
		1992	627	740	732	709	732	699
		1993	331	730	732	713	741	716
		1994	712	707	739	710	731	709
		1995	715	730	737	709	725	699
		1996	713	834	787	371	0	0
		1997	711	727	734	713	711	694
		1998	688	727	782	690	738	705
		1999	700	716	702	692	660	595
		2000	590	0	722	716	722	0
		2001	715	742	735	710	743	717
		2002	693	742	742	719	740	720
		2003	712	743	742	711	737	695
		2004	716	740	741	713	736	711
		2005	715	741	740	715	723	694
		2006	713	738	726	664	727	705
		2007	712	740	738	717	732	670
		2008	719	741	743	718	741	712
		2009	244	743	744	720	742	690
		2010	720	744	741	718	726	683
		2011	697	687	675	685	725	675
		2012	0	0	700	715	684	669
	36	1981	0	0	0	0	0	38
		1982	14	7	0	0	34	48
		1983	0	0	0	0	22	0
		1984	0	0	0	0	0	0
		1985	0	0	0	0	0	0
		1986	0	0	0	0	0	0
		1987	143	151	146	159	191	132
		1988	2	116	116	114	108	193
		1989	219	142	0	138	78	0
		1990	237	247	244	235	246	226
		1991	234	240	243	230	244	230
		1992	208	245	244	238	193	138
		1993	211	43	29	432	504	478
		1994	440	494	298	176	495	410
		1995	395	469	438	471	486	456

		1996	1418	1324	1476	1436	1467	481
		1997	**156**	**484**	**458**	**476**	**249**	**0**
		1998	1433	1461	1432	1362	1471	1430
		1999	1368	1397	1429	1439	918	1422
		2000	1428	1456	1487	1423	885	649
		2001	1440	1488	1480	1440	1486	1437
		2002	**1440**	**1484**	**1488**	**1440**	**1488**	**1440**
		2003	1432	1488	1487	1423	1473	1431
		2004	1440	1477	1488	1440	1488	1422
		2005	1434	1487	1481	1437	1476	1430
		2006	1418	1488	1486	1439	1487	339
		2007	1440	1488	1488	1440	1488	1440
		2008	1440	1488	1488	1440	1488	1440
		2009	**1426**	**1488**	**1488**	**1440**	**1488**	**1440**
		2010	586	1488	1488	1440	1488	1440
		2011	1440	1488	1488	1440	1488	1438
		2012	1440	1488	1488	1440	1488	1440
	46005	1976	0	0	0	151	245	239
		1977	0	0	0	0	158	230
		1978	215	241	240	235	246	240
		1979	239	246	256	238	246	240
		1980	211	616	742	712	744	720
		1981	719	742	744	707	720	719
		1982	**720**	**742**	**737**	**715**	**716**	**621**
		1983	711	744	743	718	743	718
		1984	716	738	737	716	739	712
		1985	239	710	707	292	343	0
		1986	**717**	**742**	**738**	**654**	**0**	**0**
		1987	0	258	738	681	742	718
		1988	719	743	737	252	246	39
		1989	704	738	731	715	741	716
		1990	238	246	123	0	0	0
		1991	**717**	**741**	**732**	**714**	**737**	**715**
		1992	717	736	732	706	728	698
		1993	0	68	525	458	741	711
		1994	**716**	**699**	**730**	**704**	**734**	**714**
		1995	715	737	741	693	736	707
		1996	708	832	785	716	537	191

		1997	**711**	**724**	**735**	**713**	**737**	**699**
		1998	686	725	780	696	740	712
		1999	720	735	723	306	425	642
		2000	711	729	739	712	733	710
		2001	713	721	736	718	726	718
		2002	**711**	**736**	**705**	**694**	**736**	**719**
		2003	720	742	740	709	741	715
		2004	715	742	737	705	743	719
		2005	0	0	0	0	0	0
		2006	719	743	739	696	738	718
		2007	716	737	742	717	740	693
		2008	122	743	743	716	738	713
		2009	**0**	**0**	**0**	**0**	**0**	**0**
		2010	120	738	731	662	648	371
		2011	606	743	6	718	743	719
		2012	720	8	0	0	0	0
Oregon	46050	**1991**	**0**	**0**	**0**	**0**	**0**	**303**
		1992	681	725	728	674	684	648
		1993	573	662	614	581	668	596
		1994	**698**	**662**	**732**	**430**	**0**	**0**
		1995	712	741	736	715	738	711
		1996	706	834	549	0	0	0
		1997	**0**	**0**	**6**	**536**	**716**	**683**
		1998	692	737	787	684	741	710
		1999	612	700	715	597	509	680
		2000	718	736	742	718	737	710
		2001	717	743	736	711	730	711
		2002	**718**	**740**	**741**	**718**	**728**	**714**
		2003	719	740	740	712	739	717
		2004	717	738	744	720	743	700
		2005	719	744	744	720	742	719
		2006	717	742	583	505	740	720
		2007	716	739	743	716	742	688
		2008	712	733	737	711	736	706
		2009	**710**	**721**	**720**	**712**	**728**	**685**
		2010	703	714	718	705	721	671
		2011	145	559	741	717	739	703
		2012	696	739	737	715	702	682

	46002	1975	0	0	0	650	716	0
		1976	249	0	195	39	204	240
		1977	47	0	19	238	245	241
		1978	0	0	211	239	246	234
		1979	715	742	741	719	739	720
		1980	719	743	743	713	741	719
		1981	715	741	744	703	720	719
		1982	**718**	**741**	**739**	**714**	**210**	**366**
		1983	707	341	443	713	703	620
		1984	0	0	0	0	0	0
		1985	718	737	717	716	738	717
		1986	**720**	**743**	**743**	**720**	**741**	**451**
		1987	715	742	742	680	740	715
		1988	0	0	0	0	743	717
		1989	703	733	732	715	738	715
		1990	167	739	742	708	739	718
		1991	**716**	**742**	**732**	**719**	**743**	**302**
		1992	718	739	736	712	730	697
		1993	707	722	709	472	734	711
		1994	**706**	**706**	**733**	**711**	**732**	**711**
		1995	716	739	741	716	744	714
		1996	712	839	790	717	734	688
		1997	**0**	**0**	**617**	**715**	**732**	**703**
		1998	686	728	786	702	0	0
		1999	0	0	0	0	0	0
		2000	715	740	739	718	733	712
		2001	716	740	739	713	728	693
		2002	**481**	**542**	**738**	**689**	**712**	**649**
		2003	0	0	0	0	0	0
		2004	75	739	742	720	742	711
		2005	718	710	0	0	0	0
		2006	167	740	615	716	739	717
		2007	717	742	349	101	734	719
		2008	162	743	744	715	741	719
		2009	**720**	**656**	**0**	**0**	**0**	**0**
		2010	0	0	0	0	0	0
		2011	715	742	742	716	736	717
		2012	719	740	742	719	727	698

Northern California	46027	1983	0	0	0	0	0	0
		1984	0	0	0	0	0	0
		1985	154	740	161	0	348	715
		1986	**717**	**739**	**219**	**0**	**0**	**616**
		1987	709	739	484	516	733	694
		1988	695	663	609	535	0	0
		1989	671	722	726	702	713	700
		1990	695	726	729	702	734	712
		1991	**718**	**734**	**736**	**715**	**294**	**0**
		1992	642	699	672	660	674	680
		1993	0	0	0	694	730	699
		1994	**707**	**704**	**738**	**699**	**727**	**684**
		1995	170	0	0	713	740	709
		1996	707	829	784	712	735	689
		1997	**0**	**0**	**0**	**0**	**0**	**0**
		1998	1	730	257	705	9	0
		1999	605	688	637	625	657	656
		2000	636	649	662	636	676	715
		2001	712	723	740	716	732	720
		2002	**707**	**740**	**719**	**719**	**721**	**720**
		2003	719	742	743	711	741	719
		2004	720	739	737	720	743	719
		2005	0	0	0	0	219	653
		2006	686	694	702	657	649	714
		2007	695	743	743	720	737	554
		2008	701	708	717	701	730	702
		2009	**705**	**721**	**672**	**691**	**737**	**700**
		2010	676	703	696	688	712	676
		2011	676	704	741	715	738	703
		2012	705	734	737	713	740	717
	46006	1977	234	244	247	239	247	240
		1978	232	248	247	239	248	122
		1979	227	240	626	708	668	703
		1980	0	0	0	0	0	0
		1981	719	744	744	704	719	704
		1982	**719**	**740**	**730**	**715**	**744**	**719**
		1983	712	742	742	717	739	717
		1984	0	0	0	0	0	0

		1985	487	0	244	717	738	718
		1986	**57**	**737**	**734**	**707**	**727**	**688**
		1987	710	741	735	677	736	711
		1988	0	0	600	709	727	681
		1989	701	707	732	695	726	703
		1990	704	731	722	680	725	702
		1991	**0**	**0**	**0**	**0**	**0**	**0**
		1992	330	742	740	708	733	696
		1993	706	732	732	711	736	712
		1994	**709**	**697**	**737**	**704**	**729**	**708**
		1995	710	731	734	699	733	634
		1996	704	825	729	710	717	681
		1997	**534**	**14**	**0**	**0**	**0**	**0**
		1998	462	430	480	588	695	692
		1999	614	615	567	549	672	654
		2000	0	0	300	713	704	657
		2001	708	741	740	700	737	701
		2002	**701**	**722**	**733**	**713**	**704**	**670**
		2003	0	83	743	712	738	720
		2004	718	740	738	720	744	716
		2005	720	743	743	720	743	720
		2006	719	743	743	719	743	462
		2007	0	0	374	664	579	636
		2008	0	0	239	711	733	688
		2009	**716**	**735**	**725**	**704**	**724**	**699**
		2010	0	0	157	658	643	644
		2011	719	744	742	719	739	717
		2012	720	744	744	720	738	719
	46022	**1982**	**697**	**737**	**739**	**713**	**737**	**718**
		1983	714	744	744	715	736	708
		1984	716	739	413	0	0	0
		1985	720	736	736	709	733	715
		1986	**716**	**744**	**739**	**716**	**739**	**149**
		1987	715	741	737	399	76	715
		1988	716	741	735	591	0	0
		1989	687	734	732	715	737	718
		1990	237	81	0	363	739	716
		1991	**716**	**737**	**732**	**717**	**737**	**714**

		1992	709	737	738	712	722	690
		1993	704	727	727	709	736	712
		1994	**708**	**706**	**733**	**713**	**721**	**696**
		1995	242	610	729	693	725	675
		1996	0	0	0	0	0	0
		1997	**708**	**723**	**731**	**708**	**737**	**700**
		1998	0	690	536	708	712	700
		1999	717	740	277	244	605	673
		2000	585	718	735	716	726	709
		2001	713	738	729	698	743	715
		2002	**716**	**715**	**711**	**714**	**729**	**712**
		2003	719	743	743	713	741	137
		2004	716	743	710	0	743	718
		2005	720	742	742	719	744	718
		2006	719	742	736	681	737	719
		2007	710	736	733	716	739	698
		2008	1	731	733	713	715	337
		2009	**720**	**743**	**744**	**720**	**742**	**719**
		2010	0	16	168	713	695	671
		2011	705	737	599	0	0	0
		2012	0	0	0	0	0	1
	46014	1981	714	388	453	303	717	719
		1982	**718**	**742**	**735**	**716**	**741**	**720**
		1983	658	742	742	719	737	712
		1984	715	735	722	700	741	712
		1985	713	729	166	599	740	718
		1986	**605**	**741**	**743**	**717**	**739**	**695**
		1987	715	738	667	680	740	719
		1988	718	742	735	641	0	0
		1989	314	734	736	713	740	719
		1990	716	738	713	687	738	717
		1991	**720**	**742**	**739**	**719**	**7**	**0**
		1992	174	739	739	658	617	574
		1993	703	728	730	712	734	706
		1994	**702**	**707**	**740**	**707**	**727**	**706**
		1995	216	5	740	716	740	713
		1996	711	837	789	717	737	694
		1997	**714**	**734**	**739**	**713**	**736**	**697**

		1998	696	735	783	700	736	712
		1999	718	742	728	707	597	686
		2000	709	736	741	718	727	713
		2001	718	743	742	715	743	718
		2002	**718**	**740**	**741**	**719**	**737**	**719**
		2003	720	741	743	712	741	720
		2004	719	740	742	715	743	719
		2005	720	743	743	720	742	719
		2006	0	0	0	567	741	715
		2007	715	152	378	718	743	703
		2008	719	743	744	719	744	720
		2009	**720**	**744**	**744**	**720**	**743**	**720**
		2010	718	744	743	719	743	662
		2011	0	511	743	719	740	718
		2012	718	743	744	717	743	718
Central California	46059	**1994**	**0**	**0**	**0**	**0**	**307**	**702**
		1995	711	738	743	711	742	714
		1996	710	830	791	713	734	685
		1997	**711**	**727**	**738**	**716**	**737**	**702**
		1998	692	733	784	706	734	708
		1999	718	729	727	709	694	687
		2000	710	733	741	718	734	713
		2001	714	737	736	712	735	715
		2002	**718**	**739**	**733**	**719**	**737**	**719**
		2003	719	743	744	712	738	720
		2004	717	741	616	716	744	716
		2005	0	0	0	0	269	719
		2006	716	742	736	678	737	711
		2007	698	720	723	698	731	689
		2008	695	711	726	707	727	710
		2009	**0**	**0**	**0**	**0**	**0**	**0**
		2010	632	611	138	719	728	685
		2011	709	732	5	718	739	716
		2012	696	0	0	0	0	0
	46013	1981	700	741	133	460	703	553
		1982	**717**	**741**	**740**	**718**	**743**	**720**
		1983	708	741	740	715	732	713
		1984	714	728	403	715	731	702

		1985	647	713	728	698	720	696
		1986	**0**	**0**	**0**	**605**	**740**	**691**
		1987	715	738	740	678	741	360
		1988	719	741	735	704	732	715
		1989	692	695	10	54	739	283
		1990	714	737	187	385	740	718
		1991	**718**	**741**	**735**	**719**	**742**	**717**
		1992	187	723	729	699	711	672
		1993	686	720	729	704	735	711
		1994	**701**	**664**	**720**	**706**	**732**	**715**
		1995	712	740	726	715	739	712
		1996	716	818	777	753	473	517
		1997	**0**	**0**	**0**	**0**	**0**	**0**
		1998	677	720	773	695	677	714
		1999	702	716	719	638	559	676
		2000	703	727	737	718	733	714
		2001	705	739	734	713	738	714
		2002	**716**	**739**	**719**	**718**	**737**	**720**
		2003	622	604	685	313	0	606
		2004	717	737	712	719	744	719
		2005	719	744	739	717	742	718
		2006	717	741	742	695	730	510
		2007	669	717	720	710	734	713
		2008	707	738	729	715	737	710
		2009	**714**	**732**	**734**	**712**	**742**	**211**
		2010	717	743	743	717	734	517
		2011	704	239	741	718	744	715
		2012	710	736	734	708	729	705
	46026	**1982**	**0**	**200**	**547**	**484**	**737**	**711**
		1983	711	740	723	713	740	704
		1984	707	736	731	717	740	664
		1985	718	731	736	709	736	703
		1986	**718**	**742**	**742**	**713**	**738**	**701**
		1987	715	301	0	0	0	0
		1988	388	743	734	328	363	715
		1989	698	711	726	301	738	711
		1990	714	119	0	304	375	718
		1991	**715**	**739**	**740**	**720**	**742**	**716**

		1992	699	488	0	0	685	698
		1993	707	729	729	713	731	715
		1994	**712**	**712**	**740**	**707**	**732**	**706**
		1995	710	739	742	712	732	714
		1996	708	836	788	715	733	692
		1997	**716**	**736**	**734**	**717**	**734**	**704**
		1998	0	0	311	702	741	649
		1999	702	737	732	709	710	674
		2000	711	735	739	716	730	716
		2001	712	744	735	700	743	717
		2002	**716**	**735**	**743**	**719**	**475**	**198**
		2003	719	742	743	712	739	717
		2004	717	740	733	719	743	706
		2005	719	743	741	719	742	719
		2006	718	742	742	702	741	718
		2007	714	738	736	714	732	706
		2008	709	732	739	713	734	712
		2009	**707**	**730**	**736**	**712**	**738**	**719**
		2010	720	744	743	720	722	695
		2011	717	685	0	433	743	713
		2012	718	742	744	718	727	712
	46012	1980	0	0	0	0	0	152
		1981	716	744	743	698	722	718
		1982	**718**	**732**	**737**	**712**	**737**	**719**
		1983	708	742	741	717	737	717
		1984	713	725	625	699	728	700
		1985	717	740	739	715	740	715
		1986	**710**	**167**	**739**	**718**	**737**	**699**
		1987	334	736	739	681	738	714
		1988	713	738	731	716	741	717
		1989	703	733	737	713	740	718
		1990	228	739	742	709	740	717
		1991	**0**	**41**	**738**	**718**	**741**	**717**
		1992	716	741	735	705	730	696
		1993	0	0	0	0	0	0
		1994	**663**	**367**	**318**	**709**	**723**	**702**
		1995	0	77	728	713	741	713
		1996	719	831	789	714	736	695

		1997	**718**	**214**	**0**	**0**	**0**	**0**
		1998	262	725	782	693	729	690
		1999	0	0	67	713	718	676
		2000	0	0	719	665	713	713
		2001	712	740	664	718	740	716
		2002	**631**	**736**	**393**	**493**	**730**	**715**
		2003	503	741	744	713	740	720
		2004	716	742	715	720	741	716
		2005	720	744	743	719	743	718
		2006	718	741	741	695	737	719
		2007	694	733	735	712	727	384
		2008	716	741	558	313	700	680
		2009	**703**	**735**	**743**	**718**	**741**	**716**
		2010	720	744	743	719	730	688
		2011	718	743	743	720	742	707
		2012	651	627	399	7	137	3
	46042	1987	0	0	0	196	0	0
		1988	684	715	707	689	708	678
		1989	680	723	722	700	734	715
		1990	706	737	739	712	741	715
		1991	**715**	**735**	**733**	**711**	**735**	**708**
		1992	714	733	733	672	688	623
		1993	666	670	675	661	719	671
		1994	**697**	**658**	**720**	**705**	**730**	**715**
		1995	716	739	734	711	738	709
		1996	720	834	782	705	736	696
		1997	**716**	**730**	**737**	**719**	**611**	**0**
		1998	261	724	770	687	733	713
		1999	0	0	612	710	715	682
		2000	708	731	740	715	731	714
		2001	717	743	684	714	740	715
		2002	**716**	**737**	**741**	**705**	**738**	**718**
		2003	720	743	743	714	740	719
		2004	719	737	704	717	709	695
		2005	690	739	731	708	742	706
		2006	683	735	734	659	709	700
		2007	632	716	725	707	634	665
		2008	482	479	386	535	449	490

		2009	**710**	**724**	**736**	**713**	**729**	**711**
		2010	719	744	743	719	743	719
		2011	720	744	743	718	744	719
		2012	713	739	743	718	1477	718
	46028	1984	387	738	735	716	744	715
		1985	719	730	743	718	738	717
		1986	**716**	**743**	**741**	**716**	**740**	**695**
		1987	713	738	739	676	694	697
		1988	706	701	698	692	304	0
		1989	712	645	0	36	740	718
		1990	715	738	743	713	741	719
		1991	**714**	**740**	**735**	**719**	**743**	**640**
		1992	438	740	737	710	734	693
		1993	104	736	727	715	739	716
		1994	**714**	**711**	**730**	**707**	**645**	**712**
		1995	712	735	739	714	738	709
		1996	714	836	784	711	736	694
		1997	**719**	**475**	**0**	**0**	**0**	**0**
		1998	0	0	437	700	736	711
		1999	715	737	372	0	0	0
		2000	701	718	736	711	728	712
		2001	702	739	734	697	742	718
		2002	**711**	**732**	**716**	**698**	**732**	**535**
		2003	714	735	740	712	729	715
		2004	698	731	716	688	708	714
		2005	705	742	743	708	742	716
		2006	716	743	738	693	741	719
		2007	708	737	736	716	738	707
		2008	635	622	621	627	639	653
		2009	**643**	**647**	**600**	**582**	**597**	**593**
		2010	580	720	677	656	704	680
		2011	666	704	668	676	741	716
		2012	711	738	742	719	743	719
Southern California	76	1983	62	117	110	98	196	185
		1984	189	233	236	175	229	205
		1985	209	216	241	232	238	235
		1986	**205**	**170**	**188**	**58**	**54**	**194**
		1987	161	172	133	146	0	209

		1988	211	208	0	0	0	0
		1989	226	194	194	200	182	196
		1990	0	0	0	0	0	0
		1991	**54**	**13**	**0**	**0**	**0**	**0**
		1992	210	246	245	233	207	230
		1993	229	225	226	235	248	240
		1994	**240**	**249**	**242**	**238**	**268**	**239**
		1995	114	218	233	0	0	0
		1996	430	477	502	461	651	478
		1997	**468**	**453**	**488**	**463**	**460**	**471**
		1998	470	483	486	464	486	663
		1999	1411	1446	1286	1433	1478	1405
		2000	1430	1451	1488	1407	1459	1404
		2001	1440	1488	1378	1440	1484	1439
		2002	**1436**	**1483**	**1488**	**1440**	**1488**	**1440**
		2003	1440	1488	1488	1428	1487	1434
		2004	1420	1488	1488	1430	1481	1439
		2005	1440	1488	1447	1440	1480	1440
		2006	1350	528	1488	1421	1488	1440
		2007	1440	976	1479	1440	1488	1438
		2008	1430	1309	1476	1014	1425	1368
		2009	**1432**	**1476**	**1470**	**1440**	**1470**	**1433**
		2010	1440	1487	1148	1440	1488	1440
		2011	1436	1417	1478	1409	1417	1423
		2012	1438	1488	1488	1440	1488	1440
	46011	1980	0	0	0	0	578	714
		1981	706	740	731	695	719	717
		1982	**718**	**728**	**687**	**717**	**742**	**720**
		1983	708	740	743	713	735	116
		1984	213	0	0	396	743	718
		1985	321	296	717	694	739	719
		1986	**714**	**740**	**739**	**544**	**335**	**0**
		1987	716	742	738	677	677	239
		1988	719	734	737	715	736	718
		1989	703	731	733	718	373	0
		1990	713	737	742	714	160	604
		1991	**715**	**742**	**739**	**720**	**225**	**0**
		1992	715	742	730	683	131	0

		1994	**0**	**0**	**530**	**709**	**732**	**714**
		1995	703	735	724	710	736	663
		1996	712	835	789	715	736	693
		1997	**712**	**734**	**735**	**711**	**735**	**707**
		1998	696	737	789	708	740	720
		1999	720	733	733	717	144	337
		2000	708	736	743	701	732	717
		2001	716	741	736	717	742	717
		2002	**690**	**740**	**744**	**720**	**738**	**719**
		2003	719	742	743	714	742	718
		2004	719	741	744	720	741	716
		2005	720	743	736	696	726	449
		2006	718	742	743	717	738	719
		2007	718	744	742	720	735	719
		2008	717	741	742	715	729	714
		2009	**714**	**741**	**728**	**714**	**722**	**528**
		2010	717	742	740	720	741	717
		2011	709	726	735	711	734	708
		2012	705	738	743	717	739	717
	46023	**1982**	**720**	**739**	**738**	**717**	**743**	**718**
		1983	709	740	742	640	648	33
		1984	710	738	727	711	741	715
		1985	681	717	725	709	738	30
		1986	**715**	**739**	**739**	**717**	**739**	**694**
		1987	713	744	743	679	34	0
		1988	711	737	732	711	741	715
		1989	676	696	732	712	741	713
		1990	712	736	743	714	742	716
		1991	**716**	**741**	**740**	**719**	**742**	**715**
		1992	715	741	738	711	736	692
		1993	712	728	732	710	741	400
		1994	**364**	**732**	**740**	**715**	**737**	**1**
		1995	692	717	719	705	736	709
		1996	325	102	0	0	0	0
		1997	**487**	**529**	**726**	**707**	**730**	**699**
		1998	679	728	785	692	741	713
		1999	718	737	736	714	722	657
		2000	705	739	741	717	729	717

		2001	718	741	737	717	743	718
		2002	**702**	**728**	**727**	**712**	**735**	**29**
		2003	719	744	744	714	741	720
		2004	720	741	736	720	743	718
		2005	720	743	707	720	744	713
		2006	709	731	713	678	282	4
		2007	695	710	706	671	696	686
		2008	712	729	719	690	705	704
		2009	**715**	**739**	**738**	**716**	**735**	**710**
		2010	694	697	653	153	0	0
	71	1998	1433	1474	1444	1275	1159	1434
		1999	1424	1463	1483	1435	1455	1434
		2000	1430	1485	1481	1436	1487	1432
		2001	1438	1458	1432	1430	1486	1376
		2002	**1433**	**1482**	**1456**	**1410**	**1464**	**1380**
		2003	1438	1484	1475	1427	1412	1401
		2004	1438	1488	1488	1438	1483	1437
		2005	1440	1475	1488	1440	1488	1440
		2006	1440	1488	1488	1440	1488	1440
		2007	1440	1488	1488	1440	1488	454
		2008	1440	1488	1488	1440	1488	1440
		2009	**1440**	**1488**	**1488**	**1440**	**1487**	**1440**
		2010	1440	1488	1488	1440	1482	1096
		2011	1440	1488	1488	1440	1488	1440
		2012	1440	1462	1418	1356	1449	1425
	46054	**1994**	**683**	**642**	**655**	**642**	**697**	**692**
		1995	704	715	699	678	721	703
		1996	717	823	764	713	734	684
		1997	**697**	**722**	**725**	**682**	**202**	**158**
		1998	695	736	776	677	728	672
		1999	704	727	701	674	704	676
		2000	704	712	734	701	715	694
		2001	706	731	664	697	664	704
		2002	**113**	**715**	**708**	**667**	**697**	**659**
		2003	691	710	722	679	712	674
		2004	713	735	725	701	735	651
		2005	445	439	560	380	498	500
		2006	387	411	428	413	360	297

		2007	394	390	321	293	219	273
		2008	496	532	465	585	456	552
		2009	**719**	**744**	**743**	**720**	**740**	**718**
		2010	717	744	741	709	736	711
		2011	648	650	680	675	735	637
		2012	212	165	99	162	246	263
	46053	**1994**	**696**	**674**	**732**	**701**	**719**	**706**
		1995	707	683	736	710	728	714
		1996	701	818	782	708	731	691
		1997	**0**	**0**	**0**	**0**	**0**	**0**
		1998	693	732	735	155	100	715
		1999	720	733	703	689	667	589
		2000	705	726	742	717	726	717
		2001	714	735	741	712	727	709
		2002	**711**	**738**	**725**	**718**	**713**	**705**
		2003	719	743	743	712	741	720
		2004	719	740	743	720	743	716
		2005	719	742	743	720	742	719
		2006	715	744	740	695	740	718
		2007	709	738	738	711	731	712
		2008	717	740	742	718	742	71
		2009	**720**	**743**	**707**	**594**	**682**	**634**
		2010	647	740	743	714	744	717
		2011	719	744	574	0	0	0
		2012	705	732	738	711	725	700
	46025	**1982**	**460**	**0**	**291**	**718**	**742**	**718**
		1983	701	733	735	699	716	700
		1984	717	735	740	715	741	715
		1985	717	735	738	716	738	718
		1986	**715**	**743**	**742**	**717**	**735**	**699**
		1987	717	741	564	0	741	715
		1988	719	742	735	716	740	717
		1989	0	0	0	0	431	719
		1990	712	735	734	463	662	716
		1991	**718**	**740**	**737**	**716**	**739**	**713**
		1992	716	740	733	711	731	676
		1993	701	714	704	691	36	0
		1994	**477**	**447**	**421**	**410**	**324**	**281**

		1995	384	499	742	716	738	711
		1996	674	820	783	712	729	684
		1997	**711**	**143**	**0**	**0**	**0**	**256**
		1998	678	728	772	689	719	693
		1999	720	741	735	716	719	680
		2000	707	736	743	719	734	714
		2001	718	744	680	714	743	716
		2002	**578**	**641**	**652**	**638**	**689**	**664**
		2003	595	699	705	690	737	718
		2004	535	628	737	718	743	712
		2005	718	743	741	719	741	718
		2006	718	742	742	698	740	719
		2007	710	740	740	718	742	695
		2008	720	743	743	720	744	720
		2009	**720**	**743**	**744**	**719**	**744**	**717**
		2010	713	741	738	718	741	703
		2011	715	738	737	717	739	714
		2012	0	0	0	0	0	171
	92	1981	111	89	122	119	119	118
		1982	**0**	**0**	**0**	**0**	**0**	**0**
		1983	0	0	0	0	0	0
		1984	0	0	0	0	0	0
		1985	0	0	0	0	0	0
		1986	**0**	**0**	**0**	**0**	**0**	**0**
		1987	0	0	0	0	0	0
		1988	0	0	0	0	0	0
		1989	0	0	0	0	0	0
		1990	0	0	0	0	0	0
		1991	**0**	**0**	**0**	**0**	**0**	**0**
		1992	0	0	0	0	0	0
		1993	0	0	0	0	0	0
		1994	**0**	**0**	**0**	**0**	**0**	**0**
		1995	0	0	0	0	0	0
		1996	0	0	0	0	0	0
		1997	**0**	**0**	**0**	**0**	**0**	**0**
		1998	1388	1395	1319	1268	1461	1425
		1999	1408	1427	1486	1426	1380	1346
		2000	1437	1486	1488	862	1485	1430

		2001	1437	1488	1488	1440	1488	1440
		2002	**1264**	**1483**	**1488**	**1440**	**1488**	**1439**
		2003	1440	1433	1488	1440	1488	1437
		2004	1440	1488	1487	1440	1488	1440
		2005	1440	1487	1469	1440	1488	1440
		2006	1440	1488	1392	1372	1453	1408
		2007	1440	1488	1488	1440	1487	1440
		2008	1440	1488	1482	1440	1488	1440
		2009	**1436**	**1488**	**1486**	**1440**	**1488**	**1438**
		2010	1440	1488	1488	1440	1488	1440
		2011	1440	1488	1488	1440	1488	1438
		2012	1440	1488	1488	1440	1488	1440
	45	**1997**	**1424**	**1433**	**1487**	**1399**	**1463**	**1327**
		1998	1436	1409	1452	751	1360	1399
		1999	1434	1438	1387	1421	1486	1437
		2000	1438	1470	1481	1440	1486	1434
		2001	1440	1488	1488	1440	1488	1432
		2002	**1439**	**1484**	**1488**	**1440**	**1487**	**1440**
		2003	1440	1487	1473	1026	1444	1428
		2004	1408	1488	1488	1439	1488	1440
		2005	1440	1486	1488	1440	1488	1440
		2006	1410	866	1477	1412	1484	1404
		2007	1434	1471	1487	1440	1488	1440
		2008	1440	1488	1488	1433	1486	1440
		2009	**1440**	**1488**	**1488**	**1440**	**1488**	**1441**
		2010	1440	1488	1487	1437	1488	1439
		2011	1439	1357	1446	1250	1488	1438
		2012	1429	1448	1487	1440	1488	1423
	93	1981	109	79	42	115	118	120
		1982	**194**	**170**	**211**	**225**	**216**	**190**
		1983	0	0	0	0	0	0
		1984	0	0	0	0	0	0
		1985	237	245	212	234	239	240
		1986	**225**	**198**	**216**	**234**	**244**	**231**
		1987	227	226	227	199	223	189
		1988	235	234	241	220	222	218
		1989	230	234	241	227	135	233
		1990	237	247	246	237	247	230

		1991	**121**	**244**	**248**	**222**	**247**	**239**
		1992	211	263	246	239	196	229
		1993	225	211	0	0	0	0
		1994	**192**	**240**	**251**	**239**	**267**	**240**
		1995	194	146	0	0	0	0
		1996	0	0	0	0	534	703
		1997	**684**	**703**	**716**	**640**	**923**	**1393**
		1998	277	0	315	0	0	0
		1999	0	0	0	0	0	0
		2000	0	0	0	0	0	0
		2001	0	0	0	0	0	0
		2002	**0**	**0**	**0**	**0**	**0**	**0**
		2003	0	0	0	0	0	0
		2004	0	0	0	0	0	0
		2005	0	0	0	0	1303	1440
		2006	1437	1476	323	162	1488	1438
		2007	938	1488	1489	1440	1488	1440
		2008	1440	1488	1488	1440	1488	1426
		2009	**1440**	**1488**	**1488**	**1440**	**1488**	**1440**
		2010	1440	1488	1488	1437	1488	1440
		2011	1440	1472	1488	1440	1488	1118
		2012	1318	1488	1488	1440	1488	1440
	46047	1992	0	0	747	626	469	669
		1993	557	606	32	0	0	0
		1994	**0**	**0**	**0**	**0**	**0**	**0**
		1995	0	0	0	0	0	0
		1996	0	0	0	0	0	0
		1997	**0**	**0**	**0**	**0**	**0**	**0**
		1998	0	0	0	0	0	0
		1999	693	698	689	612	666	612
		2000	654	652	698	676	703	678
		2001	671	696	706	718	743	716
		2002	**715**	**741**	**692**	**348**	**123**	**680**
		2003	720	739	742	712	743	720
		2004	720	739	710	720	744	718
		2005	719	744	743	720	741	719
		2006	719	742	743	693	743	720
		2007	712	743	742	719	735	716

		2008	708	737	742	719	739	718
		2009	**684**	**723**	**699**	**696**	**711**	**700**
		2010	677	727	724	692	77	0
		2011	240	237	124	421	731	692
		2012	709	739	741	231	0	54

APPENDIX B

Average Autumn Significant Wave Heights for All El Niño and Non-El Niño Years

Average autumn significant wave heights (H_{sig}) over (a) the entire season and over the months of (b) September, (c) October, and (d) November for all El Niño years and non-El Niño years. Orange cells indicate that average H_{sig} during El Niño autumn months were higher than during non-El Niño autumn months.

A.

Region	Station	Autumn Average Hsig (m)					
		All El Niño	StDev	Non-El Niño	StDev	El Niño – Non-El Niño	% Difference
Washington	46041	2.34	1.22	2.33	1.16	0.01	0.4
	46029	2.55	1.26	2.44	1.24	0.11	4.3
	36	2.15	1.07	2.20	1.09	-0.05	-2.3
	46005	2.84	1.43	2.94	1.41	-0.09	-3.2
	regional	2.47	1.28	2.46	1.26	0.01	0.4
Oregon	46050	2.60	1.30	2.51	1.22	0.09	3.4
	46002	2.75	1.32	2.75	1.26	0.00	0.0
	regional	2.69	1.31	2.65	1.25	0.04	1.6
Northern California	46027	2.31	1.00	2.19	0.93	0.12	5.3
	46006	2.82	1.40	2.78	1.36	0.03	1.2
	46022	2.42	1.10	2.35	1.04	0.07	2.9
	46014	2.28	0.98	2.27	0.97	0.01	0.3
	regional	2.46	1.16	2.42	1.13	0.05	1.9
Central California	46059	2.80	1.22	2.71	1.10	0.10	3.5
	46013	2.03	0.87	2.09	0.87	-0.07	-3.2
	46026	1.69	0.73	1.69	0.70	0.00	-0.3
	46012	2.01	0.90	1.97	0.82	0.04	2.2
	46042	2.17	0.93	2.05	0.80	0.12	5.7
	46028	2.19	0.89	2.15	0.80	0.04	2.0
	regional	2.09	0.96	2.07	0.88	0.02	1.1
Southern California	76	1.48	0.58	1.47	0.54	0.02	1.3
	46011	1.91	0.81	1.90	0.76	0.01	0.6
	46023	2.06	0.88	2.03	0.77	0.03	1.6
	71	2.09	0.86	2.10	0.76	0.00	0.0
	46054	1.95	0.81	1.91	0.72	0.04	2.0
	46053	1.16	0.46	1.14	0.43	0.02	1.4
	46025	1.02	0.38	1.03	0.37	-0.01	-1.4
	92	0.91	0.33	0.89	0.30	0.03	3.1
	45	0.88	0.28	0.89	0.25	-0.01	-1.4
	93	1.08	0.41	1.04	0.31	0.04	3.4
	46047	2.12	0.83	2.06	0.74	0.05	2.5
	regional	1.47	0.80	1.46	0.75	0.01	0.9

B.

Region	Station	September Average Hsig (m)					
		All El Niño	StDev	Non-El Niño	StDev	El Niño – Non-El Niño	% Difference
Washington	46041	1.79	0.73	1.67	0.73	0.13	7.3
	46029	1.92	0.79	1.74	0.70	0.18	9.9
	36	1.71	0.69	1.60	0.65	0.12	7.1
	46005	2.14	0.99	2.13	0.89	0.01	0.5
	regional	1.90	0.83	1.77	0.77	0.12	6.8
Oregon	46050	2.02	0.81	1.86	0.71	0.16	8.3
	46002	2.17	0.90	2.14	0.82	0.03	1.3
	regional	2.12	0.88	2.02	0.79	0.09	4.5
Northern California	46027	1.89	0.71	1.82	0.73	0.07	3.8
	46006	2.03	0.81	2.00	0.86	0.02	1.1
	46022	1.96	0.86	1.91	0.83	0.05	2.4
	46014	1.94	0.76	1.90	0.73	0.04	2.2
	regional	1.96	0.79	1.91	0.79	0.04	2.3
Central California	46059	2.24	0.84	2.25	0.81	-0.01	-0.7
	46013	1.75	0.64	1.78	0.64	-0.03	-1.4
	46026	1.45	0.53	1.42	0.47	0.03	2.0
	46012	1.69	0.64	1.62	0.57	0.07	4.2
	46042	1.83	0.57	1.73	0.57	0.10	5.5
	46028	1.86	0.55	1.86	0.57	0.00	-0.3
	regional	1.75	0.65	1.74	0.64	0.01	0.6
Southern California	76	1.29	0.36	1.22	0.34	0.07	5.8
	46011	1.65	0.54	1.62	0.51	0.03	1.7
	46023	1.79	0.60	1.72	0.51	0.07	3.8
	71	1.84	0.52	1.76	0.49	0.07	4.0
	46054	1.69	0.50	1.63	0.47	0.07	4.0
	46053	1.02	0.31	0.99	0.30	0.03	3.1
	46025	0.97	0.28	0.95	0.24	0.02	2.0
	92	0.88	0.22	0.80	0.17	0.08	9.7
	45	0.92	0.21	0.90	0.19	0.02	2.3
	93	0.97	0.24	1.02	0.21	-0.05	-5.0
	46047	1.90	0.49	1.82	0.47	0.08	4.5
	regional	1.34	0.57	1.29	0.53	0.05	3.7

C.

Region	Station	October Average Hsig (m)					
		All El Niño	StDev	Non-El Niño	StDev	El Niño – Non-El Niño	% Difference
Washington	46041	2.06	0.92	2.35	1.11	-0.29	-13
	46029	2.32	1.05	2.53	1.15	-0.21	-8.5
	36	2.00	0.88	2.31	1.07	-0.31	-14
	46005	2.76	1.30	2.94	1.38	-0.18	-6.2
	regional	2.29	1.1	2.52	1.2	-0.23	-9.7
Oregon	46050	2.40	1.12	2.56	1.13	-0.16	-6.4
	46002	2.76	1.29	2.70	1.15	0.06	2.2
	regional	2.63	1.2	2.64	1.1	-0.02	-0.6
Northern California	46027	2.20	0.76	2.23	0.93	-0.04	-1.6
	46006	2.78	1.24	2.79	1.23	-0.01	-0.2
	46022	2.35	0.91	2.37	0.98	-0.02	-0.6
	46014	2.24	0.86	2.26	0.93	-0.02	-0.8
	regional	2.41	1.0	2.43	1.1	-0.02	-0.9
Central California	46059	2.77	1.07	2.73	1.08	0.05	1.7
	46013	1.98	0.77	2.02	0.80	-0.05	-2.5
	46026	1.63	0.69	1.67	0.66	-0.04	-2.2
	46012	1.94	0.80	1.95	0.79	-0.02	-0.8
	46042	2.14	0.90	2.06	0.77	0.08	3.8
	46028	2.12	0.78	2.18	0.82	-0.06	-2.8
	regional	2.03	0.9	2.05	0.9	-0.02	-1.0
Southern California	76	1.43	0.55	1.49	0.53	-0.06	-4.0
	46011	1.88	0.79	1.92	0.73	-0.04	-2.0
	46023	2.02	0.83	2.08	0.78	-0.06	-3.1
	71	1.95	0.79	2.18	0.81	-0.23	-11
	46054	1.91	0.84	1.95	0.74	-0.04	-2.3
	46053	1.10	0.47	1.15	0.41	-0.05	-4.5
	46025	0.99	0.33	1.01	0.34	-0.01	-1.3
	92	0.88	0.32	0.89	0.29	-0.01	-1.5
	45	0.88	0.32	0.89	0.22	-0.01	-1.5
	93	1.03	0.38	1.04	0.32	-0.02	-1.6
	46047	1.96	0.79	2.12	0.79	-0.16	-7.7
	regional	1.42	0.8	1.48	0.8	-0.06	-4.1

D.

Region	Station	November Average Hsig (m)					
		All El Niño	StDev	Non-El Niño	StDev	El Niño – Non-El Niño	% Difference
Washington	46041	3.23	1.43	2.92	1.21	0.31	10
	46029	3.30	1.40	3.13	1.38	0.17	5.3
	36	2.87	1.31	2.74	1.18	0.14	4.9
	46005	3.71	1.51	3.76	1.41	-0.05	-1.4
	regional	3.28	1.45	3.11	1.35	0.18	5.5
Oregon	46050	3.35	1.47	3.12	1.37	0.22	7.0
	46002	3.41	1.45	3.41	1.40	0.00	0.1
	regional	3.39	1.46	3.29	1.39	0.10	3.0
Northern California	46027	2.85	1.19	2.52	0.98	0.33	12
	46006	3.70	1.52	3.56	1.45	0.14	3.7
	46022	2.94	1.26	2.79	1.11	0.15	5.4
	46014	2.69	1.14	2.67	1.07	0.03	1.0
	regional	3.05	1.35	2.92	1.25	0.13	4.5
Central California	46059	3.29	1.39	3.11	1.19	0.18	5.6
	46013	2.39	1.06	2.47	0.98	-0.08	-3.4
	46026	2.01	0.83	1.96	0.79	0.05	2.5
	46012	2.41	1.05	2.33	0.91	0.07	3.1
	46042	2.61	1.10	2.38	0.89	0.23	9.3
	46028	2.61	1.09	2.40	0.89	0.21	8.6
	regional	2.49	1.13	2.39	0.98	0.10	4.2
Southern California	76	1.73	0.68	1.68	0.61	0.05	2.8
	46011	2.30	0.98	2.21	0.90	0.09	3.9
	46023	2.52	1.10	2.34	0.89	0.18	7.6
	71	2.51	1.03	2.36	0.82	0.15	6.0
	46054	2.31	0.94	2.15	0.80	0.16	7.0
	46053	1.36	0.50	1.30	0.50	0.06	4.7
	46025	1.09	0.49	1.14	0.47	-0.05	-4.2
	92	0.99	0.40	0.97	0.38	0.02	2.0
	45	0.83	0.29	0.88	0.31	-0.05	-5.3
	93	1.19	0.48	1.06	0.38	0.13	12
	46047	2.43	0.99	2.28	0.84	0.15	6.5
	regional	1.66	0.98	1.60	0.87	0.06	3.5

APPENDIX C

Average Summer Significant Wave Heights for Moderate to Strong El Niño and Non-El Niño to Weak El Niño Years

Average summer significant wave heights (H_{sig}) over the (a) entire season and over the months of (b) June, (c) July, and (d) August for moderate to strong El Niño years and non-El Niño to weak El Niño years. Blue cells indicate that average H_{sig} during moderate to strong El Niño summer months were lower than during non-El Niño to weak El Niño summer months.

A.

Region	Station	Summer Average Hsig (m)					
		Mod-Str El Niño	StDev	Non-Wk El Niño	StDev	Mod-Str – Non-Wk El Niño	% Difference
Washington	46041	1.39	0.62	1.41	0.55	-0.02	-1.4
	46029	1.49	0.61	1.49	0.55	0.00	0.1
	36	1.32	0.53	1.33	0.49	-0.01	-0.5
	46005	1.69	0.71	1.70	0.65	-0.01	-0.9
	regional	1.48	0.64	1.47	0.57	0.01	0.9
Oregon	46050	1.56	0.61	1.61	0.57	-0.06	-3.7
	46002	1.74	0.63	1.77	0.62	-0.03	-1.8
	regional	1.68	0.63	1.70	0.60	-0.02	-1.5
Northern California	46027	1.72	0.76	1.72	0.70	0.00	0.2
	46006	1.60	0.62	1.63	0.63	-0.03	-1.8
	46022	1.79	0.81	1.81	0.78	-0.02	-1.0
	46014	1.86	0.74	1.94	0.72	-0.08	-4.3
	regional	1.76	0.75	1.78	0.72	-0.02	-1.3
Central California	46059	1.95	0.64	1.92	0.65	0.03	1.5
	46013	1.74	0.68	1.87	0.71	-0.13	-7.3
	46026	1.45	0.57	1.51	0.57	-0.06	-4.0
	46012	1.56	0.62	1.70	0.61	-0.13	-8.3
	46042	1.73	0.61	1.77	0.59	-0.04	-2.3
	46028	1.94	0.64	1.96	0.63	-0.02	-1.0
	regional	1.70	0.65	1.78	0.65	-0.08	-4.8
Southern California	76	1.19	0.36	1.23	0.37	-0.04	-3.5
	46011	1.61	0.54	1.68	0.56	-0.07	-4.3
	46023	1.76	0.56	1.82	0.57	-0.05	-2.9
	71	1.70	0.53	1.83	0.55	-0.14	-7.7
	46054	1.62	0.53	1.67	0.52	-0.04	-2.6
	46053	1.02	0.34	1.02	0.35	-0.01	-0.9
	46025	0.95	0.26	1.00	0.26	-0.05	-5.4
	92	0.80	0.18	0.85	0.21	-0.05	-6.3
	45	0.88	0.21	0.89	0.19	-0.01	-1.0
	93	0.92	0.22	1.00	0.23	-0.08	-8.3
	46047	1.72	0.50	1.83	0.57	-0.11	-6.4
	regional	1.29	0.56	1.33	0.58	-0.04	-3.1

B.

Region	Station	June Average Hsig (m)					
		Mod-Str El Niño	StDev	Non-Wk El Niño	StDev	Mod-Str – Non-Wk El Niño	% Difference
Washington	46041	1.50	0.77	1.56	0.66	-0.06	-3.6
	46029	1.73	0.76	1.63	0.64	0.09	5.5
	36	1.40	0.62	1.44	0.57	-0.04	-2.9
	46005	1.84	0.87	1.88	0.78	-0.05	-2.6
	regional	1.63	0.79	1.61	0.68	0.01	0.9
Oregon	46050	1.64	0.76	1.74	0.66	-0.10	-5.9
	46002	1.79	0.71	1.88	0.70	-0.09	-4.9
	regional	1.74	0.73	1.82	0.68	-0.08	-4.4
Northern California	46027	1.71	0.81	1.83	0.73	-0.13	-7.1
	46006	1.76	0.73	1.85	0.78	-0.09	-5.3
	46022	1.85	0.88	2.00	0.82	-0.15	-7.8
	46014	1.99	0.89	2.14	0.79	-0.15	-7.2
	regional	1.84	0.85	1.97	0.79	-0.12	-6.5
Central California	46059	2.05	0.60	2.06	0.70	-0.01	-0.7
	46013	1.89	0.85	2.13	0.79	-0.24	-12
	46026	1.71	0.72	1.73	0.65	-0.02	-1.1
	46012	1.74	0.77	1.99	0.75	-0.24	-13
	46042	2.02	0.78	2.00	0.69	0.02	0.9
	46028	2.18	0.78	2.20	0.74	-0.02	-0.9
	regional	1.92	0.79	2.01	0.74	-0.10	-5.0
Southern California	76	1.36	0.45	1.42	0.42	-0.06	-4.1
	46011	1.80	0.71	1.93	0.67	-0.13	-6.8
	46023	1.93	0.71	2.05	0.69	-0.12	-6.0
	71	1.90	0.68	2.06	0.66	-0.16	-8.2
	46054	1.89	0.67	1.88	0.62	0.01	0.8
	46053	1.16	0.40	1.14	0.41	0.02	1.4
	46025	1.03	0.31	1.08	0.31	-0.04	-4.2
	92	0.80	0.20	0.90	0.25	-0.10	-12
	45	0.90	0.18	0.95	0.20	-0.05	-5.2
	93	0.98	0.23	1.08	0.27	-0.11	-10
	46047	1.86	0.67	2.03	0.67	-0.17	-8.7
	regional	1.40	0.67	1.48	0.68	-0.08	-5.3

C.

Region	Station	July Average Hsig (m)					
		Mod-Str El Niño	StDev	Non-Wk El Niño	StDev	Mod-Str – Non-Wk El Niño	% Difference
Washington	46041	1.34	0.43	1.36	0.48	-0.02	-1.6
	46029	1.43	0.45	1.47	0.47	-0.04	-2.7
	36	1.27	0.38	1.30	0.42	-0.03	-2.3
	46005	1.59	0.54	1.56	0.51	0.03	2.1
	regional	1.41	0.48	1.41	0.48	0.00	0.0
Oregon	46050	1.62	0.49	1.60	0.51	0.02	1.0
	46002	1.69	0.54	1.73	0.55	-0.04	-2.1
	regional	1.67	0.53	1.67	0.54	-0.01	-0.6
Northern California	46027	1.83	0.77	1.70	0.71	0.13	7.2
	46006	1.50	0.49	1.52	0.50	-0.01	-0.9
	46022	1.90	0.82	1.76	0.80	0.14	7.7
	46014	1.96	0.68	1.93	0.70	0.03	1.6
	regional	1.82	0.73	1.74	0.71	0.08	4.5
Central California	46059	1.89	0.66	1.89	0.66	0.00	-0.1
	46013	1.76	0.57	1.79	0.66	-0.03	-1.9
	46026	1.42	0.46	1.43	0.49	-0.01	-0.7
	46012	1.57	0.47	1.63	0.54	-0.07	-4.1
	46042	1.63	0.44	1.72	0.52	-0.09	-5.4
	46028	1.86	0.52	1.89	0.57	-0.03	-1.5
	regional	1.66	0.53	1.72	0.59	-0.05	-3.0
Southern California	76	1.15	0.26	1.17	0.30	-0.02	-1.7
	46011	1.56	0.41	1.61	0.49	-0.05	-3.4
	46023	1.69	0.45	1.75	0.50	-0.07	-3.8
	71	1.66	0.40	1.77	0.48	-0.11	-6.4
	46054	1.53	0.42	1.58	0.45	-0.06	-3.7
	46053	0.94	0.26	0.98	0.33	-0.04	-4.2
	46025	0.90	0.20	0.99	0.24	-0.08	-9.0
	92	0.81	0.14	0.83	0.18	-0.02	-3.0
	45	0.84	0.20	0.86	0.16	-0.02	-2.9
	93	0.89	0.19	0.99	0.19	-0.09	-9.9
	46047	1.65	0.36	1.76	0.49	-0.12	-6.8
	regional	1.24	0.48	1.28	0.52	-0.04	-3.2

D.

Region	Station	August Average Hsig (m)					
		Mod-Str El Niño	StDev	Non-Wk El Niño	StDev	Mod-Str – Non-Wk El Niño	% Difference
Washington	46041	1.33	0.63	1.32	0.49	0.01	0.6
	46029	1.37	0.57	1.39	0.49	-0.02	-1.5
	36	1.31	0.55	1.26	0.44	0.05	4.2
	46005	1.63	0.64	1.69	0.62	-0.05	-3.2
	regional	1.43	0.62	1.41	0.54	0.02	1.4
Oregon	46050	1.41	0.53	1.51	0.51	-0.09	-6.5
	46002	1.74	0.63	1.72	0.60	0.02	1.1
	regional	1.63	0.61	1.62	0.57	0.00	0.2
Northern California	46027	1.61	0.68	1.62	0.63	-0.01	-0.7
	46006	1.55	0.59	1.55	0.54	0.00	0.2
	46022	1.62	0.70	1.68	0.69	-0.06	-3.7
	46014	1.63	0.57	1.77	0.62	-0.14	-8.3
	regional	1.61	0.64	1.66	0.63	-0.05	-3.2
Central California	46059	1.92	0.64	1.80	0.57	0.11	6.0
	46013	1.58	0.55	1.69	0.58	-0.11	-7.0
	46026	1.24	0.41	1.34	0.45	-0.09	-7.3
	46012	1.36	0.47	1.52	0.45	-0.17	-12
	46042	1.56	0.43	1.62	0.47	-0.06	-4.0
	46028	1.75	0.46	1.82	0.52	-0.07	-3.9
	regional	1.51	0.52	1.62	0.53	-0.11	-7.2
Southern California	76	1.07	0.28	1.12	0.29	-0.05	-4.4
	46011	1.49	0.42	1.51	0.42	-0.02	-1.6
	46023	1.70	0.47	1.65	0.43	0.05	2.8
	71	1.54	0.39	1.68	0.42	-0.13	-8.3
	46054	1.51	0.42	1.55	0.39	-0.03	-2.1
	46053	0.95	0.28	0.96	0.28	-0.01	-0.5
	46025	0.90	0.23	0.95	0.22	-0.05	-5.8
	92	0.79	0.18	0.82	0.17	-0.03	-3.6
	45	0.90	0.24	0.85	0.18	0.05	5.2
	93	0.90	0.22	0.93	0.19	-0.03	-3.3
	46047	1.64	0.38	1.70	0.47	-0.06	-3.6
	regional	1.22	0.48	1.23	0.48	0.00	-0.2

APPENDIX D

Average Autumn Significant Wave Heights for Moderate to Strong El Niño and Non-El Niño to Weak El Niño Years

Average autumn significant wave heights (H_{sig}) over (a) the entire season and over the months of (b) September, (c) October, and (d) November for moderate to strong El Niño years and non-El Niño to weak El Niño years. Orange cells indicate that average H_{sig} during moderate to strong El Niño autumn months were higher than during non-El Niño to weak El Niño autumn months.

A.

Region	Station	Autumn Average Hsig (m)					
		Mod-Str El Niño	StDev	Non-Wk El Niño	StDev	Mod-Str – Non-Wk El Niño	% Difference
Washington	46041	2.34	1.28	2.33	1.16	0.02	0.7
	46029	2.53	1.28	2.45	1.24	0.08	3.2
	36	2.21	1.18	2.18	1.07	0.03	1.5
	46005	2.85	1.48	2.92	1.40	-0.07	-2.4
	regional	2.50	1.34	2.45	1.25	0.05	2.0
Oregon	46050	2.61	1.36	2.52	1.21	0.09	3.5
	46002	2.76	1.36	2.75	1.26	0.01	0.4
	regional	2.70	1.36	2.65	1.24	0.05	1.8
Northern California	46027	2.33	1.05	2.20	0.93	0.12	5.5
	46006	2.84	1.42	2.78	1.36	0.05	1.9
	46022	2.43	1.13	2.35	1.04	0.07	3.0
	46014	2.30	1.01	2.27	0.96	0.03	1.4
	regional	2.46	1.18	2.42	1.13	0.04	1.8
Central California	46059	2.94	1.35	2.70	1.09	0.24	8.5
	46013	2.03	0.89	2.09	0.86	-0.05	-2.6
	46026	1.68	0.76	1.69	0.69	-0.01	-0.6
	46012	1.96	0.91	1.99	0.83	-0.02	-1.1
	46042	2.23	0.98	2.05	0.80	0.18	8.5
	46028	2.21	0.93	2.15	0.80	0.06	2.7
	regional	2.08	0.99	2.07	0.88	0.01	0.3
Southern California	76	1.55	0.65	1.46	0.53	0.10	6.4
	46011	1.95	0.86	1.89	0.75	0.05	2.7
	46023	2.10	0.91	2.02	0.77	0.08	3.8
	71	2.16	0.96	2.09	0.76	0.07	3.4
	46054	2.02	0.87	1.90	0.71	0.12	6.1
	46053	1.18	0.50	1.14	0.43	0.04	3.3
	46025	1.02	0.41	1.03	0.36	-0.02	-1.9
	92	0.94	0.38	0.89	0.30	0.05	5.5
	45	0.88	0.31	0.89	0.25	-0.01	-0.6
	93	1.09	0.43	1.04	0.31	0.05	4.6
	46047	2.31	0.97	2.05	0.73	0.26	12
	regional	1.51	0.85	1.45	0.74	0.06	4.3

B.

Region	Station	September Average Hsig (m)					
		Mod-Str El Niño	StDev	Non-Wk El Niño	StDev	Mod-Str – Non-Wk El Niño	% Difference
Washington	46041	1.75	0.70	1.69	0.74	0.06	3.6
	46029	1.91	0.79	1.77	0.72	0.14	7.7
	36	1.70	0.69	1.62	0.66	0.09	5.2
	46005	2.12	1.01	2.14	0.90	-0.03	-1.2
	regional	1.89	0.85	1.79	0.78	0.10	5.4
Oregon	46050	2.03	0.85	1.88	0.71	0.15	7.7
	46002	2.19	0.96	2.14	0.82	0.05	2.3
	regional	2.13	0.93	2.03	0.79	0.10	4.9
Northern California	46027	1.88	0.71	1.83	0.73	0.05	2.7
	46006	2.03	0.85	2.01	0.84	0.03	1.4
	46022	1.96	0.87	1.91	0.83	0.04	2.2
	46014	1.91	0.77	1.91	0.73	0.01	0.3
	regional	1.95	0.81	1.92	0.79	0.03	1.4
Central California	46059	2.30	0.93	2.24	0.80	0.06	2.8
	46013	1.72	0.62	1.79	0.64	-0.06	-3.5
	46026	1.41	0.52	1.43	0.48	-0.02	-1.7
	46012	1.59	0.56	1.65	0.60	-0.06	-3.8
	46042	1.82	0.56	1.75	0.58	0.08	4.4
	46028	1.79	0.52	1.88	0.57	-0.08	-4.6
	regional	1.69	0.63	1.76	0.65	-0.07	-3.8
Southern California	76	1.26	0.35	1.23	0.35	0.03	2.7
	46011	1.64	0.54	1.63	0.51	0.01	0.8
	46023	1.79	0.61	1.73	0.51	0.06	3.4
	71	1.80	0.48	1.78	0.50	0.02	1.3
	46054	1.70	0.52	1.63	0.47	0.07	4.2
	46053	0.99	0.30	1.00	0.31	-0.01	-0.6
	46025	0.95	0.29	0.96	0.24	-0.02	-1.7
	92	0.86	0.21	0.82	0.19	0.04	5.3
	45	0.90	0.22	0.90	0.20	0.00	-0.2
	93	0.97	0.25	1.02	0.21	-0.05	-4.9
	46047	1.97	0.48	1.82	0.47	0.15	7.8
	regional	1.33	0.58	1.30	0.54	0.03	2.3

C.

Region	Station	October Average Hsig (m)					
		Mod-Str El Niño	StDev	Non-Wk El Niño	StDev	Mod-Str – Non-Wk El Niño	% Difference
Washington	46041	1.92	0.82	2.34	1.10	-0.42	-20
	46029	2.28	1.05	2.51	1.14	-0.23	-9.8
	36	1.94	0.88	2.28	1.05	-0.34	-16
	46005	2.76	1.30	2.92	1.37	-0.16	-5.7
	regional	2.25	1.10	2.50	1.20	-0.25	-11
Oregon	46050	2.38	1.20	2.54	1.11	-0.17	-6.9
	46002	2.71	1.17	2.72	1.20	0.00	-0.2
	regional	2.59	1.19	2.65	1.17	-0.06	-2.2
Northern California	46027	2.15	0.70	2.24	0.92	-0.09	-3.9
	46006	2.69	1.11	2.80	1.26	-0.11	-4.0
	46022	2.36	0.91	2.36	0.97	0.00	0.0
	46014	2.26	0.84	2.25	0.93	0.01	0.6
	regional	2.38	0.93	2.43	1.07	-0.06	-2.3
Central California	46059	2.76	1.00	2.73	1.09	0.02	0.9
	46013	1.98	0.75	2.02	0.81	-0.04	-1.8
	46026	1.63	0.71	1.67	0.66	-0.03	-2.0
	46012	1.89	0.77	1.96	0.80	-0.08	-4.1
	46042	2.20	0.93	2.05	0.78	0.16	7.4
	46028	2.15	0.78	2.17	0.82	-0.02	-0.7
	regional	2.01	0.86	2.05	0.86	-0.04	-2.2
Southern California	76	1.51	0.60	1.47	0.52	0.04	2.6
	46011	1.94	0.83	1.90	0.73	0.04	1.8
	46023	2.06	0.84	2.06	0.78	0.00	-0.2
	71	2.01	0.89	2.13	0.80	-0.12	-5.8
	46054	1.98	0.92	1.93	0.73	0.06	3.0
	46053	1.15	0.54	1.14	0.40	0.01	1.2
	46025	1.00	0.36	1.00	0.33	0.00	0.0
	92	0.90	0.38	0.88	0.29	0.02	2.0
	45	0.89	0.35	0.89	0.23	0.01	0.6
	93	1.07	0.42	1.03	0.31	0.04	3.8
	46047	2.20	0.98	2.06	0.77	0.13	6.2
	regional	1.48	0.82	1.46	0.75	0.03	1.8

D.

Region	Station	November Average Hsig (m)					
		Mod-Str El Niño	StDev	Non-Wk El Niño	StDev	Mod-Str – Non-Wk El Niño	% Difference
Washington	46041	3.32	1.49	2.93	1.22	0.39	13
	46029	3.29	1.42	3.16	1.38	0.13	4.1
	36	3.05	1.40	2.71	1.17	0.34	12
	46005	3.84	1.58	3.72	1.40	0.12	3.2
	regional	3.38	1.50	3.11	1.34	0.27	8.4
Oregon	46050	3.41	1.53	3.13	1.37	0.28	8.6
	46002	3.58	1.60	3.37	1.37	0.20	5.8
	regional	3.51	1.57	3.27	1.37	0.23	6.9
Northern California	46027	2.95	1.29	2.54	0.97	0.42	15
	46006	3.80	1.61	3.56	1.44	0.25	6.7
	46022	3.03	1.32	2.77	1.10	0.26	8.8
	46014	2.79	1.20	2.65	1.06	0.14	5.2
	regional	3.13	1.41	2.91	1.24	0.22	7.2
Central California	46059	3.51	1.59	3.09	1.16	0.43	13
	46013	2.43	1.12	2.46	0.98	-0.03	-1.2
	46026	2.04	0.87	1.95	0.78	0.09	4.3
	46012	2.40	1.09	2.34	0.91	0.06	2.6
	46042	2.78	1.18	2.37	0.88	0.42	16
	46028	2.72	1.15	2.40	0.89	0.32	13
	regional	2.54	1.21	2.39	0.97	0.16	6.3
Southern California	76	1.87	0.76	1.66	0.60	0.21	12
	46011	2.40	1.04	2.19	0.89	0.20	8.8
	46023	2.58	1.14	2.33	0.89	0.25	10
	71	2.67	1.15	2.36	0.82	0.31	12
	46054	2.44	0.99	2.14	0.79	0.30	13
	46053	1.40	0.54	1.30	0.49	0.10	7.5
	46025	1.09	0.53	1.13	0.46	-0.04	-3.5
	92	1.05	0.46	0.96	0.37	0.09	9.1
	45	0.85	0.33	0.87	0.30	-0.02	-2.4
	93	1.21	0.52	1.07	0.37	0.14	12
	46047	2.63	1.12	2.27	0.83	0.36	15
	regional	1.74	1.06	1.59	0.86	0.15	9.0

APPENDIX E

K-S Test Results for Normalized Distributions of Individual Summer Significant Wave Height (H_{sig}) Observed Data vs. Normalized Distributions of Overall Summer H_{sig} Observed Data for Each Station

Data from El Niño summers are indicated in bold typeface. A sign on a D-statistic indicates whether the greatest difference between an individual summer's H_{sig} distribution and that of the overall summer for its station is positive or negative. Red color indicates that the results of the K-S test are not significant. Confidence levels of the observed D-statistics relative to the outcome of the Monte Carlo simulation (Figure 3.9) are also presented in the last column on the right.

Region	Station	Year	D-statistic	p < 0.05?	Monte Carlo Confidence
Washington	46041	1987	-0.070	yes	99%
		1988	0.035	yes	99%
		1989	-0.167	yes	99%
		1990	0.039	yes	99%
		1991	**-0.067**	**yes**	**99%**
		1992	-0.069	yes	99%
		1993	-0.083	yes	99%
		1994	**-0.051**	**yes**	**99%**
		1995	-0.057	yes	99%
		1996	-0.069	yes	99%
		1997	**0.087**	**yes**	**99%**
		1998	-0.143	yes	99%
		1999	-0.097	yes	99%
		2000	0.038	yes	99%
		2001	0.022	yes	99%
		2002	**0.060**	**yes**	**99%**
		2003	0.049	yes	99%
		2004	**0.069**	**yes**	**99%**
		2005	0.076	yes	99%
		2006	**-0.154**	**yes**	**99%**
		2007	0.323	yes	99%
		2008	0.065	yes	99%
		2009	**0.032**	**yes**	**99%**
		2010	0.111	yes	99%
		2011	0.062	yes	99%
		2012	0.071	yes	99%

Region	Station	Year	D-statistic	p < 0.05?	Monte Carlo Confidence
Washington	46029	1984	-0.127	yes	99%
		1985	0.216	yes	99%
		1986	**0.132**	**yes**	**99%**
		1987	0.347	yes	99%
		1991	**0.219**	**yes**	**99%**
		1992	-0.082	yes	99%
		1993	-0.148	yes	99%
		1994	**0.031**	**yes**	**99%**
		1995	-0.094	yes	99%
		1996	-0.362	yes	99%
		1997	**-0.035**	**yes**	**99%**
		1998	-0.061	yes	99%
		1999	0.091	yes	99%
		2000	-0.099	yes	99%
		2001	0.068	yes	99%
		2002	**-0.038**	**yes**	**99%**
		2003	0.030	yes	99%
		2004	**-0.051**	**yes**	**99%**
		2005	-0.097	yes	99%
		2006	**0.071**	**yes**	**99%**
		2007	-0.027	yes	99%
		2008	-0.083	yes	99%
		2009	**0.081**	**yes**	**99%**
		2010	0.104	yes	99%
		2011	0.040	yes	99%
		2012	0.155	yes	99%

Region	Station	Year	D-statistic	$p < 0.05$?	Monte Carlo Confidence
Washington	36	**1982**	**-0.371**	**yes**	**99%**
		1987	0.133	yes	99%
		1988	-0.193	yes	99%
		1989	0.104	yes	99%
		1990	-0.047	no	n/a
		1991	**-0.105**	**yes**	**99%**
		1992	-0.114	yes	99%
		1993	-0.142	yes	99%
		1994	**-0.153**	**yes**	**99%**
		1995	0.052	yes	99%
		1996	0.065	yes	99%
		1997	**-0.070**	**yes**	**99%**
		1998	-0.034	yes	99%
		1999	-0.056	yes	99%
		2000	-0.039	yes	99%
		2001	-0.037	yes	99%
		2002	**0.039**	**yes**	**99%**
		2003	0.017	no	n/a
		2004	**0.091**	**yes**	**99%**
		2005	0.098	yes	99%
		2006	**0.081**	**yes**	**99%**
		2007	-0.070	yes	99%
		2008	0.068	yes	99%
		2009	**-0.042**	**yes**	**99%**
		2010	0.082	yes	99%
		2011	-0.069	yes	99%
		2012	-0.091	yes	99%

Region	Station	Year	D-statistic	p < 0.05?	Monte Carlo Confidence
Washington	46005	**1976**	**-0.135**	**yes**	**99%**
		1977	0.278	yes	99%
		1978	-0.145	yes	99%
		1979	**-0.152**	**yes**	**99%**
		1980	-0.063	yes	99%
		1981	0.032	yes	99%
		1982	**-0.105**	**yes**	**99%**
		1983	-0.051	yes	99%
		1984	0.068	yes	99%
		1985	-0.255	yes	99%
		1986	**-0.074**	**yes**	**99%**
		1987	0.130	yes	99%
		1988	0.025	yes	99%
		1989	-0.098	yes	99%
		1990	0.087	yes	99%
		1991	**-0.046**	**yes**	**99%**
		1992	-0.051	yes	99%
		1993	0.081	yes	99%
		1994	**0.059**	**yes**	**99%**
		1995	0.069	yes	99%
		1996	-0.083	yes	99%
		1997	**-0.025**	**yes**	**99%**
		1998	0.085	yes	99%
		1999	0.092	yes	99%
		2000	-0.034	yes	99%
		2001	0.084	yes	99%
		2002	**0.030**	**yes**	**99%**
		2003	0.057	yes	99%
		2004	**0.067**	**yes**	**99%**
		2006	**-0.109**	**yes**	**99%**
		2007	0.038	yes	99%
		2008	0.054	yes	99%
		2010	-0.148	yes	99%
		2011	-0.064	yes	99%
		2012	0.139	yes	99%

Region	Station	Year	D-statistic	p < 0.05?	Monte Carlo Confidence
Oregon	46050	**1991**	**0.407**	**yes**	**99%**
		1992	-0.071	yes	99%
		1993	-0.097	yes	99%
		1994	**-0.113**	**yes**	**99%**
		1995	-0.055	yes	99%
		1996	-0.060	yes	99%
		1997	**0.221**	**yes**	**99%**
		1998	0.032	yes	99%
		1999	0.106	yes	99%
		2000	0.024	yes	99%
		2001	0.040	yes	99%
		2002	**-0.073**	**yes**	**99%**
		2003	0.038	yes	99%
		2004	**-0.032**	**yes**	**99%**
		2005	-0.100	yes	99%
		2006	**0.077**	**yes**	**99%**
		2007	-0.049	yes	99%
		2008	-0.089	yes	99%
		2009	**-0.057**	**yes**	**99%**
		2010	0.092	yes	99%
		2011	0.056	yes	99%
		2012	0.049	yes	99%

Region	Station	Year	D-statistic	p < 0.05?	Monte Carlo Confidence
Oregon	46002	1975	0.223	yes	99%
		1976	**-0.209**	**yes**	**99%**
		1977	0.030	yes	99%
		1978	-0.108	yes	99%
		1979	**-0.146**	**yes**	**99%**
		1980	-0.061	yes	99%
		1981	0.036	yes	99%
		1982	**-0.126**	**yes**	**99%**
		1983	0.082	yes	99%
		1984	0.278	yes	99%
		1985	-0.078	yes	99%
		1986	**0.029**	**yes**	**99%**
		1987	-0.059	yes	99%
		1988	0.196	yes	99%
		1989	-0.086	yes	99%
		1990	-0.052	yes	99%
		1991	**-0.092**	**yes**	**99%**
		1992	-0.055	yes	99%
		1993	0.063	yes	99%
		1994	**0.061**	**yes**	**99%**
		1995	0.076	yes	99%
		1996	-0.046	yes	99%
		1997	**0.146**	**yes**	**99%**
		1998	0.063	yes	99%
		2000	-0.122	yes	99%
		2001	0.086	yes	99%
		2002	**0.024**	**yes**	**99%**
		2003	0.188	yes	99%
		2004	**-0.059**	**yes**	**99%**
		2005	0.088	yes	99%
		2006	**0.060**	**yes**	**99%**
		2007	0.045	yes	99%
		2008	0.038	yes	99%
		2009	**-0.106**	**yes**	**99%**
		2011	-0.150	yes	99%
		2012	-0.066	yes	99%

Region	Station	Year	D-statistic	p < 0.05?	Monte Carlo Confidence
Northern California	46027	1985	-0.136	yes	99%
		1986	**0.078**	**yes**	**99%**
		1987	0.102	yes	99%
		1988	-0.060	yes	99%
		1989	-0.195	yes	99%
		1990	-0.046	yes	99%
		1991	**-0.069**	**yes**	**99%**
		1992	-0.055	yes	99%
		1993	0.041	yes	99%
		1994	**-0.020**	**yes**	**97.5%**
		1995	0.059	yes	99%
		1996	-0.042	yes	99%
		1997	**0.169**	**yes**	**99%**
		1998	-0.220	yes	99%
		1999	0.127	yes	99%
		2000	0.026	yes	99%
		2001	0.092	yes	99%
		2002	**0.031**	**yes**	**99%**
		2003	-0.024	yes	99%
		2004	**-0.038**	**yes**	**99%**
		2005	0.289	yes	99%
		2006	**0.052**	**yes**	**99%**
		2007	-0.121	yes	99%
		2008	-0.074	yes	99%
		2009	**-0.050**	**yes**	**99%**
		2010	0.094	yes	99%
		2011	-0.027	yes	99%
		2012	-0.039	yes	99%

Region	Station	Year	D-statistic	p < 0.05?	Monte Carlo Confidence
Northern California	46006	1977	-0.226	yes	99%
		1978	-0.139	yes	99%
		1979	**-0.111**	**yes**	**99%**
		1981	-0.153	yes	99%
		1982	**-0.074**	**yes**	**99%**
		1983	0.062	yes	99%
		1984	0.223	yes	99%
		1985	-0.076	yes	99%
		1986	**0.116**	**yes**	**99%**
		1987	0.042	yes	99%
		1988	0.069	yes	99%
		1989	-0.138	yes	99%
		1990	-0.077	yes	99%
		1991	**0.357**	**yes**	**99%**
		1992	-0.163	yes	99%
		1993	0.037	yes	99%
		1994	**0.075**	**yes**	**99%**
		1995	0.061	yes	99%
		1996	0.042	yes	99%
		1997	**0.210**	**yes**	**99%**
		1998	0.146	yes	99%
		1999	0.066	yes	99%
		2000	0.074	yes	99%
		2001	0.045	yes	99%
		2002	**-0.055**	**yes**	**99%**
		2003	0.161	yes	99%
		2004	**0.037**	**yes**	**99%**
		2005	0.071	yes	99%
		2006	**0.046**	**yes**	**99%**
		2007	-0.090	yes	99%
		2008	-0.078	yes	99%
		2009	**-0.067**	**yes**	**99%**
		2010	0.149	yes	99%
		2011	-0.055	yes	99%
		2012	-0.038	yes	99%

Region	Station	Year	D-statistic	p < 0.05?	Monte Carlo Confidence
Northern California	46022	**1982**	**-0.097**	**yes**	**99%**
		1983	0.054	yes	99%
		1984	-0.047	yes	99%
		1985	-0.055	yes	99%
		1986	**0.044**	**yes**	**99%**
		1987	-0.021	yes	97.5%
		1988	-0.049	yes	99%
		1989	-0.120	yes	99%
		1990	0.167	yes	99%
		1991	**-0.035**	**yes**	**99%**
		1992	-0.060	yes	99%
		1993	-0.110	yes	99%
		1994	**-0.043**	**yes**	**99%**
		1995	0.044	yes	99%
		1996	0.128	yes	99%
		1997	**-0.038**	**yes**	**99%**
		1998	0.150	yes	99%
		1999	0.118	yes	99%
		2000	-0.126	yes	99%
		2001	0.047	yes	99%
		2002	**0.030**	**yes**	**99%**
		2003	-0.055	yes	99%
		2004	**-0.032**	**yes**	**99%**
		2005	-0.048	yes	99%
		2006	**0.070**	**yes**	**99%**
		2007	-0.050	yes	99%
		208	-0.039	yes	99%
		2009	**-0.066**	**yes**	**99%**
		2010	0.145	yes	99%
		2011	-0.066	yes	99%
		2012	0.309	yes	99%

Region	Station	Year	D-statistic	p < 0.05?	Monte Carlo Confidence
Northern California	46014	1981	-0.048	yes	99%
		1982	**-0.126**	**yes**	**99%**
		1983	-0.082	yes	99%
		1984	-0.035	yes	99%
		1985	-0.073	yes	99%
		1986	**0.042**	**yes**	**99%**
		1987	0.058	yes	99%
		1988	-0.093	yes	99%
		1989	-0.140	yes	99%
		1990	-0.057	yes	99%
		1991	**-0.042**	**yes**	**99%**
		1992	-0.095	yes	99%
		1993	-0.109	yes	99%
		1994	**0.063**	**yes**	**99%**
		1995	0.059	yes	99%
		1996	0.047	yes	99%
		1997	**0.035**	**yes**	**99%**
		1998	0.098	yes	99%
		1999	0.090	yes	99%
		2000	0.025	yes	99%
		2001	0.139	yes	99%
		2002	**-0.028**	**yes**	**99%**
		2003	-0.032	yes	99%
		2004	**-0.038**	**yes**	**99%**
		2005	0.048	yes	99%
		2006	**0.142**	**yes**	**99%**
		2007	-0.031	yes	99%
		2008	-0.049	yes	99%
		2009	**-0.064**	**yes**	**99%**
		2010	0.081	yes	99%
		2011	-0.042	yes	99%
		2012	-0.021	yes	97.5%

Region	Station	Year	D-statistic	p < 0.05?	Monte Carlo Confidence
Central California	46059	**1994**	**0.289**	**yes**	**99%**
		1995	-0.059	yes	99%
		1996	-0.057	yes	99%
		1997	**-0.051**	**yes**	**99%**
		1998	0.078	yes	99%
		1999	0.065	yes	99%
		2000	-0.044	yes	99%
		2001	-0.044	yes	99%
		2002	**-0.066**	**yes**	**99%**
		2003	-0.026	yes	99%
		2004	**-0.032**	**yes**	**99%**
		2005	0.149	yes	99%
		2006	**0.051**	**yes**	**99%**
		2007	-0.055	yes	99%
		2008	-0.040	yes	99%
		2009	**-0.298**	**yes**	**99%**
		2010	0.067	yes	99%
		2011	-0.041	yes	99%
		2012	0.109	yes	99%

Region	Station	Year	D-statistic	p < 0.05?	Monte Carlo Confidence
Central California	46013	1981	-0.076	yes	99%
		1982	**-0.164**	**yes**	**99%**
		1983	0.039	yes	99%
		1984	0.121	yes	99%
		1985	-0.066	yes	99%
		1986	**-0.043**	**yes**	**99%**
		1987	-0.043	yes	99%
		1988	-0.088	yes	99%
		1989	-0.117	yes	99%
		1990	-0.049	yes	99%
		1991	**-0.041**	**yes**	**99%**
		1992	-0.037	yes	99%
		1993	0.056	yes	99%
		1994	**0.069**	**yes**	**99%**
		1995	0.030	yes	99%
		1996	0.048	yes	99%
		1997	**0.237**	**yes**	**99%**
		1998	0.083	yes	99%
		1999	0.131	yes	99%
		2000	0.052	yes	99%
		2001	0.121	yes	99%
		2002	**-0.058**	**yes**	**99%**
		2003	-0.029	yes	99%
		2004	**-0.077**	**yes**	**99%**
		2005	-0.046	yes	99%
		2006	**0.037**	**yes**	**99%**
		2007	-0.039	yes	99%
		2008	0.036	yes	99%
		2009	**-0.100**	**yes**	**99%**
		2010	0.088	yes	99%
		2011	-0.086	yes	99%
		2012	-0.035	yes	99%

Region	Station	Year	D-statistic	p < 0.05?	Monte Carlo Confidence
Central California	46026	**1982**	**-0.286**	**yes**	**99%**
		1983	-0.090	yes	99%
		1984	-0.056	yes	99%
		1985	-0.196	yes	99%
		1986	**-0.101**	**yes**	**99%**
		1987	0.091	yes	99%
		1988	-0.088	yes	99%
		1989	-0.219	yes	99%
		1990	-0.109	yes	99%
		1991	**-0.135**	**yes**	**99%**
		1992	-0.069	yes	99%
		1993	-0.100	yes	99%
		1994	**-0.049**	**yes**	**99%**
		1995	-0.061	yes	99%
		1996	-0.044	yes	99%
		1997	**0.107**	**yes**	**99%**
		1998	0.237	yes	99%
		1999	0.046	yes	99%
		2000	0.092	yes	99%
		2001	0.168	yes	99%
		2002	**0.052**	**yes**	**99%**
		2003	0.090	yes	99%
		2004	**-0.036**	**yes**	**99%**
		2005	0.055	yes	99%
		2006	**0.063**	**yes**	**99%**
		2007	0.075	yes	99%
		2008	0.102	yes	99%
		2009	**0.066**	**yes**	**99%**
		2010	0.077	yes	99%
		2011	0.094	yes	99%
		2012	0.061	yes	99%

Region	Station	Year	D-statistic	p < 0.05?	Monte Carlo Confidence
Central California	46012	1980	-0.139	yes	99%
		1981	-0.044	yes	99%
		1982	**-0.172**	**yes**	**99%**
		1983	0.057	yes	99%
		1984	-0.057	yes	99%
		1985	-0.147	yes	99%
		1986	**-0.089**	**yes**	**99%**
		1987	-0.173	yes	99%
		1988	-0.081	yes	99%
		1989	-0.183	yes	99%
		1990	-0.119	yes	99%
		1991	**-0.040**	**yes**	**99%**
		1992	-0.049	yes	99%
		1993	0.217	yes	99%
		1994	**-0.049**	**yes**	**99%**
		1995	-0.097	yes	99%
		1996	-0.026	yes	99%
		1997	**0.092**	**yes**	**99%**
		1998	-0.062	yes	99%
		1999	0.133	yes	99%
		2000	0.041	yes	99%
		2001	0.048	yes	99%
		2002	**-0.135**	**yes**	**99%**
		2003	-0.027	yes	99%
		2004	**0.078**	**yes**	**99%**
		2005	0.089	yes	99%
		2006	**0.116**	**yes**	**99%**
		2007	0.052	yes	99%
		2008	0.086	yes	99%
		2009	**0.077**	**yes**	**99%**
		2010	0.123	yes	99%
		2011	0.105	yes	99%
		2012	0.153	yes	99%

Region	Station	Year	D-statistic	p < 0.05?	Monte Carlo Confidence
Central California	46042	1987	0.263	yes	99%
		1988	-0.036	yes	99%
		1989	-0.151	yes	99%
		1990	-0.063	yes	99%
		1991	**-0.028**	**yes**	**99%**
		1992	-0.041	yes	99%
		1993	-0.041	yes	99%
		1994	**-0.046**	**yes**	**99%**
		1995	0.040	yes	99%
		1996	-0.036	yes	99%
		1997	**-0.051**	**yes**	**99%**
		1998	0.065	yes	99%
		1999	0.122	yes	99%
		2000	0.025	yes	99%
		2001	0.095	yes	99%
		2002	**-0.059**	**yes**	**99%**
		2003	-0.032	yes	99%
		2004	**-0.044**	**yes**	**99%**
		2005	-0.037	yes	99%
		2006	**0.039**	**yes**	**99%**
		2007	-0.030	yes	99%
		2008	0.045	yes	99%
		2009	**-0.053**	**yes**	**99%**
		2010	0.069	yes	99%
		2011	0.053	yes	99%
		2012	0.036	yes	99%

Region	Station	Year	D-statistic	p < 0.05?	Monte Carlo Confidence
Central California	46028	1983	0.126	yes	99%
		1984	0.069	yes	99%
		1985	-0.128	yes	99%
		1986	**0.043**	**yes**	**99%**
		1987	0.038	yes	99%
		1988	-0.145	yes	99%
		1989	-0.092	yes	99%
		1990	0.030	yes	99%
		1991	**-0.048**	**yes**	**99%**
		1992	-0.128	yes	99%
		1993	-0.099	yes	99%
		1994	**-0.051**	**yes**	**99%**
		1995	-0.060	yes	99%
		1996	-0.032	yes	99%
		1997	**0.110**	**yes**	**99%**
		1998	0.100	yes	99%
		1999	0.173	yes	99%
		2000	-0.032	yes	99%
		2001	0.113	yes	99%
		2002	**0.028**	**yes**	**99%**
		2003	-0.036	yes	99%
		2004	**0.045**	**yes**	**99%**
		2005	-0.035	yes	99%
		2006	**0.041**	**yes**	**99%**
		2007	0.047	yes	99%
		2008	0.041	yes	99%
		2009	**-0.084**	**yes**	**99%**
		2010	0.030	yes	99%
		2011	-0.031	yes	99%
		2012	-0.019	yes	95%

Region	Station	Year	D-statistic	p < 0.05?	Monte Carlo Confidence
Southern California	76	1983	0.108	yes	99%
		1984	-0.086	yes	99%
		1985	-0.251	yes	99%
		1986	**-0.243**	**yes**	**99%**
		1987	0.058	no	n/a
		1988	-0.071	yes	99%
		1989	-0.076	yes	99%
		1991	**-0.116**	**no**	**n/a**
		1992	-0.159	yes	99%
		1993	0.167	yes	99%
		1994	**-0.067**	**yes**	**99%**
		1995	-0.217	yes	99%
		1996	0.096	yes	99%
		1997	**0.056**	**yes**	**99%**
		1998	-0.078	yes	99%
		1999	0.083	yes	99%
		2000	-0.076	yes	99%
		2001	-0.086	yes	99%
		2002	**0.044**	**yes**	**99%**
		2003	-0.053	yes	99%
		2004	**-0.070**	**yes**	**99%**
		2005	0.059	yes	99%
		2006	**0.054**	**yes**	**99%**
		2007	0.071	yes	99%
		2008	0.120	yes	99%
		2009	**-0.152**	**yes**	**99%**
		2010	0.061	yes	99%
		2011	0.115	yes	99%
		2012	0.085	yes	99%

Region	Station	Year	D-statistic	p < 0.05?	Monte Carlo Confidence
Southern California	46011	1980	-0.101	yes	99%
		1981	-0.049	yes	99%
		1982	**-0.114**	**yes**	**99%**
		1983	0.063	yes	99%
		1984	0.185	yes	99%
		1985	-0.071	yes	99%
		1986	**-0.060**	**yes**	**99%**
		1987	-0.191	yes	99%
		1988	-0.079	yes	99%
		1989	-0.112	yes	99%
		1990	-0.114	yes	99%
		1991	**-0.056**	**yes**	**99%**
		1992	-0.138	yes	99%
		1994	**0.068**	**yes**	**99%**
		1995	0.037	yes	99%
		1996	-0.073	yes	99%
		1997	**0.097**	**yes**	**99%**
		1998	0.146	yes	99%
		1999	0.111	yes	99%
		2000	-0.033	yes	99%
		2001	0.100	yes	99%
		2002	**0.023**	**yes**	**99%**
		2003	-0.031	yes	99%
		2004	**-0.031**	**yes**	**99%**
		2005	0.040	yes	99%
		2006	**-0.082**	**yes**	**99%**
		2007	0.049	yes	99%
		2008	0.036	yes	99%
		2009	**-0.085**	**yes**	**99%**
		2010	0.028	yes	99%
		2011	-0.052	yes	99%
		2012	0.075	yes	99%

Region	Station	Year	D-statistic	p < 0.05?	Monte Carlo Confidence
Southern California	46023	**1982**	**-0.062**	**yes**	**99%**
		1983	0.064	yes	99%
		1984	0.102	yes	99%
		1985	-0.070	yes	99%
		1986	**0.032**	**yes**	**99%**
		1987	0.046	yes	99%
		1988	-0.051	yes	99%
		1989	-0.122	yes	99%
		1990	-0.111	yes	99%
		1991	**0.027**	**yes**	**99%**
		1992	-0.048	yes	99%
		1993	0.040	yes	99%
		1994	**-0.066**	**yes**	**99%**
		1995	0.040	yes	99%
		1996	0.129	yes	99%
		1997	**-0.045**	**yes**	**99%**
		1998	0.097	yes	99%
		1999	0.051	yes	99%
		2000	0.050	yes	99%
		2001	0.062	yes	99%
		2002	**-0.123**	**yes**	**99%**
		2003	-0.050	yes	99%
		2004	**-0.045**	**yes**	**99%**
		2005	-0.021	yes	97.5%
		2006	**0.055**	**yes**	**99%**
		2007	0.056	yes	99%
		2008	0.049	yes	99%
		2009	**-0.068**	**yes**	**99%**
		2010	0.097	yes	99%

Region	Station	Year	D-statistic	p < 0.05?	Monte Carlo Confidence
Southern California	71	1998	-0.061	yes	99%
		1999	-0.066	yes	99%
		2000	-0.066	yes	99%
		2001	-0.068	yes	99%
		2002	**0.034**	**yes**	**99%**
		2003	-0.090	yes	99%
		2004	**-0.126**	**yes**	**99%**
		2005	-0.067	yes	99%
		2006	**0.067**	**yes**	**99%**
		2007	0.116	yes	99%
		2008	0.129	yes	99%
		2009	**-0.197**	**yes**	**99%**
		2010	-0.046	yes	99%
		2011	0.102	yes	99%
		2012	0.152	yes	99%

Region	Station	Year	D-statistic	p < 0.05?	Monte Carlo Confidence
Southern California	46054	**1994**	**-0.068**	**yes**	**99%**
		1995	0.046	yes	99%
		1996	-0.038	yes	99%
		1997	**0.077**	**yes**	**99%**
		1998	0.095	yes	99%
		1999	0.086	yes	99%
		2000	0.050	yes	99%
		2001	0.058	yes	99%
		2002	**-0.136**	**yes**	**99%**
		2003	-0.057	yes	99%
		2004	**-0.056**	**yes**	**99%**
		2005	-0.080	yes	99%
		2006	**-0.027**	**yes**	**99%**
		2007	-0.050	yes	99%
		2008	-0.047	yes	99%
		2009	**-0.080**	**yes**	**99%**
		2010	0.032	yes	99%
		2011	-0.057	yes	99%
		2012	-0.026	yes	99%

Region	Station	Year	D-statistic	p < 0.05?	Monte Carlo Confidence
Southern California	46053	**1994**	**-0.074**	**yes**	**99%**
		1995	0.056	yes	99%
		1996	-0.026	yes	99%
		1998	0.026	yes	99%
		1999	0.096	yes	99%
		2000	0.046	yes	99%
		2001	0.042	yes	99%
		2002	**0.030**	**yes**	**99%**
		2003	-0.034	yes	99%
		2004	**-0.051**	**yes**	**99%**
		2005	0.015	yes	<95%
		2006	**0.047**	**yes**	**99%**
		2007	-0.036	yes	99%
		2008	-0.041	yes	99%
		2009	**-0.049**	**yes**	**99%**
		2010	0.024	yes	99%
		2011	0.050	yes	99%
		2012	-0.049	yes	99%

Region	Station	Year	D-statistic	p < 0.05?	Monte Carlo Confidence
Southern California	46025	**1982**	**-0.135**	**yes**	**99%**
		1983	0.162	yes	99%
		1984	0.146	yes	99%
		1985	0.076	yes	99%
		1986	**-0.181**	**yes**	**99%**
		1987	-0.052	yes	99%
		1988	-0.131	yes	99%
		1989	-0.091	yes	99%
		1990	-0.056	yes	99%
		1991	**-0.152**	**yes**	**99%**
		1992	-0.050	yes	99%
		1993	0.182	yes	99%
		1994	**-0.121**	**yes**	**99%**
		1995	-0.162	yes	99%
		1996	-0.049	yes	99%
		1997	**0.197**	**yes**	**99%**
		1998	0.207	yes	99%
		1999	0.114	yes	99%
		2000	0.094	yes	99%
		2001	0.070	yes	99%
		2002	**-0.077**	**yes**	**99%**
		2003	0.095	yes	99%
		2004	**-0.036**	**yes**	**99%**
		2005	-0.055	yes	99%
		2006	**0.070**	**yes**	**99%**
		2007	-0.105	yes	99%
		2008	-0.085	yes	99%
		2009	**-0.126**	**yes**	**99%**
		2010	0.040	yes	99%
		2011	-0.091	yes	99%
		2012	0.096	yes	99%

Region	Station	Year	D-statistic	p < 0.05?	Monte Carlo Confidence
Southern California	92	1981	-0.231	yes	99%
		1998	0.124	yes	99%
		1999	0.093	yes	99%
		2000	0.039	yes	99%
		2001	-0.036	yes	99%
		2002	**-0.078**	**yes**	**99%**
		2003	0.035	yes	99%
		2004	**-0.046**	**yes**	**99%**
		2005	-0.154	yes	99%
		2006	**0.050**	**yes**	**99%**
		2007	0.040	yes	99%
		2008	0.037	yes	99%
		2009	**-0.178**	**yes**	**99%**
		2010	-0.127	yes	99%
		2011	0.092	yes	99%
		2012	0.054	yes	99%

Region	Station	Year	D-statistic	p < 0.05?	Monte Carlo Confidence
Southern California	45	**1997**	**0.085**	**yes**	**99%**
		1998	0.227	yes	99%
		1999	0.095	yes	99%
		2000	0.053	yes	99%
		2001	-0.096	yes	99%
		2002	**-0.133**	**yes**	**99%**
		2003	-0.059	yes	99%
		2004	**-0.203**	**yes**	**99%**
		2005	**-0.125**	yes	99%
		2006	**0.119**	**yes**	**99%**
		2007	-0.150	yes	99%
		2008	0.113	yes	99%
		2009	**-0.025**	**yes**	**99%**
		2010	0.068	yes	99%
		2011	0.102	yes	99%
		2012	-0.085	yes	99%

Region	Station	Year	D-statistic	p < 0.05?	Monte Carlo Confidence
Southern California	93	1981	0.086	no	n/a
		1982	**-0.225**	**yes**	**99%**
		1985	-0.254	yes	99%
		1986	**-0.316**	**yes**	**99%**
		1987	-0.110	yes	99%
		1988	-0.268	yes	99%
		1989	-0.142	yes	99%
		1990	-0.049	no	n/a
		1991	**-0.357**	**yes**	**99%**
		1992	-0.199	yes	99%
		1993	0.075	yes	99%
		1994	**0.043**	**no**	**n/a**
		1995	-0.244	yes	99%
		1997	**-0.102**	**yes**	**99%**
		1998	0.250	yes	99%
		2006	**0.198**	**yes**	**99%**
		2007	-0.113	yes	99%
		2008	0.088	yes	99%
		2009	**-0.106**	**yes**	**99%**
		2010	0.091	yes	99%
		2011	0.189	yes	99%
		2012	0.035	yes	99%

Region	Station	Year	D-statistic	p < 0.05?	Monte Carlo Confidence
Southern California	46047	**1991**	**0.217**	**yes**	**99%**
		1992	-0.047	yes	99%
		1993	0.130	yes	99%
		1999	-0.052	yes	99%
		2000	0.127	yes	99%
		2001	0.088	yes	99%
		2002	**-0.044**	**yes**	**99%**
		2003	0.022	yes	99%
		2004	**-0.055**	**yes**	**99%**
		2005	-0.069	yes	99%
		2006	**-0.055**	**yes**	**99%**
		2007	-0.039	yes	99%
		2008	-0.017	yes	<95%
		2009	**-0.078**	**yes**	**99%**
		2010	0.044	yes	99%
		2011	-0.108	yes	99%
		2012	0.040	yes	99%

APPENDIX F

Summer Significant Wave Height (H_{sig}) vs. Winter Multivariate ENSO Index (MEI)

Plots of average winter MEI as a function of the percentage difference between average summer H_{sig} for each year and the overall average summer H_{sig} for every station over the time period of available summer H_{sig} data. Plots are shown in north to south latitudinal order, from off of the coast of Washington State to off of the coast of Southern California. Linear regression coefficients are listed in Table 3.4.

Washington

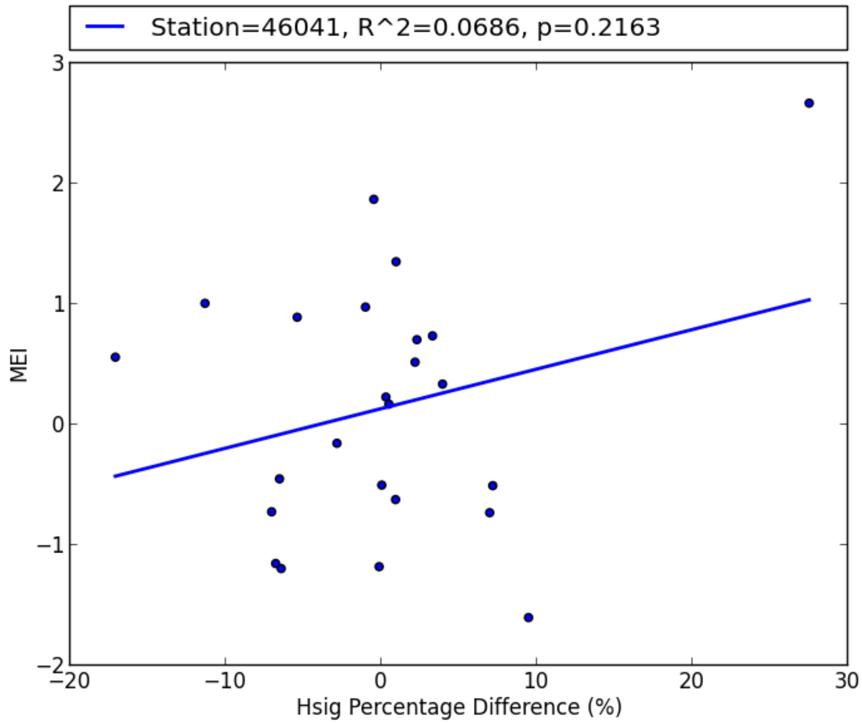
Station=46041, R^2=0.0686, p=0.2163
MEI
Hsig Percentage Difference (%)
3
2
1
0
−1
−2
−20
−10
0
10
20
30

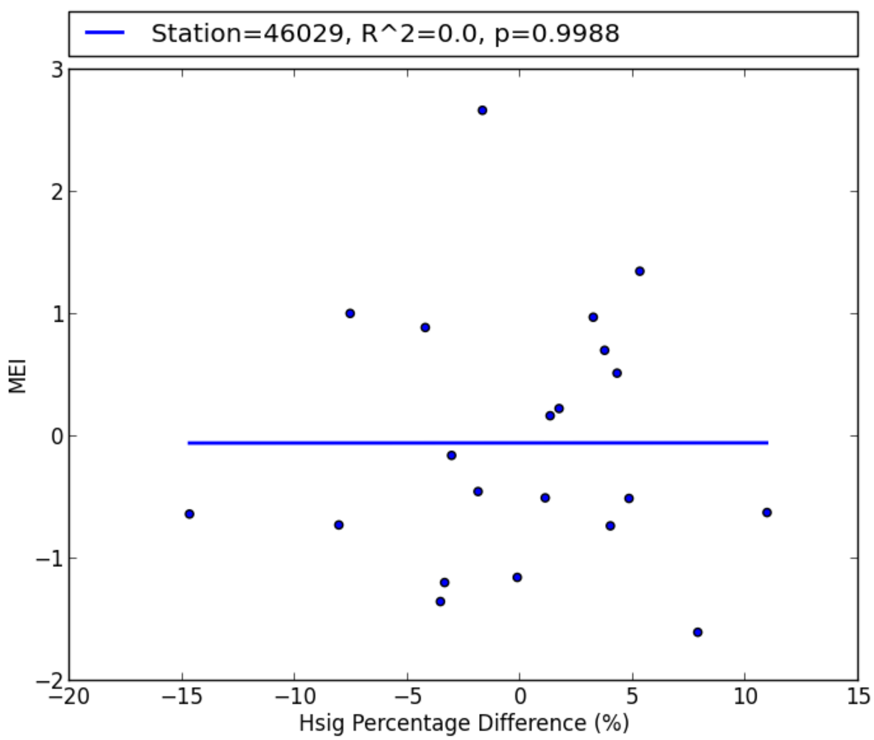
Station=46029, R^2=0.0, p=0.9988
MEI
Hsig Percentage Difference (%)
3
2
1
0
−1
−2
−20
−15
−10
−5
0
5
10
15

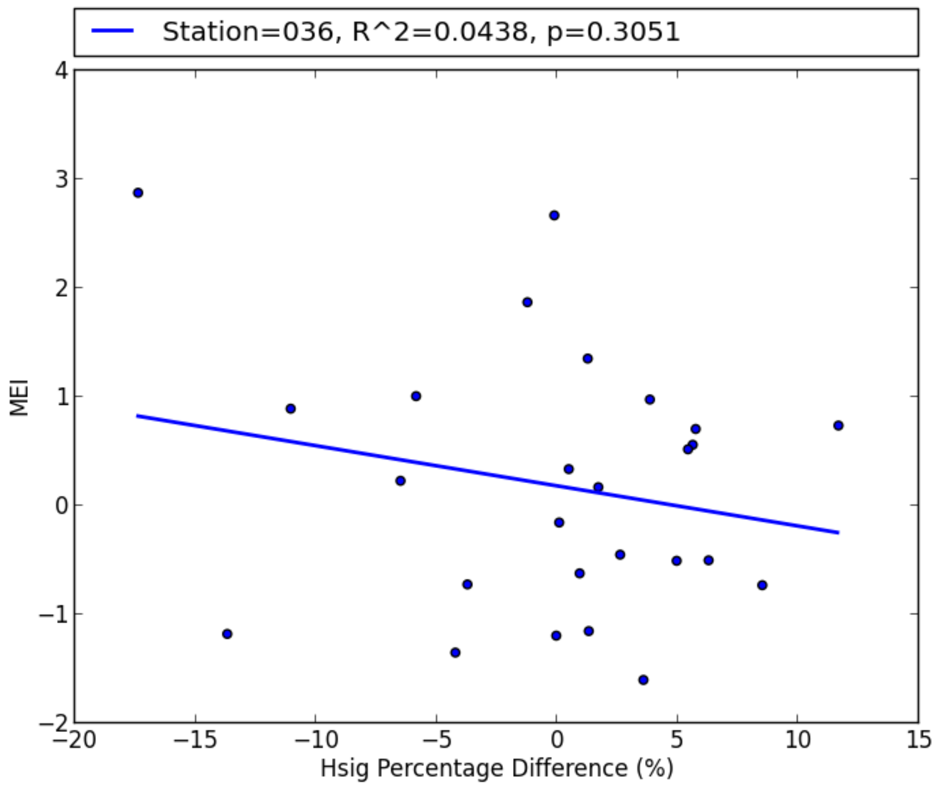
Station=036, R^2=0.0438, p=0.3051
MEI
Hsig Percentage Difference (%)

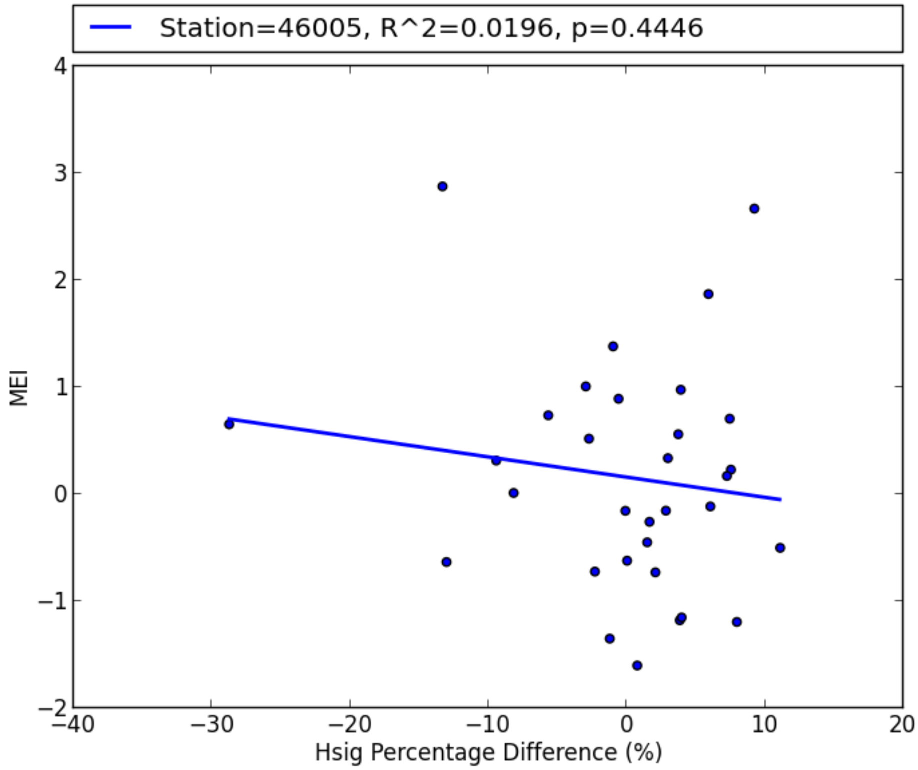
Station=46005, R^2=0.0196, p=0.4446
MEI
Hsig Percentage Difference (%)
4
3
2
1
0
−1
−2
−40
−30
−20
−10
0
10
20

Oregon

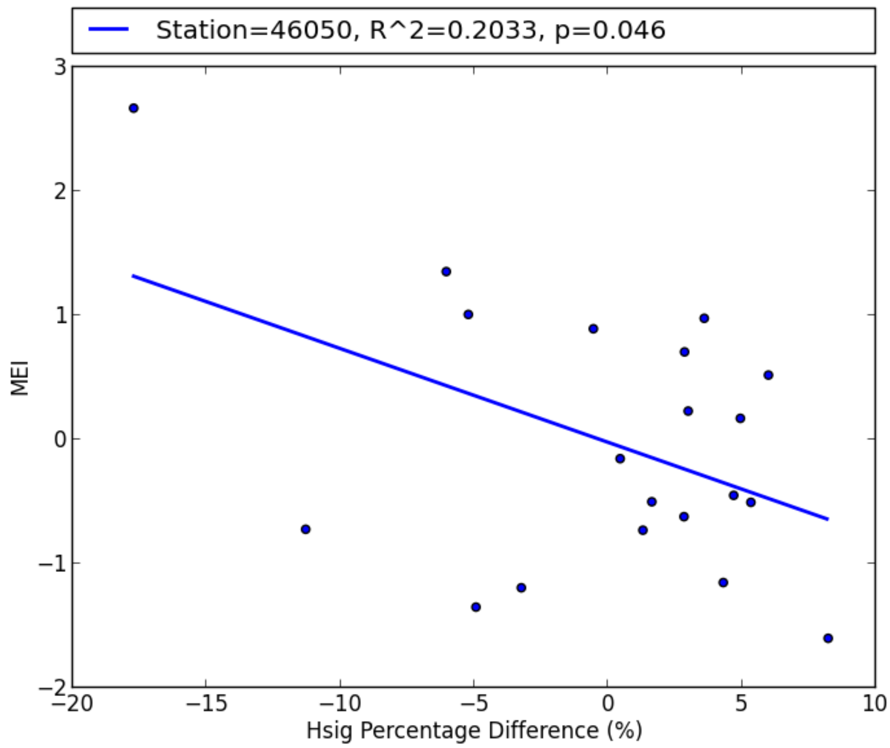
Station=46050, R^2=0.2033, p=0.046
MEI
Hsig Percentage Difference (%)
3
2
1
0
−1
−2
−20
−15
−10
−5
0
5
10

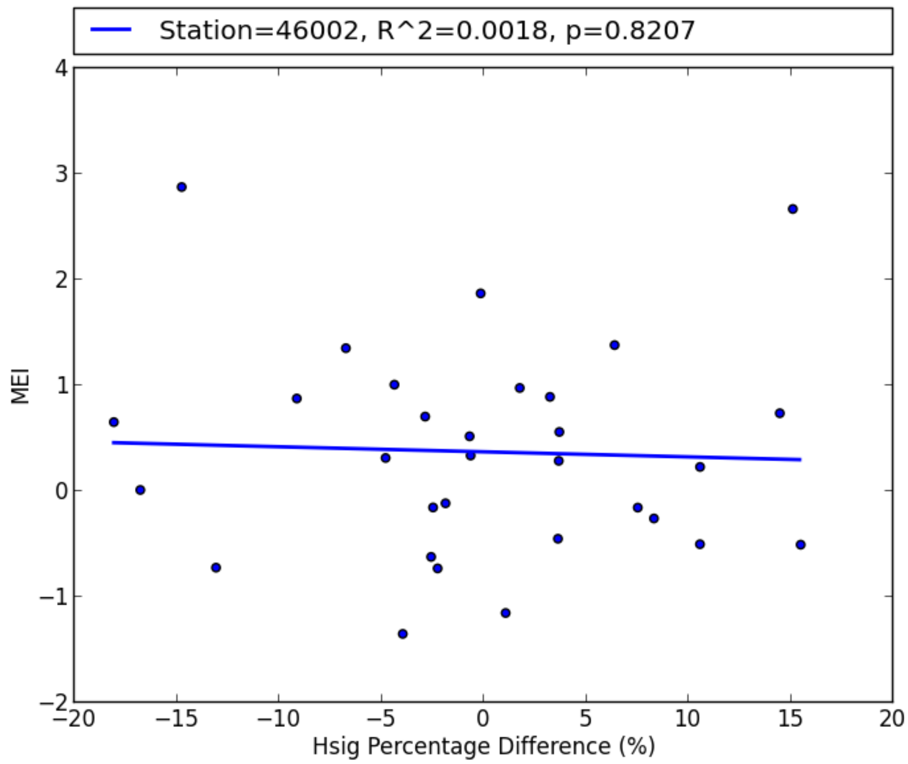

Station=46002, R^2=0.0018, p=0.8207
MEI
Hsig Percentage Difference (%)

Northern California

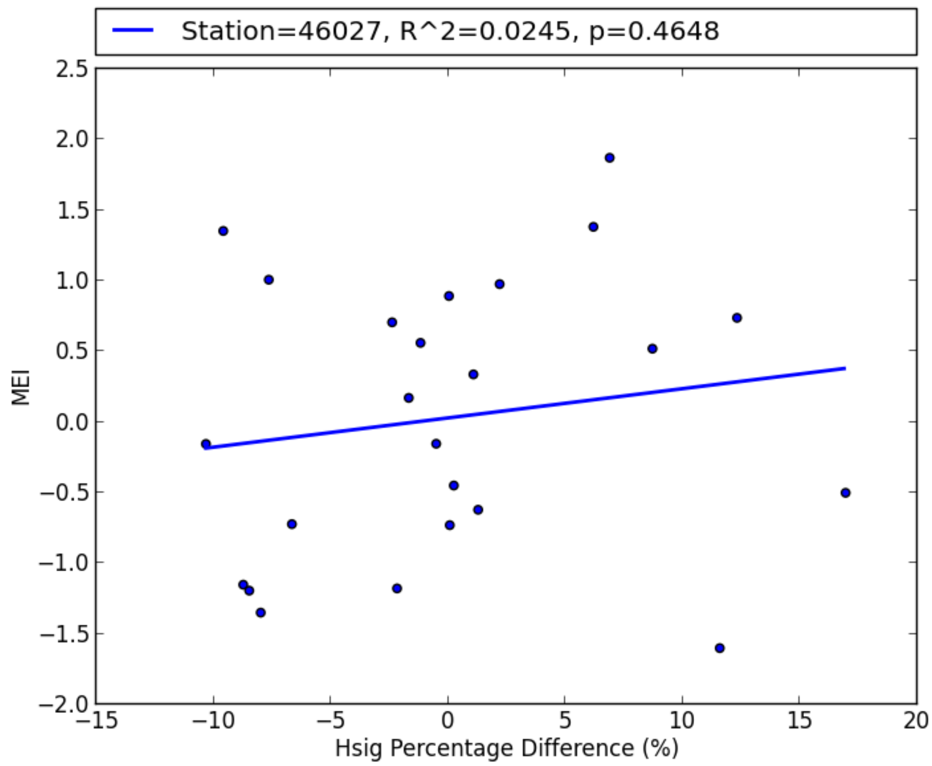

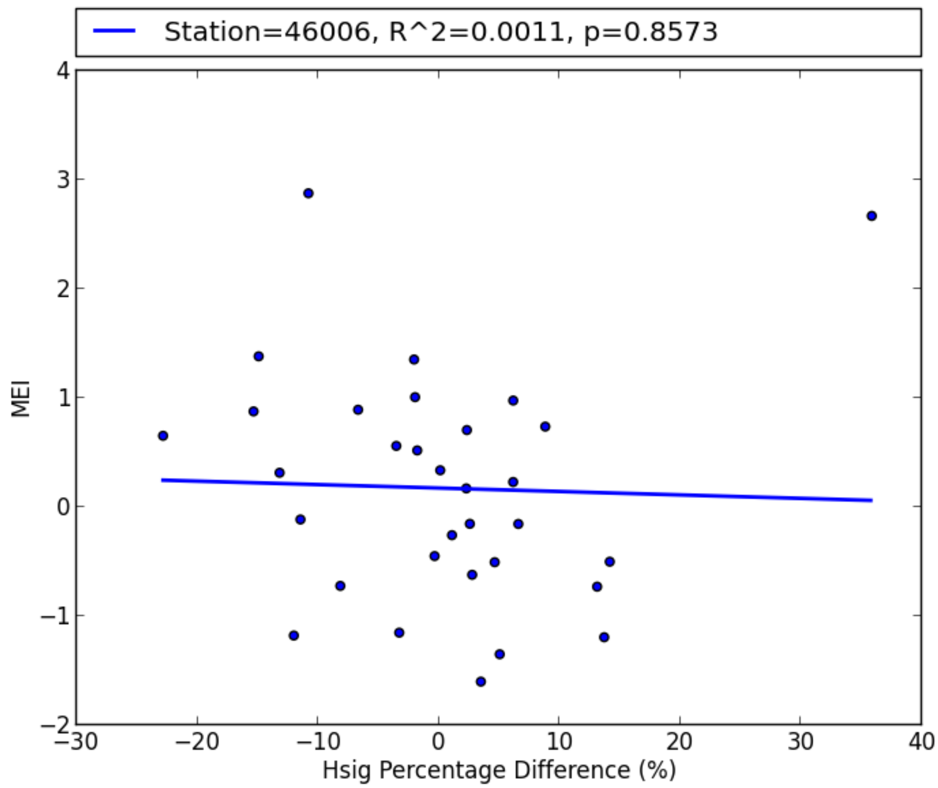

Station=46006, R^2=0.0011, p=0.8573
MEI
Hsig Percentage Difference (%)
4
3
2
1
0
−1
−2
−30
−20
−10
0
10
20
30
40

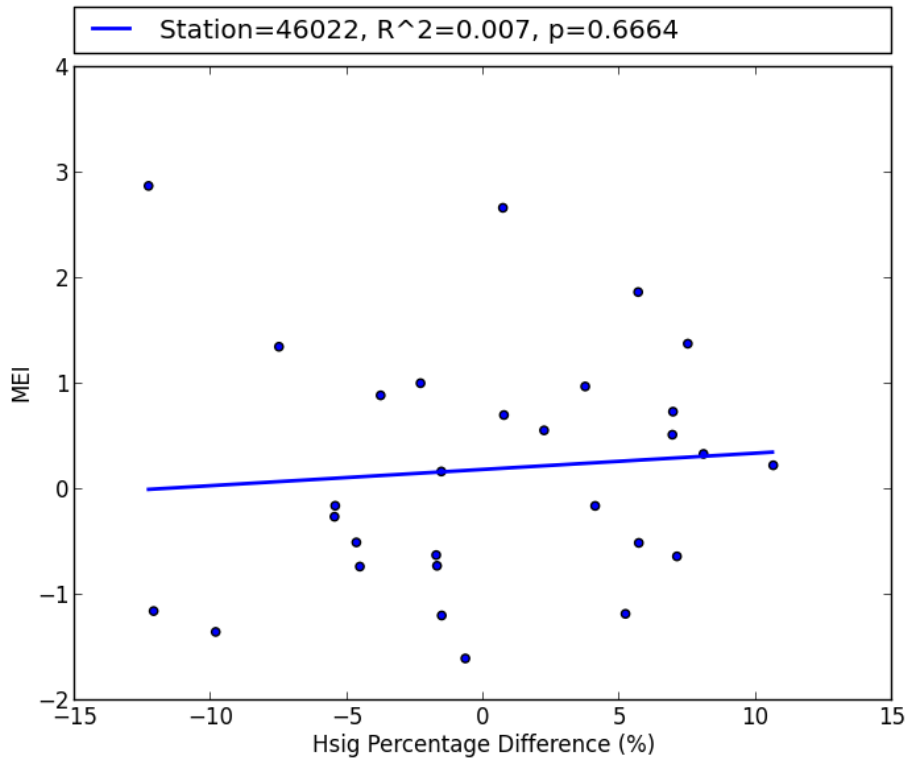
Station=46022, R^2=0.007, p=0.6664
MEI
Hsig Percentage Difference (%)
4
3
2
1
0
−1
−2
−15
−10
−5
0
5
10
15

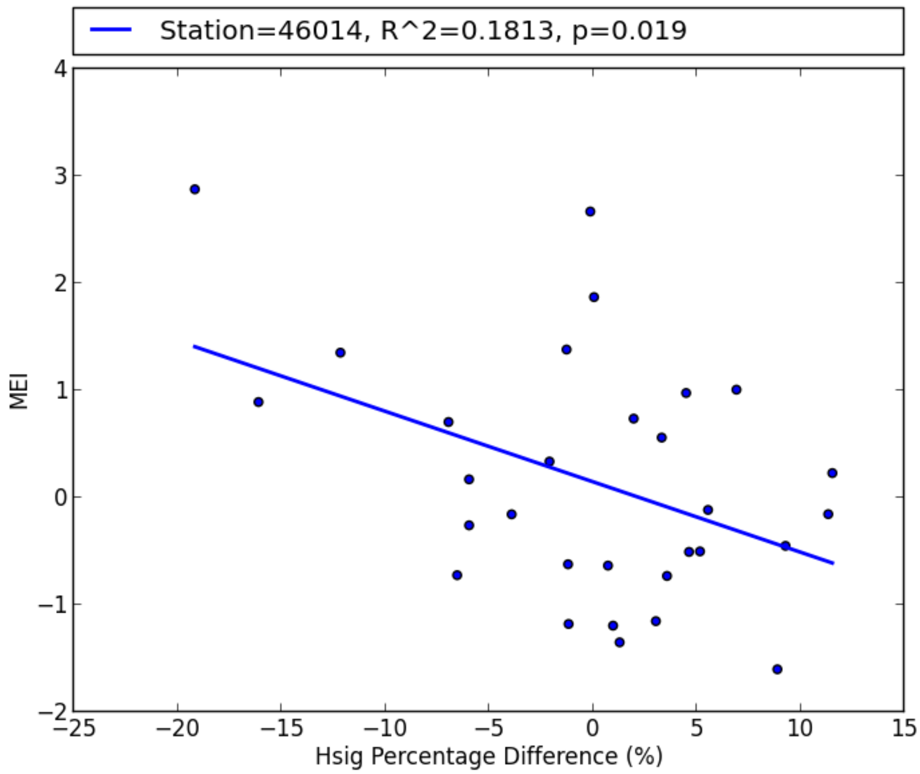

Station=46014, R^2=0.1813, p=0.019
MEI
Hsig Percentage Difference (%)
4
3
2
1
0
−1
−2
−25
−20
−15
−10
−5
0
5
10
15

Central California

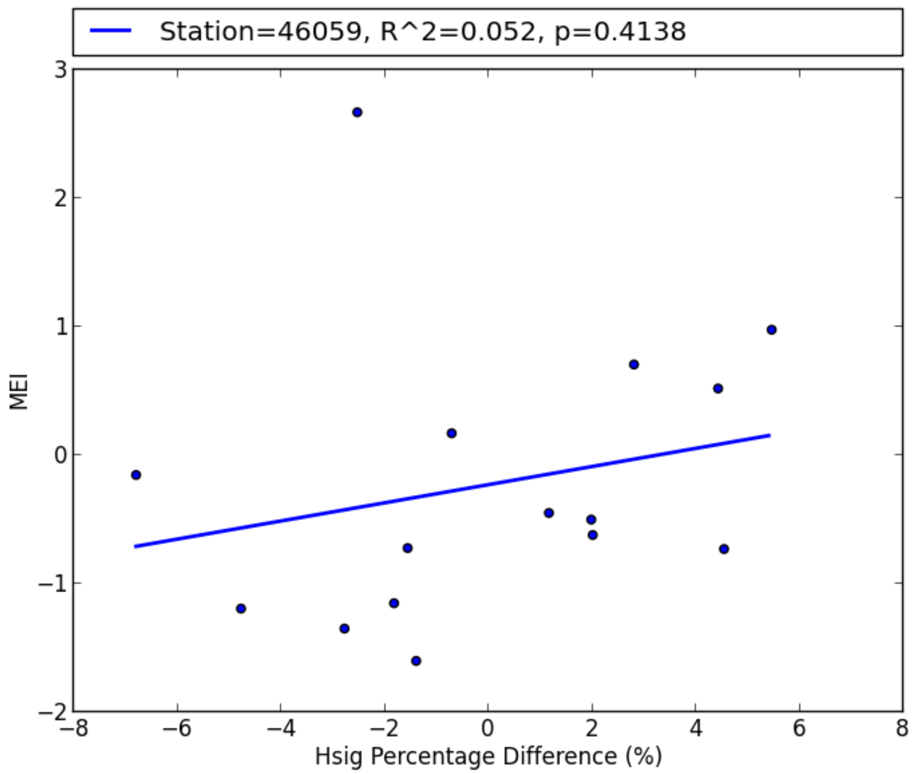

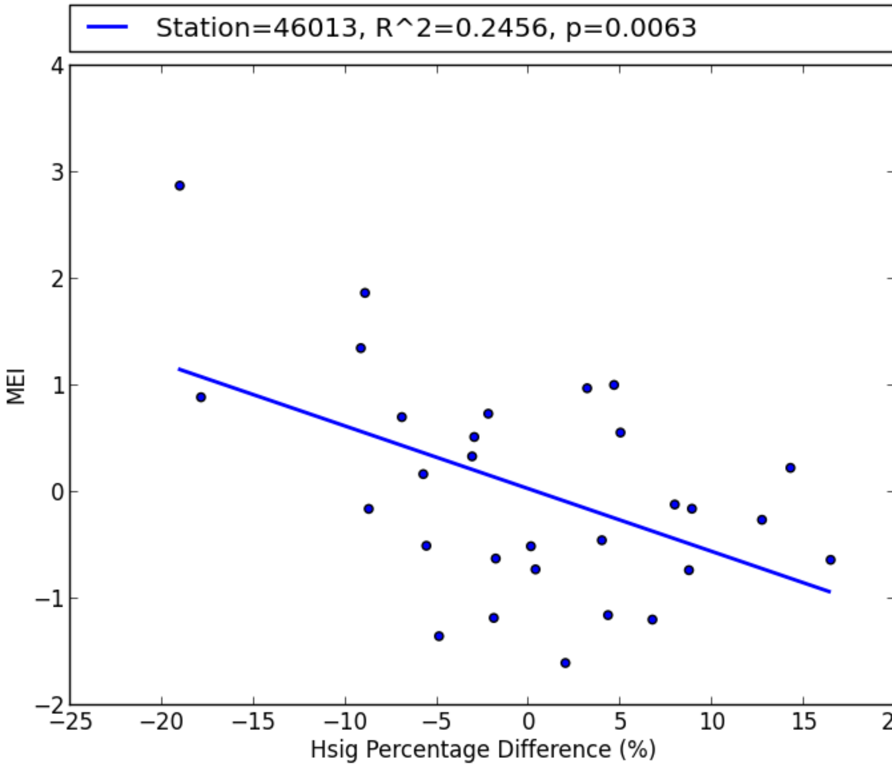

Station=46013, R^2=0.2456, p=0.0063
4
3
2
1
0
−1
−2
MEI
−25
−20
−15
−10
−5
0
5
10
15
20
Hsig Percentage Difference (%)

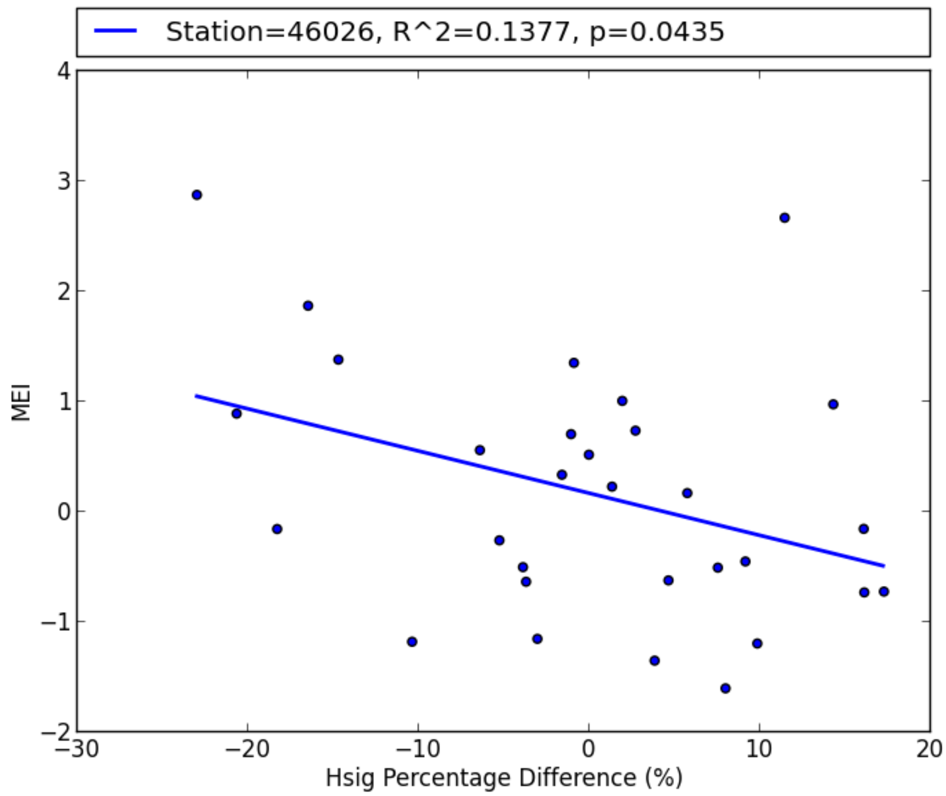
Station=46026, R^2=0.1377, p=0.0435
4
3
2
1
0
−1
−2
MEI
−30
−20
−10
0
10
20
Hsig Percentage Difference (%)

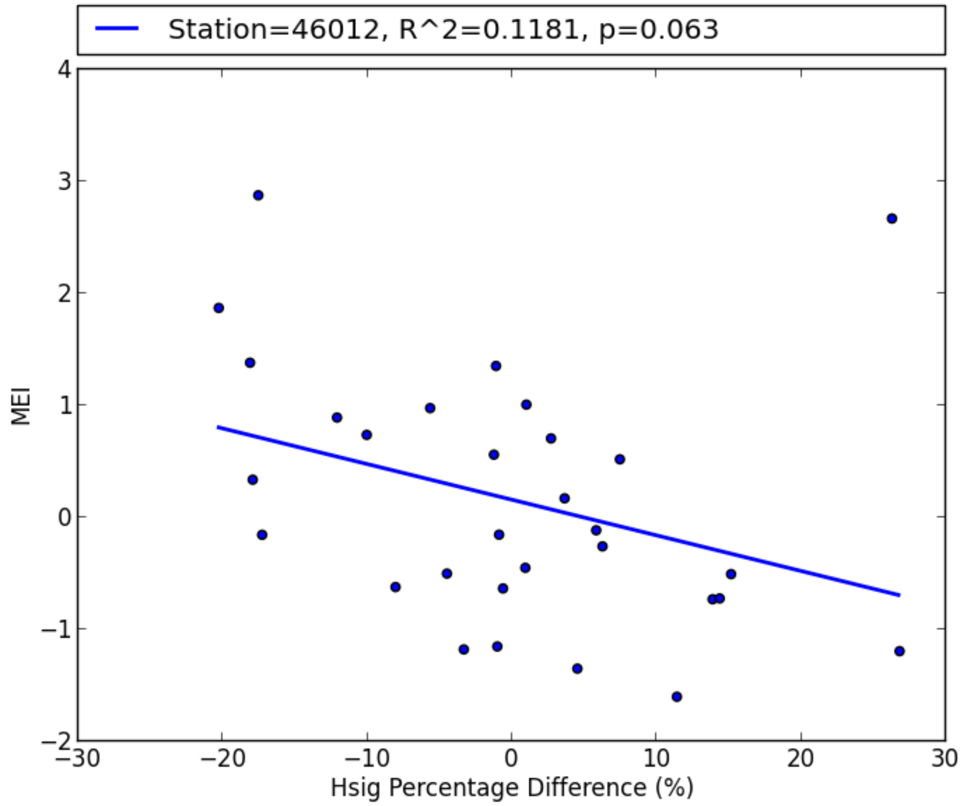

Station=46012, R^2=0.1181, p=0.063
MEI
Hsig Percentage Difference (%)

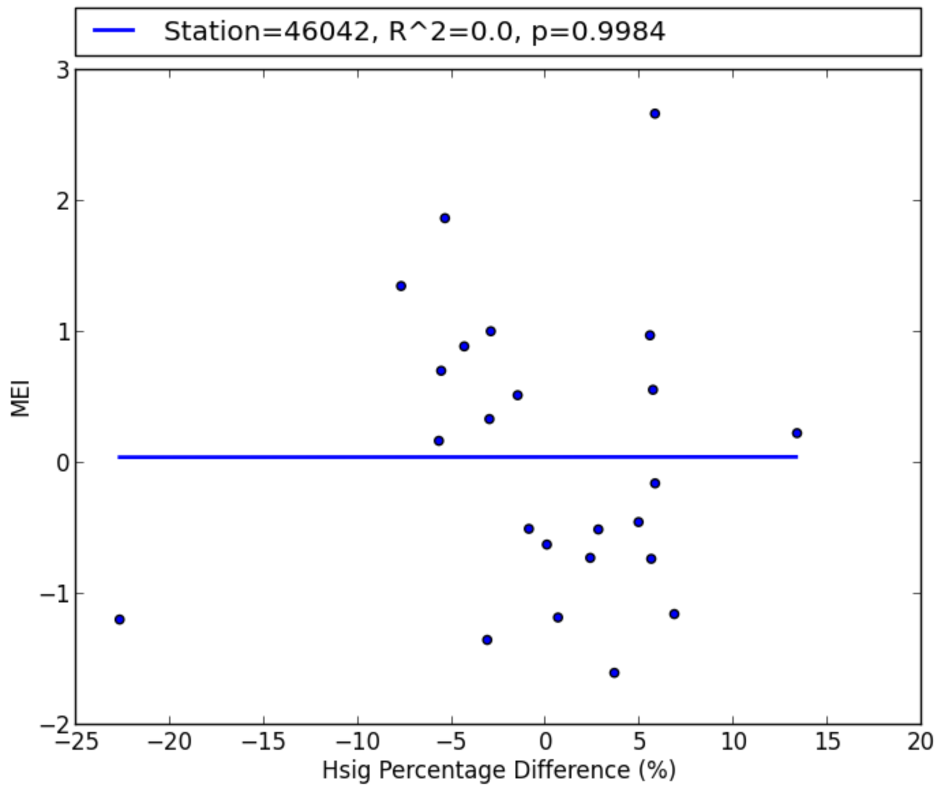

Station=46042, R^2=0.0, p=0.9984
MEI
Hsig Percentage Difference (%)
3
2
1
0
−1
−2
−25
−20
−15
−10
−5
0
5
10
15
20

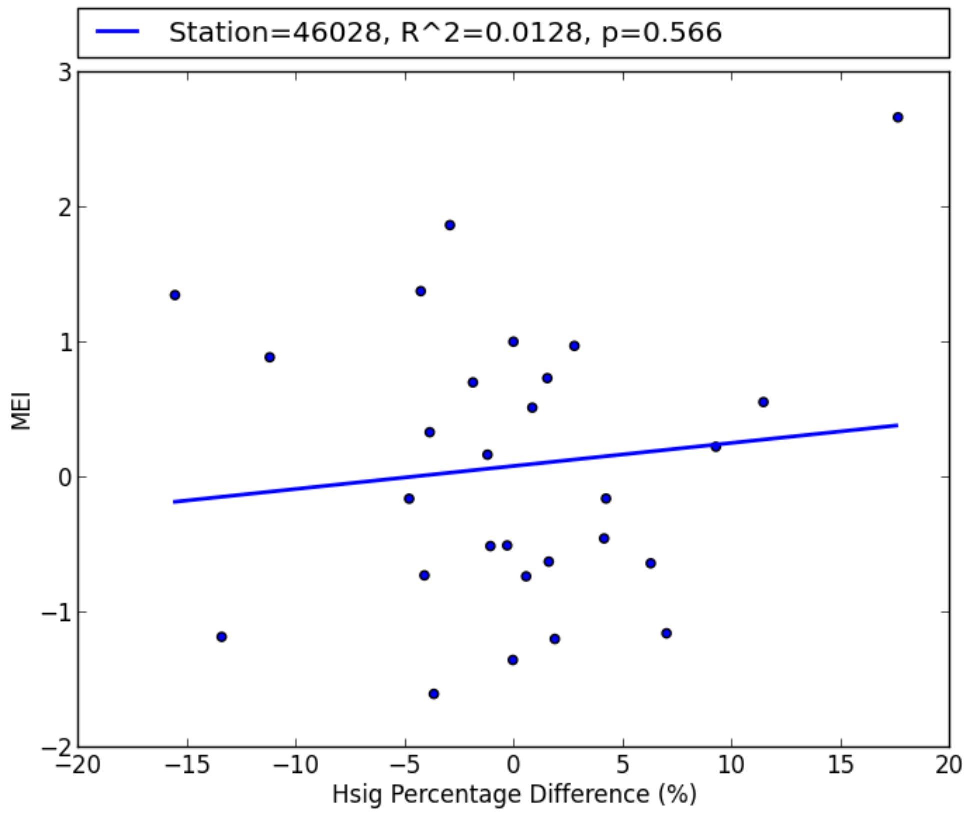
Station=46028, R^2=0.0128, p=0.566
MEI
Hsig Percentage Difference (%)
3
2
1
0
−1
−2
−20
−15
−10
−5
0
5
10
15
20

Southern California

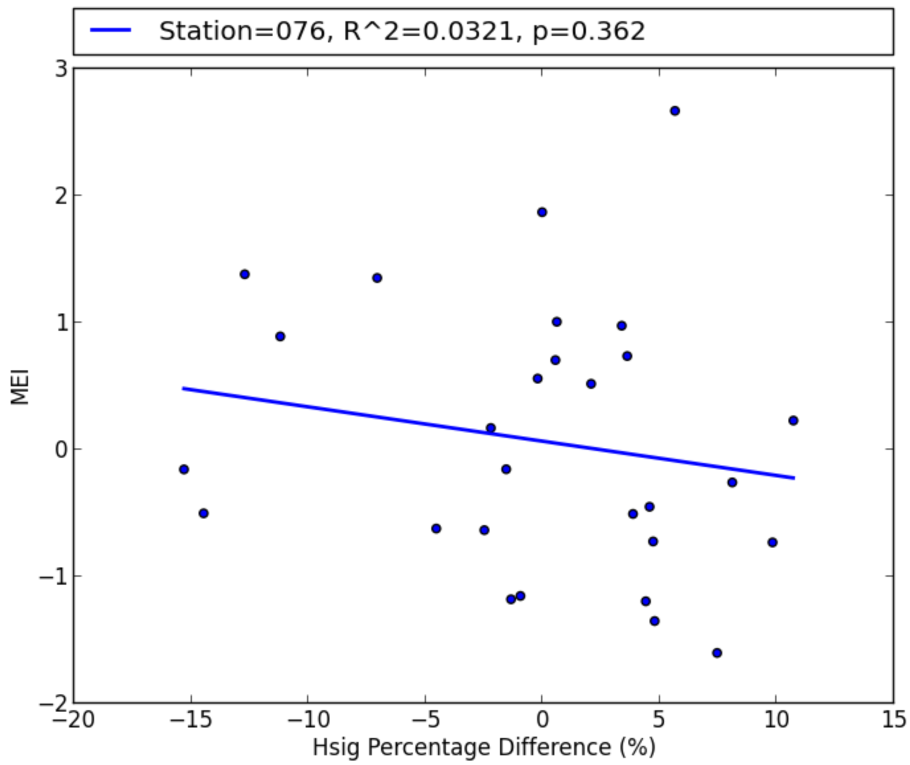

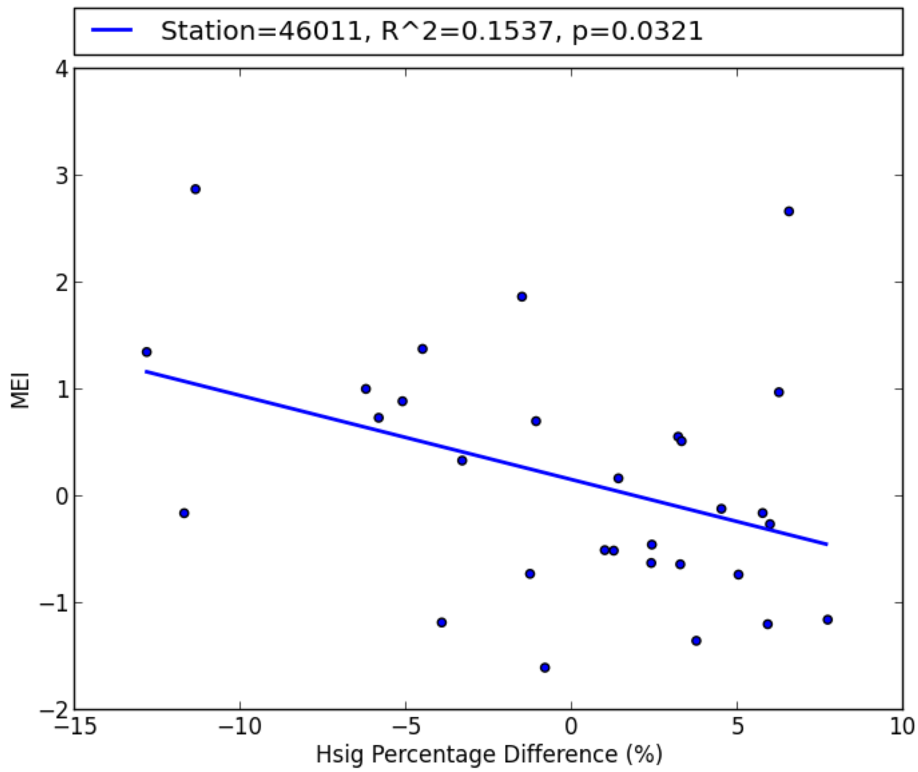

Station=46011, R^2=0.1537, p=0.0321
4
3
2
1
0
−1
−2
MEI
−15
−10
−5
0
5
10
Hsig Percentage Difference (%)

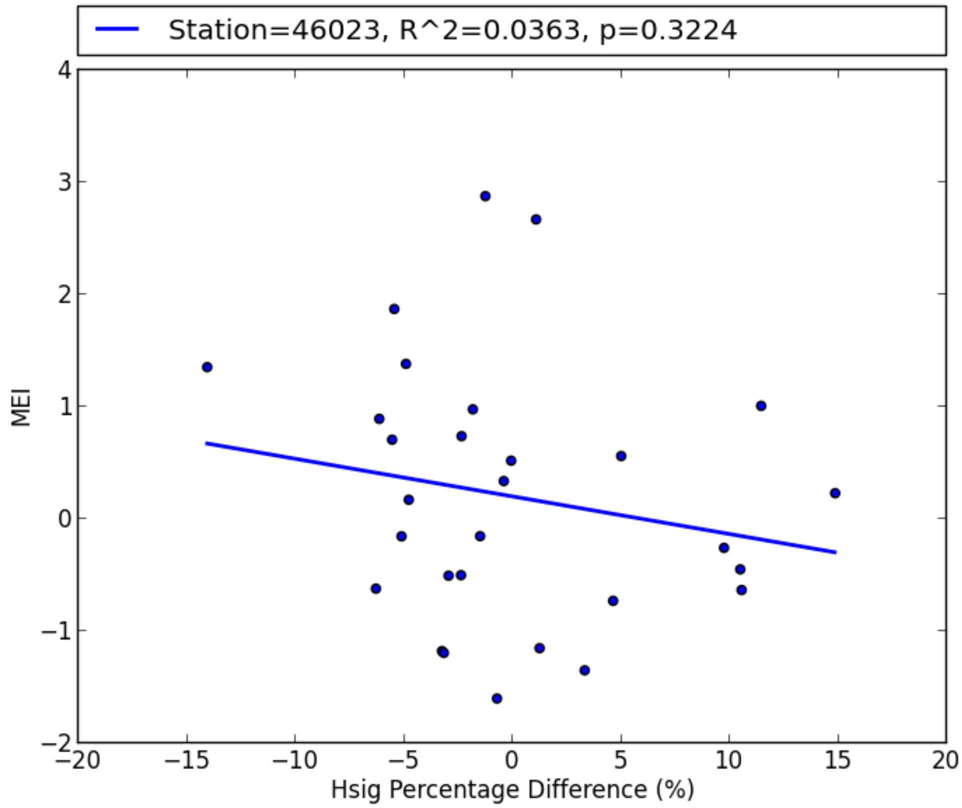

Station=46023, R^2=0.0363, p=0.3224
MEI
Hsig Percentage Difference (%)
4
3
2
1
0
−1
−2
−20
−15
−10
−5
0
5
10
15
20

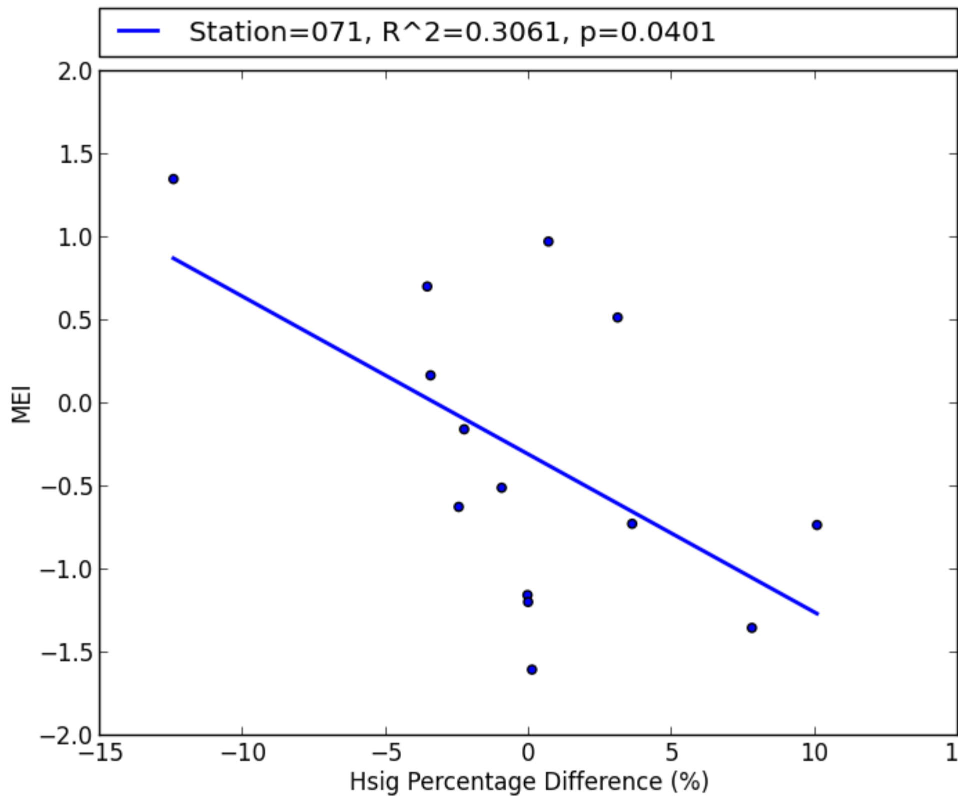
Station=071, R^2=0.3061, p=0.0401
MEI
Hsig Percentage Difference (%)
2.0
1.5
1.0
0.5
0.0
−0.5
−1.0
−1.5
−2.0
−15
−10
−5
0
5
10
15

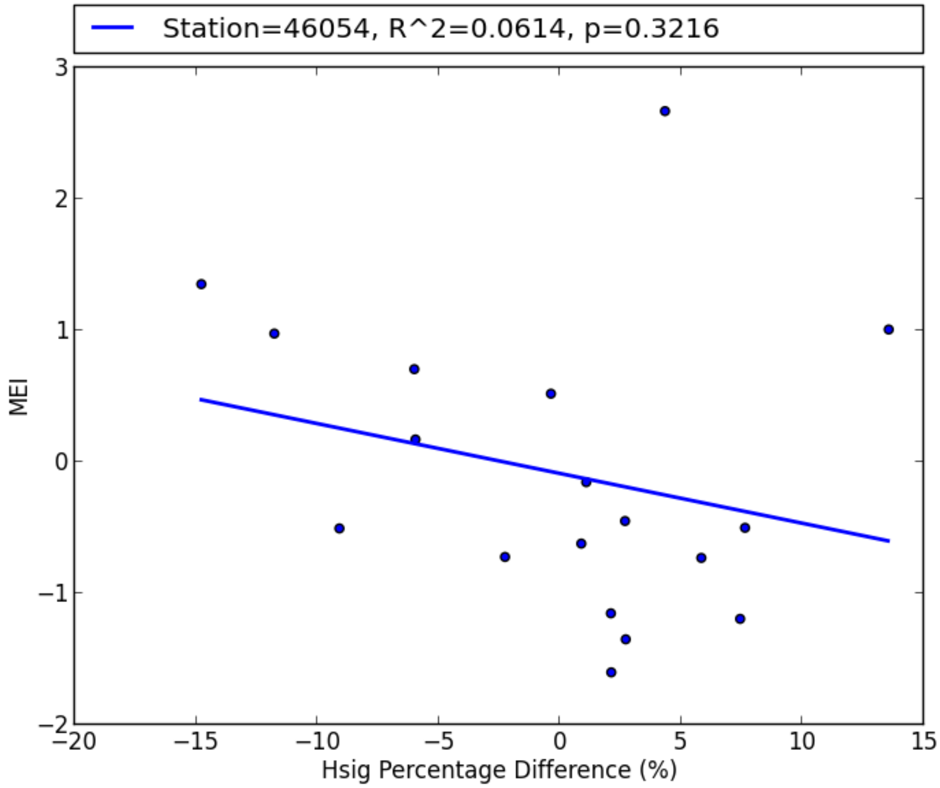
Station=46054, R^2=0.0614, p=0.3216
3
2
1
0
−1
−2
MEI
−20
−15
−10
−5
0
5
10
15
Hsig Percentage Difference (%)

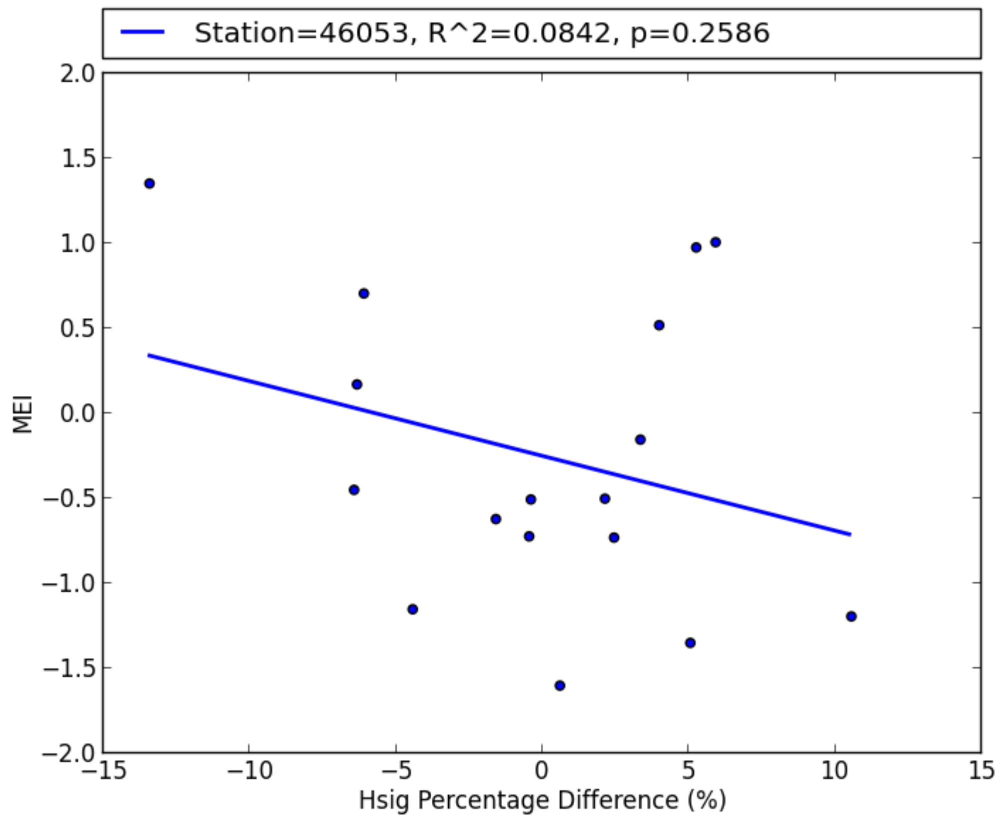
Station=46053, R^2=0.0842, p=0.2586
2.0
1.5
1.0
0.5
0.0
−0.5
−1.0
−1.5
−2.0
MEI
−15
−10
−5
0
5
10
15
Hsig Percentage Difference (%)

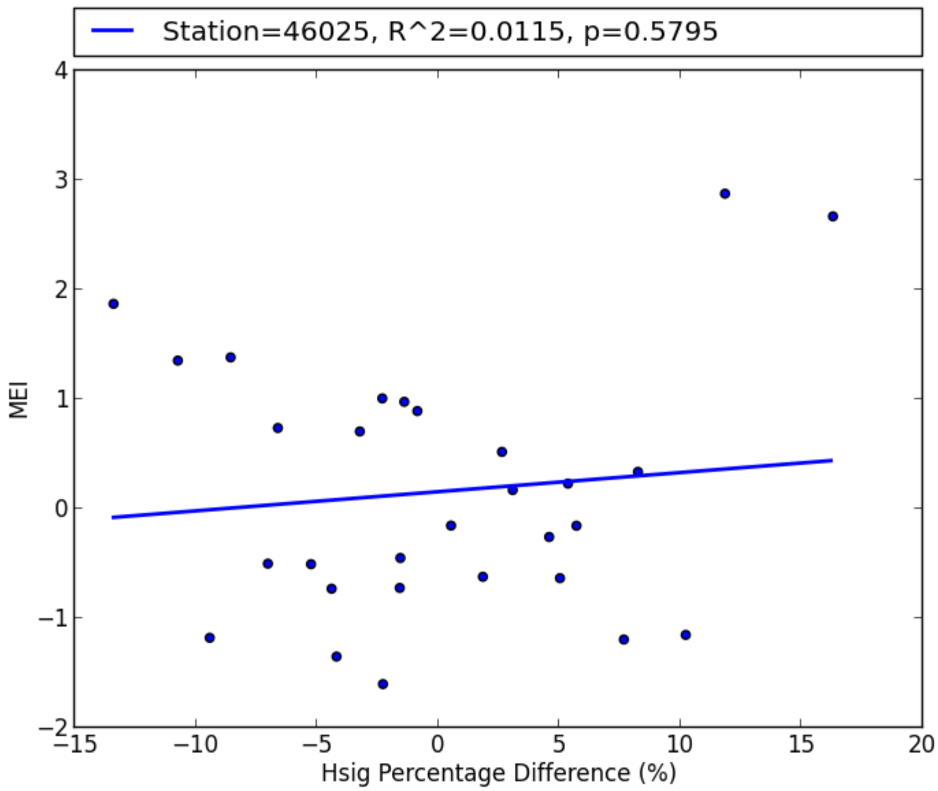
Station=46025, R^2=0.0115, p=0.5795
MEI
Hsig Percentage Difference (%)
4
3
2
1
0
−1
−2
−15
−10
−5
0
5
10
15
20

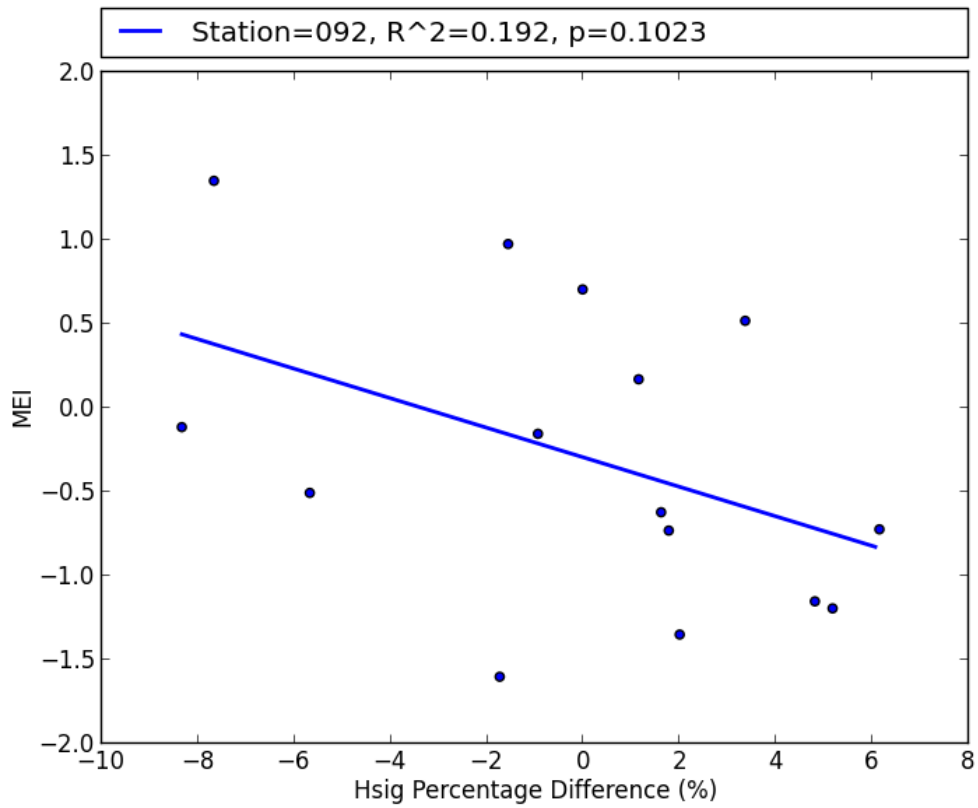

Station=092, R^2=0.192, p=0.1023
2.0
1.5
1.0
0.5
0.0
−0.5
−1.0
−1.5
−2.0
MEI
−10
−8
−6
−4
−2
0
2
4
6
8
Hsig Percentage Difference (%)

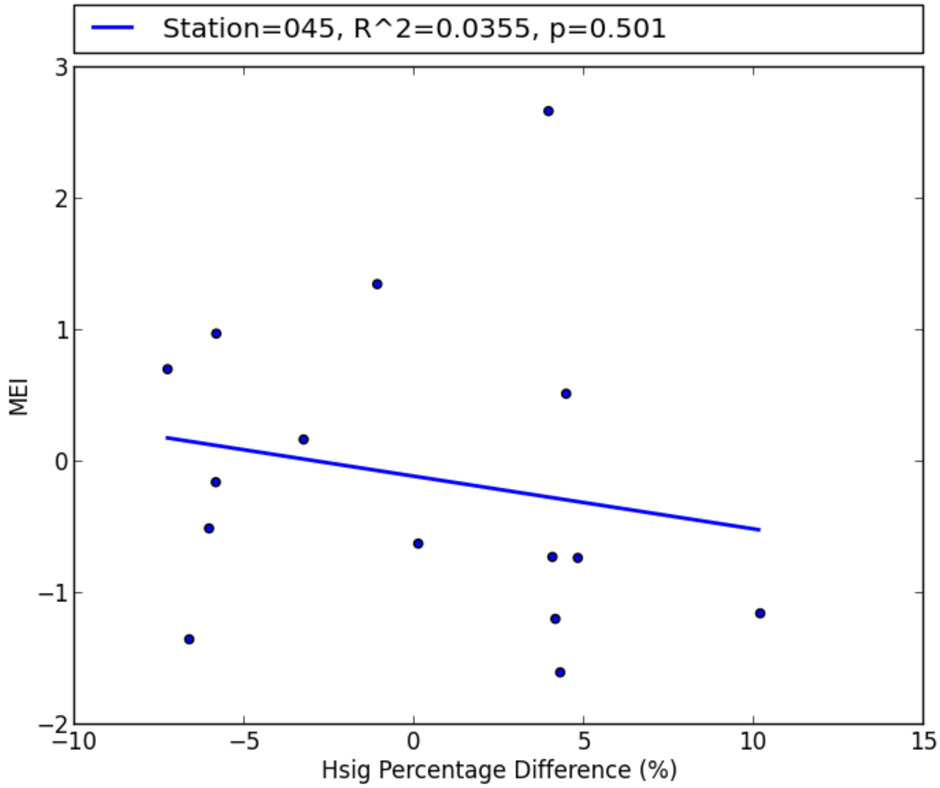
Station=045, R^2=0.0355, p=0.501
3
2
1
0
−1
−2
MEI
−10
−5
0
5
10
15
Hsig Percentage Difference (%)

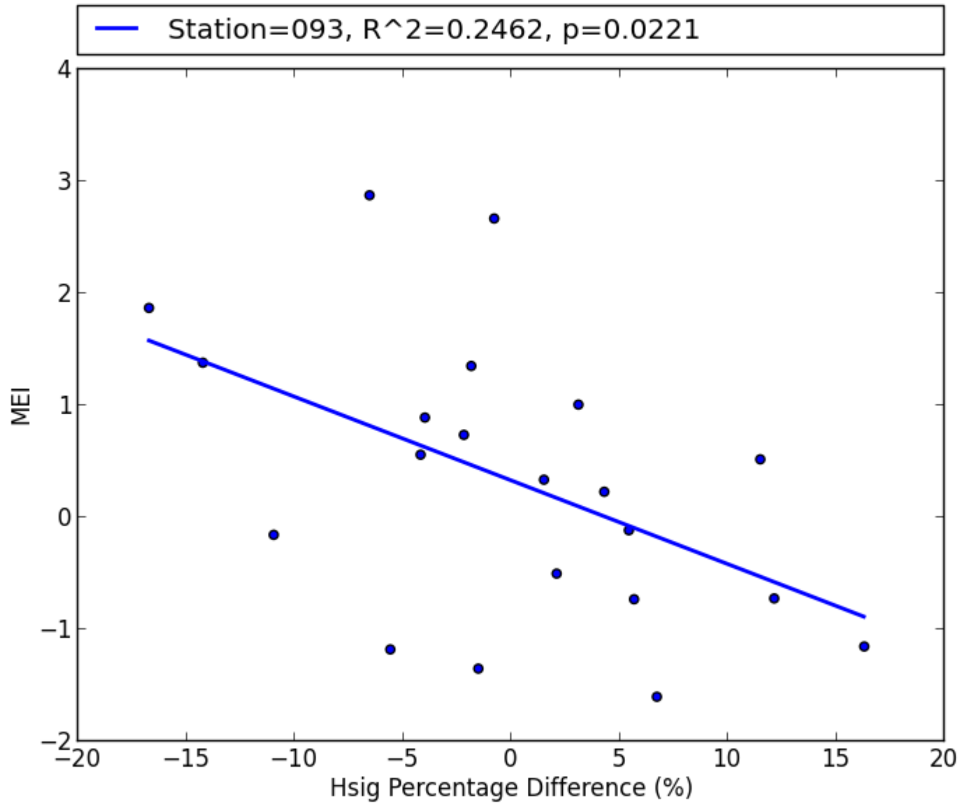
Station=093, R^2=0.2462, p=0.0221
4
3
2
1
0
−1
−2
MEI
−20
−15
−10
−5
0
5
10
15
20
Hsig Percentage Difference (%)

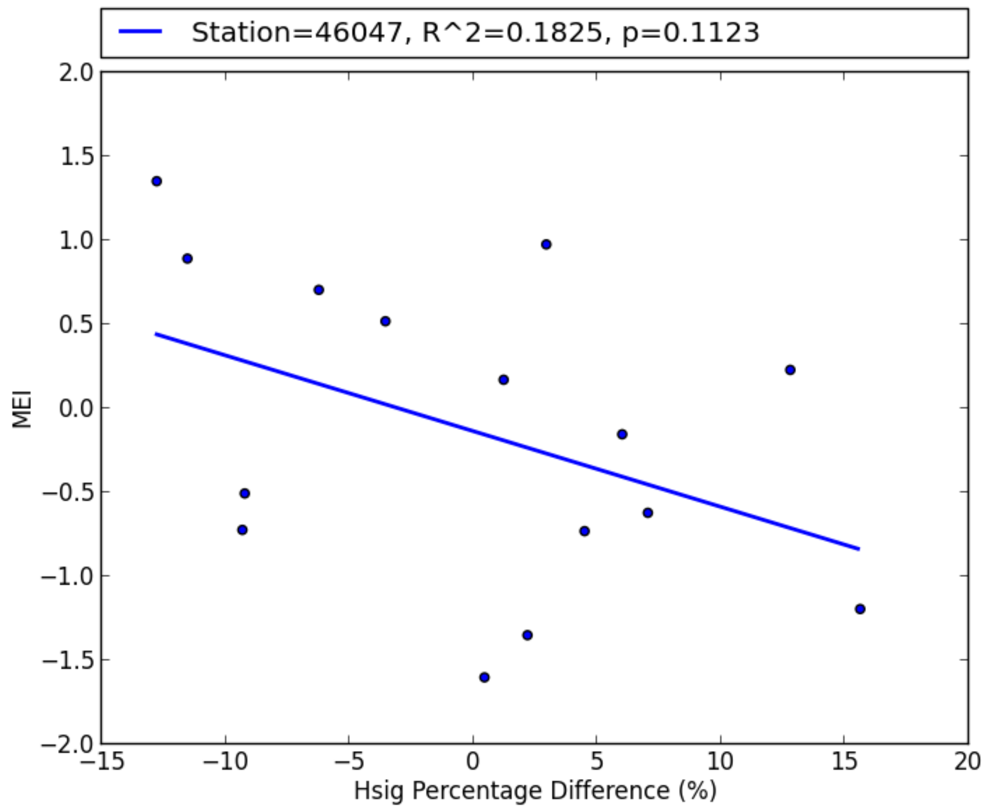

Station=46047, R^2=0.1825, p=0.1123
2.0
1.5
1.0
0.5
0.0
−0.5
−1.0
−1.5
−2.0
MEI
−15
−10
−5
0
5
10
15
20
Hsig Percentage Difference (%)

APPENDIX G

Combining the Summer Multivariate El Niño Southern Oscillation (ENSO) Index (MEI) with Summer Significant Wave Height (H_{sig}) to Forecast the Winter MEI

Results of the ordinary least-squares (OLS) multiple (linear) regression analysis for each buoy. x_1 *= average summer MEI,* x_2 *= summer average* H_{sig}*, and* y *= average winter MEI. Results are shown in north to south latitudinal order.*

Washington

Station 46041						
name of term	coef	std err	t	P > |t|	[95.0% Conf. Int.]	
x1	1.0583	0.160	6.600	0.000	0.725	1.392
x2	-0.0137	0.017	-0.826	0.418	-0.048	0.021
const	-0.255	0.137	-1.859	0.077	-0.540	0.030

Dep. Variable:	y	R-squared:	0.697
Model:	OLS	Adj. R-squared:	0.668
Method:	Least Squares	F-statistic:	24.16
No. Observations:	24	Prob (F-statistic):	3.59E-06
Df Residuals:	21	Log-Likelihood:	-20.446
Df Model:	2	AIC:	46.89
		BIC:	50.43

Omnibus:	0.589	Durbin-Watson:	1.813
Prob(Omnibus):	0.745	Jarque-Bera(JB):	0.421
Skew:	-0.304	Prob(JB):	0.810
Kurtosis:	2.775	Cond. No.	12.0

Station 46029						
name of term	coef	std err	t	P > |t|	[95.0% Conf. Int.]	
x1	1.1976	0.135	8.881	0.000	0.914	1.481
x2	0.0041	0.018	0.224	0.825	-0.034	0.042
const	-0.4307	0.113	-3.815	0.001	-0.668	-0.193

Dep. Variable:	y	R-squared:	0.814
Model:	OLS	Adj. R-squared:	0.794
Method:	Least Squares	F-statistic:	39.43
No. Observations:	21	Prob (F-statistic):	2.64E-07
Df Residuals:	18	Log-Likelihood:	-12.721
Df Model:	2	AIC:	31.44
		BIC:	34.58

Omnibus:	2.488	Durbin-Watson:	2.190
Prob(Omnibus):	0.288	Jarque-Bera(JB):	1.532
Skew:	-0.662	Prob(JB):	0.465
Kurtosis:	3.019	Cond. No.	8.12

Station 036						
name of term	coef	std err	t	P > |t|	[95.0% Conf. Int.]	
x1	1.1156	0.149	7.509	0.000	0.808	1.423
x2	-0.0319	0.019	-1.644	0.114	-0.072	0.008
const	-0.2426	0.140	-1.738	0.096	-0.531	0.046

Dep. Variable:	y	R-squared:	0.723
Model:	OLS	Adj. R-squared:	0.699
Method:	Least Squares	F-statistic:	30.01
No. Observations:	26	Prob (F-statistic):	3.89E-07
Df Residuals:	23	Log-Likelihood:	-24.126
Df Model:	2	AIC:	54.25
		BIC:	58.03

Omnibus:	0.252	Durbin-Watson:	1.878
Prob(Omnibus):	0.882	Jarque-Bera(JB):	0.122
Skew:	0.150	Prob(JB):	0.941
Kurtosis:	2.850	Cond. No.	8.84

Station 46005						
name of term	coef	std err	t	P > |t|	[95.0% Conf. Int.]	
x1	0.9575	0.154	6.207	0.000	0.642	1.273
x2	-0.0162	0.016	-0.995	0.328	-0.049	0.017
const	-0.1706	0.139	-1.232	0.228	-0.454	0.113

Dep. Variable:	y	R-squared:	0.579
Model:	OLS	Adj. R-squared:	0.550
Method:	Least Squares	F-statistic:	19.94
No. Observations:	32	Prob (F-statistic):	3.57E-06
Df Residuals:	29	Log-Likelihood:	-33.474
Df Model:	2	AIC:	72.95
		BIC:	77.34

Omnibus:	0.202	Durbin-Watson:	2.060
Prob(Omnibus):	0.904	Jarque-Bera(JB):	0.034
Skew:	-0.072	Prob(JB):	0.983
Kurtosis:	2.933	Cond. No.	10.7

Oregon

Station 46050						
name of term	coef	std err	t	P > |t|	[95.0% Conf. Int.]	
x1	1.1755	0.159	7.406	0.000	0.841	1.510
x2	-0.0056	0.020	-0.279	0.784	-0.048	0.037
const	-0.4225	0.123	-3.445	0.003	-0.681	-0.164

Dep. Variable:	y	R-squared:	0.811
Model:	OLS	Adj. R-squared:	0.789
Method:	Least Squares	F-statistic:	36.59
No. Observations:	20	Prob (F-statistic):	6.92E-07
Df Residuals:	17	Log-Likelihood:	-12.585
Df Model:	2	AIC:	31.17
		BIC:	34.16

Omnibus:	1.413	Durbin-Watson:	2.088
Prob(Omnibus):	0.493	Jarque-Bera(JB):	1.028
Skew:	-0.535	Prob(JB):	0.598
Kurtosis:	2.699	Cond. No.	9.87

Station 46002						
name of term	coef	std err	t	P > |t|	[95.0% Conf. Int.]	
x1	1.0261	0.188	5.459	0.000	0.641	1.411
x2	-0.0298	0.016	-1.921	0.065	-0.062	0.002
const	-0.1740	0.163	-1.067	0.295	-0.508	0.160

Dep. Variable:	y	R-squared:	0.516
Model:	OLS	Adj. R-squared:	0.482
Method:	Least Squares	F-statistic:	14.95
No. Observations:	31	Prob (F-statistic):	3.82E-05
Df Residuals:	28	Log-Likelihood:	-32.060
Df Model:	2	AIC:	70.12
		BIC:	74.42

Omnibus:	0.158	Durbin-Watson:	2.373
Prob(Omnibus):	0.924	Jarque-Bera(JB):	0.207
Skew:	-0.146	Prob(JB):	0.902
Kurtosis:	2.726	Cond. No.	15.1

Northern California

Station 46027						
name of term	coef	std err	t	P > |t|	[95.0% Conf. Int.]	
x1	1.0901	0.192	5.676	0.000	0.691	1.490
x2	-0.0012	0.018	-0.064	0.950	-0.039	0.037
const	-0.1731	0.135	-1.281	0.214	-0.454	0.108

Dep. Variable:	y	R-squared:	0.615
Model:	OLS	Adj. R-squared:	0.578
Method:	Least Squares	F-statistic:	16.78
No. Observations:	24	Prob (F-statistic):	4.43E-05
Df Residuals:	21	Log-Likelihood:	-21.673
Df Model:	2	AIC:	49.35
		BIC:	52.88

Omnibus:	0.489	Durbin-Watson:	1.877
Prob(Omnibus):	0.783	Jarque-Bera(JB):	0.138
Skew:	-0.186	Prob(JB):	0.933
Kurtosis:	2.982	Cond. No.	11.1

Station 46006						
name of term	coef	std err	t	P > |t|	[95.0% Conf. Int.]	
x1	1.0427	0.151	6.897	0.000	0.734	1.352
x2	-0.0253	0.011	-2.229	0.034	-0.049	-0.002
const	-0.2013	0.131	-1.536	0.135	-0.469	0.067

Dep. Variable:	y	R-squared:	0.622
Model:	OLS	Adj. R-squared:	0.596
Method:	Least Squares	F-statistic:	23.83
No. Observations:	32	Prob (F-statistic):	7.56E-07
Df Residuals:	29	Log-Likelihood:	-31.219
Df Model:	2	AIC:	68.44
		BIC:	72.83

Omnibus:	3.154	Durbin-Watson:	2.707
Prob(Omnibus):	0.207	Jarque-Bera(JB):	1.804
Skew:	-0.477	Prob(JB):	0.406
Kurtosis:	3.666	Cond. No.	15.5

Station 46022						
name of term	coef	std err	t	P > |t|	[95.0% Conf. Int.]	
x1	1.0122	0.166	6.082	0.000	0.670	1.354
x2	0.0142	0.023	0.615	0.544	-0.033	0.062
const	-0.2255	0.158	-1.429	0.165	-0.550	0.099

Dep. Variable:	y	R-squared:	0.590
Model:	OLS	Adj. R-squared:	0.559
Method:	Least Squares	F-statistic:	18.72
No. Observations:	29	Prob (F-statistic):	9.21E-06
Df Residuals:	26	Log-Likelihood:	-31.811
Df Model:	2	AIC:	69.62
		BIC:	73.72

Omnibus:	0.68	Durbin-Watson:	2.229
Prob(Omnibus):	0.712	Jarque-Bera(JB):	0.120
Skew:	0.127	Prob(JB):	0.942
Kurtosis:	3.185	Cond. No.	8.40

Station 46014						
name of term	coef	std err	t	P > |t|	[95.0% Conf. Int.]	
x1	0.9248	0.159	5.819	0.000	0.599	1.251
x2	-0.0356	0.019	-1.913	0.066	-0.074	0.003
const	-0.1916	0.142	-1.347	0.189	-0.483	0.100

Dep. Variable:	y	R-squared:	0.637
Model:	OLS	Adj. R-squared:	0.610
Method:	Least Squares	F-statistic:	23.67
No. Observations:	30	Prob (F-statistic):	1.16E-06
Df Residuals:	27	Log-Likelihood:	-30.725
Df Model:	2	AIC:	67.45
		BIC:	71.65

Omnibus:	1.389	Durbin-Watson:	2.130
Prob(Omnibus):	0.499	Jarque-Bera(JB):	0.561
Skew:	-0.299	Prob(JB):	0.755
Kurtosis:	3.300	Cond. No.	10.1

Central California

Station 46059						
name of term	coef	std err	t	P > |t|	[95.0% Conf. Int.]	
x1	1.1811	0.138	8.589	0.000	0.881	1.481
x2	0.0380	0.033	1.157	0.270	-0.033	0.109
const	-0.4211	0.115	-3.675	0.003	-0.671	-0.171

Dep. Variable:	y	R-squared:	0.867
Model:	OLS	Adj. R-squared:	0.845
Method:	Least Squares	F-statistic:	39.23
No. Observations:	15	Prob (F-statistic):	5.45E-06
Df Residuals:	12	Log-Likelihood:	-7.1352
Df Model:	2	AIC:	20.27
		BIC:	22.39

Omnibus:	6.259	Durbin-Watson:	1.641
Prob(Omnibus):	0.044	Jarque-Bera(JB):	3.266
Skew:	-1.047	Prob(JB):	0.195
Kurtosis:	3.917	Cond. No.	4.37

Station 46013						
name of term	coef	std err	t	P > |t|	[95.0% Conf. Int.]	
x1	0.8726	0.159	5.471	0.000	0.545	1.200
x2	-0.0439	0.014	-3.126	0.004	-0.073	-0.015
const	-0.2236	0.126	-1.777	0.087	-0.482	0.035

Dep. Variable:	y	R-squared:	0.649
Model:	OLS	Adj. R-squared:	0.622
Method:	Least Squares	F-statistic:	24.07
No. Observations:	29	Prob (F-statistic):	1.21E-06
Df Residuals:	26	Log-Likelihood:	-26.136
Df Model:	2	AIC:	58.27
		BIC:	62.37

Omnibus:	0.195	Durbin-Watson:	2.222
Prob(Omnibus):	0.907	Jarque-Bera(JB):	0.386
Skew:	0.129	Prob(JB):	0.825
Kurtosis:	2.497	Cond. No.	12.5

Station 46026						
name of term	coef	std err	t	P > |t|	[95.0% Conf. Int.]	
x1	0.9609	0.151	6.356	0.000	0.651	1.271
x2	-0.0268	0.012	-2.272	0.031	-0.051	-0.003
const	-0.2059	0.140	-1.474	0.152	-0.492	0.081

Dep. Variable:	y	R-squared:	0.655
Model:	OLS	Adj. R-squared:	0.629
Method:	Least Squares	F-statistic:	25.58
No. Observations:	30	Prob (F-statistic):	5.85E-07
Df Residuals:	27	Log-Likelihood:	-29.992
Df Model:	2	AIC:	65.98
		BIC:	70.19

Omnibus:	3.349	Durbin-Watson:	2.247
Prob(Omnibus):	0.187	Jarque-Bera(JB):	2.240
Skew:	-0.659	Prob(JB):	0.326
Kurtosis:	3.238	Cond. No.	14.9

Station 46012						
name of term	coef	std err	t	P > |t|	[95.0% Conf. Int.]	
x1	1.0036	0.147	6.818	0.000	0.702	1.306
x2	-0.0249	0.010	-2.446	0.021	-0.046	-0.004
const	-0.1931	0.133	-1.451	0.158	-0.466	0.080

Dep. Variable:	y	R-squared:	0.676
Model:	OLS	Adj. R-squared:	0.652
Method:	Least Squares	F-statistic:	28.16
No. Observations:	30	Prob (F-statistic):	2.47E-07
Df Residuals:	27	Log-Likelihood:	-29.062
Df Model:	2	AIC:	64.12
		BIC:	68.33

Omnibus:	2.596	Durbin-Watson:	2.675
Prob(Omnibus):	0.273	Jarque-Bera(JB):	1.558
Skew:	-0.542	Prob(JB):	0.459
Kurtosis:	3.267	Cond. No.	16.4

Station 46042						
name of term	coef	std err	t	P > |t|	[95.0% Conf. Int.]	
x1	1.1570	0.148	7.823	0.000	0.849	1.465
x2	-0.0201	0.017	-1.175	0.253	-0.056	0.015
const	-0.2684	0.124	-2.164	0.042	-0.526	-0.010

Dep. Variable:	y	R-squared:	0.745
Model:	OLS	Adj. R-squared:	0.720
Method:	Least Squares	F-statistic:	30.60
No. Observations:	24	Prob (F-statistic):	5.98E-07
Df Residuals:	21	Log-Likelihood:	-19.154
Df Model:	2	AIC:	44.31
		BIC:	47.84

Omnibus:	1.598	Durbin-Watson:	1.457
Prob(Omnibus):	0.450	Jarque-Bera(JB):	0.509
Skew:	0.261	Prob(JB):	0.775
Kurtosis:	3.485	Cond. No.	9.43

Station 46028						
name of term	coef	std err	t	P > |t|	[95.0% Conf. Int.]	
x1	1.0907	0.148	7.348	0.000	0.785	1.396
x2	-0.0208	0.018	-1.185	0.247	-0.057	0.015
const	-0.2462	0.124	-1.984	0.058	-0.502	0.009

Dep. Variable:	y	R-squared:	0.668
Model:	OLS	Adj. R-squared:	0.663
Method:	Least Squares	F-statistic:	27.51
No. Observations:	28	Prob (F-statistic):	4.83E-07
Df Residuals:	25	Log-Likelihood:	-24.341
Df Model:	2	AIC:	54.68
		BIC:	58.68

Omnibus:	1.343	Durbin-Watson:	2.143
Prob(Omnibus):	0.511	Jarque-Bera(JB):	0.532
Skew:	0.310	Prob(JB):	0.767
Kurtosis:	3.267	Cond. No.	9.64

Southern California

Station 076						
name of term	coef	std err	t	P > |t|	[95.0% Conf. Int.]	
x1	0.9607	0.144	6.672	0.000	0.664	1.257
x2	-0.0393	0.018	-2.196	0.038	-0.076	-0.002
const	-0.2783	0.132	-2.101	0.046	-0.551	-0.005

Dep. Variable:	y	R-squared:	0.652
Model:	OLS	Adj. R-squared:	0.624
Method:	Least Squares	F-statistic:	23.41
No. Observations:	28	Prob (F-statistic):	1.87E-06
Df Residuals:	25	Log-Likelihood:	-25.877
Df Model:	2	AIC:	57.75
		BIC:	61.75

Omnibus:	0.089	Durbin-Watson:	1.910
Prob(Omnibus):	0.957	Jarque-Bera(JB):	0.157
Skew:	-0.110	Prob(JB):	0.924
Kurtosis:	2.707	Cond. No.	9.18

Station 46011						
name of term	coef	std err	t	P > |t|	[95.0% Conf. Int.]	
x1	0.9922	0.143	6.961	0.000	0.700	1.285
x2	-0.0616	0.021	-2.879	0.008	-0.105	-0.018
const	-0.1891	0.129	-1.470	0.153	-0.453	0.075

Dep. Variable:	y	R-squared:	0.697
Model:	OLS	Adj. R-squared:	0.675
Method:	Least Squares	F-statistic:	31.08
No. Observations:	30	Prob (F-statistic):	9.92E-08
Df Residuals:	27	Log-Likelihood:	-28.048
Df Model:	2	AIC:	62.10
		BIC:	66.30

Omnibus:	0.291	Durbin-Watson:	2.379
Prob(Omnibus):	0.865	Jarque-Bera(JB):	0.045
Skew:	-0.094	Prob(JB):	0.978
Kurtosis:	2.976	Cond. No.	7.56

Station 46023						
name of term	coef	std err	t	P > |t|	[95.0% Conf. Int.]	
x1	1.0171	0.158	6.445	0.000	0.693	1.342
x2	-0.0387	0.021	-1.837	0.078	-0.082	0.005
const	-0.2202	0.149	-1.473	0.153	-0.527	0.087

Dep. Variable:	y	R-squared:	0.629
Model:	OLS	Adj. R-squared:	0.600
Method:	Least Squares	F-statistic:	22.04
No. Observations:	29	Prob (F-statistic):	2.53E-06
Df Residuals:	26	Log-Likelihood:	-30.200
Df Model:	2	AIC:	66.40
		BIC:	70.50

Omnibus:	0.492	Durbin-Watson:	2.228
Prob(Omnibus):	0.782	Jarque-Bera(JB):	0.198
Skew:	0.201	Prob(JB):	0.906
Kurtosis:	2.965	Cond. No.	8.77

Station 071						
name of term	coef	std err	t	P > |t|	[95.0% Conf. Int.]	
x1	1.2122	0.249	4.862	0.001	0.663	1.761
x2	-0.0432	0.027	-1.628	0.132	-0.102	0.015
const	-0.4115	0.128	-3.217	0.008	-0.693	-0.130

Dep. Variable:	y	R-squared:	0.780
Model:	OLS	Adj. R-squared:	0.740
Method:	Least Squares	F-statistic:	19.46
No. Observations:	14	Prob (F-statistic):	2.44E-04
Df Residuals:	11	Log-Likelihood:	-7.6608
Df Model:	2	AIC:	21.32
		BIC:	23.24

Omnibus:	9.789	Durbin-Watson:	1.534
Prob(Omnibus):	0.007	Jarque-Bera(JB):	5.761
Skew:	-1.404	Prob(JB):	0.056
Kurtosis:	4.409	Cond. No.	10.3

Station 46054						
name of term	coef	std err	t	P > |t|	[95.0% Conf. Int.]	
x1	1.2312	0.142	8.690	0.000	0.929	1.533
x2	-0.0174	0.016	-1.106	0.286	-0.051	0.016
const	-0.4001	0.115	-3.465	0.003	-0.646	-0.154

Dep. Variable:	y	R-squared:	0.844
Model:	OLS	Adj. R-squared:	0.824
Method:	Least Squares	F-statistic:	40.71
No. Observations:	18	Prob (F-statistic):	8.69E-07
Df Residuals:	15	Log-Likelihood:	-10.135
Df Model:	2	AIC:	26.27
		BIC:	28.94

Omnibus:	5.786	Durbin-Watson:	1.972
Prob(Omnibus):	0.055	Jarque-Bera(JB):	3.294
Skew:	-0.964	Prob(JB):	0.193
Kurtosis:	3.821	Cond. No.	9.69

Station 46053						
name of term	coef	std err	t	P > |t|	[95.0% Conf. Int.]	
x1	1.3740	0.225	6.097	0.000	0.891	1.857
x2	-0.0134	0.021	-0.643	0.530	-0.058	0.031
const	-0.4023	0.119	-3.383	0.004	-0.657	-0.147

Dep. Variable:	y	R-squared:	0.749
Model:	OLS	Adj. R-squared:	0.714
Method:	Least Squares	F-statistic:	20.94
No. Observations:	17	Prob (F-statistic):	6.19E-05
Df Residuals:	14	Log-Likelihood:	-9.9737
Df Model:	2	AIC:	25.95
		BIC:	28.45

Omnibus:	10.512	Durbin-Watson:	2.214
Prob(Omnibus):	0.005	Jarque-Bera(JB):	7.227
Skew:	-1.392	Prob(JB):	0.0270
Kurtosis:	4.567	Cond. No.	11.2

Station 46025						
name of term	coef	std err	t	P > |t|	[95.0% Conf. Int.]	
x1	1.0898	0.163	6.671	0.000	0.754	1.426
x2	-0.0145	0.020	-0.729	0.472	-0.055	0.026
const	-0.2998	0.151	-1.987	0.058	-0.610	0.010

Dep. Variable:	y	R-squared:	0.635
Model:	OLS	Adj. R-squared:	0.607
Method:	Least Squares	F-statistic:	22.66
No. Observations:	29	Prob (F-statistic):	2.01E-06
Df Residuals:	26	Log-Likelihood:	-30.203
Df Model:	2	AIC:	66.41
		BIC:	70.51

Omnibus:	1.681	Durbin-Watson:	2.359
Prob(Omnibus):	0.432	Jarque-Bera(JB):	0.596
Skew:	-0.127	Prob(JB):	0.742
Kurtosis:	3.655	Cond. No.	9.84

Station 092						
name of term	coef	std err	t	P > |t|	[95.0% Conf. Int.]	
x1	1.2666	0.244	5.200	0.000	0.736	1.797
x2	-0.0399	0.030	-1.316	0.213	-0.106	0.026
const	-0.3921	0.125	-3.126	0.009	-0.665	-0.119

Dep. Variable:	y	R-squared:	0.752
Model:	OLS	Adj. R-squared:	0.710
Method:	Least Squares	F-statistic:	18.15
No. Observations:	15	Prob (F-statistic):	2.35E-04
Df Residuals:	12	Log-Likelihood:	-8.614
Df Model:	2	AIC:	23.23
		BIC:	25.35

Omnibus:	5.072	Durbin-Watson:	2.229
Prob(Omnibus):	0.079	Jarque-Bera(JB):	2.965
Skew:	-1.082	Prob(JB):	0.227
Kurtosis:	3.250	Cond. No.	8.49

Station 045						
name of term	coef	std err	t	P > |t|	[95.0% Conf. Int.]	
x1	1.2323	0.146	8.459	0.000	0.915	1.550
x2	-0.0337	0.023	-1.473	0.167	-0.084	0.016
const	-0.4280	0.128	-3.348	0.006	-0.707	-0.149

Dep. Variable:	y	R-squared:	0.861
Model:	OLS	Adj. R-squared:	0.838
Method:	Least Squares	F-statistic:	37.31
No. Observations:	15	Prob (F-statistic):	7.07E-06
Df Residuals:	12	Log-Likelihood:	-8.382
Df Model:	2	AIC:	22.76
		BIC:	24.89

Omnibus:	2.243	Durbin-Watson:	2.157
Prob(Omnibus):	0.326	Jarque-Bera(JB):	1.671
Skew:	-0.767	Prob(JB):	0.434
Kurtosis:	2.433	Cond. No.	6.89

Station 093						
name of term	coef	std err	t	P > |t|	[95.0% Conf. Int.]	
x1	1.0009	0.146	6.836	0.000	0.693	1.309
x2	-0.0553	0.016	-3.352	0.004	-0.090	-0.021
const	-0.1077	0.148	-0.729	0.475	-0.418	0.202

Dep. Variable:	y	R-squared:	0.790
Model:	OLS	Adj. R-squared:	0.767
Method:	Least Squares	F-statistic:	33.94
No. Observations:	21	Prob (F-statistic):	7.81E-07
Df Residuals:	18	Log-Likelihood:	-17.781
Df Model:	2	AIC:	41.56
		BIC:	44.70

Omnibus:	0.031	Durbin-Watson:	2.315
Prob(Omnibus):	0.984	Jarque-Bera(JB):	0.161
Skew:	-0.076	Prob(JB):	0.923
Kurtosis:	2.598	Cond. No.	10.8

Station 46047						
name of term	coef	std err	t	P > |t|	[95.0% Conf. Int.]	
x1	1.1508	0.179	6.427	0.000	0.761	1.541
x2	-0.0191	0.014	-1.393	0.189	-0.049	0.011
const	-0.3747	0.115	-3.245	0.007	-0.626	-0.123

Dep. Variable:	y	R-squared:	0.816
Model:	OLS	Adj. R-squared:	0.785
Method:	Least Squares	F-statistic:	26.60
No. Observations:	15	Prob (F-statistic):	3.88E-05
Df Residuals:	12	Log-Likelihood:	-6.7155
Df Model:	2	AIC:	19.43
		BIC:	21.56

Omnibus:	0.960	Durbin-Watson:	1.863
Prob(Omnibus):	0.619	Jarque-Bera(JB):	0.859
Skew:	-0.470	Prob(JB):	0.651
Kurtosis:	2.299	Cond. No.	14.2

APPENDIX H

Summer Significant Wave Height (H_{sig}) vs. Summer Northern Pacific (NP) Index

Plots of monthly summer H_{sig} percentage difference as a function of monthly summer NP Index over the period of available summer H_{sig} data through 2010 for each buoy. Plots are shown in north to south latitudinal order. Linear regression coefficients are listed in Table 3.8.

Washington

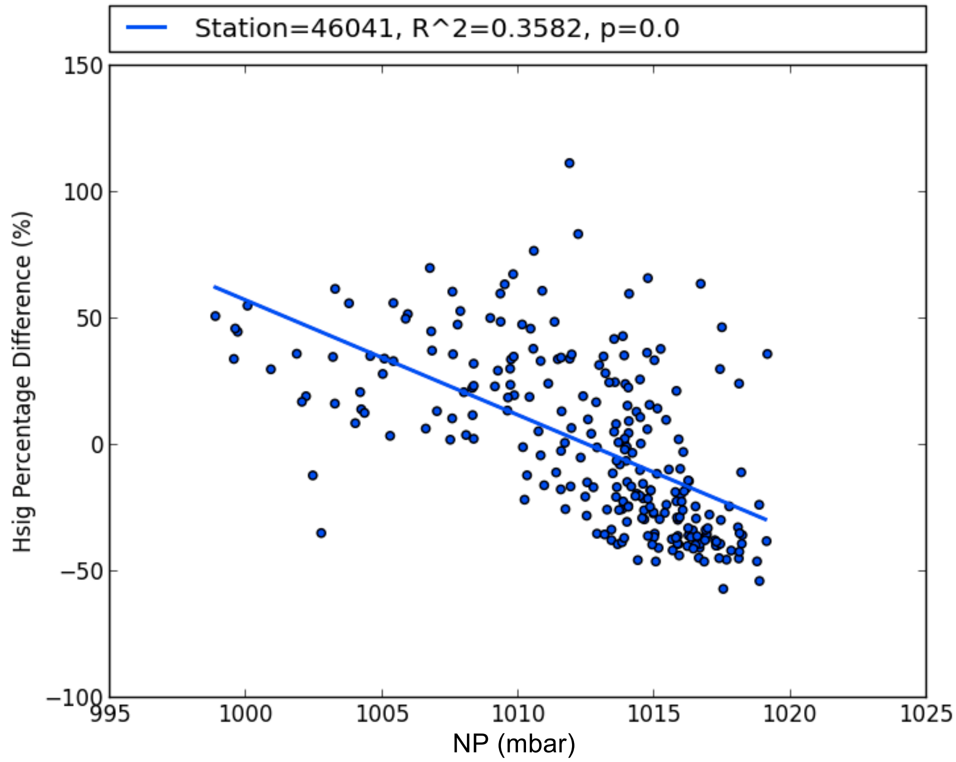

Station=46041, R^2=0.3582, p=0.0
150
100
50
0
−50
−100
Hsig Percentage Difference (%)
995
1000
1005
1010
1015
1020
1025
NP (mbar)

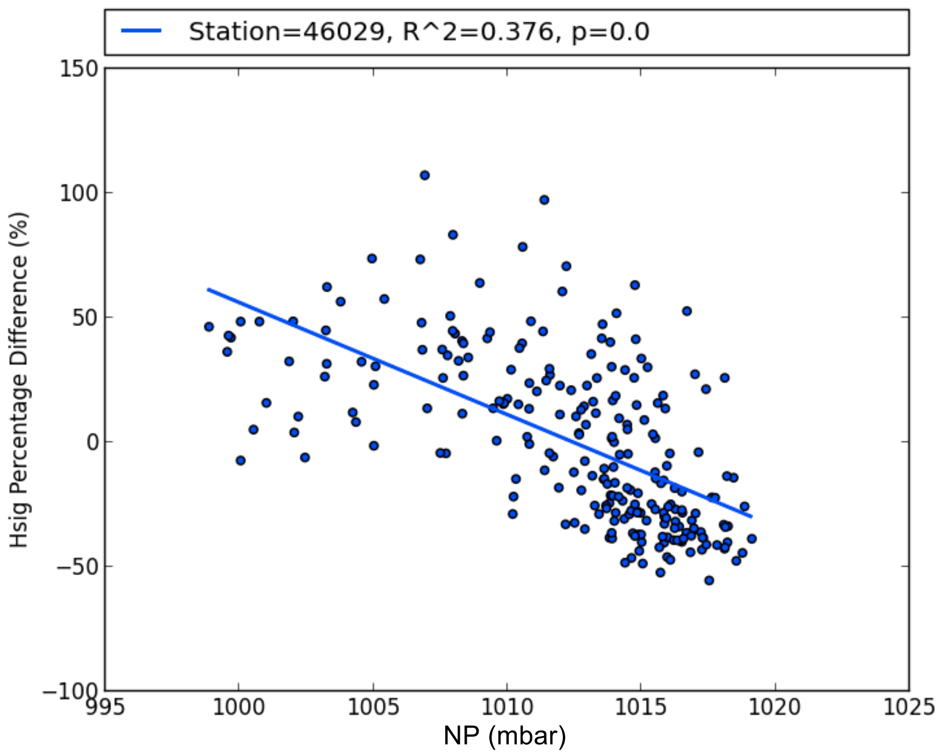
Station=46029, R^2=0.376, p=0.0
150
100
50
0
−50
−100
995
1000
1005
1010
1015
1020
1025
Hsig Percentage Difference (%)
NP (mbar)

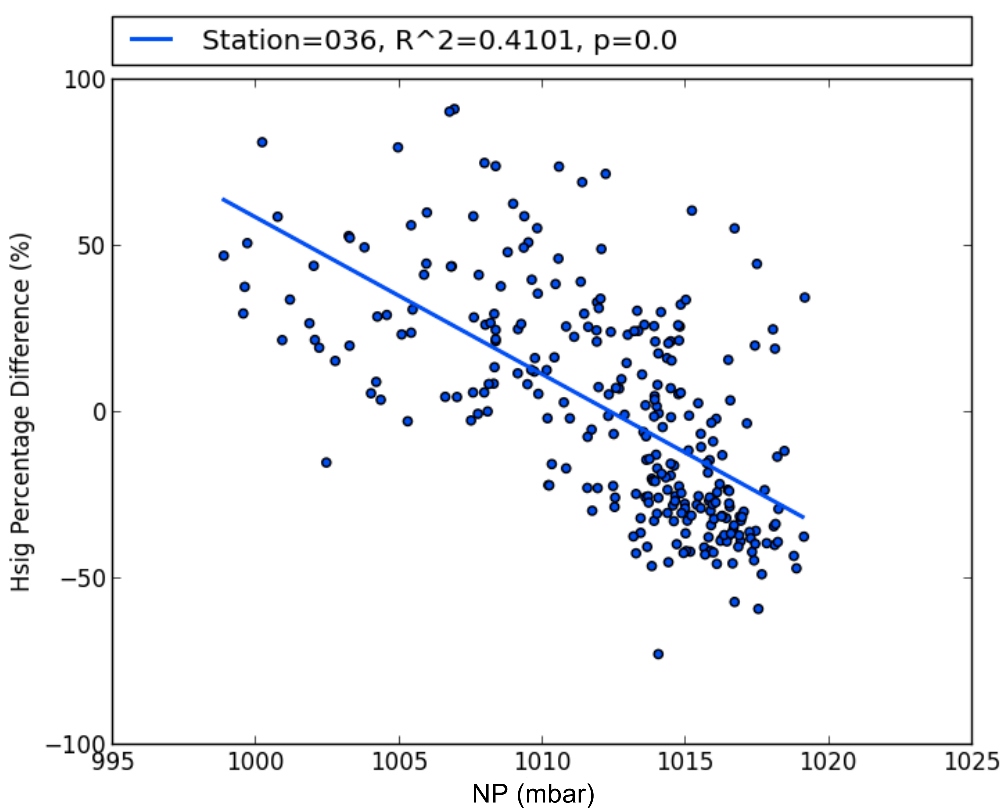
Station=036, R^2=0.4101, p=0.0
100
50
0
−50
−100
995
1000
1005
1010
1015
1020
1025
Hsig Percentage Difference (%)
NP (mbar)

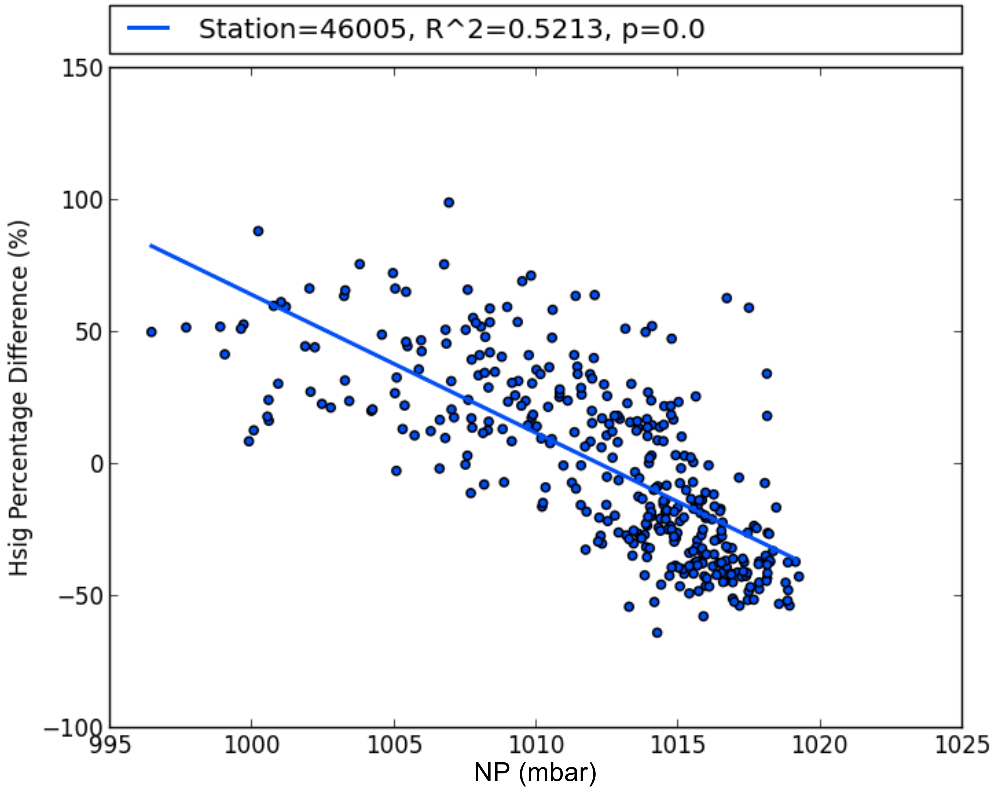
Station=46005, R^2=0.5213, p=0.0
Hsig Percentage Difference (%)
NP (mbar)
150
100
50
0
−50
−100
995
1000
1005
1010
1015
1020
1025

Oregon

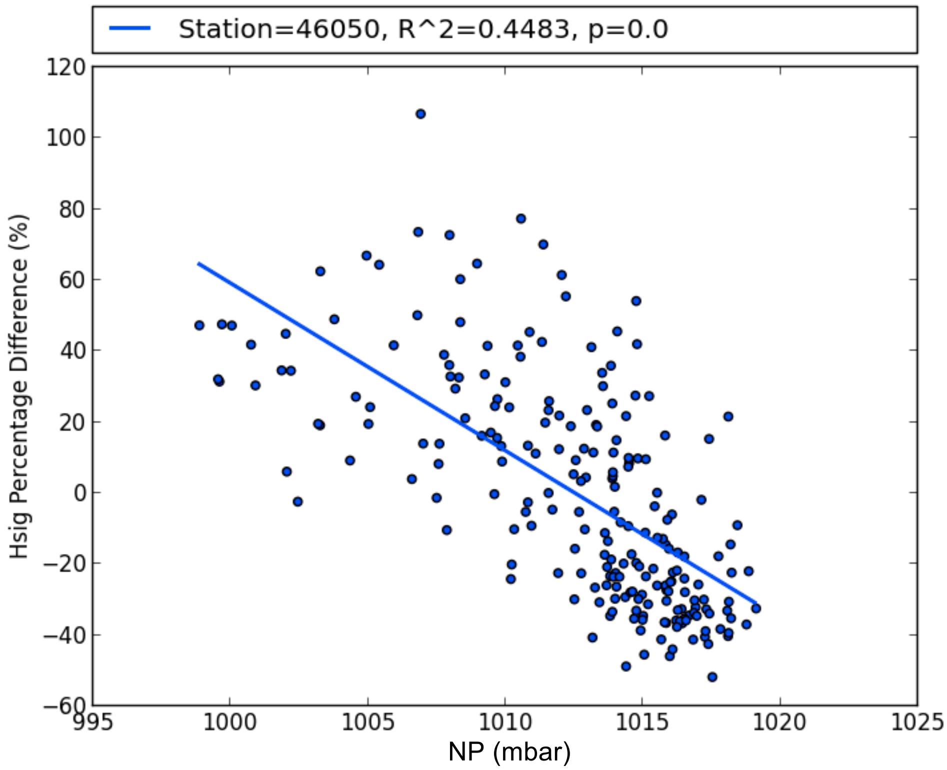

Station=46050, R^2=0.4483, p=0.0
Hsig Percentage Difference (%)
NP (mbar)
120
100
80
60
40
20
0
−20
−40
−60
995
1000
1005
1010
1015
1020
1025

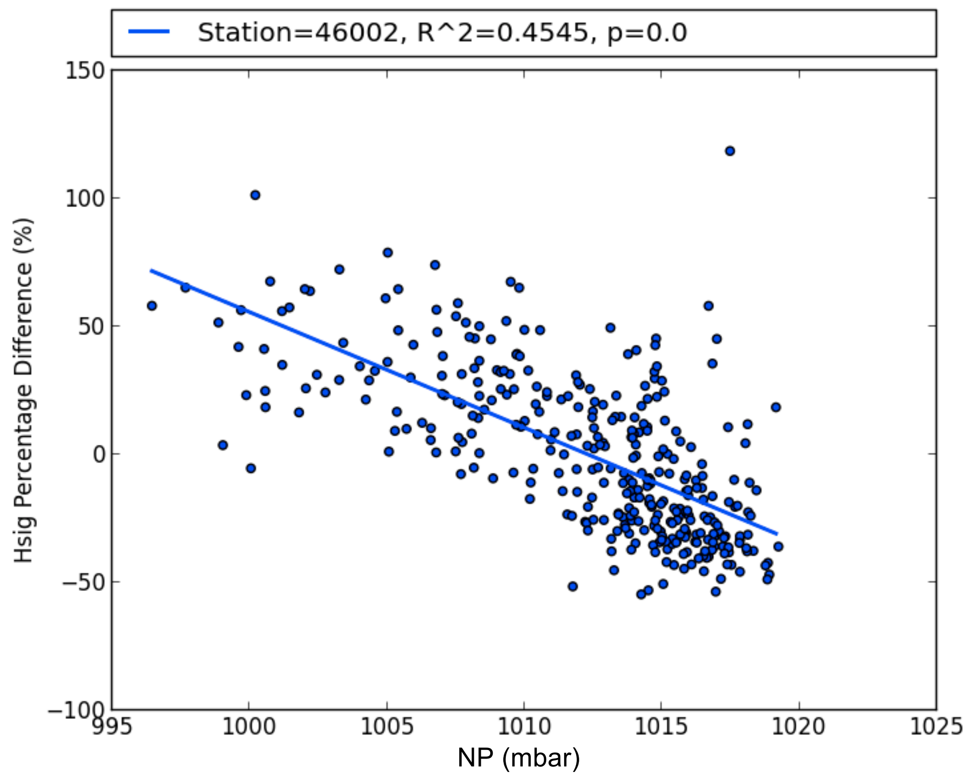

Station=46002, R^2=0.4545, p=0.0
150
100
50
0
−50
−100
Hsig Percentage Difference (%)
995
1000
1005
1010
1015
1020
1025
NP (mbar)

Northern California

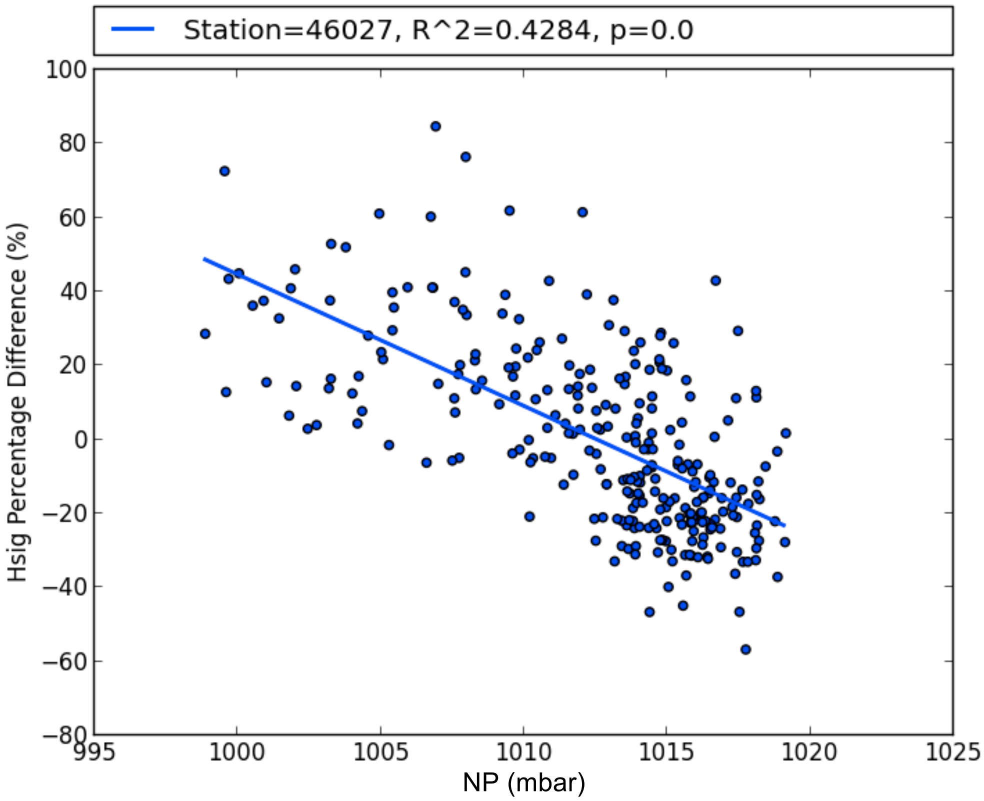

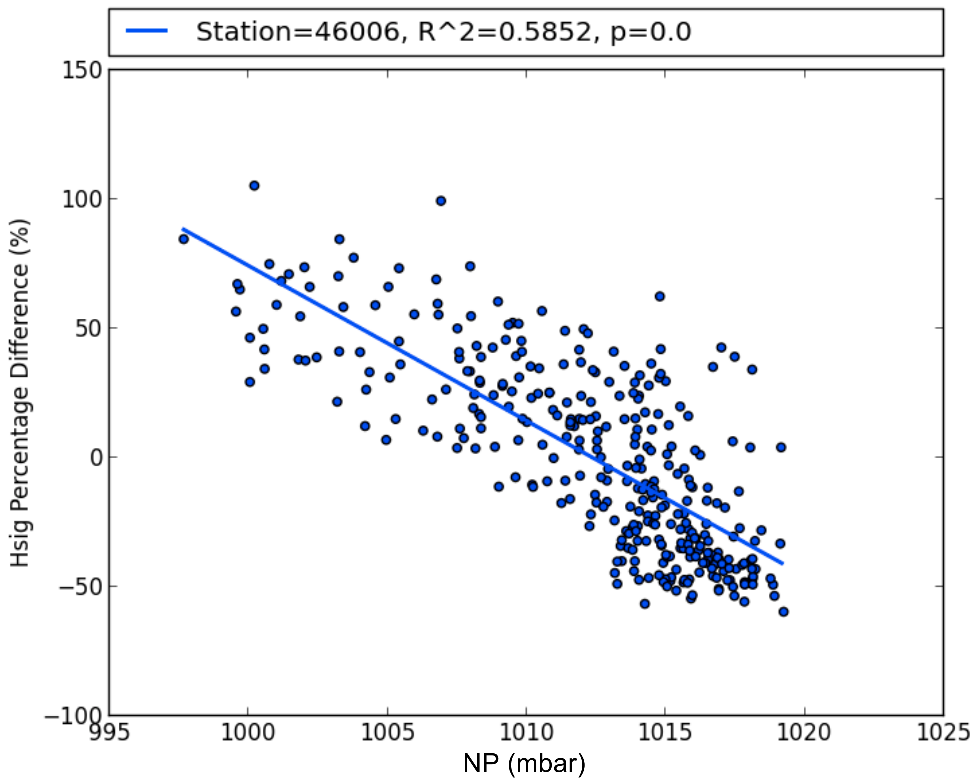
Station=46006, R^2=0.5852, p=0.0
150
100
50
0
−50
−100
Hsig Percentage Difference (%)
995
1000
1005
1010
1015
1020
1025
NP (mbar)

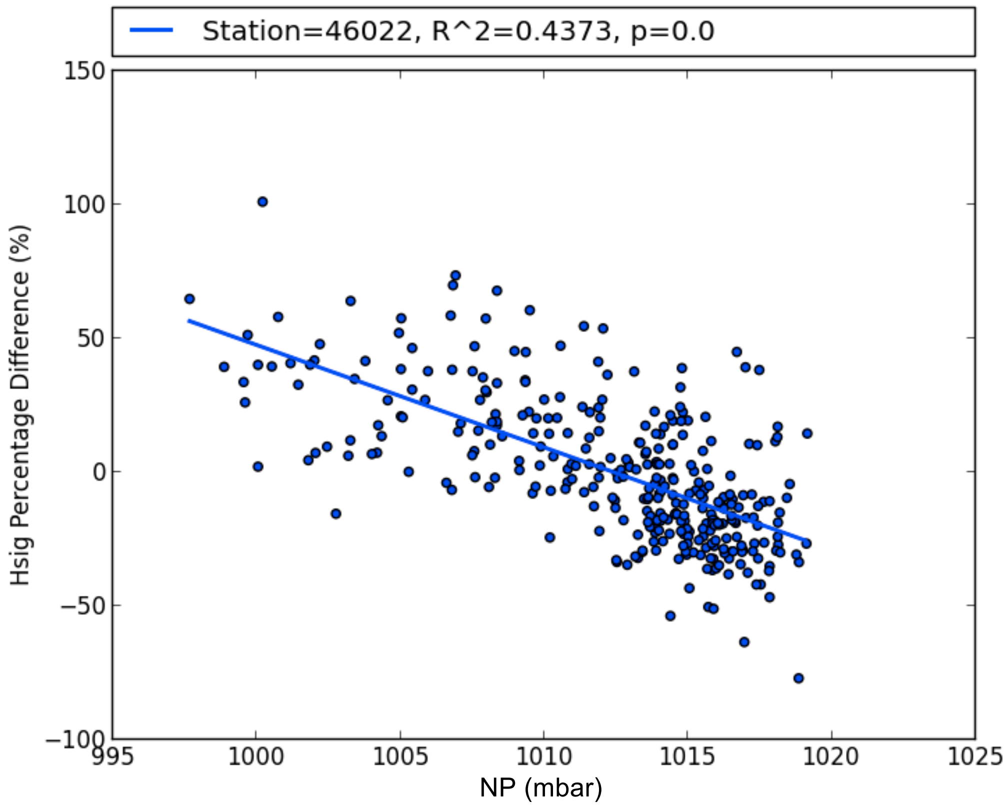

Station=46022, R^2=0.4373, p=0.0
Hsig Percentage Difference (%)
150
100
50
0
−50
−100
995
1000
1005
1010
1015
1020
1025
NP (mbar)

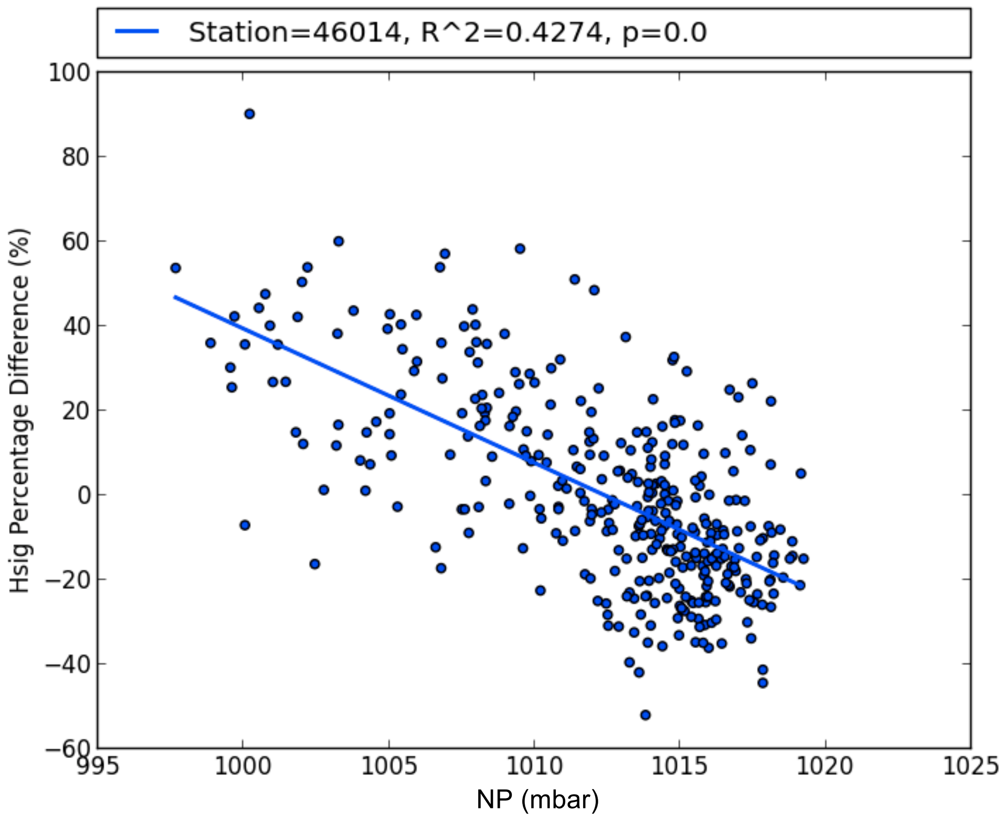
Station=46014, R^2=0.4274, p=0.0
Hsig Percentage Difference (%)
NP (mbar)
100
80
60
40
20
0
−20
−40
−60
995
1000
1005
1010
1015
1020
1025

Central California

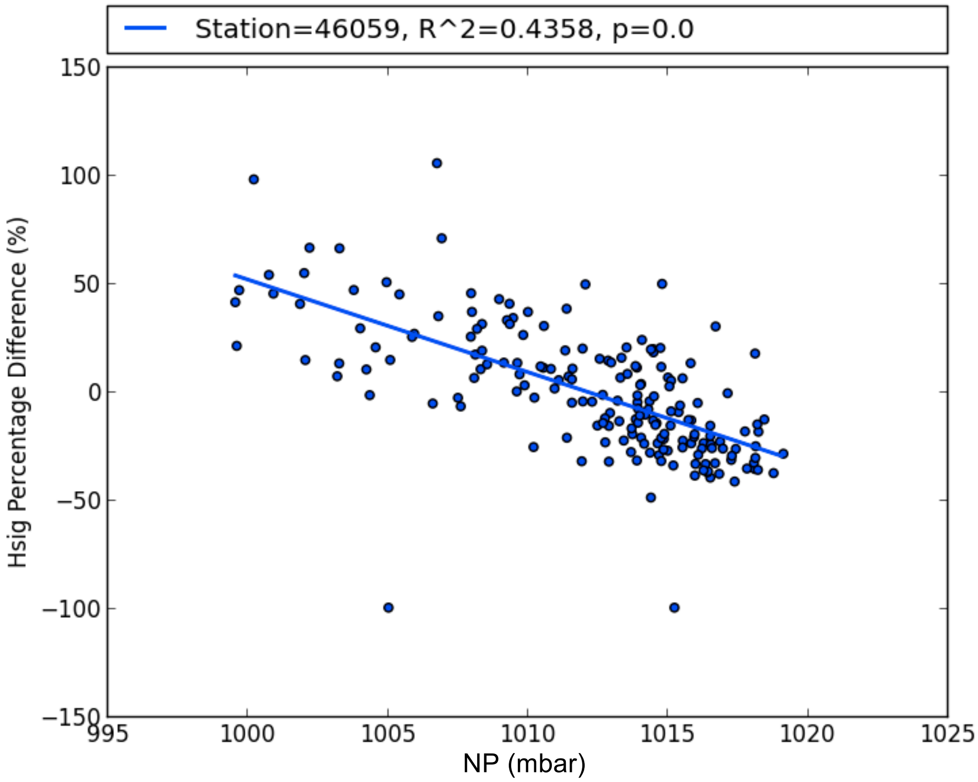

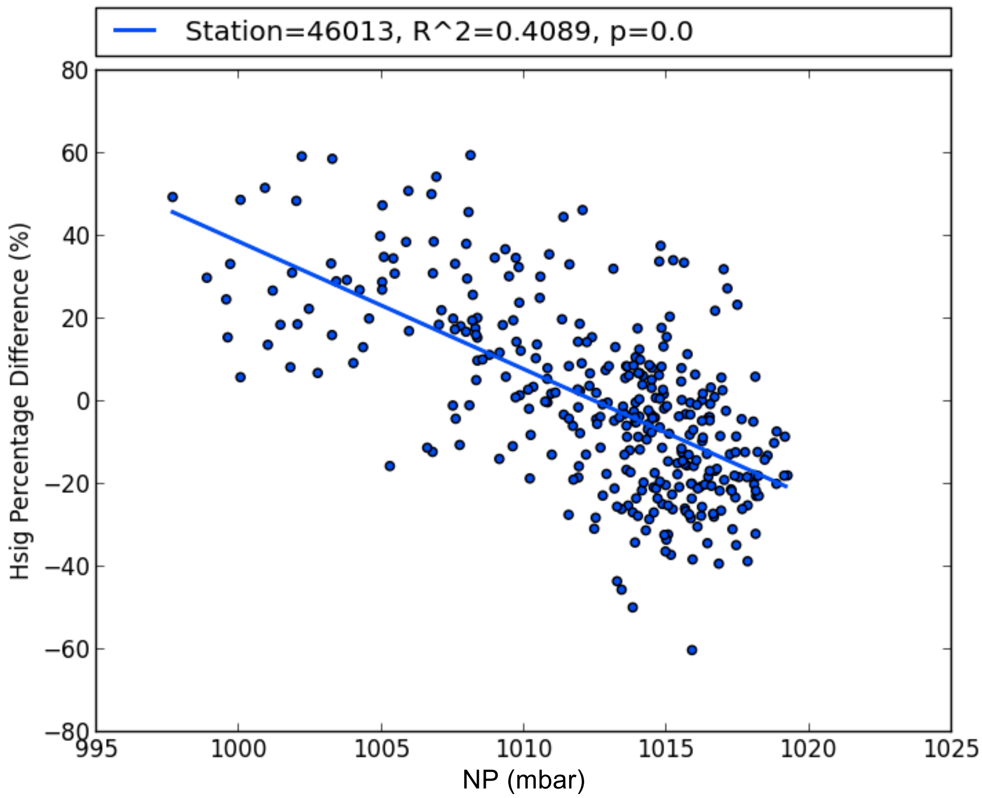
Station=46013, R^2=0.4089, p=0.0
Hsig Percentage Difference (%)
NP (mbar)
80
60
40
20
0
−20
−40
−60
−80
995
1000
1005
1010
1015
1020
1025

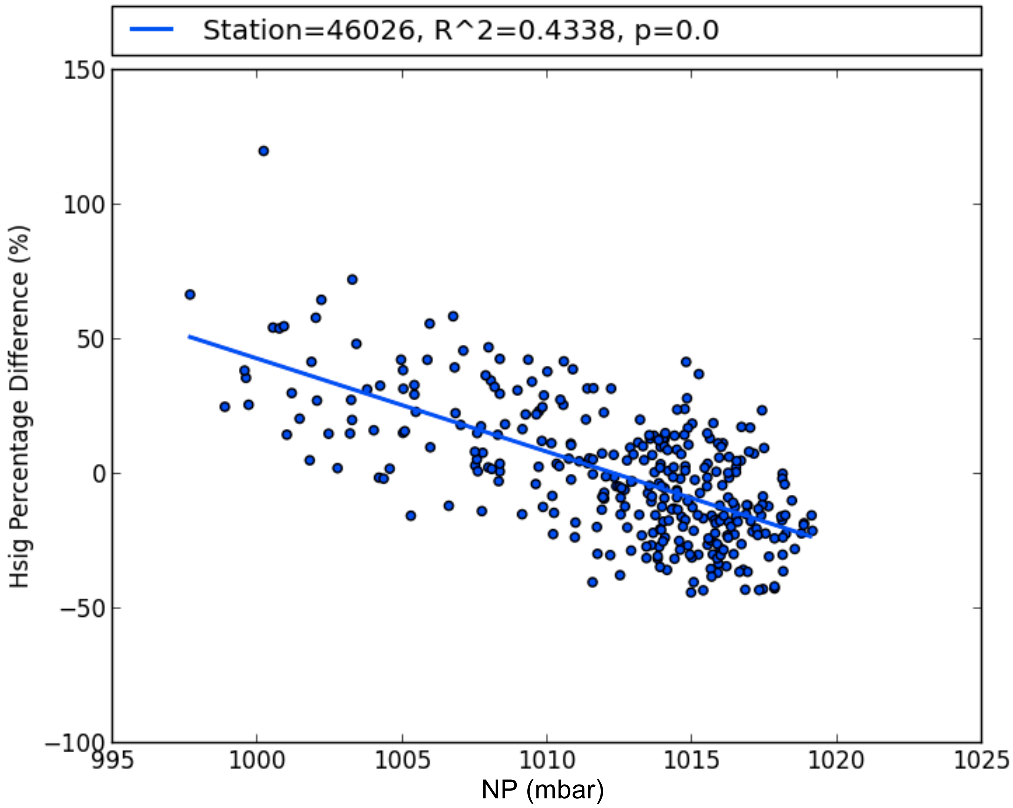
Station=46026, R^2=0.4338, p=0.0
150
100
50
0
−50
−100
995
1000
1005
1010
1015
1020
1025
Hsig Percentage Difference (%)
NP (mbar)

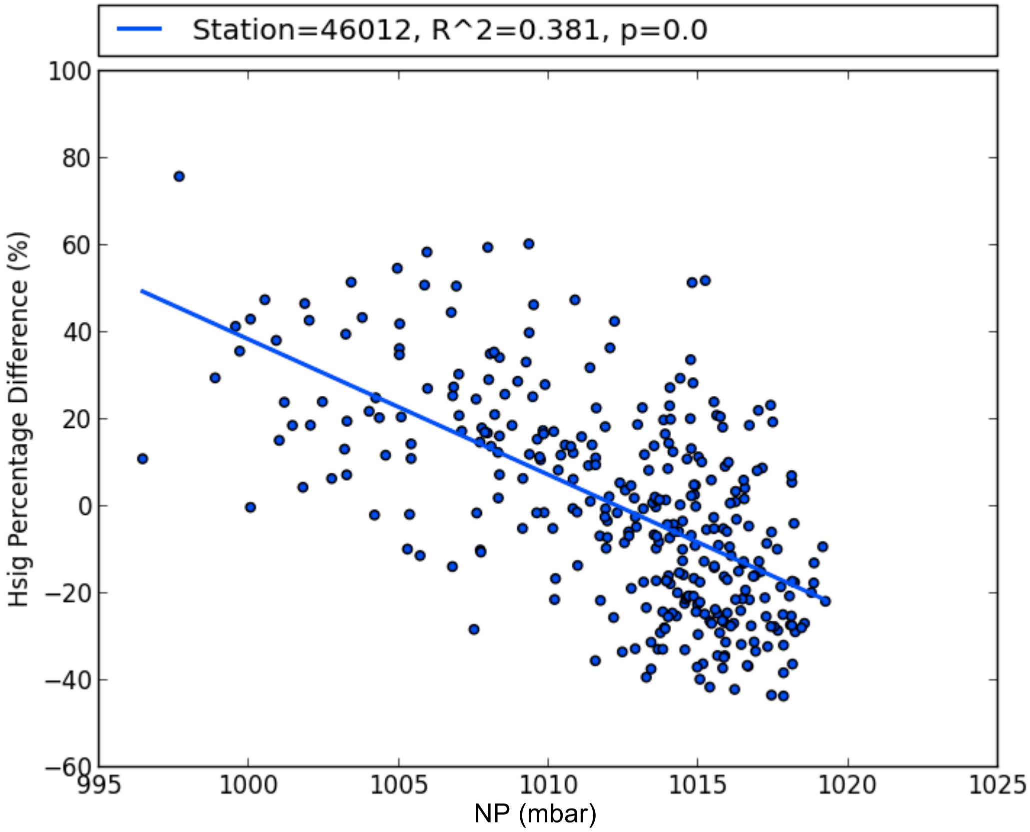

Station=46012, R^2=0.381, p=0.0
100
80
60
40
20
0
−20
−40
−60
995
1000
1005
1010
1015
1020
1025
Hsig Percentage Difference (%)
NP (mbar)

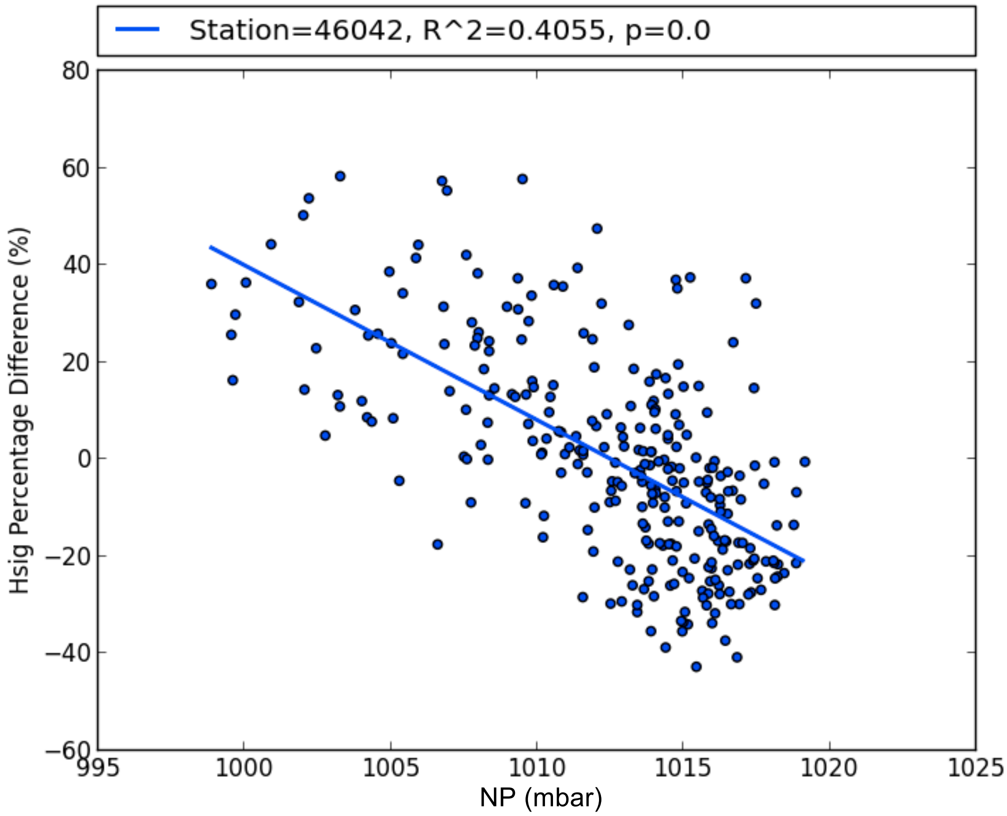

Station=46042, R^2=0.4055, p=0.0
80
60
40
20
0
−20
−40
−60
Hsig Percentage Difference (%)
995
1000
1005
1010
1015
1020
1025
NP (mbar)

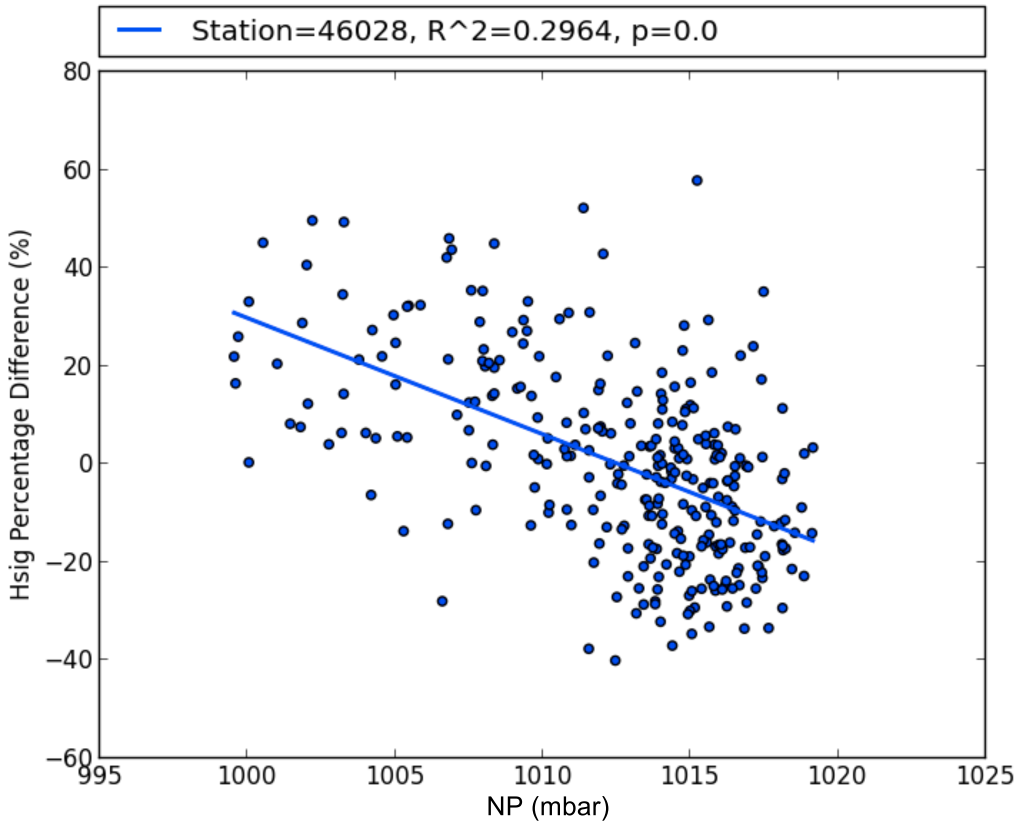

Station=46028, R^2=0.2964, p=0.0
80
60
40
20
0
−20
−40
−60
995
1000
1005
1010
1015
1020
1025
Hsig Percentage Difference (%)
NP (mbar)

Southern California

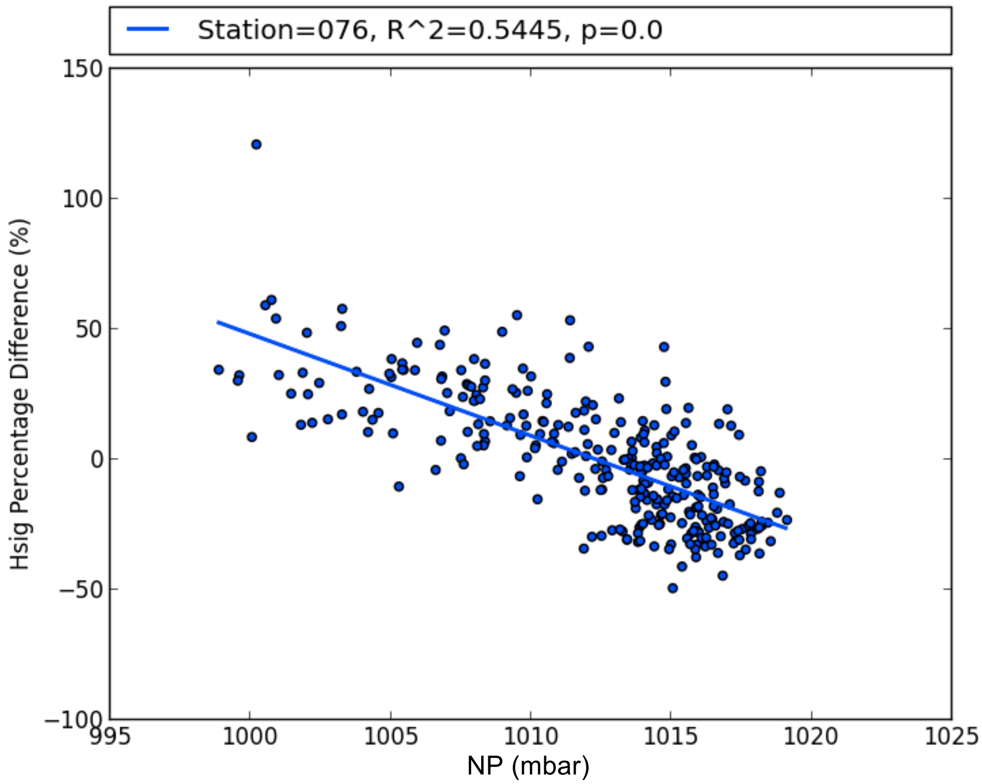

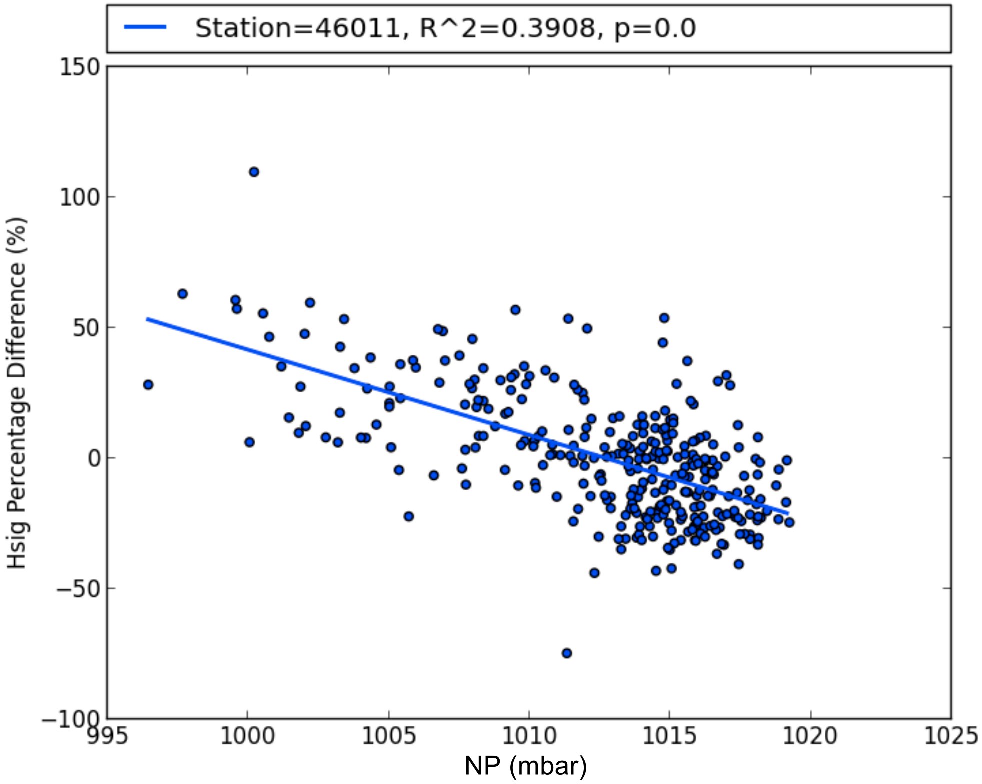
Station=46011, R^2=0.3908, p=0.0
Hsig Percentage Difference (%)
NP (mbar)
150
100
50
0
−50
−100
995
1000
1005
1010
1015
1020
1025

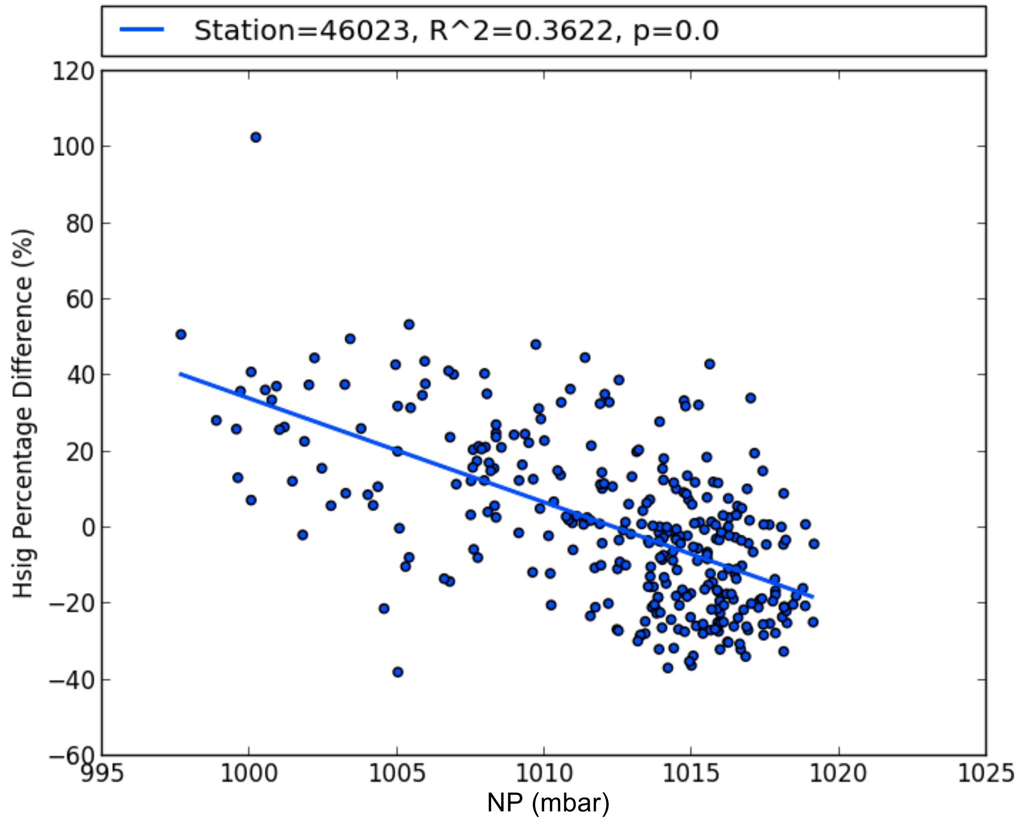

Station=46023, R^2=0.3622, p=0.0
Hsig Percentage Difference (%)
NP (mbar)
120
100
80
60
40
20
0
−20
−40
−60
995
1000
1005
1010
1015
1020
1025

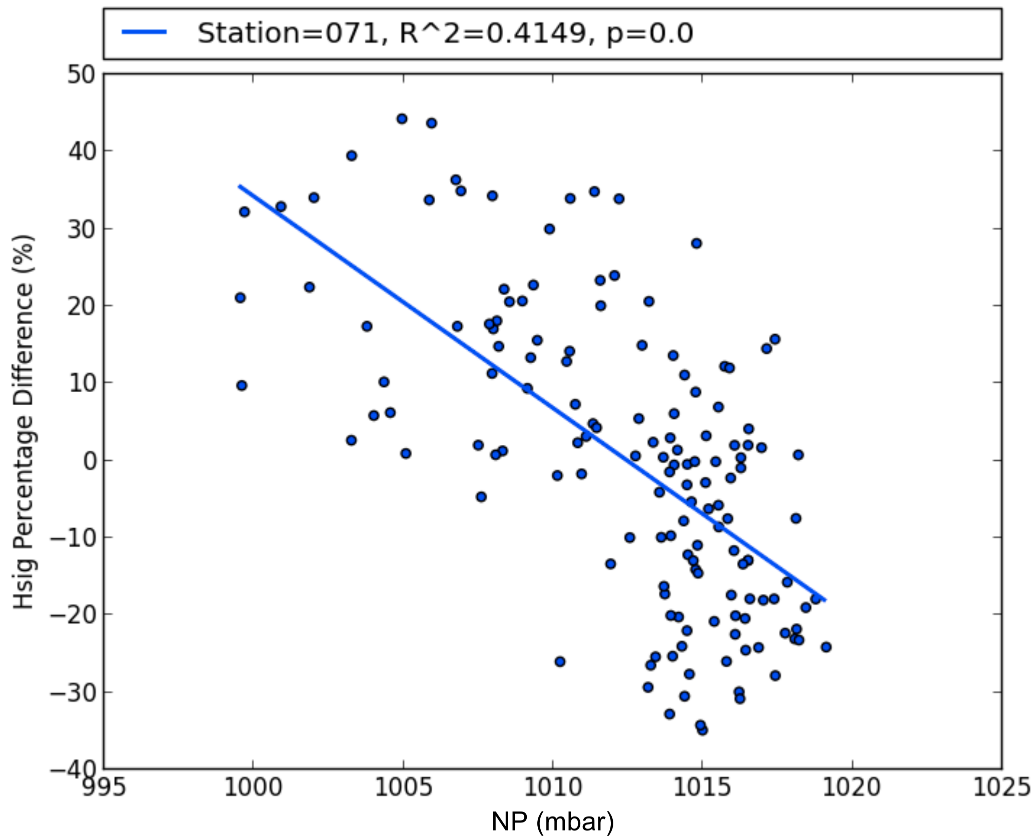
Station=071, R^2=0.4149, p=0.0
50
40
30
20
10
0
−10
−20
−30
−40
995
1000
1005
1010
1015
1020
1025
Hsig Percentage Difference (%)
NP (mbar)

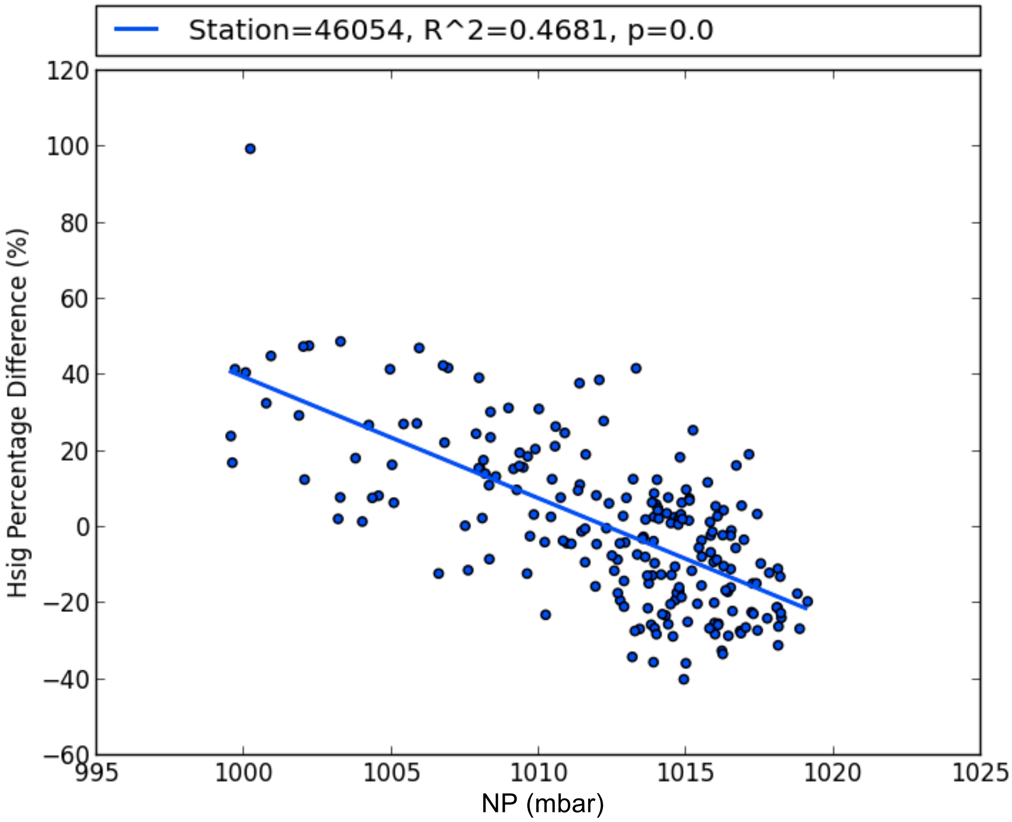
Station=46054, R^2=0.4681, p=0.0
Hsig Percentage Difference (%)
NP (mbar)
120
100
80
60
40
20
0
−20
−40
−60
995
1000
1005
1010
1015
1020
1025

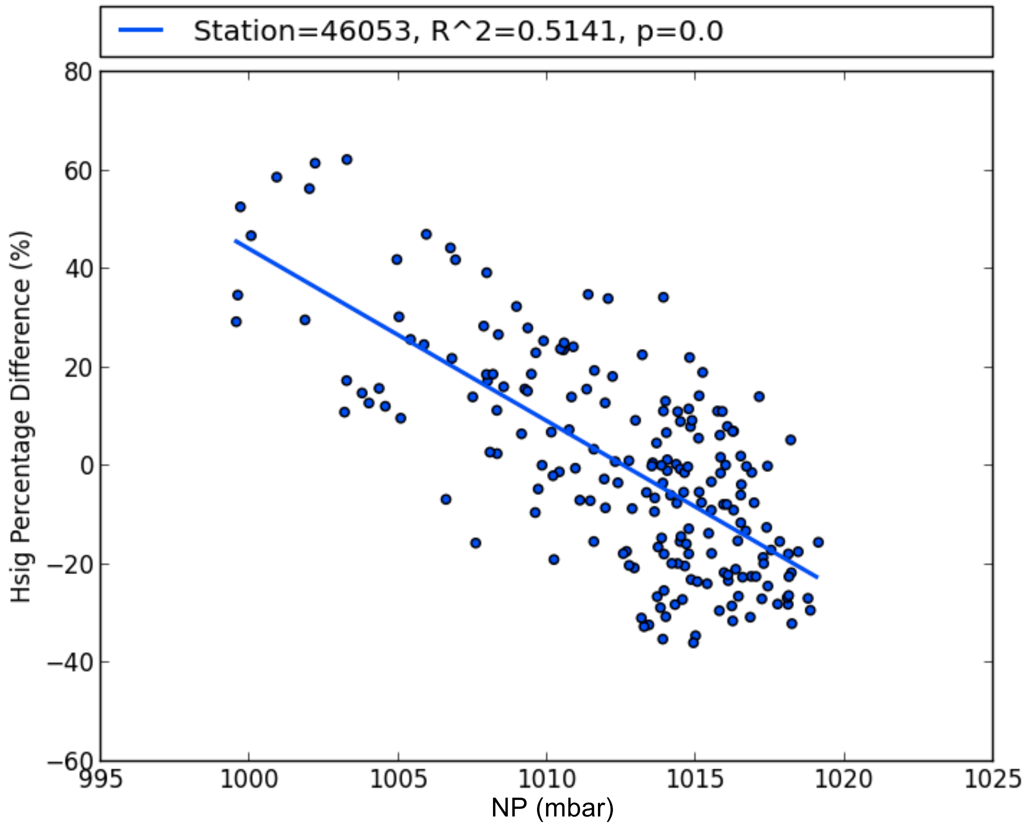
Station=46053, R^2=0.5141, p=0.0
80
60
40
20
0
−20
−40
−60
995
1000
1005
1010
1015
1020
1025
NP (mbar)
Hsig Percentage Difference (%)

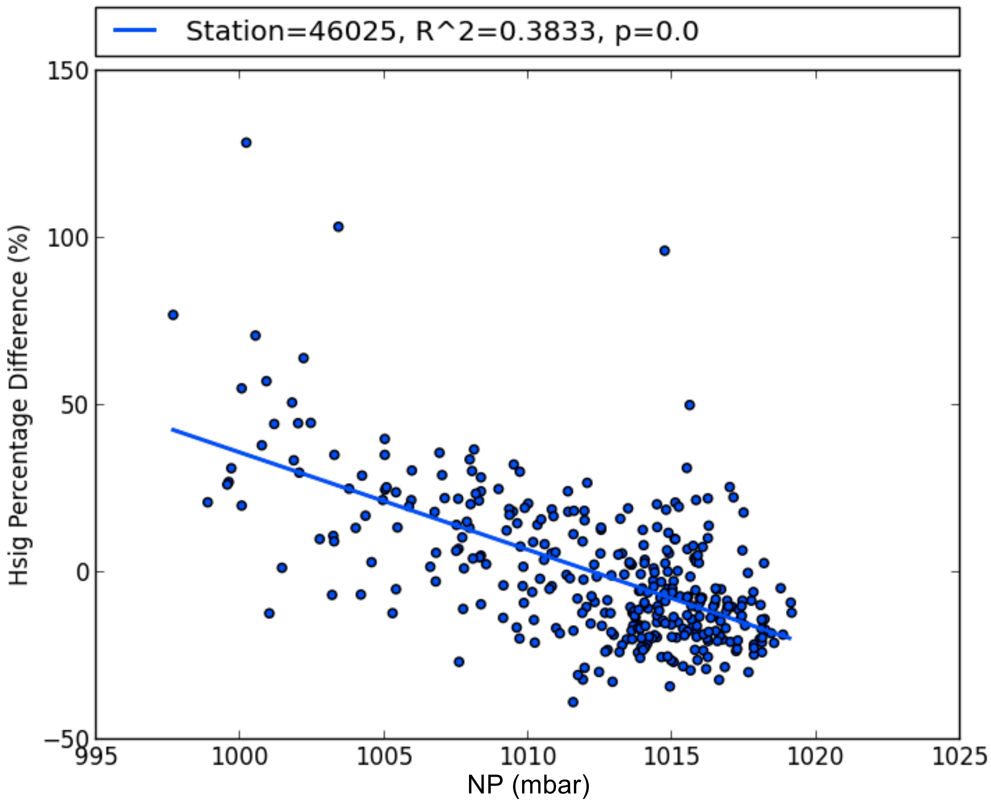
Station=46025, R^2=0.3833, p=0.0
150
100
50
0
−50
Hsig Percentage Difference (%)
995
1000
1005
1010
1015
1020
1025
NP (mbar)

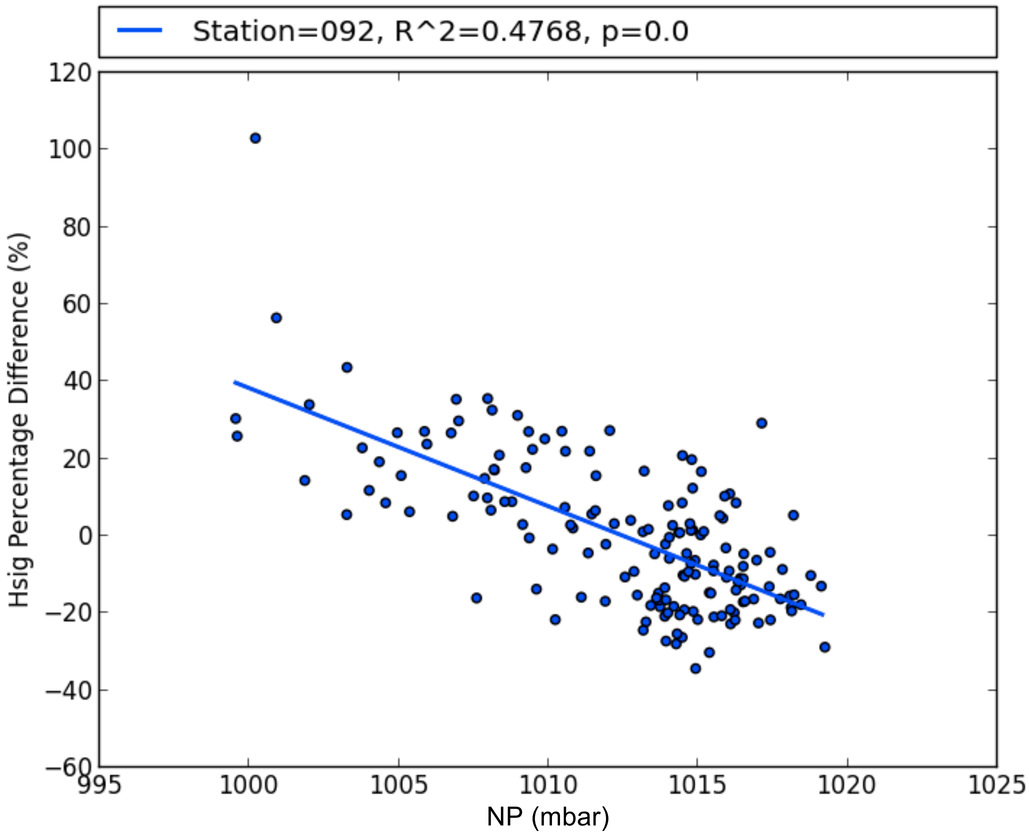

Station=092, R^2=0.4768, p=0.0
Hsig Percentage Difference (%)
NP (mbar)
120
100
80
60
40
20
0
−20
−40
−60
995
1000
1005
1010
1015
1020
1025

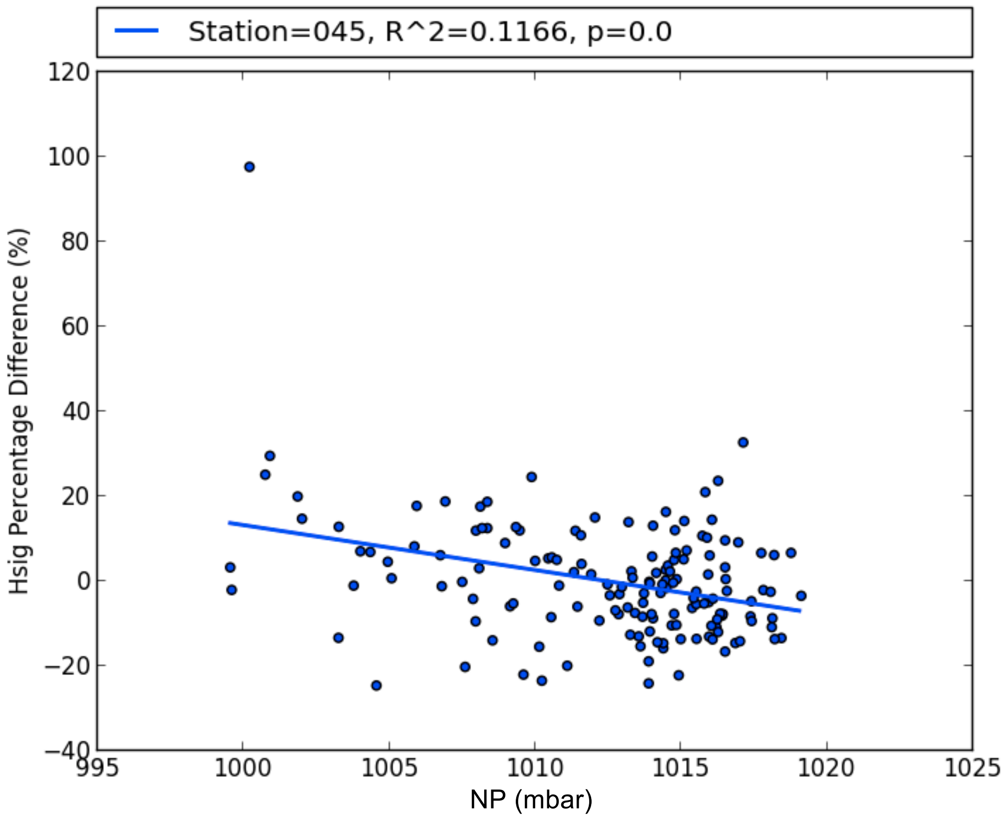
Station=045, R^2=0.1166, p=0.0
120
100
80
60
40
20
0
−20
−40
995
1000
1005
1010
1015
1020
1025
Hsig Percentage Difference (%)
NP (mbar)

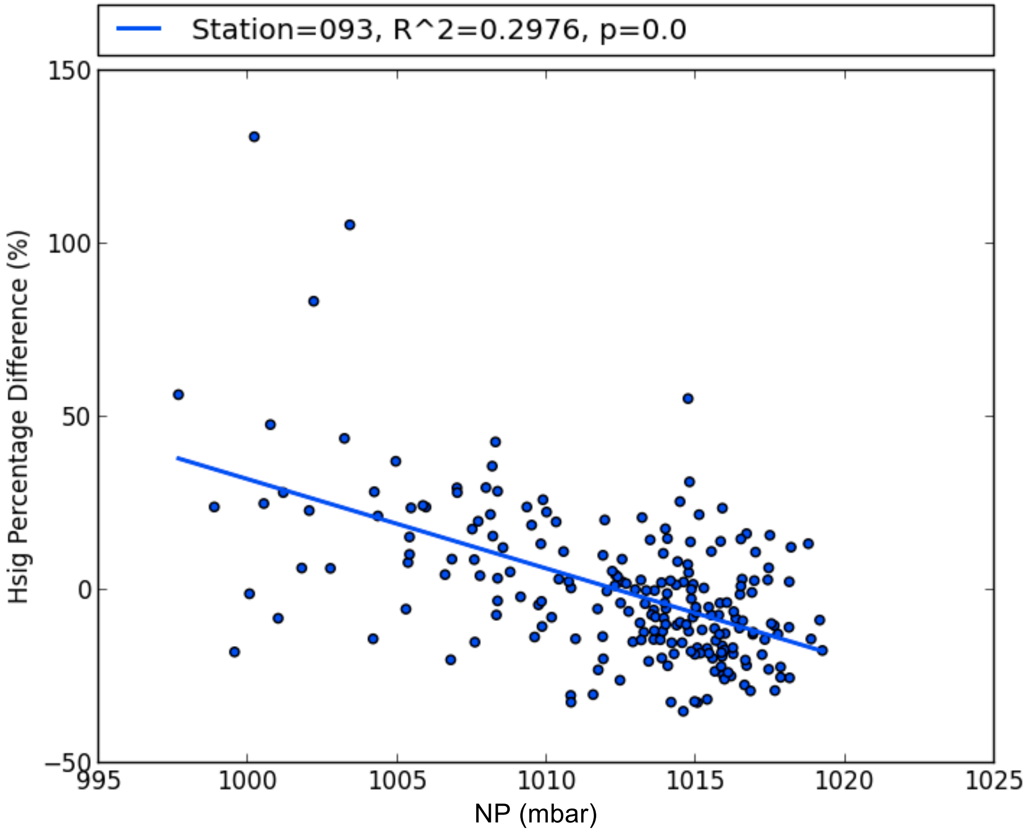
Station=093, R^2=0.2976, p=0.0
150
100
50
0
−50
995
1000
1005
1010
1015
1020
1025
Hsig Percentage Difference (%)
NP (mbar)

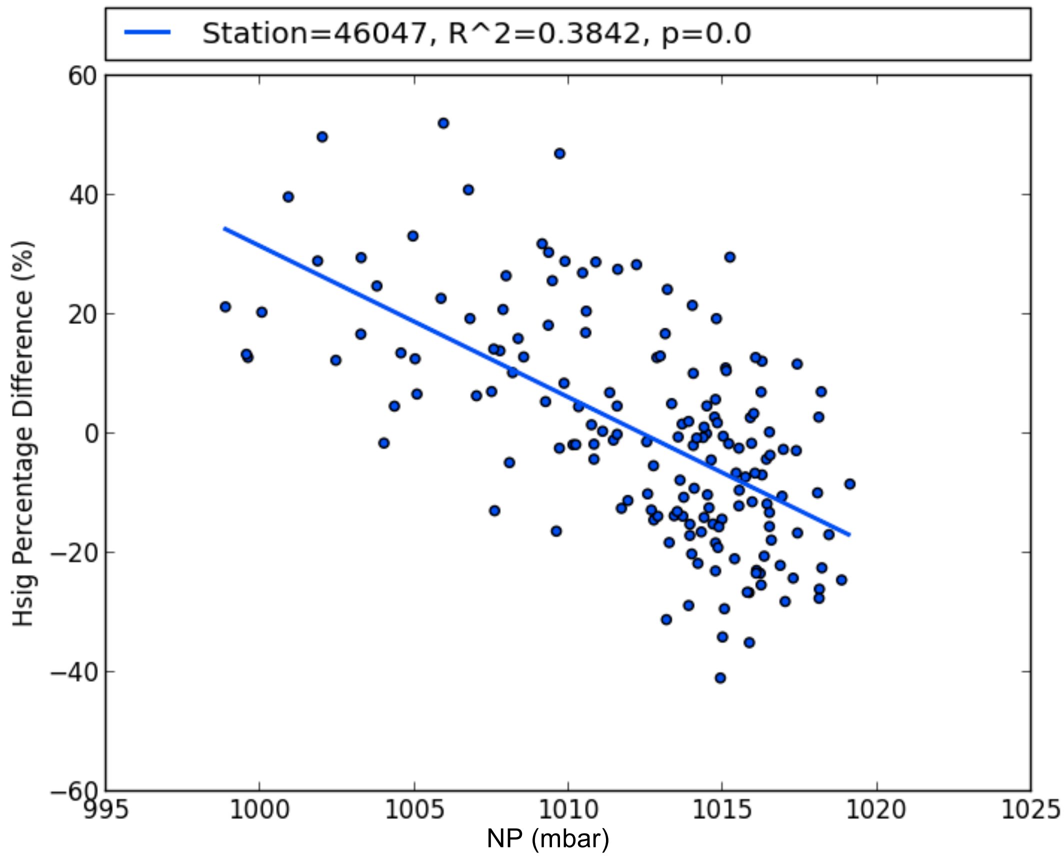
Station=46047, R^2=0.3842, p=0.0
60
40
20
0
−20
−40
−60
Hsig Percentage Difference (%)
995
1000
1005
1010
1015
1020
1025
NP (mbar)

LIST OF SUPPLEMENTAL FILES

File One	Adapting to Sea-Level Rise: A Guide for California's Coastal Communities
File Two	City of Santa Barbara Sea-Level Rise Vulnerability Study
File Three	Appendix A.csv
File Four	Appendix B.csv
File Five	Appendix C.csv
File Six	Appendix D.csv
File Seven	Appendix E.csv
File Eight	Appendix G.csv

FULL BIBLIOGRAPHY

Akaike, H. (1974), A new look at the statistical model identification, *IEEE Transactions on Automatic Control*, *19*, 716-723.

Allan, J.C., and P.D. Komar (2002), Extreme storms on the Pacific Northwest Coast during the 1997–98 El Niño and 1998–99 La Niña, *Journal of Coastal Research*, *18*(1), 175–193.

Allan, J.C., and P.D. Komar (2006), Climate controls on US West Coast erosion processes, *Journal of Coastal Research*, *22*(3), 511–529, doi:10.2112/030108.1.

AMEC Earth & Environmental Inc. (2010), *Proposed Final Program Environmental Impact Report for the Plan Santa Barbara General Plan Update.* Santa Barbara, California, 762 pp.

Barnard, P.L., J. Allan, J.E. Hansen, G.M. Kaminsky, P. Ruggiero, and A. Doria (2011), The impact of the 2009–10 El Niño Modoki on U.S. West Coast beaches, *Geophysical Research Letters*, *38*, L13604, doi:10.1029/2011GL047707.

Barnard, P.L., D.L. Revell, D. Hoover, J. Warrick, J. Brocatus, A.E. Draut, P. Dartnell, E. Elias, N. Mustain, P.E. Hart, and H.F. Ryan (2009). *Coastal processes study of Santa Barbara and Ventura County, California*. U.S. Geological Survey Open-File Report 2009-1029. 904 pp. http://pubs.usgs.gov/of/2009/1029/.

Barnett, T.P., N.E. Graham, N.A. Cane, S.E. Zebiak, S.C. Dolan, J.J. O'Brien, and D.M. Legeler (1988), On the prediction of the El Niño of 1986-1987, *Science*, *241*, 192-196.

Barnett, T.P., N. Graham, S. Pazan, W. White, M. Latif, and M. Flügel (1993), ENSO and ENSO-related predictability, Part I: Prediction of equatorial Pacific sea surface temperature with a hybrid coupled ocean–atmosphere model, *Journal of Climate*, *6*, 1545-1566.

Barnston, A.G., M.H. Glantz, and Y.X. He (1999), Predictive skill of statistical and dynamical climate models in SST forecasts during the 1997/98 El Niño episode and the 1998 La Niña onset, *Bulletin of the American Meteorological Society*, *80*, 217-243.

Barnston, A.G., and C.F. Ropelewski (1992), Prediction of ENSO episodes using canonical correlation analysis, *Journal of Climate*, *5*, 1316-1345.

Barnston, A.G., H.M. van den Dool, S.E. Zebiak, T.P. Barnett, M. Ji, D.R. Rodenhuis, M.A. Cane, A. Leetma, N.E. Graham, C.R. Ropelewski, V.E. Kousky, E.A. O'Lenic, and R.E. Livezey (1994), Long-lead seasonal forecasts—where do we stand?, *Bulletin of the American Meteorological Society*, *75*, 2097-2114.

Barth, M.C., and J.G. Titus, eds. (1984). *Greenhouse Effect and Sea Level Rise: A Challenge for the Generation*. Van Nostrand, New York: 238 pp. http://epa.gov/climatechange/effects/coastal/SLR-Challenge.html

Battisti, D.S., and A.C. Hirst (1989), Interannual variability in a tropical atmosphere-ocean model: Influence of the basic state, ocean geometry, and nonlinearity, *Journal of Atmospheric Science*, *46*, 1687-1712.

Benumof, B.T., C.D. Storlazzi, R.J. Seymour, and G.B. Griggs (2000), The relationship between incident wave energy and seacliff erosion rates: San Diego County, California, *Journal of Coastal Research*, *16*, 1162-1178.

Bjerknes, J. (1969), Atmospheric teleconnections from the equatorial Pacific, *Monthly Weather Review*, *97*, 163-172.

Bromirski, P.D., D.R. Cayan, and R.E. Flick (2005), Wave spectral energy variability in the northeast Pacific, *Journal of Geophysical Research*, *110*, 15 pp.

Bromirski, P.D., R.E. Flick, and D.R. Cayan (2003), Storminess variability along the California coast: 1858–2000, *Journal of Climate*, *16*(6), 982–993, doi:10.1175/1520-0442(2003)016<0982:SV A TCC>2.0.CO;2.

Bromirski, P.D., A.J. Miller, R.E. Flick, and G. Auad (2011), Dynamical suppression of sea level rise along the Pacific Coast of North America: Indications for imminent acceleration, *Journal of Geophysical Research*, *116*, C07005, doi:10.1029/2010JC006759.

Brönnimann, S., J. Luterbacher, J. Staehelin, T.M. Svendby, G. Hansen, and T. Svenøe (2004), Extreme climate of the global troposphere and stratosphere in1940-42 related to El Niño, *Nature*, *431*, 971-974.

Burnham, K.P., and D.R. Anderson (2002), *Model selection and multimodel inference: A practical information-theoretic approach*, Springer.

California Coastal Commission (1978). *Wave damage along the California coast: December 1977-March 1978.* San Francisco, California.

California Resources Agency (2009). *California Climate Adaptation Strategy*. 200 pp.

Cane, M.A., M. Munnich, and S.E. Zebiak (1990), A study of self-excited oscillations of the tropical ocean-atmosphere system. Part 1: Linear analysis, *Journal of Atmospheric Science*, *47*, 1562-1577.

Cane, M.A., and S.E. Zebiak (1985), A theory for El Niño and the Southern oscillation, *Science*, *228*, 1085-1087.

Cane, M.A., S.E. Zebiak, and S.C. Dolan (1986), Experimental forecasts of El Niño, *Nature*, *321*, 827-832.

Cayan, D., P. Bromirski, K. Hayhoe, M. Tyree, M. Dettinger, and R. Flick (2006), *Projecting future sea level rise*. California Climate Change Center, 64 pp.

Chelton, D.B., and R.E. Davis (1982), Monthly mean sea-level variability along the west coast of North America, *Journal of Physical Oceanography*, *12*, 757-784.

Chen, D., and M.A. Cane (2008), El Niño prediction and predictability, *Journal of Computational Physics*, 227, 3625-3640.

Chen, D., M.A. Cane, A. Kaplan, S.E. Zebiak, and D. Huang (2004), Predictability of El Niño over the past 148 years, *Nature*, *428*, 733-736.

Clarke, A.J., and S. Van Gorder (2003), Improving El Niño prediction using a space-time integration of Indo-Pacific winds and equatorial Pacific upper ocean heat content, *Geophysics Research Letters*, *30*, 1399, doi:10.1029/2002GL016673.

Climate Impacts Group, Joint Institute for the Study of the Atmosphere and Ocean, University of Washington and King County, Washington (2007), *Preparing for climate change: A guidebook for local, regional, and state governments*. 186 pp. cses.washington.edu/cig/fpt/guidebook.shtml

Committee on Sea-Level Rise in California, Oregon, and Washington; Board on Earth Sciences and Resources; Ocean Studies Board; Division on Earth and Life Studies; National Research Council (2012), *Sea-level rise for the coasts of California, Oregon, and Washington: Past, present, and future*. Washington, DC: National Academies Press, 275 pp. http://www.nap.edu/catalog.php?record_id=13389

Corral, A., A. Ossó, and J.E. Llebot (2010), Scaling of tropical-cyclone dissipation, *Nature Physics*, *6*, 693-696.

Dare, J. (2005). *Coastal erosion and armor database for California*. California Coastal Commission, 1 CD-ROM.

Dasgupta, S., B. Laplanate, C. Meisner, D. Wheeler, and J. Yan (2009), The impact of sea level rise on developing countries: A comparative analysis, *Climatic Change, 93*, 379-388

Davis, M. (2001), *Late Victorian Holocausts: El Niño Famines and the Making of the Third World*, Verso, London.

Department of Commerce, National Oceanic and Atmospheric Administration, National Ocean Service, Coastal Services Center (2011), *2009-2011 CA Coastal Conservancy Coastal Lidar Project*. NOAA's Ocean Service, Coastal Services Center (CSC).

Domurat, G. (1978), Selected coastal storm damage in California, winter of 1977-78, *Shore & Beach*, *46*, 15-20.

Donges, J.F., Y. Zou, N. Marwan, and J. Kurths (2009), The backbone of the climate network, *EPL (Europhysics Letters)*, *87*, 48007.

Donnelly, J.P., and J.D. Woodruff (2007), Intense hurricane activity over the past 5,000 years controlled by El Niño and the West African monsoon, *Nature*, *447*, 465-468.

Emery, K.O., and G.G. Kuhn (1982), Sea cliffs: Their processes, profiles and classification, *Geological Society of America Bulletin*, *93*(7), 644-654.

Enfield, D.B., and J.S. Allen (1980), On the structure and dynamics of monthly mean sea level anomalies along the Pacific coast of North and South America, *Journal of Physical Oceanography*, *10*, 557–578, doi:10.1175/1520-0485(1980)010<0557:OTSADO>2.0.CO;2.

Finzi Hart, J.A., P.M. Grifman, S.C. Moser, A. Abeles, M.R. Myers, S.C. Schlosser, and J.A. Ekstrom (2012), Rising to the Challenge: Results of the 2011 coastal California adaptation needs assessment. USCSG-TR-01-2012.

Flick, R.E. (1994), *Shoreline Erosion Assessment and Atlas of the San Diego Region,* Volume 1, Sacramento, California: Department of Boating and Waterways and the San Diego Association of Governments, 135 pp.

Flick, R.E. (1998), Comparison of tides, storm surges, and mean sea level during the El Niño winters of 1982-83 and 1997-98, *Shore & Beach*, *66*, 7-17.

Gemmrich, J., B. Thomas, and R. Bouchard (2011), Observational changes and trends in Northeast Pacific wave records, *Geophysical Research Letters*, *38*, L22601, 5 pp.

Goddard, L., S.J. Mason, S.E. Zebiak, C.F. Ropelewski, R. Basher, and M.A. Cane (2001), Current approaches to seasonal to interannual climate predictions, *International Journal of Climatology*, *21*, 1111-1152.

Gozolchiani, A., S. Havlin, and K. Yamasaki (2011), Emergence of El Niño as an autonomous component in the climate network, *Physical Review Letters*, *107*, 148501.

Graham, N.E., and H.F. Diaz (2001), Evidence for intensification of North Pacific winter cyclones since 1948, *Bulletin of the American Meteorological Society*, *82*, 1869–1893, doi:10.1175/1520-0477(2001)082<1869:EFIONP>2.3. CO;2.

Graham, N.E., J. Michaelsen, and T.P. Barnett (1987), An investigation of the El Niño-Southern oscillation cycle with statistical models. 2. Model results, *Journal of Geophysical Research*, *92*, 14271-14289.

Greene, H.G., L.Y. Murai, P. Watts, N.A. Maher, M.A. Fisher, C.E. Paull, and P. Eichhubl (2006), Submarine landslides in the Santa Barbara Channel as potential tsunami sources, *Natural Hazards and earth System Sciences*, *6*, 63-88.

Griggs, G.B. (2005), The impacts of coastal armoring, *Shore & Beach*, *73*(1), 13-22.

Griggs, G.B. (2010). *Introduction to California's beaches and coast*. University of California Press, Berkeley, California: 311 pp.

Griggs, G.B., and K. Brown (1998), Erosion and shoreline damage along the Central California coast: A comparison between the 1997-98 and 1982-83 winters, *Shore & Beach*, *66*(3), 18-23.

Griggs, G.B., and K.W. Fulton-Bennett (1987), Failure of coastal protection at Seacliff State Beach, Santa Cruz, California, *Environmental Management*, *11*, 175-182.

Griggs, G.B., and R.E. Johnson (1983), The impact of the 1983 storms on the coastline of northern Monterey Bay, *California Geology*, *36*, 163-174.

Griggs, G.B., K.B. Patsch, and L.E. Savoy (2005). *Living with the changing California coast*. University of California Press, Berkeley, California: 540 pp.

Griggs, G.B., J.E. Pepper, and M.E. Jordan (1992), *California Coastal Hazards: A Critical Assessment of Existing Land-Use Policies and Practices*. Special Publication of California Policy Seminar Program, Berkeley, California: 224 pp.

Griggs, G.B., and N.L. Russell (2012), *City of Santa Barbara Sea-Level Rise Vulnerability Study*. Sacramento, California: California Energy Commission, Public Interest Environmental Research Program, 87 pp.

Hapke, C.J., and D. Reid (2007), National assessment of shoreline change part 4: Historical coastal cliff retreat along the California coast, USGS Open File Report, 2007-1133, 51 pp. http://pubs.usgs.gov/of/2007/1133/

Hapke, C.J., D. Reid, B.M. Richmond, P. Ruggiero, and J. List (2006), National assessment of shoreline change part 3: Historical shoreline change and associated coastal land loss along sandy shorelines of the California coast, USGS Open File Report, 2006-1219, 72 pp. http://pubs.usgs.gov/of/2006/1219/

Heberger, M., H. Cooley, P. Herrera, P.H. Gleick, and E. Moore (2009a), *The impacts of sea-level rise on the California coast*. The Pacific Institute, 99 pp. www.pacinst.org/reports/sea_level?rise/report.pdf

Heberger, M., H. Cooley, P. Herrera, P.H. Gleick, and E. Moore (2011b), Potential impacts of increased coastal flooding in California due to sea-level rise, *Climatic Change*, *109*, 229-249.

Huyer, A., and R.L. Smith (1985), The signature of El Niño off Oregon, 1982–1983, *Journal of Geophysical Research*, *90*(C4), 7133–7142, doi:10.1029/JC090iC04p07133.

Inoue, M., and J.J. O'Brien (1984), A forecasting model for the onset of El Niño, *Monthly Weather Review*, *112*, 2326-2337.

International Research Institute for Climate and Society Earth Institute, IRI/CPC ENSO Quick Look, available at http://iri.columbia.edu/our-expertise/climate/forecasts/enso/.

Ji, M., A. Kumar, and A. Leetma (1994), An experimental coupled forecast system at the National Meteorological Center: Some early results, *Tellus*, *46A*, 398-418.

Ji, M., and A. Leetma (1997), Impact of data assimilation on ocean initialization and El Niño prediction, *Monthly Weather Review*, *125*, 742-753.

Jin, F.F. (1997), An equatorial recharge paradigm for ENSO. Part I: Conceptual model, *Journal of Atmospheric Science, 54*, 811–829, doi:10.1175/1520-0469(1997)054<0811:AEORPF>2.0.CO;2.

Kaminsky, G.M., P. Ruggiero, and G.R. Gelfenbaum (1998), Monitoring coastal change in southwest Washington and northwest Oregon during the 1997/98 El Niño, *Shore & Beach*, *66*(3), 42–51.

Kildow, J.K., and C.S. Colgan (2005). *California's Ocean Economy, National Ocean Economics Program*. Prepared for California Resources Agency, 156 pp.

King, P.G., A.R. McGregor, and J.D. Whittet (2011), *The economic costs of sea-level rise to California beach communities*. California Department of Boating and Waterways and San Francisco State University, 97 pp. http://www.dbw.ca.gov/PDF/Reports/CalifSeaLevelRise.pdf

Kirtman, B.P., J. Shukla, M. Balmaseda, N. Graham, C. Penland, Y. Xue, and S. Zebiak (2002), Current status of ENSO forecast skill. A report to the Climate Variability and Predictability (CLIVAR) Numerical Experimentation Group (NEG), CLIVAR Working Group on Seasonal to Interannual Prediction.

Kirtman, B.P., J. Shukla, B. Huang, Z. Zhu, and E.K. Schneider (1997), Multiseasonal predictions with a coupled tropical ocean global atmosphere system, *Monthly Weather Review*, *125*, 789-808.

Kleeman, R. (1991), A simple model of the atmospheric response to ENSO sea surface temperature anomalies, *Journal of Atmospheric Science*, *48*, 3-18.

Komar, P.D., J.C. Allan, and P. Ruggiero, (2011), Sea level variations along the U.S. Pacific Northwest coast: Tectonic and climate controls, *Journal of Coastal Research, 27*(5), 808–823. West Palm Beach (Florida), ISSN 0749-0208.

Kovats, R.S., M.J. Bouma, S. Hajat, E. Worrall, and A. Haines (2003), El Niño and health, *Lancet*, *362*, 1481-1489.

Kron, W. (2008). *Coasts: The riskiest places on Earth*. Pp. 3-21 in: Proceedings of the 31st International Conference on Coastal Engineering. J.McKee Smith, ed., World Scientific, Hamburg, Germany.

Landsea, C.W., and J.A. Knaff (2000), How much skill was there in forecasting the very strong 1997/98 El Niño?, *Bulletin of the American Meteorological Society*, *81*, 2107-2119.

Latif, M., D. Anderson, T. Barnett, M. Cane, R. Kleeman, A. Leetmaa, J. J. O'Brien, A. Rosati, and E. Schneider (1998), A review of the predictability and prediction of ENSO, *Journal of Geophysical Research*, *103*, 14,375–14,393, doi:10.1029/97JC03413.

Lester, C.F. (2005). An overview of California's coastal hazards policy. In: *Living with the Changing California Coast*. University of California Press, Berkeley, California, 138-162.

Ludescher, J., A. Gozolchiani, M.I. Bogachev, A. Bunde, S. Havlin, and H.J. Schellnhuber (2013), Improved El Niño forecasting by cooperativity detection, *Proceedings of the National Academy of Sciences*, *110*, 11742-11745.

Ludescher, J., A. Gozolchiani, M.I. Bogachev, A. Bunde, S Havlin, and H.J. Schellnhuber (2014), Very early warning of next El Niño, *Proceedings of the National Academy of Sciences*, *111*, 2064-2066, doi: 10.1073/pnas.1323058111.

Massey, F.J., Jr. (1951), The Kolmogorov-Smirnov Test for goodness of fit, *Journal of the American Statistical Association*, *46*(253), 68-78.

Matsumoto, M, and T. Nishimura (1998), Mersenne Twister: A 623-dimensionally equidistributed uniform pseudo-random number generator, *Association for Computing Machinery Transactions on Modeling and Computer Simulation*, *8*, 3-30.

McGranahan, G., D. Balk, and B. Anderson (2007), The rising tide: Assessing the risks of climate change and human settlements in low elevation coastal zones, *Environment and Urbanization*, *19*, 17-37.

McPhaden, M.J. (1999), Genesis and evolution of the 1997-98 El Niño, *Science*, *283*, 950-954.

McPhaden, M.J. (2003), Tropical Pacific Ocean heat content variations and ENSO persistence barriers, *Geophysics Research Letters*, *30*, 1480, doi:10.1029/2003GL016872.

McPhaden, M.J., A.J. Busalacchi, R. Cheney, J.-R. Donguy, K.S. Gage, D. Halpern, M. Ji, P. Julian, G. Meyers, G.T. Mitchum, P.P. Niiler, J. Picaut, R.W. Reynolds, N. Smith, and K. Takeuchi (1998), The Tropical Ocean-Global Atmosphere observing system: A decade of progress, *Journal of Geophysical Research*, *103*, 14169-14240.

Metropolis, N., and S. Ulam (1949), The Monte Carlo method, *Journal of the American Statistical Association*, *44*, 335-341.

Milliman, J.D., J.M. Broadus, and F. Gable (1989), Environmental and economic implications of rising sea level and subsiding deltas: The Nile and Bengal examples, *Ambio*, *18*, 340-345.

Moffatt and Nichol Engineers (1989), *Historic Wave and Sea Level Data Report, San Diego Region*, Coast of California Storm and Tidal Waves Study 88-6, Los Angeles, California: U.S. Army Corps of Engineers.

Moser, S.C. (2007), Is California preparing for sea-level rise?, *California Coast and Ocean*, *22*(4), 24-30.

Moser, S.C. (2009). *Good Morning, America! The Explosive U.S. Awakening to the Need for Adaptation*. Sacramento, California and Charleston, South Carolina. California Energy Commission and NOAA-Coastal Services Center.

Moser, S.C., and J. Tribbia (2007). *Vulnerability to coastal impacts of climate change: Coastal managers' attitudes, knowledge, perceptions, and action*. PIER Project Report, California Energy Commission, 35 pp. http://www.susannemoser.com/documents/Moser-Tribbia_attitudesknowledgeperceptionsactions_CEC-500-2007-082.PDF

National Oceanic and Atmospheric Administration (2010), *Adapting to climate change: A planning guide for state coastal managers*. NOAA Office of Ocean and Coastal Resource Management, 138 pp. http://coastalmanagement.noaa.gov/climate/docs/adaptationguide.pdf

National Research Council (2010). *Adapting to the impacts of climate change*. The National Academies Press, Washington, D.C., 244 pp.

National Research Council (2011). *America's Climate Choices*. The National Academies Press: Washington, D.C.

Neelin, J.D. (1990), A hybrid coupled general circulation model for El Niño studies, *Journal of Atmospheric Sciences*, *47*, 674-693.

Neelin, J.D., D.S. Battisti, A.C. Hirst, F.-F. Jin, Y. Wakata, T. Yamagata, and S.E. Zebiak (1998), ENSO theory, *Journal of Geophysical Research*, *103*, 14261-14290.

Neelin, J.D., M. Latif, and F. Jin (1994), Dynamics of coupled ocean-atmosphere models: The tropical problem, *Annual Review of Fluid Mechanics*, *26*, 617-659.

Nichols, R.J. (2010), *Impacts of and responses to sea level rise*. In Understanding Sea Level Rise and Variability. Wiley-Blackwell, 17-51.

Nichols, R.J. (2011), Planning for the impacts of sea level rise, *Oceanography*, *24*(2), 144-157, doi:10.5670/oceanograp.2011.34.

Nichols, R.J., P.P. Wong, V.R. Burkett, J.O. Codignotto, J.E. Hay, R.F. McLean, S. Ragoonaden, and C.D. Woodroofe (2007). *Coastal systems and low-lying areas*, Chapter 6 in Climate Change 2007: Impacts, Adaptation and Vulnerability. Cambidge University Press, Cambridge, U.K. http://www.ipcc.ch/pdf/assessment-report/ar4/wg2/ar-wg2-chapter6.pdf.

O'Reilly, W.C., and R.T. Guza (1993), A comparison of two spectral wave models in the Southern California Bight, *Coastal Engineering*, *19*, 263-282.

O'Reilly, W.C., and R.T. Guza (1998), Assimilating coastal wave observations in regional swell predictions. Part I: Inverse methods, *American Meteorological Society*, *28*, 679-691.

Orme, A.R., G.B. Griggs, D.L. Revell, J.G. Zoulas, C.C. Grandy, and J. Koo (2011), Beach changes along the Southern California coast during the twentieth century: A comparison of natural and human forcing factors, *Shore & Beach*, *79*(4), 38-50.

Patsch, K., and G. Griggs (2006a). *Littoral cells, sand budgets and beaches: Understanding California's shoreline*. Institute of Marine Sciences, University of California Santa Cruz and California Department of Boating and Waterways. 39 pp.

Patsch, K., and G. Griggs (2006b). *Development of sand budgets for California's major littoral cells: Eureka, Santa Cruz, Southern Monterey Bay, Santa Barbara, Santa Monica (including Zuma), San Pedro, Laguna, Oceanside, Mission Bay, and Silver Strand littoral cells*. Report for California Coastal Sediment Management Workgroup. 111 pp.

Patsch, K.B., and G.B. Griggs (2008), A sand budget for the Santa Barbara littoral cell, California, *Marine Geology*, *252*, 50-61.

PWA Ltd. (2009). *California coastal erosion responses to sea level rise-analysis and mapping*. Prepared for the Pacific Institute, 65 pp.

Revell, D.L., and G.B. Griggs (2006), Beach width and climate oscillations along Isla Vista, Santa Barbara, California, *Shore & Beach*, *74*(3), 8-16.

Revell, D.L., and G.B. Griggs (2007), Regional shoreline and beach changes in the Santa Barbara sandshed, *Proc. Coastal Sediments* 2007. ASCE.

Ruggiero, P., P.D. Komar, and J.C. Allan (2010), Increasing wave heights and extreme value projections: The wave climate of the U.S. Pacific Northwest, *Coastal Engineering*, *57*, 539-552.

Runyan, K.B., and G. Griggs (2003), The effects of armoring sea cliffs on the natural sand supply to the beaches of California, *Journal of Coastal Research*, *19*(2), 336-347.

Russell, N.L, and G.B. Griggs (2012), *Adapting to sea-level rise: A guide for California's coastal communities.* Sacramento, California: California Energy Commission, Public Interest Environmental Research Program, 52 pp.

Russell, N.L., and G.B. Griggs (2013a), California sea-level rise vulnerability and adaptation guidance document: A summary report, *Shore & Beach*, *81*(1), 23-29.

Russell, N.L., and G.B. Griggs (2013b), City of Santa Barbara sea-level rise vulnerability assessment: A summary report, *Shore & Beach*, *81*(4), 38-51.

Ryan, H.F., and M. Noble (2002), Sea level response to ENSO along the central California coast: How the 1997–1998 event compares with the historic record, *Progress in Oceanography*, *54*, 149–169, doi:10.1016/S0079-6611(02)00047-2.

Sallenger, A.H., W. Krabill, J. Brock, R. Swift, S. Manizade, and H. Stockton (2002), Sea-cliff erosion as a function of beach changes and extreme wave runup during the 1997–1998 El Niño, *Marine Geology*, *187*, 279–297, doi:10.1016/S0025-3227(02)00316-X.

Seager R., N. Naik, M. Ting, M.A. Cane, N. Harnik, and Y. Kushnir (2010), Adjustment of the atmospheric circulation to tropical Pacific SST anomalies: Variability of transient eddy propagation in the Pacific–North America sector, *Quarterly Journal of the Royal Meteorological Society*, *136*, 277–296, doi:10.1002/qj.588.

Seymour, R.J. (1998), Effects of El Niño on the west coast wave climate, *Shore & Beach*, *66*(3), 3-6.

Seymour, R.J. (2011), Evidence for changes to the Northeast Pacific wave climate, *Journal of Coastal Research*, *27*, 194-201.

Shum, C., and C. Kuo (2011). *Observation and geophysical causes of present-day sea level rise*. In: Climate Change and Food Security in South Asia, R. Lai, M. Kivakumar, S. Faiz, A. Rahman, and K. Islam (Eds.), Part 2, Chapter 7, 85-104.

Stahl, S. (2006), The evolution of the normal distribution, *Mathematics Magazine*, *79*, 96-113.

Storlazzi, C.D., and G.B. Griggs (1998), The 1997-1998 El Niño and erosion processes along the central coast of California, *Shore & Beach*, *66*(3), 12-17.

Storlazzi, C.D., and G.B. Griggs (2000), Influence of El Niño-Southern Oscillation (ENSO) events on the evolution of central California's shoreline, *Geological Society of America Bulletin*, *112*(2), 236-249.

Storlazzi, C.D., C.M. Willis, and G.B. Griggs (2000), Comparative impacts of the 1982-83 and 1997-98 El Niño winters on the central California coast, *Journal of Coastal Research*, *16*(4), 1022-1036.

Storlazzi, C.D., and D.K. Winfield (2005), *Spatial and temporal variations in oceanographic and meteorologic forcing along the Central California coast*, 1980-2002, Scientific Investigations Report 2005-5085, U.S. Geological Survey, Denver, CO, 39 pp. http://pubs.usgs.gov/sir/2005/5085

Swisher, M.L. (1983). *Preliminary report on January 1983 coastal storm damage*. San Francisco, California Coastal Commission: 15 pp.

Takeuchi, K. (1976), Distribution of informational statistics and a criterion of model fitting, *Suri-Kagaku (Mathematical Sciences)*, *153*, 12-18.

Tang, F.T., W.W. Hsieh, and B. Tang (1997), Forecasting the equatorial Pacific sea surface temperature by neural network models, *Climate Dynamics*, *13*, 135-147.

Tollefson, J. (2014), El Niño tests forecasters, *Nature*, *508*, 20-21.

Trenberth, K.E., and J.W. Hurrell (1994), Decadal atmosphere-ocean variations in the Pacific, *Climate Dynamics*, *9*, 303-319.

Tsonis, A.A., K.L. Swanson, and P.J. Roebber (2006), What do networks have to do with climate?, *Bulletin of the American Meteorological Society*, *87*, 585-595.

United States Agency for International Development (2009). Adapting to climate change: A guidebook for development planners, 164 pp. http://www.crc.uri.edu/download/CoastalAdaptationGuide.pdf

Vermeer, M., and S. Rahmstorf (2009). *Global sea level linked to global temperature.* Proceedings National Academy of Sciences, 106(51): 21527-21532.

Warrick, R.A., E.M.I. Barrow, and T.M.L. Wigley, eds. (1993). Climate and sea level change: Observations, projections, implications. Cambridge University Press, Cambridge, UK: 448 pp.

Webster, P.J. (1995), The annual cycle and the predictability of the tropical coupled ocean-atmosphere system, *Meteorology and Atmospheric Physics*, *56*, 33-55.

Wen, C. (2002), Impacts of El Niño and La Niña on the cycle of the East Asian winter and summer monsoon, *China Journal of Atmospheric Sciences*, *5*, 595-610.

Wolter, K., and M.S. Timlin (1993), Monitoring ENSO in COADS with a seasonally adjusted principal component index, *Proceedings of the 17th Climate Diagnostics Workshop*, Norman, OK, NOAA/NMC/CAC, NSSL, Oklahoma Climate Survey, CIMMS and the School of Meteorology, University of Oklahoma, 52-57.

Wolter, K. and M.S. Timlin (1998), Measuring the strength of ENSO events: How does 1997/98 rank? *Weather, Royal Meteorological Society*, *53*(9), 315–324.

Wolter, K., and M.S. Timlin (2011), El Niño/Southern Oscillation behaviour since 1871 as diagnosed in an extended multivariate ENSO index (MEI. ext), *International Journal of Climatology*, *31.7*, 1074-1087.

Xu, J.S., and H. Storch (1990), Principal oscillation patterns – prediction of the state of ENSO, *Journal of Climate*, *3*, 1316-1329.

Xue, Y., A. Leetmaa, and M. Ji (2000), ENSO prediction with Markov models: The impact of sea level, *Journal of Climate*, *13*, 849-871.

Yamasaki, K., A. Gozolchiani, and S. Havlin (2008), Climate networks around the globe are significantly affected by El Niño, *Physical Review Letters*, *100*, 228501.

Zebiak, S.E., and M.A. Cane (1987), A model El Niño-Southern oscillation, *Monthly Weather Review*, *115*, 2262-2278.